THE EFFECTIVENESS OF ENERGY STORAGE IN HYBRID VEHICLES

Daniel Cole

A thesis submitted in partial fulfilment of the requirement of the University of the West of England, Bristol for the Doctorate of Philosophy

Department of Engineering, Design and Mathematics, Faculty of Environment and Technology, University of the West of England, Bristol

February 2016

Abstract

Public awareness of finite oil resources and concerns over climate change have spurred efforts to improve vehicle efficiency and reduce emissions by road transport. Hybrids have become an increasingly popular alternative to conventional powertrain vehicles. Large fuel savings are claimed (typically 70 + mpg) (Toyota, 2014), however, collective anecdotal evidence from owners of these vehicles suggests a more modest performance. A literature review yielded an abundance of literature relating to specific hybrid vehicle technologies, and control strategies, however the variation in energy savings over different journey types for different classes of vehicle has received less attention. A simulation tool was developed to compare the energy saving effectiveness of parallel hybrid powertrains with regenerative braking and energy storage across a broad range of vehicle and journey types. The realism of the simulation (in non-hybrid mode) was evaluated by comparison with practical trials. A range of validation methods showed that average fuel consumption could be calculated to within +/- 5-10% of measured consumption and, in cases where detailed data for a vehicle was available, this improved to within 3%. Simulated fuel consumption was around 15% greater that manufacturers' claims – reasons for this were explored. Using the backward and forward looking simulation it was possible to calculate likely fuel savings in various scenarios. Results indicate a trend of improved potential savings with increased vehicle mass. Over urban journeys results ranged from around 16 to 23% energy savings for a small car and large coach respectively. On extra-urban journeys much more modest savings were calculated ranging from a maximum of 0 - 4 % across the same range of vehicles. The likely effects of vehicle mass and drag coefficient has also been explored along with the energy saving potential of start-stop engine technology, often used in hybrids and non-hybrids alike. The broad part of the study confirmed quantitatively that greatest fuel savings might be achieved on urban routes with public transport buses. The study then narrowed to consider this application, particularly with respect to exhaust emissions which are cause for growing concern. Possible reductions in exhaust NOx and PM emissions of up to 10 to 12% respectively were predicted through the application of parallel hybrid powertrains to existing bus designs and simulated on the MLTB cycle.

Table of Contents

List of Figures

Nomenclature and abbreviations used

		Units
A	Maximum cross section area of vehicle	m^2
a	Acceleration	m/s^2
α	Gradient	°
C_d	Drag coefficient	--
C_{rr}	Coefficient of rolling resistance	--
F	Force	N
m_v	Mass of vehicle	kg
F_{aero}	Aerodynamic drag	N
F_{roll}	Rolling resistance	N
F_{grad}	Gradient resistance	N
F_{tract}	Traction force	N
F_{brake}	Braking force	N
$B_{brakelim}$	Simulation over-speed constant to trigger braking	m/s
g	Gravitational acceleration = 9.81 m/s^2	
v	Velocity	m/s or *mph*
t	Time	seconds
v_{sim}	Simulated velocity	m/s
v_{dem}	Demand velocity	m/s
ρ	Density of air	kg/m^3
ESS_{cap}	Energy storage system capacity	J
thr_{clutch}	Throttle during clutch slip condition	%

T	Torque	N.m
η_{eng}	Overall engine efficiency	--
η_{trans}	Transmission efficiency	--
DOD	Depth of Discharge	%
SoC	State of Charge	%
SoC_{min}	Maximum state of charge	%
SoC_{max}	Minimum state of charge	%
SoC_{init}	Initial state of charge	%
$\omega_{upshift}$	Engine speed for gear change up	rpm
$\omega_{downshift}$	Engine speed for gear change down	rpm
$v_{clutchslip}$	Speed below which clutch slip occurs	mph
C_{PID}	PID Control term	--
EB_{lim}	Engine braking force limit	N
E_{idle}	Engine fuel consumption at idle	j
$F_{engbrconst}$	Engine braking constant	--
F_{engbr}	Engine braking force	
BSFC	Brake specific fuel consumption	g/kWhr (g=grams)
CVT	continuously variable transmission	
EPA	Environmental protection Agency (US)	
ECE	Economic Commission for Europe	
ESS	Energy storage system	
FTP	Federal Test Procedure (US)	
HEV	hybrid electric vehicle	

ICE	internal combustion engine
KESS	kinetic energy storage system
NEDC	New European Drive Cycle
LOE	Level of Energy
SOC	state of charge
RB&ES	regenerative braking and energy storage
ESP	electronic stability program
EV	Electric vehicle
HV	Hybrid Vehicle
SP-HEV	Series-parallel hybrid electric vehicle
PM	Particulate matter
NO_x	Nitrogen Oxides
MLTB	Millbrook London Transport Bus cycle
LowCVP	Low Carbon Vehicle Partnership
EMPA	Swiss Federal Laboratories for Materials Science and Technology
TfL	Transport for London
PEMS	Portable Emissions Monitoring System

Dedication

To my family

Acknowledgements

I would like to express my thanks to a number of people who helped to make this work possible. In particular I would like to thank Dr. Mike Ackerman, Dr. Vince Coveney and Dr. Matthew Studley for their help, encouragement and guidance throughout this project, I was very fortunate that they agreed to supervise this project. I am also grateful to Dr Terry Davies who was my Director of Studies in the early stages of the project and contributed to defining the research aims. In addition to the supervisory team, Dr. John Kamalu kindly assisted with advice and encouragement.

Throughout this project I have been fortunate to have the encouragement and friendship of my colleague, and fellow part-time research student, Nathan Townsend (MPhil) and I thank him for his help. Thanks are also in order for Przemyslaw Kukian who gave helpful advice and encouragement during his time as a PhD student in the department and who also assisted in collecting validation data. Additional validation data was recorded on test runs kindly driven by Rachel Szadziewska using her own car which was much appreciated.

Studying part-time whilst working full time in a busy department has involved plenty of challenges and I would like to thank UWE for supporting me, but especially Nick Tidman and Huw Dobson for giving me the opportunity to study part-time.

I owe a great deal to my Mother and Father, Kath and Graham, along with the rest of my family for their love, encouragement and support throughout my studies and life in general. They have taught me the most important things of all. Finally I would like to thank Jane whose, love, encouragement and patience has been so vital.

The following individuals and organisations have generously made technical and test data available which has been very useful for this project and for planned future work.

Finn Coyle (TfL)
Brian Robinson (LCVP)
Phil Hinde (Crossrail)
Thomas Beutler EMPA (Swiss Federal Laboratories for Materials Science and Technology)

For their assistance, and the interest they have expressed in this work, I am very grateful.

CHAPTER 1

INTRODUCTION

1.1 Background

Efforts to improve vehicle efficiency and reduce emissions by road transport have increased in recent years for several reasons including increasing awareness of finite oil resources, concerns over greenhouse gas emissions and associated climate change, and impacts on human health. At present 20% of global greenhouse gases are attributed to transport (The Royal Society, 2008) and 74% of oil is used in the manufacture of petrol and diesel for road transport (TRANSform Scotland, 2007). The 700 million vehicles currently in use worldwide is set to rise to 2.5 billion (Chan, 2002). Pressure from governments and consumers has begun to force manufacturers to investigate ways to increase fuel economy of vehicles and lower exhaust emissions, particularly through use of hybrid power train systems. These combine different propulsion and energy storage technologies in an attempt to optimise efficiency. Hybrid power trains can be divided into two broad types: series and parallel, terms which refer to the flow of energy through the system. The basic principle of these two formats is shown in sections 3.3.1 and 3.3.2. Before looking further into the details of hybrid vehicles and the technology employed, background issues relating to transport energy requirements have been considered.

1.1.2 Growth of hybrid vehicle market

Government legislation and increasing consumer demand for more energy efficient and less polluting vehicles have led to increased development of hybrid vehicles and associated technologies over the last 15 or so years. Over 25,000 new hybrid vehicles were registered in the UK in 2012 compared with fewer than 15,000 in 2009 (SMMT 2013). Over the past decade, a new category of cars has emerged known as alternatively fuelled vehicles (AFV). The group includes electric vehicles and various forms of hybrid vehicle including diesel/electric, petrol/electric and ‘plug-in’ hybrids (incorporating batteries that can be recharged from a household mains socket or special charging point). Figure 1.1 shows the rise in popularity of Hybrid and other AFVs. Growth in this sector continues and 49,528 AFVs were registered in the UK in 2014 (SMMT, 2014).

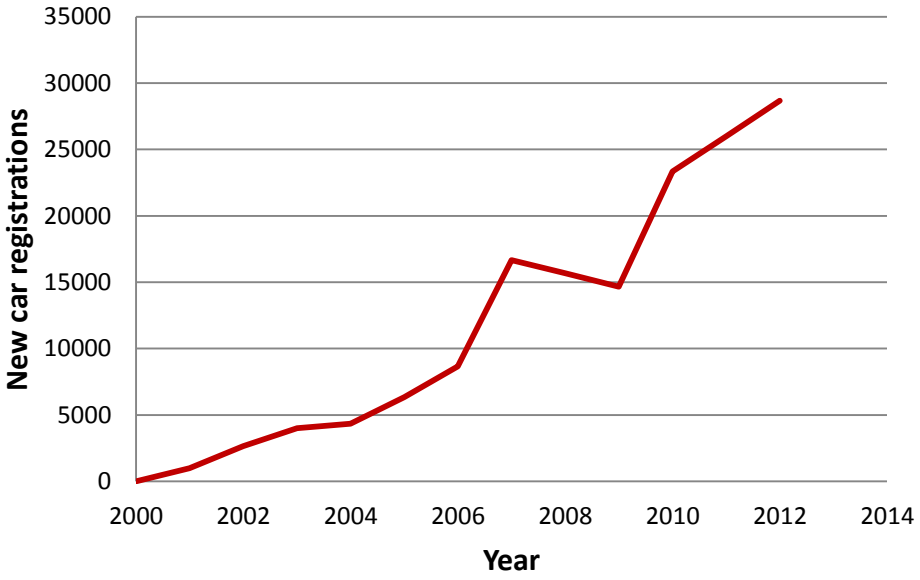

Figure 1.1: New car registrations AFVs, 2000 – 2012 (replotted from SMMT, New Car CO2 Report, 2013)

Although drivers may feel they are helping the environment using hybrids, the real situation is rather more complex and vehicles which are comparatively fuel efficient and have low exhaust emissions are, at best, doing *less* damage to the environment.

1.1.3 Global environmental issues and climate change

It is generally acknowledged that climate change was first suggested by Joseph Fourier (1768-1830) who described how the composition of the earth's atmosphere could have an effect on climatic conditions (Weart 2013). These early concepts were developed further by Svante Arrhenius (1859-1927) who first proposed the correlation between increased atmospheric CO_2 levels from the burning of fossil fuels and increased temperatures. By the late 1980's the idea of climate change being accelerated by human activity had gained wide acceptance within the scientific community and the wider public. Since that time there has been a great deal of research carried out in the field of climate modelling to predict future climatic conditions (Maslin, 2004).

It is likely that the widespread knowledge and acceptance of climate change has influenced the car buying public and helped to generate interest in vehicles that are fuel efficient and have low emissions. With hybrid vehicle sales increasing annually as shown in Figure 1.1, the affordability of these vehicles has improved with models such as the Toyota Prius (1997 – present(2016)) gaining mainstream status.

1.1.4 Local environmental issues – air quality

Air pollution in conjunction with climatic conditions, caused at least 4000 deaths single night in London during December 1952, and led to the introduction of the Clean Air Act (1956). Globally, the United Nations Environment Programme estimates that urban air pollution is linked to as many as one million premature deaths each year and a further one million pre-natal deaths (UNEP 2013).

The combustion processes of vehicle engines make a significant contribution to air pollution in the form of emissions of carbon monoxide, hydrocarbons, nitrogen oxides (NOx), and particulate matter (PM) (Heywood, 1988), some of which react in the presence of sunlight to produce ozone (O_3) (Haagen-Smit, 1952). Many studies have shown links between vehicle emissions and specific health problems, for example Kampa and Castanas (2008) linked PM, NOx, O_3 and volatile organic compounds (hydrocarbons) to respiratory and cardiac disease and reduced life expectancy; Gehring *et al* (2010) established a link between levels of traffic pollution and asthma; Yim and Barrett (2012) estimated that combustion emissions from transport cause approximately 7500 early deaths per year; and a recent review of medical studies has shown that exposure to gaseous and particulate matter pollution - including those emitted by vehicles - increased the immediate risk of stroke (Shah et al, 2015).

Governments have implemented various restrictions on vehicles in attempts to improve air quality and also to reduce congestion which reduces the concentration of emissions. For example California has stringent exhaust emission limits, and a congestion charging zone exists in central London where motorists pay a charge to enter a specified zone.

Despite increasing legislation to limit vehicle exhaust emissions increasing levels of traffic continue to present serious air quality problems. The European Commission has launched infringement proceedings against the UK Government over exceedances of EU PM air quality standards in London, and the current annual urban air pollution limits for NO_x and PM were exceeded within the first week of 2016 in areas of central London (Vaughan, 2016).

Increasing global development continues to fuel a rapid rise in private car ownership. In China, for example, the numbers of cars is predicted to rise from approximately 800

million in 2002 to more than two billion in 2030 (Dargay *et al*, 2007). The resultant lowering of air quality from vehicle emissions is of particular concern.

1.2. The Cost of Energy and the Spectre of Peak Oil

The term 'peak oil' was first used in 1956 by M. King Hubbert a geologist working for the Shell Oil Company. He calculated the future rate of oil extraction and calculated that world-wide oil production would hit a maximum level, as crude oil takes millions of years to form and, therefore it is a non-renewable energy source on human timescales. Figure 1.2 shows the skewed bell shaped curve that he determined.

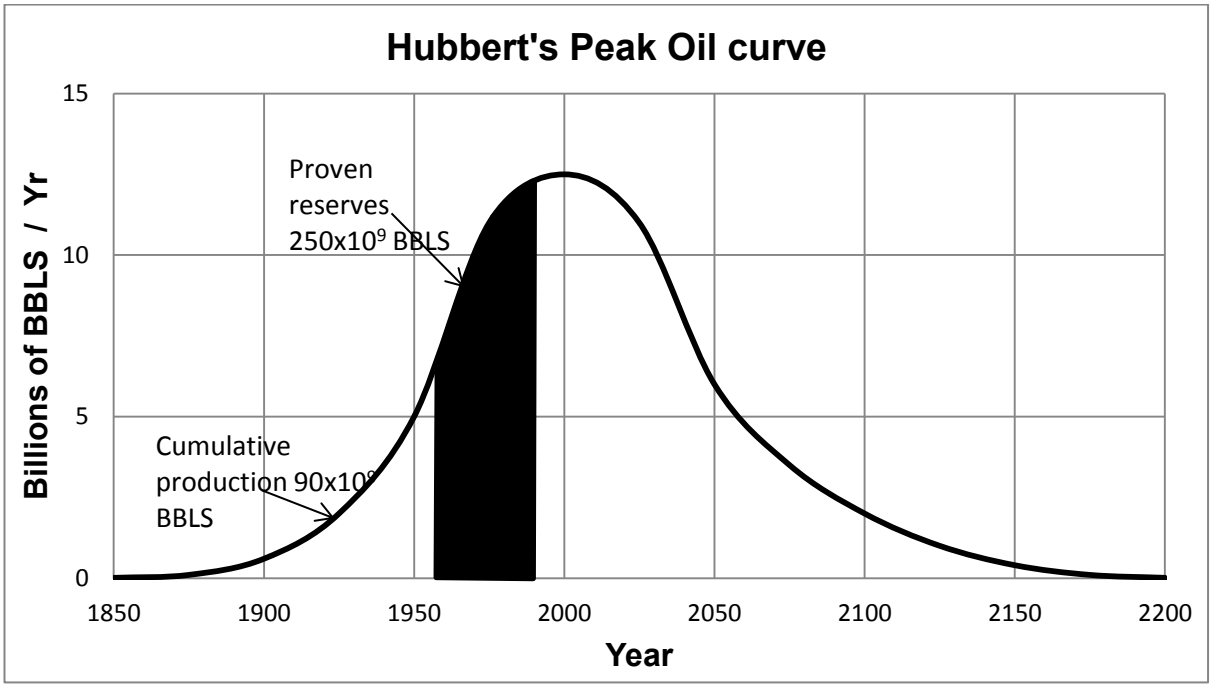

Figure 1.2: Hubbert's peak oil curve (replotted from Hubbert, 1956). BBLS = Barrels of oil, 1 Barrel of oil is usually defined as having a capacity of 42 U.S. gallons

Although there is a degree of uncertainty over exactly when peak oil has occurred or will occur, more recent forecasts including further oil discoveries and improved extraction technologies, are strikingly similar to Hubbert's predictions. Energy demands are increasing as the global population rises and living standards improve in developing countries. Along with this is an expectation of car ownership and the associated demand for petrol and diesel (derived from crude oil). In China, for example, the number of civilian vehicles registered has risen from 1.78 million in 1980 to around 78 million in 2010 (NBSC 2012). This represents an approximately 44 fold increase in 30 years.

Improvements in fuel efficiency are increasingly necessary to offset air pollution from greater numbers of road vehicles. In recent years although improvements have been made in fuel economy, these improvements have been relatively modest compared to the marked gains in horsepower, see Figure 1.3 below. 0-60 mph times have steadily fallen, which suggests that improvements in engine efficiency have been partly negated by increases in engine power. A similar trend is apparent in the European market although fuel economy Figures are generally higher for European cars.

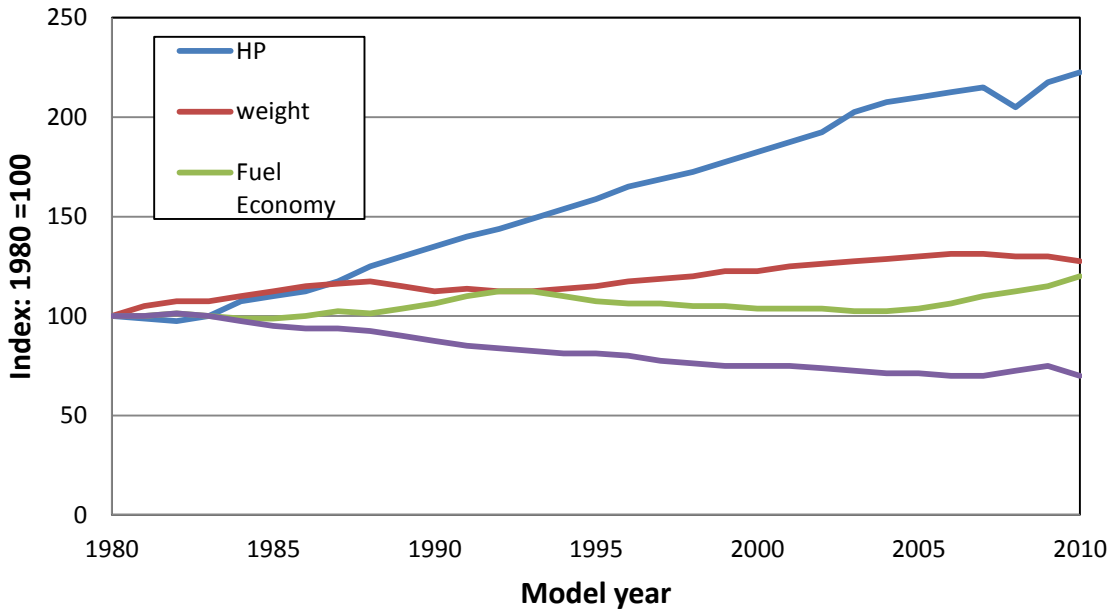

Figure 1.3: Changes in weight, horsepower and fuel economy for light vehicles from 1980 – 2010 (replotted from US Energy Information Administration, 2011)

1.3 Political Factors, Economic Issues and Financial Incentives

1.3.1 Energy costs - supply and demand

Despite the rising popularity of electric vehicles the majority of vehicles on the road still rely on petrol or diesel and as overall vehicle numbers rise, the demand for fuel continues to increase. The price of crude oil is largely influenced by demand, however it is also affected by a number of rather complex geopolitical and socio political factors including oil fields becoming exhausted, new sources being discovered, conflicts and changes in political systems and relations between regions. Natural disasters such as tropical storms, floods and tsunamis as well as man-made disasters such as oil spills and platform fires can also affect oil price. Figure 1.4 shows how fuel prices have varied between 1947 and 2010. The effects of events such as revolutions, wars and recessions can be clearly seen.

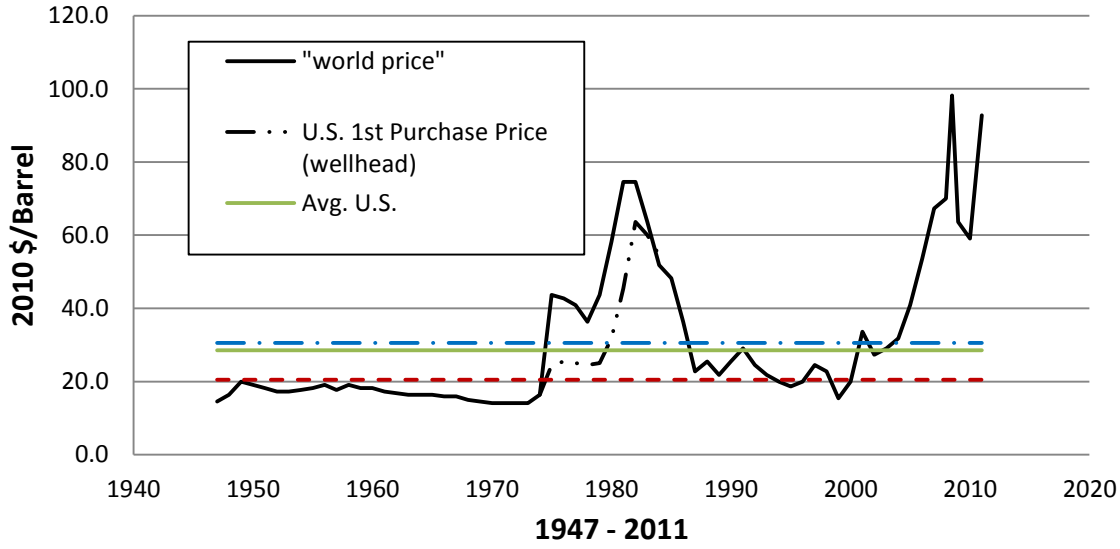

Figure 1.4: Crude Oil Prices 1947 – 2010 (replotted from WTRG, 2016)

Fuel prices influence the price of other products partly because many businesses depend on transporting goods large distances by land, sea and air. Within the scope of this research road transport energy requirements are of particular interest. OPEC (Organisation of Petroleum Exporting Countries) play a key role in setting oil prices and the complex details behind how prices are adjusted are beyond the scope of this work. However, increases in fuel efficiency resulting in lower running costs will be attractive to consumers. In addition to the environmental concerns that many motorists have, this is a further incentive for consumers to consider AFVs (alternative fuelled vehicles) including hybrid vehicles that claim, to varying extents, attractive fuel economy along with good performance. The depletion of fossil fuel sources has contributed to increased oil and gas prices and associated increased domestic fuel and transport costs. These financial costs may be most noticeable in the developed world where far more energy is used per head of population than in less developed nations. However, the physical environmental damage is often wrought in the less developed regions where fossil fuels are extracted. The human cost associated with this environmental damage is difficult to quantify.

1.3.2 Reduced taxation class for low carbon emission vehicles

Many government taxation policies offer incentives to use low emissions vehicles providing additional financial benefits to users of hybrids. Within the UK, for example, rates of vehicle tax are charged according to manufacturer-registered vehicle emissions of carbon dioxide (CO_2). In 2015 new cars that emit less than100g CO_2/km are exempt from vehicle tax. Above this emission Figure there is a sliding scale up to a maximum charge of £505 for vehicles emitting 255 g CO_2/km and above (UK Government, 2015). The fees are slightly reduced in the case of alternatively fuelled vehicles (AFVs) e.g. £495 maximum charge. This offers a substantial reduction in the fixed annual running costs for both private and fleet users in addition to the possible savings from reduced fuel consumption.

1.3.3 Company car tax saving when using hybrid vehicles

Employees are taxed on the benefit of having a company car, however this tax rises with increased CO_2 emissions varying from 0% (of the vehicle's value) annually for a vehicle with 0g CO_2/km at point of use (i.e. electric vehicles), up to 37% for a vehicle with 230g CO_2/km or more (Next greencar.com 2015), thus providing an incentive for businesses to provide electric cars for their employees.

1.3.4 Hybrid vehicles in London congestion zone

Vehicles with CO_2 emissions below 100g/km were originally exempt from the London congestion charge. The low emissions for hybrids widely reported by manufacturers' has encouraged businesses and private motorists within the Congestion Zone to purchase low emission vehicles including many hybrids such as the Toyota Prius. The extensions to the scheme made in 2013 reducing the exemption limit from 100 g CO_2/km to 75 g CO_2/km (Lydall, 2013) caused controversy amongst owners of low emissions vehicles as many lost exemption status.

1.3.5 Background Summary

As shown from the overview in sections 1.1-1.3, two principal challenges exist for future road (and other) vehicles.

(i) Fuel supplies: Dwindling finite supplies of fossil fuels – i.e. oil.
(ii) Emissions: On a local to global scale (direct human health impacts and climate change respectively).

Hybrid vehicles and associated technologies present opportunities to address the growing need for improvements in vehicle fuel economy and reduced emissions. Existing road transport examples include a range of cars and some public transport applications. An area requiring further investigation is how possible energy savings vary across a range of transport and journey types.

1.4 A Brief History of Hybrid Vehicles

Over the last 15 years hybrid vehicles (HVs) have been gaining acceptance and popularity. Although they are often considered new technology, it is widely acknowledged that one of the first examples – a series hybrid- was designed and built in 1899 by Dr Ferdinand Porsche (Bergsson, 2005), shown in Figure 1.5. By 1915 parallel hybrids were being produced in small numbers (Modak & Sane, 2006).

Figure 1.5: The Lohner-Porsche series hybrid (Hybrid Vehicle History website).
(Image redacted for copyright reasons)

1.5 Recent Developments in Hybrid Vehicles

1.5.1 Widely adopted technology

Although early examples were relatively basic, modern hybrid vehicles are highly sophisticated, utilising a combined series - parallel approach incorporating power split transmissions and computer control of the energy balance between the ICE and energy storage, such as that used in the Toyota Prius, shown in Figure 1.6 below. An explanation of the key features of series, parallel and series – parallel powertrains is given in sections 3.3.1 and 3.3.2. Features such as regenerative braking are now incorporated whereby the electrical machines used for traction can work as generators to provide braking force and generate electricity which can be stored for use later as required.

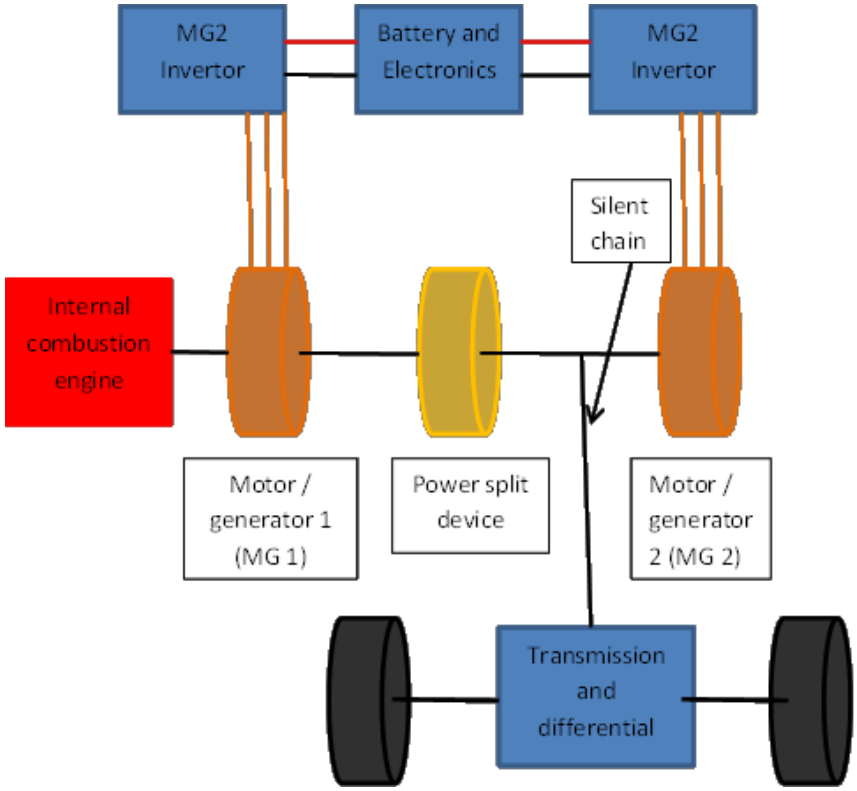

Figure 1.6: Block diagram of the Toyota Prius Parallel Hybrid Power train System (redrawn from Roper, 2014)

In Figure 1.6 the MG1 is a relatively small motor generator which performs the task of starter motor and alternator. This direct coupled unit makes frequent starting practical and enables a reliable start-stop feature to be incorporated. Current applications for hybrid systems such as cars and four wheel drive vehicles use technology, that according to manufacturers' data, exhibit significantly increased fuel economy.

At present, fuel efficiency figures quoted for hybrid vehicles and conventional European vehicles are based on the New European Driving Cycle (NEDC). This cycle includes components representing urban, extra urban and combined driving conditions. All new vehicles are subject to this standard test, although manufacturers often use rolling road tests (factored to take account of resistive forces) to ensure control over all test parameters. Whilst a useful standard for comparison purposes, independent tests and anecdotal evidence from car drivers, suggest that the manufacturer's quoted mpg figures are rarely attained in practice. An independent test conducted by the US Department of Energy showed a 2010 Toyota Generation III Prius hybrid achieved a combined fuel consumption figure of 44.3mpg (US Dept. of Energy, 2011). Equivalent UK findings of 47 mpg appear to be typical for the 2009 model (RAC, 2009). The figure quoted by Toyota is 65.69 mpg (Toyota, 2010), approximately 39% higher than the US findings.

The variations between quoted and actual fuel efficiency figures can be influenced by several factors such as driver behaviour and methods used in official testing of vehicles (discussed further in 3.12). An in depth investigation of the different factors is outside the scope of this research, however work carried out by Hari *et al* (2012) showed fuel savings of 7.6% - 12% from driver behaviour alone.

1.5.2 Public transport applications

The application of HV technology is not limited to personal transport. Increasingly, public transport vehicles such as buses are emerging with hybrid power trains.

In 2006 Transport for London (TfL) introduced hybrid buses and by May 2012, 225 diesel-electric hybrid buses were in operation. These buses incorporate regenerative braking and use batteries for on-board energy storage. The environmental benefits claimed include a 30% reduction in fuel use, a minimum 30% reduction in CO_2, reduced oxides of nitrogen and carbon monoxide along with lower noise levels (TfL, 2012). Lothian Buses (Scotland) currently run 15 hybrid buses and claim a 30% reduction in fuel consumption and reduced emissions (Lothian Buses, 2012).

Parry People Movers Ltd (PPM), are a UK based company constructing hybrid light rail and tram vehicles that combine a small ICE with a large flywheel for energy storage to smooth variations in power demand. Figures 1.7a and 1.7b show how the system is said to aid performance.

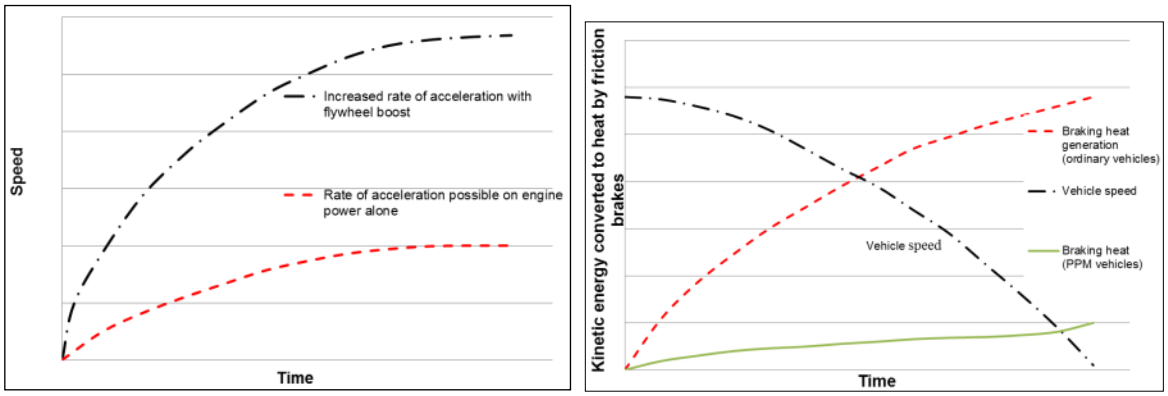

Figure 1.7a (left): How PPM flywheel Aids performance. Figure 1.7b (right): How thermal energy, normally dissipated during mechanical braking, is conserved and stored using flywheel. No units given as quantitative data not available, Figures reproduced from PPM literature demonstrating general performance trends of system. (Parry People Movers, 2009).

1.5.3 Motorsport applications

In 2009 regenerative braking was incorporated into Formula one racing. Cars are fitted with motor generator units and energy storage. Early versions of systems used were claimed to provide maximum performance of an additional 60kW of power for 6.7 seconds per lap. For recent developments it is claimed that the system can contribute an extra 120kW for up to 33 seconds per lap (Formula 1.com, 2014). As with other motorsports technologies, investment in hybrid systems is likely to have long term benefits for the wider transport field.

1.5.4 The application of hybrid technology

Much existing research in the field deals with specific aspects of hybrid vehicle technology. As suggested earlier, less attention has been given to the question of where and how it can be used to best effect in terms of energy savings across a wide range of vehicle and journey types.

The effectiveness, in terms of energy savings of hybrid vehicles, using regenerative braking and energy storage for a range of vehicle and journey types, is the central theme of this work.

CHAPTER 2

AIMS AND OBJECTIVES

2.1 Aim

The aim of this research is to critically evaluate the overall energy saving effectiveness of regenerative braking and on-board energy storage in hybrid vehicles under a variety of transport scenarios. The scope of vehicle classes investigated ranges from small lightweight vehicles through to large vehicles such as buses and coaches. In the course of this work alternative approaches to energy saving are also considered. The emphasis of the study is to investigate how the energy requirement might be reduced through the use of regenerative braking and energy storage in hybrid power trains, across a broad range of scenarios and to establish where the greatest benefits might be sought. These can then be explored in greater depth to assess potential reductions in exhaust emissions.

2.2 Objectives

(i) Carry out a thorough literature review to evaluate existing work in this field to study existing applications of regenerative braking and energy storage in hybrid vehicles and establish how this work contributes to the field.

(ii) Develop and/or study a simulation tool or tools to predict energy savings across a range of vehicles and journey types.

(iii) Validate and/or compare the simulation tools using data from experimental trials and where necessary refine the simulation tools to give an acceptable level of realism while optimising the simplicity and flexibility of the tool.

(iv) Apply the simulation to investigate energy usage across a wide range of vehicle and journey types with and without regenerative braking and on-board energy storage to compare potential benefits.

(v) Use the results from vehicle energy study to identify across which vehicle classes and journey types the greatest reduction in energy requirement might be achieved.

(vi) Having identified where regenerative braking and energy storage might be most usefully employed, study in greater depth the energy efficiency improvements and reduction in emissions that might be made within these transport scenarios - including consideration of alternative approaches for energy saving.

(vii) Draw conclusions from the work conducted and identify areas for further study.

CHAPTER 3

LITERATURE REVIEW

Before developing the simulation tool and generating results, relevant literature regarding approaches to modelling vehicle performance, vehicle energy efficiency, hybrid vehicles, regenerative braking, energy storage systems and associated technologies was studied. This enabled the author to evaluate research that has been carried out by others and study existing systems, technology and findings.

3.1 Approaches to Vehicle Modelling

Methods considered in this chapter are based on numerical modelling techniques.

3.1.1 Forward vs backward looking modelling of vehicles

(i) Forward looking simulation

In forward looking simulations driver response to a demand condition is modelled. At any given moment the output (road speed) is compared with the demand and the driver model sets the throttle position or braking effort accordingly. The throttle position output from the driver model is used in the engine model to determine engine torque. The torque data is then used in the transmission part of the vehicle model where transmission ratio and efficiency are taken into account such that output torque at the driving wheels and corresponding tractive force, and therefore acceleration, can be found. In the case of braking conditions, the driver model controls braking torque acting through the driving wheels and the resultant negative acceleration is found. Once the vehicle acceleration has been determined over a given time period the speed in the next time step can be found and the calculations can be repeated.

(ii) Backward looking simulation

The backward looking model is, in general, a simpler approach as no driver model is required since it is assumed that the speed vs time journey profile is met. The force required to meet the demand speed is calculated backwards throughout the vehicle drivetrain to determine the energy required to meet the journey profile specified. In general, the simpler nature of the backward looking simulation results in quicker processing time. Initial simulation work was simply based on tractive effort against road

speed to simulate vehicle acceleration. Many of the advantages of the backward looking approach are demonstrated in the work of Baglione (2007). A performance comparison of forward and backward looking modelling in the context of subway trains is detailed in Horrein *et al* (2012). This study concludes that because the forward looking approach requires some form of control (driver model) any scenario can be modelled without the necessity of a drive cycle data. Importantly their findings show that for the drive cycle studied the difference in total energy required between the 2 models was 2.5%.

Mierlo and Maggetto (2004) detail the development of an iteration algorithm for use in vehicle simulation and point out that many backward simulations do not include iteration. Explanation is provided for the limitations in simulation accuracy if closed-loop iteration is not used.

3.1.2 Integration methods

For both the forward and backward looking modelling approaches described in 3.1.1 a range of integration methods can be applied. A comparison of the performance of different types of numerical integration is given in Houcque (2006) – including forward Euler, backward Euler and Runge-Kutta . Many types of integration are provided as standard in software such as Matlab. For many integration methods such as the forward Euler, there is always some step size above which the behaviour is not stable (the solution becomes impossibly inaccurate and generally grows without limit because of the errors). The forward Euler method cannot be used above the step size stability limit and becomes extremely inaccurate at step sizes approaching it. The step size stability limit can be very low for the forward Euler method when used in "difficult" problems such as strongly non-linear problems. Whereas the forward Euler method is *explicit,* the backward Euler is *implicit* (iteration is likely to be needed at any given time step). Whereas the forward Euler method is very susceptible to instability, the backward Euler method is extremely stable. Error estimation and step-size stability limit are important subjects in their own right. Borse (1997, p 410) points out that for the forward Euler method the percentage error in integration is proportional to the step size, provided that rounding errors can be ignored. So integration errors can be monitored by step-size reduction.

In section 4.2 & 4.3 the development of a forward looking simulation is described. In section 4.7 a backward looking version is introduced for comparison studies of a range of

vehicles and journey types. The results in sections 5.2 onwards were generated with the backward looking simulation whilst the work in section 5.7.2 studying the effect of driver behaviour required the use of the forward looking simulation.

3.2 Modelling of Vehicles with Conventional Powertrains

In modelling conventional vehicles with an ICE either the forward or backward looking approach mentioned in 3.1.1 can be used. Some popular Matlab / Simulink models such as ADVISOR combine a Forward and backward looking approach.

3.2.1 Engine modelling

Principles of the petrol/gasoline and the diesel ICE including their idealisations in the air-standard Otto cycle and the air standard Diesel cycle are described by Heywood (1988) and Zemansky (1968). In a forward looking vehicle model, engine torque vs speed characteristics are required to enable accurate simulation of vehicle performance, fuel consumption and emissions. In backward looking models the drive cycle leads the model and according to vehicle parameters the required engine power is calculated. In this case knowledge of the torque vs speed data is not required. However, unless an emissions model is included such as the power based examples described by Wang and Fu (2010) and Leung (2000), or a statistical type as developed by Cappiello *et al* (2002), engine emissions and fuel consumption look-up maps are required – see 3.2.3.

3.2.2 Modelling transmission and clutch/ torque convertors

In forward looking modelling, available torque at the vehicle drive wheels can be calculated based on engine torque and appropriate gear ratios in the gearbox (manual or automatic) and final drive. In the case of the NEDC (New European Driving Cycle) the gear shift regime is specified as part of the test cycle. Other drive cycles, such as the MLTB developed jointly by Millbrook and Transport for LowCVP (2014), do not specify a gear shifting regime since, for buses with automatic transmissions, gear shifting will occur depending on load and engine speed conditions.

(i) Manual Transmissions

For manual transmissions, the realistic modelling of clutch behaviour may be desired if a high level of model detail is required. Serrarens *et al* (2004) consider the Karnopp model control optimization and propose a modified version with improved drive comfort. The

Karnopp approach has the advantage of using one system description for both the slipping and gripping modes of clutch operation. Bautaus *et al* (2011) investigate the hyperbolic tangent, classic and Karnopp dry clutch models and the Stribeck effect. They conclude that all the models considered perform with acceptable accuracy providing they are well tuned, but with varying degrees of efficiency.

(ii) Automatic Transmissions

An automatic transmission with dual clutches and planetary gears is modelled in detail and control optimized by Samanuhut (2011), whilst Baglione (2007) describes the simulation of automatic torque converter transmission. Lijun (2010) describes the use of PID (proportional, integral, differential) control to model and optimise automatic transmission clutch slipping. The modelling of transmissions is itself a complex subject and when looking at more generalised study a simplified approach may be appropriate.

As with conventional drivetrains, optimisation of powertrain transmission ratios is required to maximise hybrid vehicle efficiency. In conventional vehicles, CVT (continuously variable transmission) has not been widely used until recent years when such transmissions have increased in popularity with manufacturers including Honda, Nissan, Subaru and Audi all utilising CVT transmission on some vehicles in their range. The benefits of infinite variability in gear ratio between the upper and lower limits means that engine speed and load conditions can be controlled such that the engine efficiency is optimised for a given scenario. Such systems have been demonstrated by Pour and Golabi (2014) showing a predicted reduction in fuel consumption of up to 17.12% for the 0-16 km/h segment of the NEDC and 1.52% for the 50 -70 km/h segment. In addition to fuel savings, the planetary CVT gearbox was also found to improve the vehicle acceleration performance. In the context of CVT control in Parallel HEVs, Feng *et al* (2007) have demonstrated the use of a novel regenerative braking control algorithm for a system incorporating a CVT that can yield increased energy recovery during the braking process compared to a conventional algorithm. The fundamental aspects and performance of all commonly used varieties of vehicle transmissions are considered in detail by Naunheimer *et al* (2011).

3.2.3 Calculating fuel consumption and engine exhaust emissions

Vehicle engine emissions can be modelled by several methods:

(a) A detailed ICE combustion simulation can be employed such as the example described by Buttsworth (2002) who demonstrated the reliability of revised Matlab engine simulation routines compared to existing simulations. The work of Ben-Chaim *et al* (2013) describing the development of an analytical model offers an alternative approach avoiding a full engine model by generating a theoretical two dimensional BSFC map based on a pair of single dimension polynomial equations. Correlation between theoretical and experimental fuel consumption was found to be in the 2% to 7% range)

(b) Lookup tables or maps can be used where emissions in grams / second (g/s) are collated in table form indexed by engine speed (ω) and torque (T) as used in many vehicle simulations including ADVISOR. This table can be produced either from experimental data or based on data generated from an external detailed combustion model. If the simulated vehicle engine speed (ω) and load conditions (T) are known at a point in time it is possible, providing suitable data is available for a particular exhaust gas, to use a look–up table to find the engine emissions during each time step.

Other approaches to modelling emissions include statistical models such as those described by Afotey *et al* (2013) (specifically dealing with CO_2) and Cappiello *et al* (2002) where CO_2, CO, HC and NO_x emissions are predicted with a useful level of accuracy along with fuel consumption. Particular difficulty was encountered in simulating catalyst performance which is heavily dependent on temperature. For this reason only hot-stabilised conditions were considered in the EMIT (EMIssions from Traffic) simulation described by Cappiello *et al* (2002). A power based model can also be used to predict emissions as described in Leung *et al* (2000) with good general correlation to experimental data. The variation in exhaust emissions between nominally identical vehicle types is highlighted by Leung *et al* (2000). Repeated dynamometer trials carried out on behalf of TfL (Coyle, 2016) using a 67 seat double decker bus with a 6.7 Litre engine also shows a spread in results with a (standard deviation / mean) figure of between 0.04 and 0.3 across a range of emissions (for HC, CO, NO_x and PM). Wang and Fu (2010) also show the significant variation in experimental data especially at low and high engine power and state that model accuracy gradually improved as a larger number of PEMS (Portable Emissions Monitoring System) samples were available to refine data used in the model. Ongoing improvements in vehicle engine management may result in less variation in results of new cars, however

maintenance, wear and other factors will still result in variable emissions. A range of commercial simulation tools for detailed engine modelling are available such as WAVE developed by Ricardo which can be used to explore many engine characteristics including emissions of NO_x, CO and HC (Ricardo, 2015).

3.3 Modelling of Electric and Hybrid Electric Vehicles

3.3.1 Modelling of electric vehicles (EV)

The physical modelling of EVs can be carried out using principles common to those used for conventional vehicles since in terms of the whole vehicle the same fundamental physical forces are present (i.e. inertial, aerodynamic, friction and gradient forces). For purely electric vehicles the fundamentals are clearly summarised in Schaltz (2007), including different approaches to modelling batteries and outlining principles involved in simulating EVs in Matlab /Simulink. Efficiency maps for electric motors are also introduced. General principles are described in detail in many sources. The powertrain is less complex than in the case of conventional and hybrid vehicles as there is usually direct drive and a clutch, and multi ratio transmission is not required. The development of a detailed EV simulation for a 4 wheel drive vehicle is described by Pusca *et al* (2002). In addition to 4WD features, Anti-locking Braking System (ABS), Anti Slip Regulation (ASR) and Electronic Stability Program (ESP) are incorporated. A move to fuzzy logic for speed estimation is proposed to improve the quality of simulation results. Both EV and Hybrid Electric Vehicle (HEV) models require traction electric motors which are currently more widely used in trains, where electrified lines/rails supply power, or diesel ICEs are used to generate electrical power. A principal weakness of electric cars is the relatively low energy density of batteries compared to gasoline or diesel fuel, <200W-h/ kg or <720kJ/kg as opposed to ~45MJ/kg (Doucette & McCulloch, 2011; Thomas, 2009). Electric motors can have a power density of approximately 2kW/kg. The BMW “e Drive” motor was developed to have a high power density whilst minimising the use of rare earth magnets, and achieves a power density of 2.5kW/kg compared to 1.38kW/kg stated for the 2011 Nissan Leaf (Green Car Congress, 2015) . These power densities are rather higher than for commonly available internal combustion engines for passenger cars, which range from 0.25 to 0.5 (Heywood, 1988). In principle, the size and weight of electric motors could be reduced dramatically by superconducting technology - using well established superconductors such as niobium titanium (NbTi) or niobium tin (Nb_3Sn) or using newer,

higher – but still cryogenic – temperature superconductors such as Magnesium Diboride (MgB_2) or emergent higher temperature superconductors (Superconductor Week, 2015). Many permutations in the design and arrangement of components in the powertrain and energy storage system are possible and here a selection of principle types is considered. A comprehensive review of current configurations and powertrain control techniques is presented by Bayindir *et al* (2011). In 3.3.2 to 3.3.4 principle varieties of hybrid powertrain configurations are considered.

3.3.2 Series hybrid

An example of a simple series hybrid would be a conventional internal combustion engine (ICE) running under near optimum conditions for efficiency and power output coupled to an electrical machine (generator) that converts the kinetic energy output from the ICE into electrical energy. This generator output is used to charge batteries or other electrical storage devices . Stored energy can then power electric motors to provide the tractive effort for the vehicle. Since the prime mover and final transmission are physically uncoupled, no conventional gearbox is required. This series example involves the conversion of energy in three steps. Firstly from chemical to mechanical in the ICE, then from mechanical to electrical in the generator and finally back from electrical to mechanical at the tractive motor. When energy is converted from one form to another there are inevitable losses in the various sub-systems. In general the efficiency losses in double energy conversion of this type are greater than for a conventional mechanical transmission between the engine and drive wheels (Reif, Dietsche *et al*, 2011). Despite these losses a series hybrid system offers potential advantages over a conventional powertrain. There is the possibility of running the ICE (or other prime mover) at, or close to, its optimum conditions whilst allowing some energy storage device (often an electrical battery) to act as a buffer to respond to variations in demand. The electric traction motor can also be configured to work as a generator under braking conditions recapturing some of the energy usually dissipated as heat and noise through friction associated with conventional braking. This can potentially increase the overall system efficiency and is claimed to do so in many instances. An example series hybrid configuration is shown in Figure 3.1.

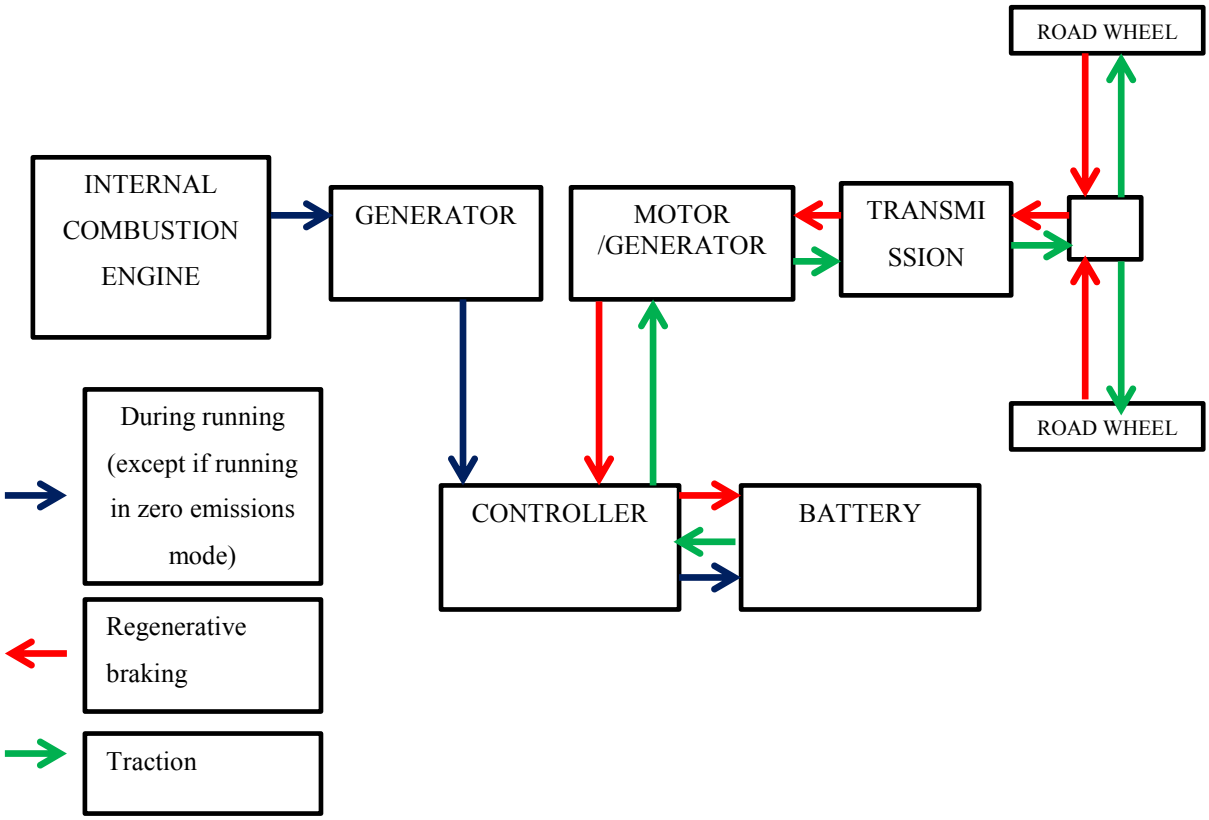

Figure 3.1: Example of a series hybrid powertrain showing energy flow during traction and braking, (re-drawn from Bosch, 2011).

3.3.3 Parallel hybrid configuration

In a parallel system the ICE and tractive motor can run together to provide tractive effort, or independently depending on the conditions and requirements. They can be combined via a gearbox, in which case the tractive motor/s are usually incorporated into the drivetrain alongside the engine or built into the engine itself. An alternative arrangement is to have the electric motors driving the wheels of one axle whilst the ICE drivetrain powers the wheels on the other axle. In some cases 'in-wheel' electric motors are utilised and combined with conventional drive shafts from the ICE gearbox. The need for running one or other branch of the system independently may arise for a number of reasons. For example if long distance, high speed driving is called for, the battery capacity would limit the effective range of the vehicle, in which case the ICE would be mostly, if not exclusively, used. If a busy city traffic scenario is encountered, the electric motor may predominately be employed to give zero emissions operation at point of use. In many

driving scenarios a combination of the two drives will be used and will be continually varying with changing conditions. When rapid acceleration is called for the two parts of the system can be configured to run together. This feature allows hybrid vehicles of a given size to be designed with comparatively small capacity engines and still be capable of brisk acceleration compared to non-hybrid vehicles of the same engine capacity or equivalent power output. In commercially available parallel hybrid vehicles, the balance between the ICE and electrical drive within the system is computer controlled and takes account of battery condition, accelerator / brake inputs along with many other subtle variables. The control of energy flow and balance in hybrid vehicles is a substantial topic in its own right and has been investigated in some depth in recent years. In particular, Feng *et al* (2007) describe the development of a regenerative braking algorithm for a Parallel system with CVT. Also Mukhitdinov *et al* (2006) studied the optimization of control strategies for a CVT of a hybrid vehicle during regenerative braking, and proposed four different approaches to optimising battery charging. They conclude that in order to maximise battery state of charge (SOC) it is necessary to control the transmission ratio of the CVT taking into account the performance characteristics and specification of the electric motor / generator unit. A schematic of a typical parallel hybrid system is shown in Figure 3.2.

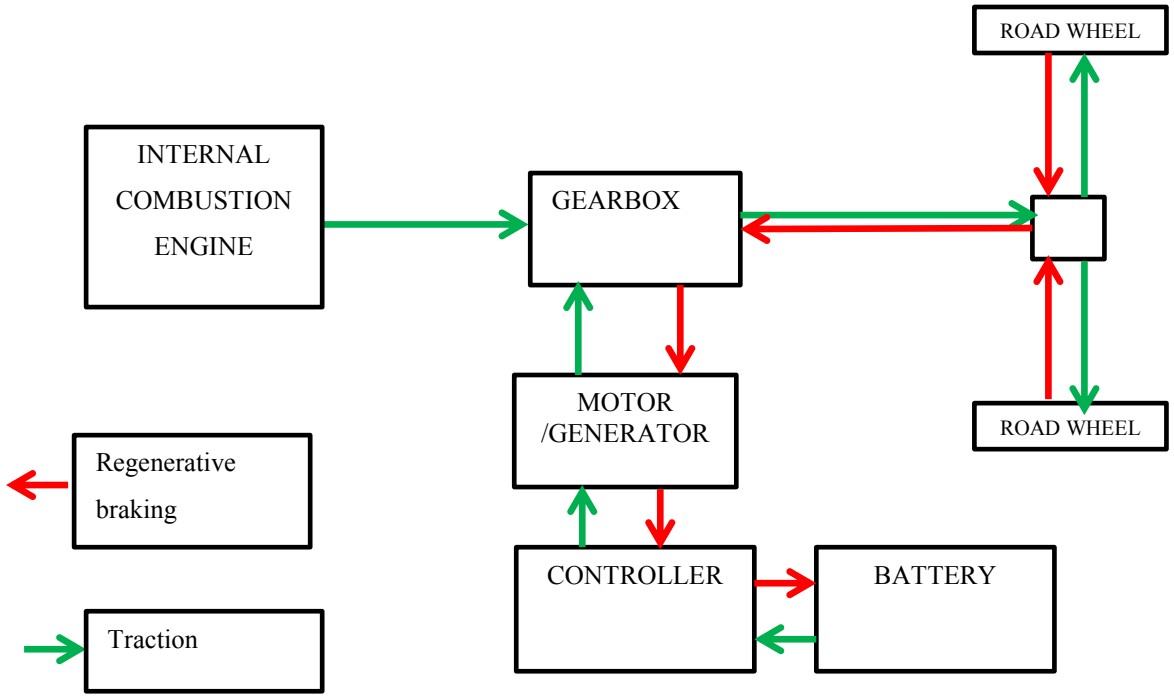

Figure 3.2: Example of parallel hybrid powertrain showing energy flow during traction and braking (Re-drawn from Bosch, 2011).

Tesla, who manufacture electric sports cars, incorporate regenerative braking into their designs and claim a 'wheel-to-battery' and 'battery-to-wheel' efficiency of 80% this implies an overall wheel to wheel efficiency for the regenerative braking and energy storage system of 64% (0.8 *0.8 =0.64) Tesla (2014). Although this is a purely electric system rather than a HEV, this efficiency figure is a useful benchmark. The hybrid vehicle simulation developed in Chapter 4 is configured as a basic parallel system as represented in Figure 3.2 above.

3.3.4 Series-parallel hybrid configuration

In series-parallel hybrids the drivetrain can run in either the series or parallel mode (described earlier in this section) depending on driving conditions and local restrictions. This is made possible by the inclusion of a clutch between the two electrical machines. When the clutch engages, the system runs as a parallel hybrid which is typically most useful at relatively high speeds.

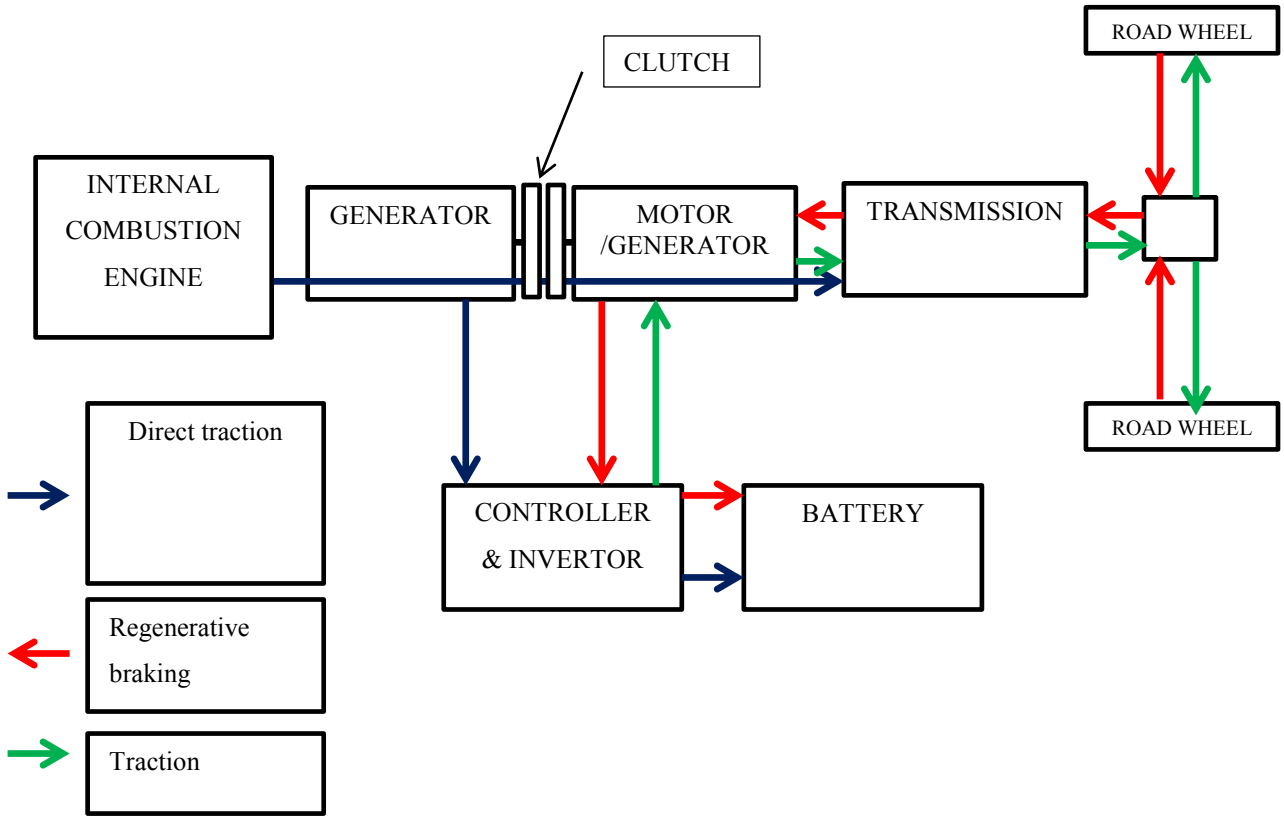

Figure 3.3: Energy flow in a series-parallel (SP-HEV) or power-split hybrid (Re-drawn from Bosch, 2011)

3.3.5 Regenerative braking

An efficient regenerative braking system is essential if effective use is to be made of any energy storage system integrated into a vehicle powertrain. A variety of methods can be employed however the options are influenced by the choice of energy storage system.

Many commercially available hybrid vehicles including the Toyota Prius, use lithium ion battery packs for energy storage, and electric machines (motor / generators) to provide tractive effort and electrical braking. The recently announced *Hybrid Air* concept from the PSA Peugeot Citroen group uses a compressed air energy storage system combined with hydraulic motor/pump units to provide tractive effort and regenerative braking respectively Brugier-Corbiere, C & deServigny, L. (2013).

Before hybrid vehicles were widely available – that is prior to the introduction of the Toyota Prius in 1997 and the Honda Insight 1999, regenerative braking had been adopted in a range of other vehicles. Examples from across the spectrum of vehicle size include the light-weight 2 seat human power / electric hybrid the Twike 1, launched in 1986 (electricbike.com 2014) through to the trains operating on the London underground. Alstom (2013) have developed a system known as Harmonic Energy Saving Optimiser (HESOP) and are conducting trials on the London Underground Victoria Line. Alstom claim that the HESOP system makes it possible to recover 99% of the traction energy converted during braking. Precise definitions are not given and at the time of writing no confirmed performance data was available for review. A large driver for regenerative braking on the London underground is to reduce air heating effects caused by the heat dissipated from friction brakes; the energy savings are a welcome secondary benefit. It is claimed that regenerative braking using a 3rd rail on existing DC train network could result in an efficiency increase of up to 20% (Railway People 2008) although no data has been published. Feng *et al* (2007) detail a study using a Matlab / Simulink simulation to develop an optimised regenerative braking algorithm for parallel hybrid electric vehicles with CVT. Results indicate improved performance compared to conventional regenerative systems.

Before investigating the energy saving potential of regenerative braking and energy storage across a range of vehicle types and journeys, relevant existing work has been studied. Simulation work carried out by Baglione (2007) indicates how fuel energy is converted throughout vehicle systems, see Figures 3.4 and 3.5 below.

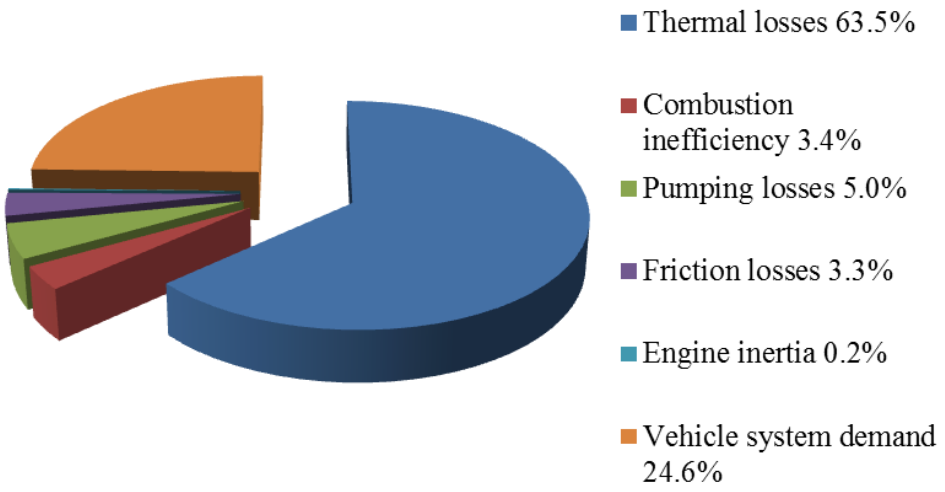

Figure 3.4: Analysis of energy transfer on the American FTP (Federal Test Procedure) urban drive cycle. Re-plotted from Baglione (2007).

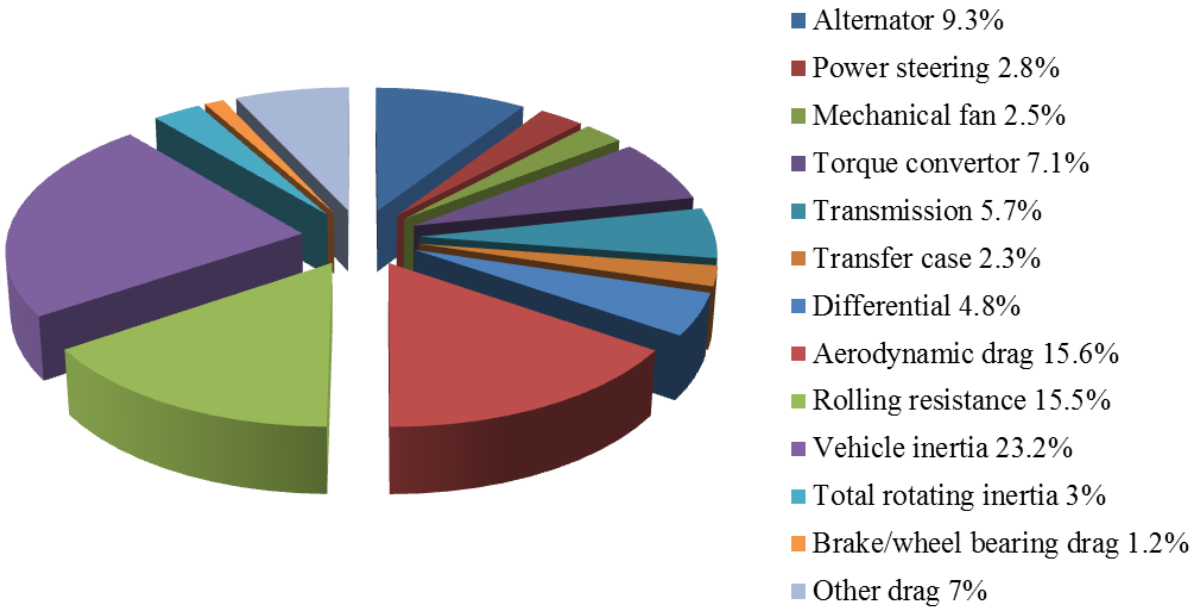

Figure 3.5: Analysis of energy transfer on the American FTP urban drive cycle (shown in Figure 3.6) for a 2,700kg truck with a V8 petrol engine. Re-plotted from Baglione (2007).

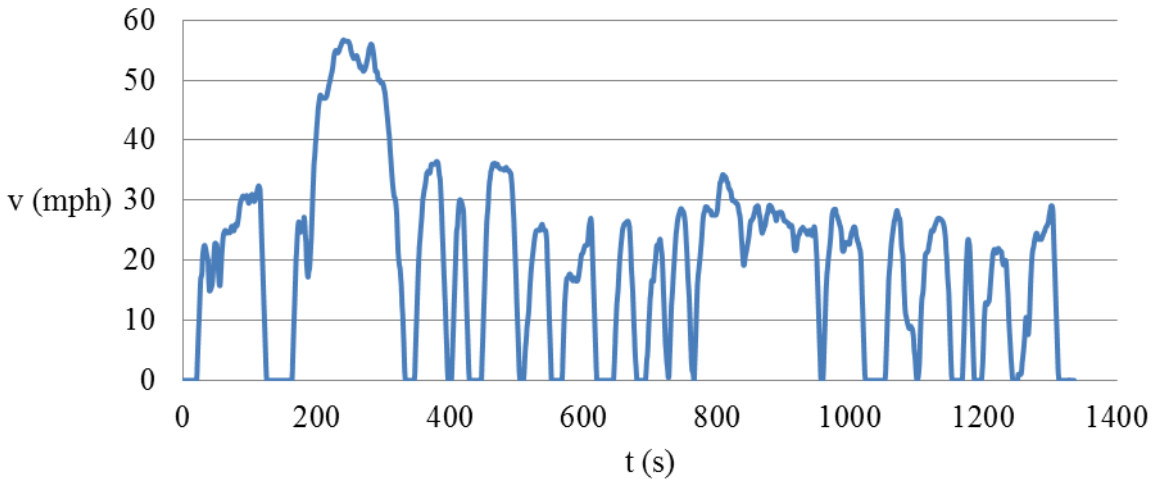

Figure 3.6 The American FTP urban drive cycle (Plotted using data from EPA (2013).

Although Figures 3.4 and 3.5 relate to results obtained from tests of a 2,700kg American truck with a V8 petrol engine - with different technical specifications to European road vehicles, they highlight relevant general issues. The proportion of fuel energy entering the engine that is lost to surroundings in the form of thermal energy is shown to be 63.5%. In total approximately 75.4% of the fuel energy is lost as heat at the engine through friction and used for powering ancillary equipment, leaving only 24.6% of the energy to run the vehicle systems. Of the 24.6% available, about 23.2 % is converted to provide kinetic energy to the vehicle. It is this share of energy which can potentially be recovered using regenerative braking. In terms of fuel energy converted by the engine this inertial energy is:

$$E_{ffr} = E_{ffv}.E_{ffi} \qquad (3\text{-}1)$$

Where:

E_{ffr} is fraction of fuel energy potentially recoverable by regenerative braking.

E_{ffv} is fraction of fuel energy available for other vehicle systems.

E_{ffi} is fraction of vehicle system energy converted to overcome vehicle inertia.

Thus, according to Baglione's figures:

$$E_{ffr} = 0.246\,.\,0.232 = 0.057 - \text{or } 5.7\% \qquad (3\text{-}2)$$

This indicates that approximately 5.7% of the fuel energy converted by the vehicle (via the engine, transmission and other systems) is used to endow the vehicle with linear kinetic energy. However any energy recovered via regenerative braking will be in the form of kinetic energy. Therefore theoretically savings of up to 23% could be achieved in the case study shown in Figures. 3.4 and 3.5. In practice however savings will be lower depending on the efficiency of the regenerative braking and energy storage system. The variation of theoretical percentage savings across different vehicle types and journey cycles are likely to vary significantly - largely because of differences in the proportions of energy required to overcome the various resistive forces. The simulation developed by the author, and outlined in Chapter 4, is used to find equivalent figures for a variety of vehicle types over different journey profiles in order to compare possible savings. The simulation work described by Baglione (2007) involves modelling of various vehicle sub-systems .The modelling described in Chapter 5 is more general in addressing directions and insight.

The limitations on the energy saving potential of any regenerative braking and on-board energy storage system in a hybrid or electric vehicle include:

- the maximum braking force that can be applied by the regenerative braking system;
- the rate at which energy can be transferred from the regenerative braking system to the energy storage system; and
- the capacity of the energy storage system.

In this regard an obvious benefit of vehicles that are connected to a power grid, such as with trains or trams, is that the system is so large that it can be considered infinite in capacity. Aside from other loads on the grid, at any one time, if many vehicles are travelling, some will be accelerating and drawing upon the grid whilst others are braking and contributing to the energy pool. Localised systems with wayside energy storage also offer opportunities for useful energy savings as shown by Lawson *et al* (1981) who determined that a wayside energy storage system (WESS) using a large underground flywheel energy storage system could save up to 23% of the standard energy requirement for freight trains depending on the rail gradients and locomotive operation techniques.

3.3.6 Safety considerations and vehicle stability under braking conditions

Historically tyre performance was thought to exhibit a balance between grip, rolling resistance and wear. Work by Williams and co-workers, (Williams & Lees, 1970; Williams *et al*, 1972; Bond, 1985) loosened this triangular relationship although there remain trade-offs between these properties. A range of tyres are now available that claim reduced rolling resistance such as the Michelin Energy Saver™ (Michelin, 2016).

The decceleration during braking with any vehicle is limited by the friction between the vehicle tyres and the road surface. This will vary depending on the type of surface and the condition of the surface, this latter factor being heavily influenced by weather. Air temperature will also have an effect. Before temperatures drop sufficiently to cause ice to form on the road surface the tribology of the elastomers used in the manufacture of the tyre will alter significantly and also affect tyre performance. Some hybrid vehicles have electric drive on the rear wheels which can be used for regenerative braking. However, the regenerative braking force that can be applied to rear wheels is limited if proper control of the vehicle is to be maintained, particularly when the road surface friction coefficient, μ, is relatively low when roads are wet or icy. If the braking force is sufficient to cause wheel lock the vehicle will become unsafe and no further energy is recovered and the rear tyres stop gripping. Work carried out by Hancock *et al* (2006) indicates that on surfaces with high μ the reduction in vehicle stability can be effectively controlled by ESP (electronic stability programme). However on low μ surfaces the reduction in stability is too severe to be managed by ESP. They propose two possible solutions to this problem, one involving automatic switching to friction braking when the longitudinal slip on either back wheel reaches a specified threshold. Another proposal involves the locking of a centre coupling between front (conventional ICE drive train) and rear (electric drivetrain) axle transmissions. However this second proposal may have an impact on the performance of ESP and ABS systems and sub-limit vehicle handling (i.e. handling in more moderate driving conditions). If the vehicle's motor/generator units are connected to all road wheels then, in principle it should be possible for more energy to be recovered through regenerative braking before vehicle stability is compromised providing there is proper control of the braking balance between front and rear axles.

3.3.7 Control strategies for hybrid vehicles

Schiffer *et al* (2005) discuss strategies for managing stored energy and controlling the energy balance between an energy storage system (ESS) and other components in the drive train. They suggest that since at low speeds there is little vehicle kinetic energy which could be converted to stored energy through regenerative braking the ESS level of energy (LOE) should be kept relatively high. Conversely at high speeds the LOE can be relatively low since the vehicle has kinetic energy that can be converted to stored energy during the next regenerative braking phase i.e. stored energy is inversely proportional to vehicle kinetic energy. Schiffer *et al* (2005) define this strategy by:

$$E_{kin}(t) + E_{electr.}(t) = const. \quad (3\text{-}3)$$

Where:

E_{kin} = Vehicle kinetic energy (3-4)

$E_{electr.}$ = Stored electrical energy (3-5)

3.4 Electrical Energy Storage

In order to develop and use a simulation tool it is necessary to know the characteristics and performance of energy storage technologies.

Energy can be stored in chemical, electrical or mechanical form. In order to optimize the efficiency of any particular Hybrid Vehicle powertrain the selection of the most appropriate system / technologies is an important factor. This section includes an overview of existing and emerging technologies along with comments regarding their potential in hybrid vehicle power trains. A wide range of energy storage systems have been evaluated by Doucette and McCulloch (2011). Overall findings suggest that in the application considered (a fuel cell series HEV) high-speed flywheels are a realistic alternative to other widely adopted energy storage technologies such as Li-ion cells and ultra-capacitors.

Electrical batteries have been employed in vehicles since the 1830's, although electrically powered vehicles with batteries that could be recharged did not become a practical proposition until the 1880's. (Erjavik, 2013). The idea of electrically powered vehicles which can be recharged from a mains source has been tried many times and in some areas trials have been conducted. Currently small 'city cars' and 'quadricycles' such as the 2 seat 'G-Whiz' are commercially available although they have not been widely adopted.

Generally the use of electric vehicles has not until recently become practical, previously being restricted to specialist applications such as goods deliveries in urban areas and vehicles operating inside buildings where zero emissions is an essential requirement. Electric vehicles are gaining popularity in London, particularly within the congestion charge zone where they are exempt. A limiting factor for road EVs has been the weight of the batteries required. Recent advances in battery technology, resulting in higher energy and power densities, have improved the practicality of EVs. An explanation of the different battery types along with their merits and shortfalls for EV and HEV use is given in the next section.

3.4.1. Lead acid batteries

Lead acid batteries are still used almost exclusively in automotive applications for starting, lighting and ignition (SLI) The technology is well tried and tested, affordable and suitably robust for vehicle applications. (Woodbank Communications, 2009) The main disadvantages of lead acid cells for primary energy storage in vehicles are their physical size and weight. In some applications such as electric delivery vehicles this does not preclude their use and they have been used in small numbers for electric car applications. However their range and performance are limited. The following sections indicate advantages and disadvantages of various battery types in relation to hybrid electric vehicles (HEV) applications based on information from the Woodbank Communications website (2009).

(i) Advantages

Lead Acid cells are low cost and low internal impedance. They are reliable, physically robust and tolerant to overcharging. Lead acid batteries can deliver high currents allowing for high torque to aid starting and acceleration. Trickle charging can be used over long periods. A very wide range of capacities, shapes and sizes of lead acid battery are available and the lead in lead acid cells can quite simply be recycled.

(ii) Shortcomings

A disadvantage of lead acid cells, particularly in regard to vehicle applications, is their high density and physical volume. Typically, a coulombic charge efficiency of only 70% is achieved although this can be as high as 85% to 90% for special designs. Lead acid cells are not suitable for fast charging and there can be a risk of over-heating during charging.

Battery life is relatively low at 300 to 500 cycles. The chemicals used in the electrolyte are toxic and corrosive whilst a limiting factor of these cells is a lower operating temperature of 15°C

Energy efficiency of lead acid cells:

Efficiency,η, = E_D / E_C (3-6)

Where:

E_C = Total energy received during charge = $v$batt (-$i$batt) dt $V_C I_C T_C$ (3-7)

E_D = Total energy delivered during discharging = $v$batt -$i$batt dt $V_D I_D T_D$ (3-8)

Energy efficiency = $\left(\frac{V_D}{V_C}\right)\left(\frac{I_D T_D}{I_C T_C}\right)$ = *(voltage efficiency)* (coulomb efficiency)* (3-9)

Coulomb efficiency = (discharge A – hrs) / (charge A – hrs) (3-10)

Voltage efficiency = (discharge voltage) / (charge voltage) (3-11)

Typical net coulomb efficiency = 90%

Typical voltage efficiency = (2V)/(2.3V) = 87%

Energy efficiency = (87%) (90%) =78%

For lead acid cells a commonly used estimate is 75%

Equations (3-6) to (3-11) from York (2014)

Battery Capacity C-Factor and Peukert's Law:

The value, *C*, is the current that will cause a battery to discharge over 1 hour. Battery capacity can be denoted as *C* amp-hours. When a battery is discharged at a current below the value *C*

For example at a current of $\frac{C}{5}$ the battery will not run for 5 hours as one might expect but will instead discharge more slowly since battery capacity and discharge current do not

follow a linear relationship. When operating at a fast discharge current, less energy can be recovered from a lead-acid cell than when running at a lower discharge current.

The relationship between battery capacity and discharge current is defined by Peukert's law:

$$C_p = I^k t \tag{3-12}$$

York (2014)

Where: C_p = The amp-hour capacity at a discharge current of 1 Amp

I = The discharge current in Amps

t = The discharge time in hours

k = The Peukert coefficient, typical value = 1.1 – 1.3

$$C_p = C^k \tag{3-13}$$

York (2014)

From this the Amp-hour capacity can be defined as:

$$It = Ct^{1-\frac{1}{k}} \tag{3-14}$$

York (2014)

The relationship shown in equation 3.12 is significant factor for HVs and EVs where depending on the journey type and the control regime large discharge currents are quite possible and in many cases likely. In a Parallel HV, high discharge rates can, in principle, be avoided. Optimal control of the power split between electrical machines (traction motors) and the IC engine will, however, limit the useful contribution of the electrical machines towards the overall tractive effort and is likely to impose a significant limitation on performance when operating in 'electric only' (zero emissions). As with many aspects of vehicle design, a compromise between energy efficiency and performance is required.

3.4.2 Nickel-Cadmium Batteries

Nickel Cadmium (Ni-Cad) batteries have been mass-produced since the early 1960's. They are arranged in 1.2volt cells and have an energy density approximately twice that of Lead Acid battery (Woodbank -Communications, 2009)

The following summaries showing the advantages and disadvantages of this battery type is from information on the Woodbank Communications website (2009).

(i) Advantages of Ni-Cd cells

Ni-Cd cells have low internal resistance and high Coulombic efficiency. High rates of charge and discharge are possible. They exhibit a flat discharge characteristic, but charge falls rapidly towards the end of the discharge cycle. Deep discharges can be tolerated and they can be deep cycled. Ni-Cd cells can operate at temperatures up to 70˚C and cycle life is typically over 500 cycles. Sealed Ni-Cd cells can be stored in a charged or discharged state without degradation occurring. A wide range of sizes and capacities are available.

(ii) Shortcomings of Ni-Cd cells

Ni-Cd cells are susceptible to 'memory effect', a characteristic more accurately described as voltage depression where charge capacity is reduced due to incomplete discharging between charge cycles discharging it each time it is used. This can be avoided when charging from the mains electricity by using a specialist NiCad battery charger which has a built-in discharge circuit. If used in a HV the discharge circuit would need to be incorporated into the charge control circuits. Ni-Cd cells are also prone to damage from over charging, another factor which can be prevented by correctly designed charging circuits. The charging regime within a HV using Ni-Cd cells for energy storage needs careful control if maximum battery life is to be achieved. At present the author has found no reference to Ni-Cd cells being used in production hybrid vehicles.

3.4.3 Nickel Metal Hydride

Nickel metal hydride batteries which have superior energy density and performance characteristics have been popular for use in many EV and HEV applications.

Nickel-metal-hydride batteries are similar to nickel-cadmium batteries and also have a cell voltage of 1.2 volts. The NiMH battery was developed by Stanford Ovshinsky and patented in 1986. NiMH batteries can exhibit a "memory effect" although to a lesser extent than Ni-Cd batteries. At present they are more expensive than Ni-Cd but they present less of an environmental problem. They exhibit a high energy density, 40% higher than Ni-Cds

and more than double that of Lead Acid cells. Higher charge and discharge rates can be used as well as micro–cycles making NiMH suitable for novel applications (Woodbank Communications, 2009). NiMH batteries have recently been utilised in various automotive applications including 2 popular HEVs; the Toyota Prius and the Honda Insight. The information below is based on information from the Woodbank Communications website (2009).

(i) Advantages

Ni-MH batteries have low internal impedance, high energy density and can be deep cycled. Typical cycle life is approximately 500 cycles but generally fewer than for Ni-Cd cells. As with Ni-Cd cells, Ni-MH exhibit flat discharge characteristic but charge falls off rapidly at the end of the cycle. They are Robust and can tolerate over charge and over discharge conditions which simplifies battery management. Rapid charging of Ni-MH cells is possible in as little as 1 hour and they can be stored indefinitely either fully charged or fully discharged. They have a wide operating temperature range and are considered less environmentally damaging that Ni-Cd cells.

(ii) Shortcomings

Ni-MH cells have a very high self-discharge rate and also suffer from 'memory' effect though not as pronounced as experienced with Ni-Cd batteries. Their high rate discharge characteristics are not as good as found with Ni-Cds and they are less tolerant of overcharging than Ni-Cds. The coulombic efficiency of nickel metal hydride batteries is typically only about 66% and diminishes the faster the charge. While Ni-MH batteries may have a high capacity, this is not necessarily all available since the cells may only deliver full power down to 50% DOD (Depth of Discharge) depending on the application. As with Ni-Cds, the cell voltage is low at only 1.2 volts which means many cells are required to make up high voltage batteries. The Toyota Prius and Honda insight hybrid both use Ni-MH batteries for on-board energy storage.

3.4.4 Lithium Ion

(i) Advantages

Lithium Ion batteries have a high cell voltage of 3.6 volts meaning fewer cells and associated connections. Individual cells of up to 1000Ah capacity are available and they are immune from leaking. They have a high energy density approximately 4 times that of lead acid cells and also have a very high power density. High rates of discharge are

possible making them suitable for hybrid vehicle applications. Fast charging and deep cycling are permissible. Lithium Ion cells exhibit a very low self-discharge rate and a very high coulombic efficiency. They can also tolerate micro-cycles and do not suffer from any 'memory effect' issues. These batteries have a long cycle life and the cycle life can be extended significantly by using protective circuits to limit the permissible depth of discharge (DOD) of the battery which helps to mitigate the high initial costs of the battery. (Woodbank Communications, 2009)

(ii) Shortcomings

Lithium Ion cells can suffer from capacity loss or thermal runaway when overcharged and can suffer degradation at high temperatures or when discharged below 2 Volts. If Lithium Ion cells are crushed venting and possible thermal runaway can occur. Due to these issues protective circuitry is required in cell installations for safety reasons.

Lithium Ion batteries are employed in several currently available EVs including the Tesla sports car (Tesla, 2014) and some HEV vehicles such as the current 7 seat Toyota Prius (Toyota, 2014).

There have been concerns raised over recent years that Lithium, like oil, is a finite natural resource and available for economically viable extraction from a limited number of regions throughout the world. Although the author has been unable to find a consensus of when approximately peak Lithium is likely to occur it is clear that demand is increasing, as shown in Figure 3.7 and the supply is limited.

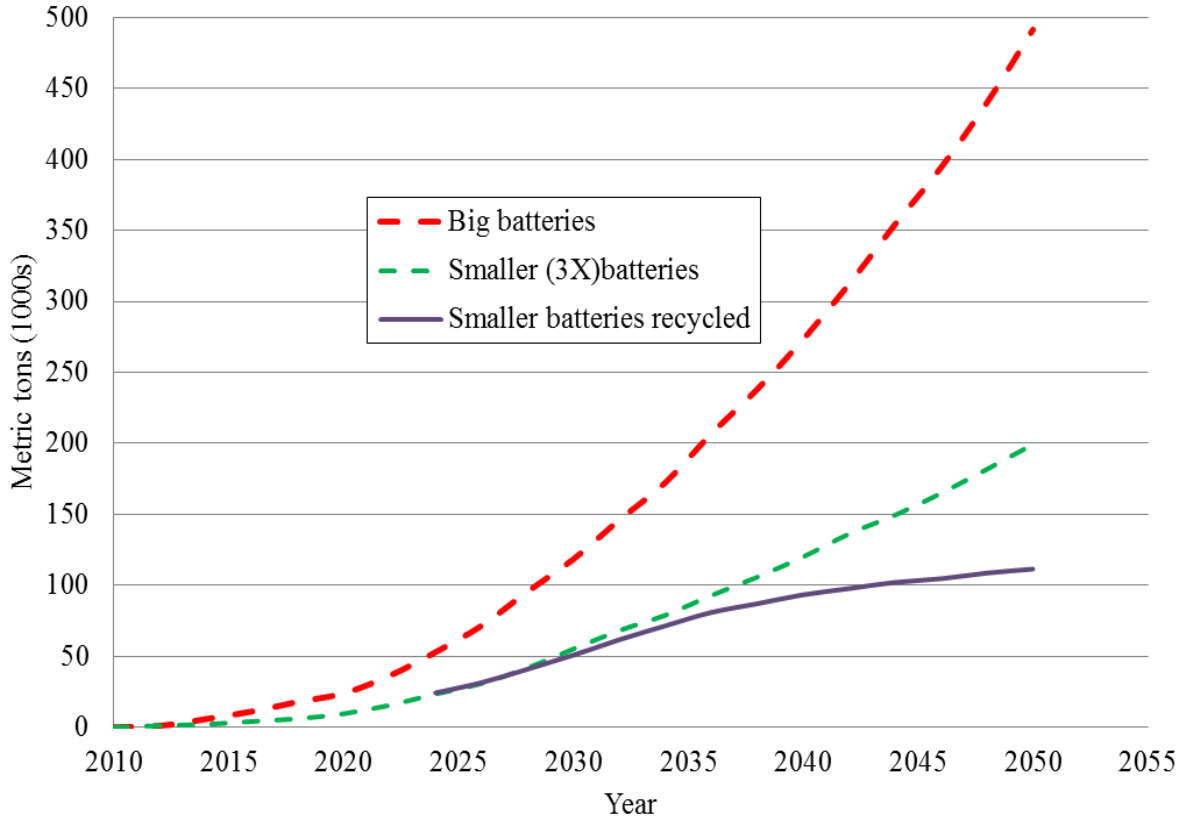

Figure 3.7: World Lithium demand (Barnes, 2009)

This has implications for the future expected growth in demand for EVs and HEVs. At present Li-Ion batteries are proving to be highly effective for powering a wide range of portable electronic devices due in part to the positive attributes already outlined. This popularity has in recent years spread to widespread use in EVs and HEVs where much larger numbers of cells are required. Tahil (2006) argues that sustainability for future transportation needs might be better met by the use of "Zebra" Sodium Nickel Chloride batteries and/ or Zinc air batteries. Whilst these technologies potentially offer some benefits they are not yet in widespread us so are not considered further in this work.

3.4.5 Battery power density and energy density summary

For HEV applications two important considerations for any energy storage system are power density and energy density. These two measures of performance are summarized in Figure 3.8.

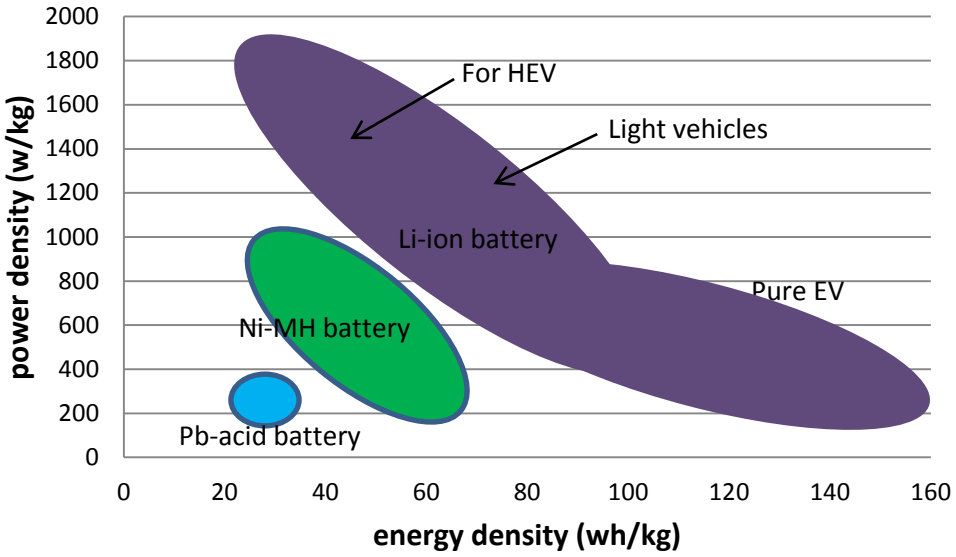

Figure 3.8: Power density / energy density for a range of batteries (replotted from Hitachi. 2008)

Figure 3.8 shows quite clearly the advantages offered by Li ion and Ni-Mh for vehicle applications in terms of energy and power density. Thomas (2008) estimates upper limit of energy density for practical Li-ion batteries at around 150Wh/kg (540kJ/kg), Doucette & McCulloch, 2011 set the value somewhat higher at just over 200Wh/kg (720kJ/kg).

Other factors such as cost, physical size and reliability/longevity are also important when selecting a battery type for a given vehicle application. In addition, the environmental impact of batteries should be considered along with recyclability.

3.4.6. Supercapacitors

Supercapcitors have been investigated as ESS for HV applications in a number of studies including Doucette and McCulloch (2010) and Barrero et al (2008). Doucette and McCulloch (2010) found ultra-capacitors to be a viable alternative to flywheels or batteries and assessed the performance and cost trade-offs of these 3 ESS types in detail from a study involving simulation over the NEDC and Artemis drive cycles. Doucette and McCulloch (2010) evaluated 3 alternative supercapacitor systems in the simulation of light rail hybrid applications and found them to be a practical means of energy storage to

provide energy savings of between 23 % and 33% with results depending heavily on the drive cycle used.

3.5 Mechanical Energy Storage

3.5.1 Energy storage in elastic materials/ gases

Potential energy has been stored in mechanical systems for centuries, most commonly in small scale applications such as watches and clocks. This type of system requires the use of material with suitable elastic behaviour. A wide range of materials behave elastically but only those which have an appropriate modulus of elasticity and sufficiently good fatigue properties are suitable for energy storage in everyday items such as clocks and timers. Other suitable applications include emergency torches where use of alkaline, Ni-Cad or Ni-Mhd batteries is not ideal as their condition is likely to deteriorate in the long periods between uses inherent with these devices. Despite being popular and practical on a small scale, this form of energy storage has not been adopted successfully on a larger scale. The main challenges include the difficulty of physically containing the required amounts of energy safely within some elastic device and the issue of safely transferring that stored energy to the wheels of the vehicle in a controllable manner. Although the author has been unable to find any examples of working prototypes of vehicles incorporating energy storage using mechanical elastic system there has been some theoretical work carried out in this area. Hoppie (1982) published research regarding regenerative braking using elastomeric energy storage. The concept of using elastomers for energy storage in vehicles was also considered in the 1960's by the Malaysian Rubber Producers Association (MRPRA) (Coveney 2008). There are records of a number of patents for kinetic energy storage systems for smaller transport applications such as bicycles. One example of this is the 'Lever Actuated Bicycle Energy Storage System', the subject of U.S Patent no. 6,035,970. This particular system includes a number of interesting and novel features but there appears to be no evidence of this or other similar systems being developed to a stage where they are practicable. There are fleeting references to trials carried out by amateur enthusiasts involving modified bicycles however no data or published papers on these trials have been found. Patents filed by Jayner (1979) and Gill (1984) in the USA also propose the use of elastomers to store energy that would otherwise be dissipated as heat via friction brakes during braking. Jayner (1979) details a system that uses a synthetic or natural

rubber as the energy storage medium connected to the vehicle powertrain via steel cables, gears and clutches. A system proposed by Gill (1984) includes the use of hydraulic motors / pumps in the transmission and a variable volume vessel to store the energy by means of either a sliding piston acting against an elastomeric material or the walls of the vessel being made of an elastic material. Various materials are suggested ranging from synthetic polymers through to natural rubber with or without fibre reinforcement. Although the details within these two patents are of technical interest there are no records of either system being proven through practical trials or of any commercial applications. Equations relating to energy storage in elastic material:

Energy stored in a deformed spring:

$$F_s = -kx \tag{3-15}$$

$$PE_s = \frac{1}{2}kx^2 \tag{3-16}$$

Where: F_s = Force acting on the spring (N)

k = Spring constant (N.m^{-1})

x = Spring extension (m)

Energy stored in elastomeric materials can be estimated from the Neo-Hookean constituative law usually expressed in terms of the elastic energy stored per unit volume (Treloar, 1975):

$$U_V = \frac{G}{2}\left(\lambda_1^2 + \lambda_2^2 + \lambda_3^2 - 3\right) \tag{3-17}$$

(Treloar, 1975)

Where:

G= Shear Modulus

λ_1, λ_2 & λ_3 are the principal extension ratios, i.e. extended over original lengths in the three principal directions.

Research carried out by Kirby *et al* (1997) indicated that natural rubber would be a suitable material for this application. In order to store the kinetic energy of a typical car travelling at 30mph, approximately 45litres ($\approx 45kg$) of natural rubber would be required. Initial results from Kirby *et al* (1997) suggested large improvements in efficiency ($\approx 60\%$) are theoretically possible although work by others including Baglione (2007) and subsequent regenerative braking simulation work by the author would suggest that these figures are optimistic. A study carried out by a group of students as part of an ME Capstone project (2008), investigated the use of superelastic shape memory metals for elastic regenerative braking. This work found that a nickel titanium alloy known as Nitinol was particularly suitable for this application due to its comparatively high energy density and high cycle life.

3.5.2. Compressed gas storage

Energy storage using compressed air is widely used to power air tools of all sizes. As far as the author can establish, there are no compressed air powered cars on the market at the present (August 2015), although they have been proposed by several manufacturers. Limited performance figures have been quoted by manufacturers but little in the way of detailed data has been published in the public domain. In 2002 at the New York Motor Show, Ford unveiled a mock-up of a possible future version of its F-350 'Tonka' truck incorporating an ESS. The proposed system used hydraulic pumps and compressed Nitrogen gas to store energy for use under acceleration. Ford claimed that this system could recoup 80% of the energy normally lost in braking (Motavalli, 2002). It is claimed that braking from 32mph to a standstill will result in sufficient stored energy to accelerate the truck from a standstill to 25mph. These figures suggest that the regenerative braking system is approximately 61% efficient which is comparable to the motor / generator and Li-ion battery system used in the Tesla EV sports car (Tesla, 2014). The technical feasibility of such a system has also been investigated by other researchers. Wicks, Maleszweski, Wright and Zarybnicky (2002) suggest that with a thermally enhanced regenerative system the quantity of energy can be further increased. The overall conclusion of this report is that such a system could potentially be competitive and *may* offer advantages over electric or flywheel energy storage. This system has not become commercially available to customers and Ford do not refer to it on their website at the present (February 2016). A 2008 press release announced the launch of 'OneCAT' concept car that utilises compressed air energy storage. Harrabin (2008) reported that the glass fibre vehicle weighing just 350 kg would be driven by compressed air stored in

carbon fibre tanks within the vehicle's structure. A novel feature of this design is the use of a fuel burner which can be used to heat the compressed air to raise the amount of energy available to the air engine and increase range when required. Obviously this requires energy input for the fuel burner but a wide range of fuel types can be used for this. Re-charging can be carried out from an external compressor in three minutes or by plugging in to a mains electrical socket and using a small on-board compressor which takes four hours. On long journeys, it is claimed that the vehicle will achieve an equivalent of 120mpg. The designer, Guy Neagre, is working in collaboration with the large Indian company Tata and hoped to bring the vehicle to market in 2009/2010. However, at present (2016), this vehicle is not commercially available and there is no mention of the model on the Tata website. In January 2013 PSA Peugeot Citroen group announced their 'Hybrid Air' system which is planned for release in 2016 (Brugier-Corbiere deServigny, 2013). This system uses compressed air for energy storage that is converted to hydraulic pressure to provide tractive effort via hydraulic motors. The energy stored within the compressed air is converted during regenerative braking and also when surplus energy is available from the ICE running at optimum efficiency. Fuel savings of up to 45% are predicted when driving in urban areas (PSA Peugeot Citroen, 2013). The certified fuel consumption for a combined cycle is quoted as 2.9l /100km (98.12 mpg) with CO_2 emissions in the region 69g/km when incorporated into the existing Citroen C3 or Peugeot 208 platforms (compared to 104g/km for existing conventional models with manual transmission) (PSA Peugeot Citroen, 2013). The Hybrid Air system is a parallel / series type hybrid and when running in compressed air mode produces zero emissions at the point of use. Peugeot Citroen claim that in urban driving, depending on traffic conditions, vehicles could run for 60-80% of the time in 'Air Power' mode alone owing to the energy recovered through regenerative braking (PSA Peugeot Citroen, 2013). Amongst the benefits claimed by the manufacturers is the ease of recycling the materials used in the system compared to petrol / electric hybrid system using Lithium Ion batteries (PSA Peugeot Citroen, 2013). Possible energy savings of up to 45% are claimed in urban areas (Mokaddem, 2013). As of January 2016, no test data was available for the Hybrid Air system. Aside from energy storage in vehicles, a number of proposals have been made for large scale and small scale applications. An Irish company, Gaelectric, recently embarked on a large scale £175 million project in the Larne Area of County Antrim, Northern Ireland (Pendick, 2011). The proposed system will be used to level out supply and demand for electricity – this is very large scale application but of technical interest.

3.5.3 Kinetic energy storage

There is evidence that simple flywheels were used to maintain the rotation of potters' wheels from as early as 3000BC (Bryant, 1994) and it is one of the oldest known ways of storing energy for short time periods (Jenson, 1980). In most forms of reciprocating engine flywheels are used for very short term (ms range) energy storage to maintain crankshaft inertia between firing / power strokes. The requirement for heavy flywheels in engines has reduced and current high performance ICEs used in vehicles the lightest flywheels possible to smooth out power pulses from each cylinder whilst allowing quick acceleration to produce a light, responsive engine. The use of flywheels for storage of energy over extended periods is a more recent application. Such applications require flywheels with very high rotational speeds and this is becoming practical due to advances in bearing technology and materials science.

The energy stored in a rotating flywheel is as follows:

$$U = \frac{1}{2} I\, \omega^2 \tag{3-18}$$

Where:

U= energy stored (J)

I= moment of inertia (kgm^2)

ω = angular velocity (rad/sec)

I, the moment of inertia, is determined by the mass and the shape of the flywheel. It can be defined thus:

For a uniform disc:

$$I = \frac{mR^2}{2} \tag{3-19}$$

From the above equations it is clear that the energy content is affected by the mass to the first power and by the speed to the second power. When attempting to maximise energy storage potential it is more useful to increase the rotational speed rather than the mass of the flywheel. To find the energy density of the rotating system, W_m, i.e. the amount of energy stored per kg, we simply divide by m

$$U_m = \frac{1}{2} r^2 \omega^2 \tag{3-20}$$

To find the volume energy density W_{vol} we substitute *m* with *m* expressed as the mass density ρ multiplied by the volume.

$$U_{vol} = \frac{1}{2} \rho \, r^2 \, \omega^2 \tag{3-21}$$

When considering flywheel energy storage systems for vehicle applications energy and power density are particularly important factors. Developments in composite materials technology have made it possible for light-weight high speed flywheels to be developed with rotational speeds of 60,000 rpm possible. As shown in eqt. (3-21), these comparatively high rotational speeds have significant benefits on the energy density possible.

3.5.4 Flywheel "Windage"

A significant factor to consider when optimising the efficiency of a KESS (Kinetic Energy Storage System) is that of windage, that is the losses due to the aerodynamic effect between the rotating part (the flywheel) and the surrounding enclosure. The magnitude of windage losses is partly determined by the size and geometry of the flywheel and enclosure (and the relation between the two), the shape of the flywheel and the surface finish of the rotating part and the enclosure. For high speed flywheels, windage loss is the single greatest factor in the overall system losses (Ajisman *et al*, 1997). One method of reducing windage losses is to enclose the rotating parts inside a vacuum containment. If the space is partially evacuated of air there is reduced air resistance acting upon the flywheel. In mechanical systems it is sometimes not practical to achieve a high vacuum especially where rotating input/output shafts are present. Another possibility for reducing windage losses in flywheels is the use of low density gasses within the sealed chamber around the flywheel. Ajisman *et al* (1997) carried out research to study the possible benefits of using a He SF_6 (helium sulphur-hexafluoride) gas mixture. Although the low density of helium reduced windage losses it was necessary to introduce SF_6 to increase the electric breakdown voltage. It was found that a ratio of between 5 and 15% of He SF_6 mixture reduced the windage losses by 40-50%.

3.5.5. Flywheel energy storage in Transport application

Examples of flywheels being used for energy storage in vehicles include the Parry People Movers Ltd (PPML) light trams and light railcars that have been in operation for over a decade. An automotive ICE is employed along with a 1m diameter steel flywheel weighing 500kg for energy storage. The flywheel runs at a maximum speed of 2500rpm and being of a low technology design is easy to maintain (PPML, 2012). Flywheels were used in the Swiss Oerlikon 'gyro-bus' in the 1950s which used a 1500kg 1.5 m diameter steel flywheel (Hoimoja, 2006). More recently, in 2011Ricardo Engineering reported in a press release that testing had commenced on a flywheel energy storage system for buses (Ricardo, 2011). Lawson *et al* (1981) investigated wayside energy storage for recuperating potential energy for freight trains. This study focused on the application of large underground flywheels and electrical machine. The storage system stored potential energy (usually dissipated through braking) from locomotives descending a gradient and this stored energy contributed towards the energy requirement of locomotives. The investigation showed that energy savings of up to 23% were possible. The wheel to wheel efficiency of this system was 60%. Despite requiring major infrastructure the system was shown to be economically viable for a number of sites considered.

3.5.6 Gyroscopic effects and vehicle stability

An important factor when considering this type of energy storage is the gyroscopic effect that such a system may have on the handling characteristics and stability of the vehicle in which it is used. Rotating flywheels are used to make systems stable and also to control the motion of spacecraft during flight. The difficulty in vehicles is that although the flywheel is spinning in a stable fashion, vehicles tend to experience road shocks and vibration. The flywheel will not easily be displaced by these forces therefore the bearings, the wheel itself and in fact the whole vehicle could easily be damaged as they absorb these shocks. The rotating mass could also affect the handling characteristics of the vehicle and could make cornering difficult.

3.6 Sources of Power Loss in Vehicles

3.6.1 Resistance due to drivetrain friction

Mechanical transmission systems inevitably incur frictional and inertial losses which need to be taken into account in vehicle energy simulation work. This resistance can be considered as an overall percentage of the torque supplied from the engine crankshaft or characterised by separate losses for individual components or sub-systems within the transmission. The data represented earlier in figure 3.5 from Baglione (2007) shows that for the vehicle considered (a 2700 kg pick-up truck with v8 engine and 5 speed transmission) the energy loss, as a percentage of the total vehicle system demand, from the transmission is 12.8% for the mechanical transmission plus a further 7.1% for the torque convertor - a significant proportion. Hawley et. al. (2010) showed the influence on transmission oil viscosity on vehicle fuel efficiency over the NEDC. Findings suggested that use of a reduced viscosity oil and preheated the oil to further reduce viscosity could yield reductions in fuel consumption of up to 1.5%.

3.6.2 Aerodynamic resistance

Aerodynamic resistance in road and rail vehicles is normally described in terms of an approximate expression for force which is proportional to the speed of the vehicle; the influence of complicating factors such as winds, including cross-winds, and of complex motion of the vehicle is often ignored (Barkan, 2009; Doucette & McCulloch, 2011).

3.6.3 Rolling resistance

The local interaction between a rubber tyre and road or steel wheel and track (for trains) is complex and many vehicle models rely on a simplified estimation of rolling resistance. The mechanisms for rolling resistance on rail and road differ: primarily very local plastic deformation and primarily viscoelastic respectively.

As mentioned in 3.3.6 in the 1970s and 1980s Williams, Bond and co-workers succeeded in “uncoupling” rolling resistance from wet grip. The former was argued to be related to

viscoelastic response at frequencies below 120Hz and the latter to frequencies from 50 kHz to 1MHz (Bond, 1985); the original theory has been subsequently refined by Persson (Persson 2001; Klüppel & Heinrich, 2000). Despite the advances outlined by Bond (1985) the rolling resistance coefficient for truck tyres is about 2-4 times and the rolling resistance coefficient of cars is about 5 times that of railway wheels which have are widely considered to have a rolling resistance coefficient of around 0.0020 (5AT, 2015)

3.7 Comparison of Energy and Power Density for Various Forms of Energy Storage Technology

Having discussed some of the different types of energy storage technologies available it is useful to summarise some key performance criteria. Two factors which are particularly relevant to engineers concerned with the development of hybrid vehicles (incorporating regenerative braking and energy storage) are the energy and power density of these systems. The energy volume of energy storage systems is also important if hybrid vehicles are to be designed for practical use without significant compromises being made in regard to passenger and driver comfort and luggage space. Figure 3.9 gives a comparison of key performance data for some of the energy storage systems discussed in this work.

	Conventional battery			**Mechanical storage**		
	Lead Acid	NiCd	Li-ion	CAES	FES-LS	FES-HS
Roundtrip efficiency (%)	70-82	60-70	85-98	57-85	70-95	70-95
Self-discharge (% energy /day)	0.033-0.03	0.067-0.6	0.1-0.3	0	100	1.3-100
Cycle lifetime (cycles)	100-2k	800-3.5k	1k-10k	n/a	20k-100k	20k-100k
Expected lifetime (yrs)	3—20	5--20	5--15	20-40	15-20	15-20
Specific energy (Wh/kg)	30-50	50-75	75-200	30-60	10--30	10--30
Specific power (W/kg)	75-300	150-300	150-315	0	400-1.5k	400-1.5k
Energy density (Wh/L)	50-80	60-150	200-500	3--6	20-80	20-80
Power density (W/L)	10-400	*	*	0.5-2	1k-2k	1k-2k
Power cost ($/kW)	175-600	150-1500	175-4000	400-800	250-360	250-400
Energy cost($/kWh)	150-400	600-1500	500-2500	2-140	230-60k	580-150k

Figure 3.9: Summary of energy storage device parameters (re-drawn from Bradbury, 2010) CAES = Compressed air energy storage, FES-LS/HS = Flywheel energy storage low speed / high speed

In relation to hybrid vehicle use, the discharge time at rated power and the power rating are also key parameters in evaluating the suitability of different energy storage systems for vehicle applications. Figure 3.10 replotted from APS (2007) gives an overview comparison of a range of systems.

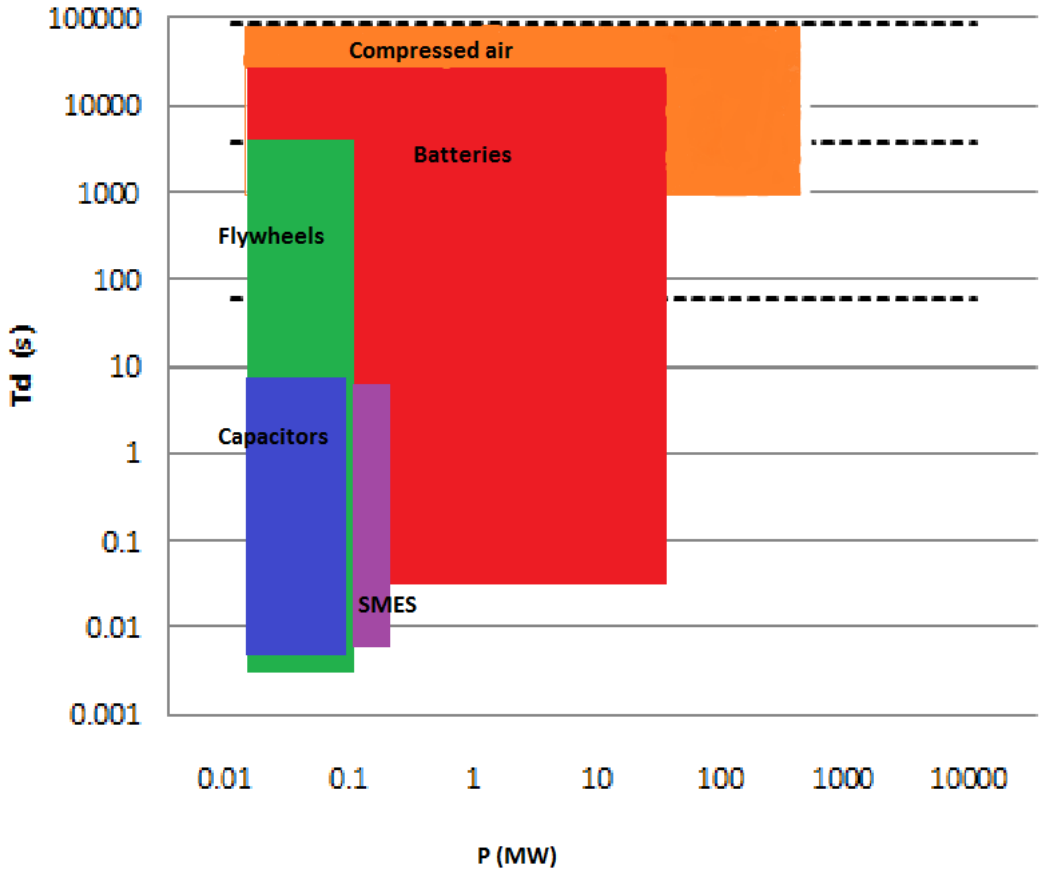

Figure 3.10: Schematic diagram of discharge time (T_d) range against system power range for various types of energy storage system. Replotted from APS (2007) Note: SMES = superconducting magnetic energy storage

3.8 Total Energy

Whilst considering different technologies that can be used for energy storage in vehicles, it is important to consider the issue of total energy, that is, the total amount of energy converted during the entire life cycle of a vehicle. From a technical and engineering perspective the purpose of regenerative braking and energy storage in hybrid vehicles is to use energy more efficiently, and to convert less energy in the process of covering a given journey. There are, of course, other factors that can make energy saving technology attractive from a commercial or marketing perspective as detailed in sections 1.3.1 - 1.3.3. When considering hybrid vehicles from an energy perspective there are two aspects to consider: The total life cycle energy requirement (including manufacturing processes and obtaining /processing scarce materials) and the energy used during the working life of the vehicle. The comparison between these energy requirements is a key issue however it is a large subject in its own right and not considered further here.

3.9 Realism and Validity of Driving Cycles

Close scrutiny of some government and industry standard driving cycles such as the NEDC gives rise to questions about the validity and realism of the drive cycles themselves. This subject is discussed at length in a range of papers. The work of Andre (2004) recognises a requirement for a more realistic drive cycle whilst identifying the importance of driving cycles being periodically updated as traffic conditions change. Tzirakis *et al* (2006) also highlight how certain European cities, such as Athens, have typical journey cycles that vary a great deal from the NEDC. There are also some discrepancies about the way in which the cars under test are prepared to give optimum performance. In a draft paper Cole *et al* (2012) discuss the validity of car manufacturers' fuel efficiency and emissions testing indicating that, in some cases, manufacturers' efficiency claims can be up to 15% greater than that found by independent tests and customers' experience. The question over the reliability of manufacturer's data gives rise to some uncertainty since, for initial simulation development where a conventional power train was modelled, the performance of the simulation was checked against manufacturer's data. Manufacturer's data provided a readily accessible point of reference for comparison purposes, even if it may not always be representative of real world performance. The subtleties of how testing is carried out by manufacturers is an important issue central to the integrity of advertising and marketing material. The methods used to evaluate vehicle performance in terms of fuel consumption and emissions are considered in more detail in 3.12.

3.10 Methods Used by Vehicle Manufacturers in Vehicle Type Approval Testing

Fuel efficiency and emissions tests are based around standard drive cycles and carried out on a rolling road to give adequate control of all variables. More detail on these cycles including speed against time plots are shown in section 4.1.3. The Drive Cycle used is often dictated by a government directive and national standard. In the EU the 'New European Drive Cycle' is used in accordance with European Directive 80/1268/EC, amended by 2004/3/EC. The details of the formal test protocol are explained by Schmidt (2011). The Artemis Drive Cycle has also been developed as a more realistic cycle and is used by some manufacturers and consultancies such as Ricardo (Little, 2011) but is not currently an official government standard. Andre (2004) describes the development of the Artemis cycle which is based on real road data evaluated using statistical analysis. Other

specific cycles have been developed to represent particular scenarios such as the MLTB (Millbrook London Transport Bus) TfL (2015) cycle to model journey typically undertaken by public transport buses in London. In the USA the Environmental Protection Agency (EPA) uses a range of test Drive Cycles including the Highway Fuel Economy Test (HWFET) Driving Schedule and the New York City Cycle (NYCC) Driving Schedule for evaluating the fuel efficiency and emissions of new cars. To determine rolling resistance, aerodynamic drag and other resistance forces to factor into to rolling road (dynamometer) tests 'coast down' tests are conducted. The recently developed WLTP (Worldwide harmonized Light Vehicles Test Procedures) are intended to provide a range of cycles that will harmonise the emissions testing of light vehicles and, by being more representative of real journeys, make official test results more closely match real world performance (UNESCO, 2016).

3.10.1. Coast down testing

This enables a series of constants to be established to represent resistive forces acting on the vehicle without recourse to expensive wind-tunnel testing and is conducted on a flat test track or road. The vehicle is accelerated up to an appropriate chosen speed and, whilst recording speed/time data neutral gear is selected and the vehicle is allowed to coast to a standstill. The required complete lack of wind is rarely encountered in real testing conditions and accordingly it is usual for this test to be repeated in each direction to help minimise wind effects. Further repeat tests in each direction are recommended (minimum 3 but commonly up to 10) to allow for statistical analysis of results. There is no fixed start speed for the test and it will be influenced in part by vehicle type. In general however, start speeds in the order of 60mph upwards are favoured for consistent results where aerodynamic drag forces have a significant influence. A test procedure is outlined in SAE J1263, Road Load Measurement and Dynamometer Simulation Using Coast-down Techniques, Society of Automotive Engineers, (1996). The coast down test can also be used to investigate specific areas. For example a practical study by Cai *et al* (2012) produced a comprehensive set of data regarding the effect of tyre pressures on rolling resistance in coast-down testing and velocity against time plots for the 2009 Saturn Vue 2-Mode Hybrid Vehicle (an American market car). However, there are no specific rules regarding how the coast down test is conducted. Notwithstanding advances in laboratory testing and simulation of road vehicles, there are limitations.

3.10.2 Factors affecting rolling resistance, engine performance, and aerodynamic drag

For most simulations and for almost all specified journey profiles and rolling road tests used to assess fuel consumption and exhaust emissions of road vehicles, much of the following is largely ignored;

(i) *Factors affecting rolling resistance, which can include:*
Lateral and vertical acceleration and the effect of a road that is not flat at mm scale and above – e.g. climb and descent, cornering, road camber, curvature of rolling roads. The weight – e.g. vehicle inclusive of removable seats, equipment etc., driver and passengers, luggage and fuel – and its distribution in the road vehicle will also have an effect. So will aerodynamic loads.

(ii) *Details of road surface*: e.g. road surface geometry at cm scale and below; presence of tyre dust, water etc. on the road surface.
Details listed in (i) & (ii) affect tyre road interaction, hence rolling resistance.
Tyre construction and types of rubber material used affect rolling resistance as does tyre pressure and the gas mixture within the tyre.
Tyre temperature has a strong effect on rolling resistance. So air temperature, road temperature, radiant heat, speed, acceleration and duration will have an effect.

(iii) *Factors affecting engine performance, which can include:*
Fuel temperature; air temperature, pressure and composition – including water content etc..
The mass (vehicle mass inclusive of removable seats, equipment, driver and passengers, luggage and fuel) and road gradient.
Details of the exhaust path.

(iv) *Factors affecting aerodynamic drag, which can include:*
Details of the externals of the body – e.g. wing mirrors, windscreen wipers, aerials, wheel covers, underside of body – including exhaust pipe etc.
Air temperature
.Winds - including cross-winds.

(v) *Other vehicle power requirements*
The number of powered ancillaries in passenger cars has grown dramatically since the 1980s. Air conditioning units are one of the most power hungry – Lee *et al* (2013) report test results indicating that fuel consumption can often increase by ~20% or more with air conditioning switched on.

An issue with electric vehicles, and to some extent hybrid electric vehicles, that is a problem -particularly in extreme climates- is that of heating/cooling the car interior. Using electric heating in a vehicle running in 'electric only' mode could cut the range by around half in Northern Europe for example (Little, 2012). This essentially makes the vehicle impractical during cold conditions, not just in terms of driver comfort but also safety in terms of clearing misted/icy windscreens. In warm conditions using air conditioning could cut range by 20-30% (Chan and Chau, 1997).When considering vehicle efficiency, published Figures from manufacturers need careful cross checking, where possible, with results from independent trials. The NEDC is considered within the industry as a relatively 'soft' cycle (Little, 2014). The Artemis cycles include greater rates of acceleration and deceleration. European type approval testing of new vehicles is emissions based rather than fuel economy based. However if stoichiometric combustion is taking place minimising CO_2 will also result in minimised fuel consumption.

3.11 Exhaust Emissions

Drive cycles such as the NEDC, MLTB and EPA HFET are employed for exhaust emissions data, the generalised study described in chapter 5 is principally concerned with energy requirements. However in chapter 6, exhaust emissions on bus urban routes (where emissions are a particular concern in terms of human health) are considered in detail. European requirements for vehicle testing are all emissions based and are not directly concerned with fuel consumption (although some emissions, such as CO_2, are broadly proportional to fuel consumption). This is partly due to air quality requirements such as the Clean Air Act (1993) and legislation such as the Climate Change Act (2008). European regulations from 2009 put binding targets in place for the reduction of CO_2 emissions to 130g CO_2/km by 2015. In addition a further target aims for CO_2 emissions to reduce to 95g CO_2/km by 2020 (DFT, 2014). The importance of vehicle exhaust emissions and their effects on human health along with the larger scale environmental issues such as climate change are now widely recognised. At a local level in built up areas, poor air quality due to road traffic pollution is widely accepted as being a contributory factor towards respiratory illness – particularly in young people. A study by Gehring *et al* (2010) found an increased risk of asthma in children living near roads carrying heavy traffic during the first 8 years of life. Despite the popularity of diesels there are growing concerns over emissions from diesels and the resultant effects on air quality and public health -particularly in cities. In London there are proposals to increase the congestion charge by £10 for diesel cars to discourage drivers from bringing them in to the city centre (Independent 2014).

3.12 Other Possibilities for Improvements in Vehicle Fuel Economy

3.12.1 Engine efficiency

There is potential scope for modest improvements in engine efficiency through the use of reduced viscosity lubricating oil as shown by Hawley *et al* (2010) with fuel savings ranging from 5.5% in the urban part of the NEDC when oil is not at maximum operating temperature but lowering to an overall saving of 1.5% over the whole NEDC. Using heating elements to raise the oil temperature showed very slight improvements in economy across the NEDC of 0.5% to 1.4% depending on the heating power and whether or not pre-heating was used before the cycle. It was considered by the authors that the small savings resulting from oil heating and the additional complication and cost involved meant that this feature was unlikely to be viable in production vehicles.

3.12.2 Improving driver behavior, moving towards automation?

Work carried out by Hari *et al* (2012) on a driver behaviour improvement tool that gave drivers audible prompts to influence and improve driving style showed in prolonged trials carried out on a fleet of 15 delivery vehicle that average fuel savings of 7.6% were achieved with the highest saving being 12%.

A prototype self-driving car developed by Oxford University has undergone rigorous testing and hints at a future where many vehicles may be automatically controlled (Lee, 2013). Google have been developing driverless cars technology in California where the testing of such vehicles on public roads has been recently approved. The testing of driverless cars has also been approved in the States of Florida and Nevada. In Japan, Nissan have also been undertaking testing on public roads with self-driving cars (Lee, 2013). In July 2014 the department of transport approved the use of driverless cars on UK roads from January 2015 (BBC, 2014). The general experience of road users is that driving styles vary greatly and that a proportion of drivers drive in an erratic fashion, accelerating rapidly and braking suddenly. This style of driving seems to be especially prevalent in high volume traffic where the bunching and spreading of traffic is commonplace. This occurrence can lead to wave formations in traffic distribution and is sometimes attributed to competitive driving where drivers are trying to ‘get ahead’ of the dense area of traffic. Often this phenomenon can be seen from the air when driving over motorways and other roads. Work by Sugiyama *et al* (2008) has shown this behaviour experimentally and

quantified the speed at which the compression wave moves back through the traffic. In dense traffic this phenomenon leads to the formation of serious bottlenecks even where no clear cause, such as obstruction due to a broken down vehicle, is apparent. At present much of the publicity surrounding technology related to automation of driving is focussed on reducing driver fatigue and improving road safety. Little mention is made, in the literature referenced in this section, of the potential for these systems to reduce energy use. However, if configured to give optimum energy efficiency through moderate acceleration and braking, and also by preventing the formation of waves which promote energy intensive driving (due to repeated acceleration and deceleration) significant energy savings may be possible especially if car control systems were integrated with traffic management systems such as traffic lights. This is a possibly an area worthy of further investigation but is not considered further in this work.

3.12.3 Engine Downsizing

A number of approaches to improve vehicle fuel economy and reduce exhaust emissions have been investigated ranging from configurations of hybrid powertrains Katrasˇnik (2007) through to the adoption of measures to increase specific power out of engines to Botes (2014) who considered boosting in greatly downsized engines.

3.12.4 Weight Reduction

Regardless of the type of energy storage system employed, in the case of any 'on board' energy storage system, as the energy capacity increases, so too does the system mass. Any additional vehicle mass will increase the energy required to enable the vehicle to complete a given journey cycle. Casadei and Broda (2007) found that for mid-sized cars on an EPA (United States Environmental Protection Agency) combined cycle, fuel consumption reduces by 1% per 100 lb (45.4 kg) weight reduction. The possible weight savings in vehicles due the cascading effects of secondary weight savings in vehicle structures is explored by Alonso *et al* (2012). Findings suggest that for every 1 kg primary weight reduction a further 0.5kg can be saved from secondary weight reduction.

3.12.5 Start / stop technology

A number of current car models incorporate various technologies claiming to improve energy efficiency and reduce emissions. The effectiveness of such technologies can be difficult to quantify but some systems such as the start / stop system built into several models in the current Volvo range (similar systems are also used by other manufacturers

including VW and BMW) have obvious potential in situations where traffic is at a stand-still for long periods i.e. many city journeys at peak traffic times. The systems employed in some current cars cause the engine to shut down after the vehicle has been stationary for a given period to save fuel wastage in heavy traffic where significant proportions of journey times can be spent at a standstill. As soon as the accelerator is depressed the engine automatically restarts ready for forward motion to resume. A trial study using a Toyota Crown in the early 1970s, and reported in New Scientist reported a 10% saving in fuel when tested in Tokyo traffic (Dunham 1974). Another early example of this technology being incorporated into a production car was the Fiat Regata ES in the early 1980s (Pederson 2009). At the time of writing (2016) this technology is becoming ubiquitous.

CHAPTER 4

DEVELOPMENT OF A VEHICLE SIMULATION TOOL

4.1 Introduction and Overview

4.1.1 Introduction

As discussed in Chapter 2, the aim of this research is to compare the energy saving effectiveness of a range of hybrid vehicles incorporating regenerative braking in different scenarios. To investigate this area a model was used to evaluate the performance of hybrid vehicles in order to avoid an impractical number of physical tests. A range of commercial simulation software packages are available, such as the 'Advisor' (ADvanced VehIcle SimulatOR) package developed by NERL (National Energy Research Laboratory 2009), part of the U.S Department of Energy. Some are concerned with simulating vehicle performance in terms of energy efficiency whereas others are aimed at modelling the dynamic behaviour of the vehicle, concentrating on vehicle handling and ride quality. Rather than use a commercial software package the author has worked from first principles to develop the simulation tool. This approach has afforded complete control of the simulation design and provided significant insight into some of the subtleties and difficulties involved in vehicle energy simulation. This chapter outlines the simulation development and the most significant findings and initial results found in validation work.

4.1.2 Overview of simulation development

A time stepping algorithm, implemented using Microsoft Excel, was used for the simulation. Although a spreadsheet package is less sophisticated than the programming languages used in some vehicle simulation-software packages, MS Excel allows the simulation to be designed from scratch, giving complete control over the development. It is also suited to time-stepping forward Euler integration analysis whilst allowing convenient representation of data in graphical form. The steps in the development of the simulation are summarised in parts (i) & (ii) within this section. The generalities of forward-looking & backward looking approaches for vehicle simulation were discussed in 3.1.1.

(i) Forward Looking simulation (Version1):

Early work was based on a forward looking algorithm and was used to check agreement against manufacturers' published figures for acceleration and maximum

speed for conventional drivetrain vehicles. Gear-shifting and PID driver modelling was introduced and evaluated and BSFC data was incorporated to enhance realism. A parallel hybrid system was incorporated into the model to allow savings through regenerative braking and energy storage to be studied for hypothetical cases.

(ii) Backward Looking simulation (versions 2 and 3):

Following this a backward looking version was developed. As detailed in 3.1.1 this configuration does not require a driver model and is subsequently simpler, more efficient and stable and offers greater robustness. After testing the simulation with fixed engine efficiency a simplified speed dependant engine efficiency function was introduced. However since this approach was valid only for constant speed scenarios, a gear shifting sub routine and BSFC look-up were added. A hypothetical regenerative braking system was included and the model was developed to allow SOC to be considered. To investigate emissions a look-up Brake Specific Emissions feature was included. This final simulation is referred to as Ver. 3.

Conventional ICE (internal combustion engine) powered vehicles were simulated to enable assessment of the simulation's performance before parallel hybrid vehicles (with regenerative braking and energy storage) were subsequently modelled. Since the simulation was designed to compare possible energy savings across a range of vehicles and journey scenarios it was designed to be flexible such that the same simulation could be applied to a range of vehicles including, for example, a small car, a large family car, a mini-bus and a coach. Accordingly the simulation needed to include a sufficient level of detail to produce meaningful results whilst at the same time avoiding any extraneous complications. For example some intricate details of powertrain systems, such as clutch slip during take-off / gear changing were simplified as described in this chapter. Whilst such powertrain details are of technical interest, within the broad scope of this study the simplification of some aspects was considered reasonable.

4.1.3 Drive Cycles used

For the work described in this chapter simulation results were compared with manufacturers' data so it was appropriate that an industry standard journey profile or

driving cycle was used. As discussed in 3.12 the standard journey profile used by vehicle manufacturers to ascertain fuel efficiency and emissions data is the New European Driving Cycle (NEDC). This cycle consists of two distinct sections. The first section represents a notional journey in an urban area with low peak speeds and frequent acceleration and deceleration. The latter region is intended to represent an extra-urban journey. The two parts of the cycle are used independently to establish fuel efficiency and emissions data for urban and extra-urban scenarios, and together to establish data for combined usage. The NEDC profile is shown in Figure 4.1.

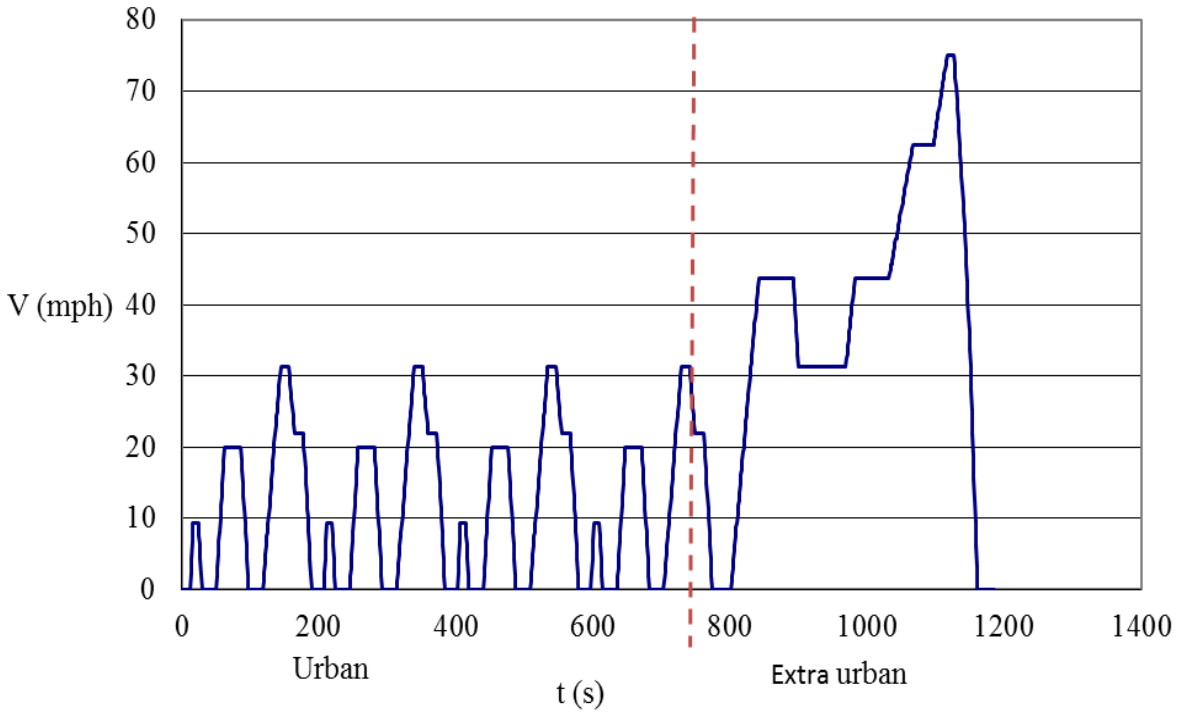

Figure 4.1: Plot of *v*, (vehicle speed) against t (time) for the New European Driving Cycle (NEDC) (from www.ecotest.eu).

The Artemis Drive Cycle has also been developed as a more realistic cycle and is used by some manufacturers and consultancies but is not currently an official government standard. Andre (2004) describes the development of the Artemis cycle which is based on real road data evaluated using statistical analysis.

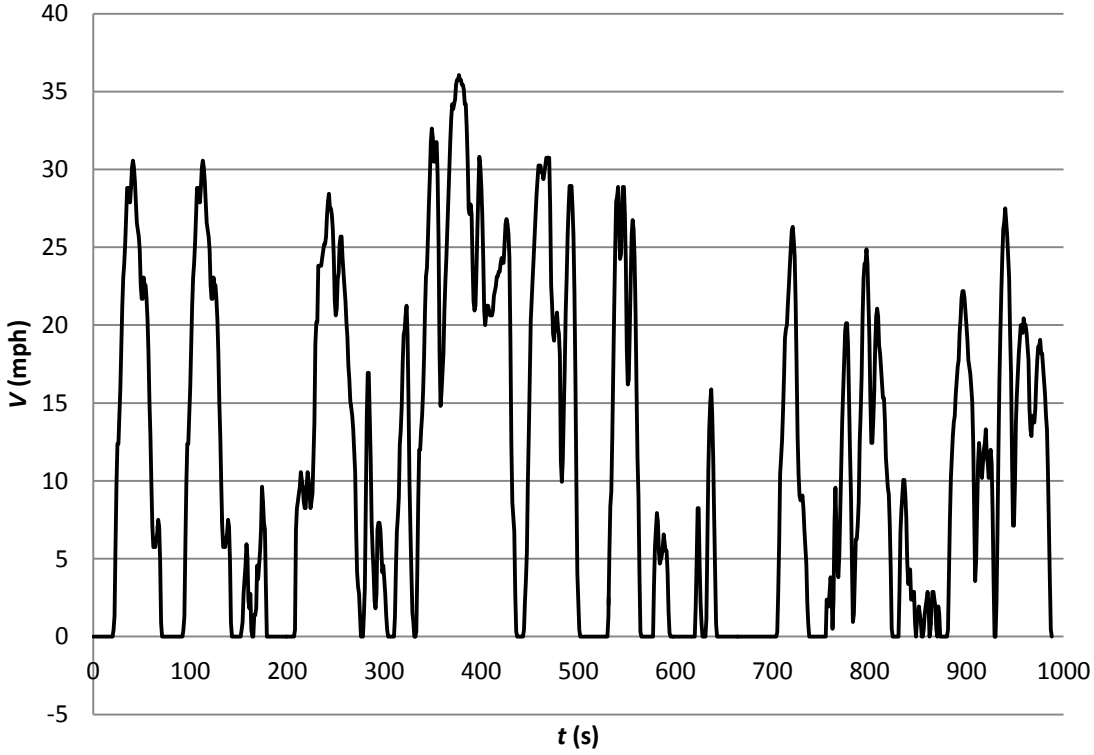

Figure 4.2: Plot of *v* (vehicle speed) against t (time) for the Artemis Urban Cycle (Andre, 2004).

For the practical validation of the simulation, actual speed / time data sets were recorded from a range of journeys with test vehicles to allow comparison between actual fuel consumption and simulation results for the vehicle under test. It was not possible to do this for many vehicle types but a practical validation on several vehicles gave some indication of the simulation's realism as outlined in 4.5 & 4.7.2. In Chapter 5 the simulation was used with NEDC & Artemis cycles and in Chapter 6 the MLTB cycle. The MLTB is based on real speed *vs* time data recorded on a working London Bus, operating on Route 159 (Streatham – Oxford street – Whitehall) (Lowcvp, 2015).

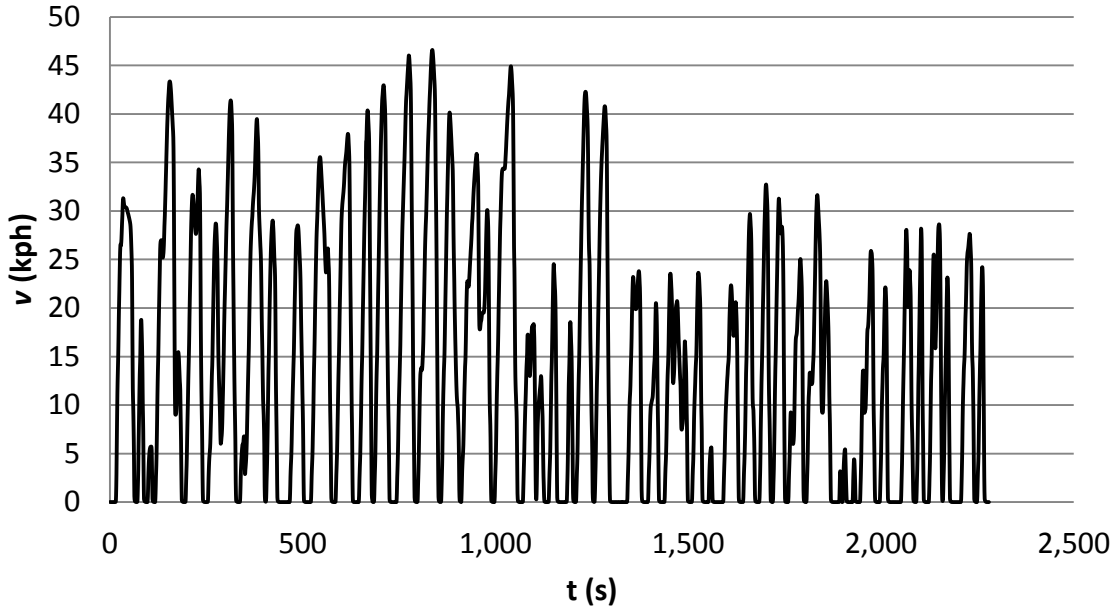

Figure 4.3: The MLTB cycle (TfL 2009) Plot of vehicle speed *v* (kph) against time t (s)

As the simulation was developed, it was applied to urban, extra urban and combined cycles for a range of vehicles. Validation work was initially by comparison with manufacturers' data and later with drive cycle data recorded from example road journeys. Further comparison was made against independent test data provided by TfL (2015) for 'bus 1'considered in chapters 5 and 6.

Initially the standard New European Driving Cycle (NEDC) was used to validate the calculated energy usage against published fuel economy data for a several domestic vehicles types. Since this cycle is currently used to determining the published fuel consumption and CO_2 emissions figures for new vehicles, this was an appropriate comparison. For assessing the fuel energy requirement for other vehicles such as buses, coaches and HGVs, a large range of other appropriate cycles exist as detailed by Barlow *et al* (2009). For the emissions simulation work on buses described in Chapter 6 bus scenario the MLTB was used.

4.2 Initial Development Work

4.2.1. Calculation of vehicle performance and validation of simulation

Before describing the detail of the simulation work undertaken to address the research aims, the principle forces acting on a road vehicle are defined in Figure 4.4 below.

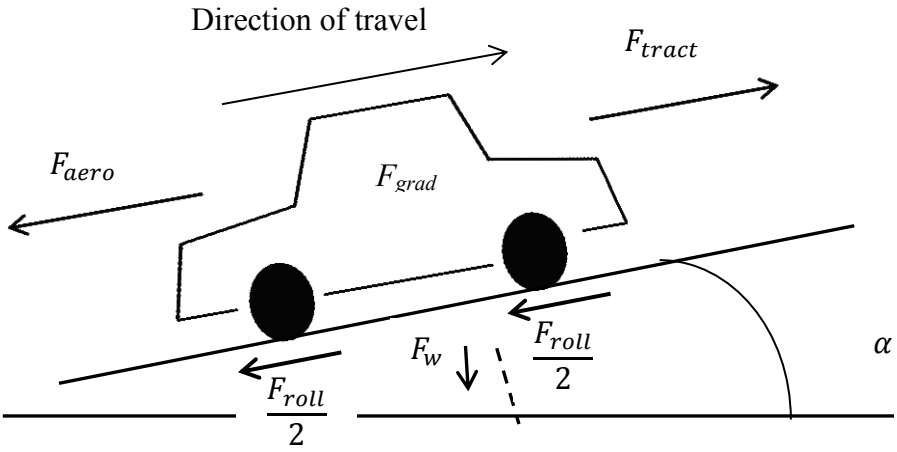

Figure 4.4: Forces acting on a vehicle.

F_{tract} = Traction force (N)

F_{aero} = Aerodynamic force (N)

F_{grad} = Force due to gradient (N)

F_{roll} = Total Force from rolling resistance (N)

F_w = Force from vehicle weight (N)

The calculation of vehicle performance within each time step of the simulation relies on data from the previous time step and on a range of vehicle specific data, particularly engine torque / engine speed, all gear ratios wheel and tyre size. Aerodynamic data is also required, specifically the vehicle drag coefficient and frontal area. The frontal area for particular vehicles is rarely quoted and, in most cases was estimated from vehicle dimensions. General parameters such as the vehicle weight and rolling resistance were also required. Some data was available from manufacturers or independent sources however, it was often necessary to make informed judgements for values based on a range of literature. The vehicle data used in each simulation is shown in Appendix I. The performance was then calculated using Newtonian laws of motion, conservation of energy equation and appropriate equations to allow for aerodynamic forces, rolling resistance and forces due to gradients. Within each step a constant rate of acceleration is used and the average velocity is calculated which is used to determine the distance travelled during the time step. Initially

a time increment of 0.1s was chosen to provide adequate resolution in the calculations whilst allowing for quick processing. A detailed study into the effects of time-step length is included in section 4.4. Before developing the simulation ultimately used to investigate the research question a preliminary model was produced to validate that the general principles being applied would output realistic vehicle performance. This early work is outlined in Appendix I.

The principal resistive forces on the vehicle were calculated using the following widely used equations:

$$F_{aero} = C_d \frac{1}{2} \rho V^2 A \qquad (4\text{-}1)$$

Where: C_d = drag coefficient
ρ = density of air
V = velocity
S = Frontal area

Limitations of this formula are as follows: The formula relies on the drag coefficient, C_d, based on either manufacturer's data or an approximate figure for a generic shape or style of vehicle body. Some typical values for C_d are shown in Figure 4.5.

Vehicle type	Drag Coefficient
Typical early car (pre ww2)	0.7 - 0.9
Toyota Prius	0.26
Vauxhall Vectra	0.29
Typical Bus	0.6 - 0.8
Typical Truck	0.8 - 1.0
Typical articulated Truck	0.96

Figure 4.5: Typical approximate vehicle drag coefficients (from: www.engineeringtoolbox.com 2012).

The exact frontal area is difficult to measure and for the simulation work undertaken this was estimated from the dimensions quoted by vehicle manufacturers (i.e by multiplying quoted width by height). Whilst this is a reasonable approximation for buses, for vehicles of non-rectangular cross section, photographic / graphic methods will provide a more

accurate estimate. Air density varies with height above sea level and this should be taken into account when undertaking simulation work involving vehicles used at high altitudes. Next, rolling resistance is considered.

$$F_{roll} = C_{rr} F_n \quad (4\text{-}2)$$

Where: C_{rr} = Coefficient of rolling resistance
F_n = Force normal to the direction of travel = $m_v g$ (m_v = vehicle mass, g = gravitational field strength)

Limitations of this formula are: Rolling resistance data is not always readily available for particular tyre types and in many cases an estimate based on generic figures has to be used.

Therefore, rolling resistance = $C_{rr}\, m_v\, g$ (4-3)

Resistance due to gradient = $\sin \alpha\, m_v g$ (4-4)

Where: α = angle of gradient

For initial simulation work the road was assumed to be level with no gradient, however a feature was introduced to allow gradient profiles to be included in the simulation. Using an engine torque vs speed relationship as described in appendix II maximum acceleration and speed performance was modelled for a Citroen C1, Volvo C70 and 17 seat LDV mini-bus and compared with manufacturers' data. Figure 4.6 shows these initial results.

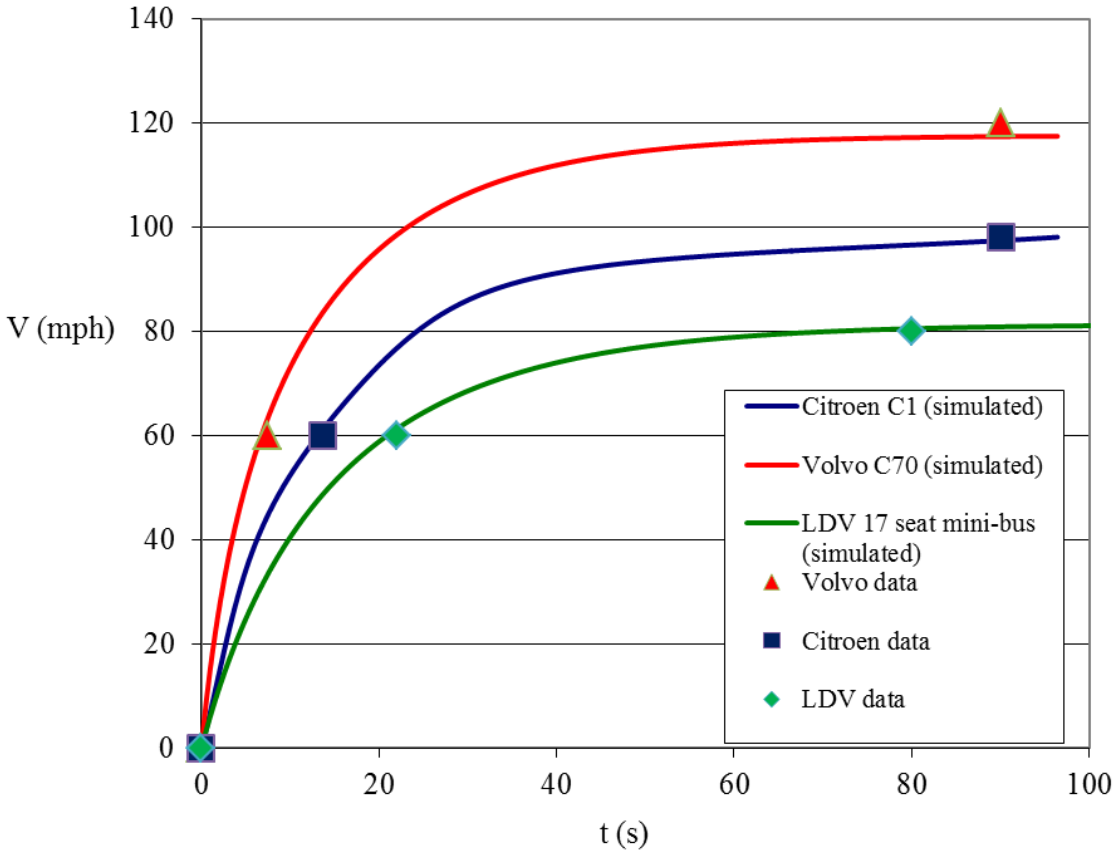

Figure 4.6: Simulated acceleration times for different classes of existing conventional vehicle.

4.2.2 Discussion of 0-60 and maximum speed results

These initial results gave some degree of confidence that the simulation could give a realistic indication of vehicle performance in terms of maximum and peak speed. Possible reasons for the small differences between simulated and quoted performance data include the following:

(i) Limitations of data used in the simulation

Some vehicle data is approximated and based on sources other than the vehicle manufacturer. Most car companies for example will not reveal the drag coefficient on their cars (unless it is outstandingly low and can be used for marketing as with the Mercedes Intelligent Aerodynamic Automobile (Barry, 2015). Generic 'typical' data tables are available showing figures for different general types of vehicle, saloon car, estate car, bus, van and truck. The accuracy of these figures is questionable and for a more thorough test

of the simulation, accurate drag coefficient figures from experimental work would be needed. These difficulties also apply for vehicle rolling resistance. Existing research carried out by Clark and Dodge (1979) provides useful data in this area but it also gives insight into the complexities involved and the need for establishing coefficients from experimental work. For the initial simulation work carried out in this project however the simplified equation was regarded as being acceptable. Other issues were more problematic:

(ii) Instability of polynomial function close to maximum speed

A polynomial function was required to achieve a representation of the tractive effort / speed relationship. The equation was generated by the Excel trend-line feature to fit a manually smoothed 'best fit' curve following the data calculated from engine torque and vehicle gear ratios. This smoothed line did not precisely follow the actual data and it was simplified in order to make it possible to fit the polynomial equation. It was also found that in one case near the maximum vehicle speed, the polynomial graph showed an exponential increase. If the simulation calculated a maximum speed above the expected figure the acceleration and speed all increased exponentially which rendered this particular version of the simulation unusable.

(iii) Lack of flexibility

Another limitation of this simulation becomes apparent if it is necessary to run the simulation with some change in vehicle power train characteristics, i.e. different engine torque characteristics or gear ratios. This requires plotting a new approximated torque / speed relationship and fitting a new polynomial equation. The shortcomings of this method for defining the relationship between vehicle speed and tractive effort meant that although it had provided a useful starting point and shown that vehicle acceleration could be modelled to an acceptable level of accuracy it was clear that a more detailed model was required.

Version 1 of the simulation described in 4.1.2 was developed as a forward looking model. The reason for initially choosing a forward looking approach for simulation work was to allow for the possible study of driver aggressiveness. At the beginning of this project it was considered that driving style might be studied in some depth and the inclusion of a driver model using PID control may facilitate such investigations. However, as determined by Horrein *et al* (2012) and others there are advantages to the backward looking model and

later versions 2 & 3 of the simulation were developed as a backward looking configuration since as the focus of the project settled upon those outlined in Chapter 2 the driver model was not essential. The development of the forward looking simulation provided useful insight into the various subtleties of vehicle modelling which might not have been apparent when using an established commercial package. This version is useful for calculating vehicle performance characteristics (0-60mph, maximum speed etc.). This last feature is particularly useful if the simulation is to be used for downsizing studies and comparison of performance characteristics between standard vehicles and those with down sized power-plants.

4.3 Development of the Version 1 Simulation (Ver. 1)

This version of the simulation used the engine torque characteristics from published manufacturers' data (or independent results) along with other relevant vehicle data as the starting point for all the vehicle performance calculations. The final calculations that determine the speed and acceleration of the vehicle in each time step are the same as in the first simulation. The main difference is the way in which the gross tractive effort at each time step is calculated. Rather than being calculated from a large polynomial equation (based on tractive effort/vehicle speed under optimum acceleration conditions) the tractive effort is calculated from the engine performance data, the gear ratios and other relevant transmission data. One key difference with this simulation is the requirement to follow a given journey profile, that is a speed / time profile of either a simulated journey (such as the NEDC) or a real journey. In the latter case, data of speed / time would have to be recorded during a real vehicle journey then entered into the simulation.

4.3.1 Simulating Clutch Slip

Various detailed clutch models are discussed in Chapter 3. For this work a simplified approach was taken using a logic statement which stated that if the vehicle speed was below a certain threshold (which can be manually set) then the engine speed defaults to a pre-determined (and easily adjustable) 'clutch slip' speed. This allows the starting to occur in a way that approximately represents real driving. This could be refined by monitoring actual engine speeds and vehicle speeds during initial starting for a range of vehicles and basing the settings on the results. Once the simulation accelerates above 'clutch slip' speed the engine speed is calculated from road speed, gear selected and appropriate transmissions ratios.

4.3.2 Simulating driver throttle response

The forward looking nature of this version requires a throttle position during each time-step – effectively a driver model. A first attempt at a simplified linear proportional throttle response performed poorly and was superseded by PID control function.

The overall architecture of the simulation is most clearly represented using a flow chart format. Figure 4.7 shows an overview of the algorithm that was developed for this version of the simulation. This chart only shows the conventional vehicle simulation. The development of this was refined and results checked against manufacturers' vehicle performance data and independent test data before the regenerative braking and energy storage sub-routines were added in order to address the main questions posed.

Figure 4.7: Flow chart of Ver. 1 Simulation with PID control and BSFC incorporated

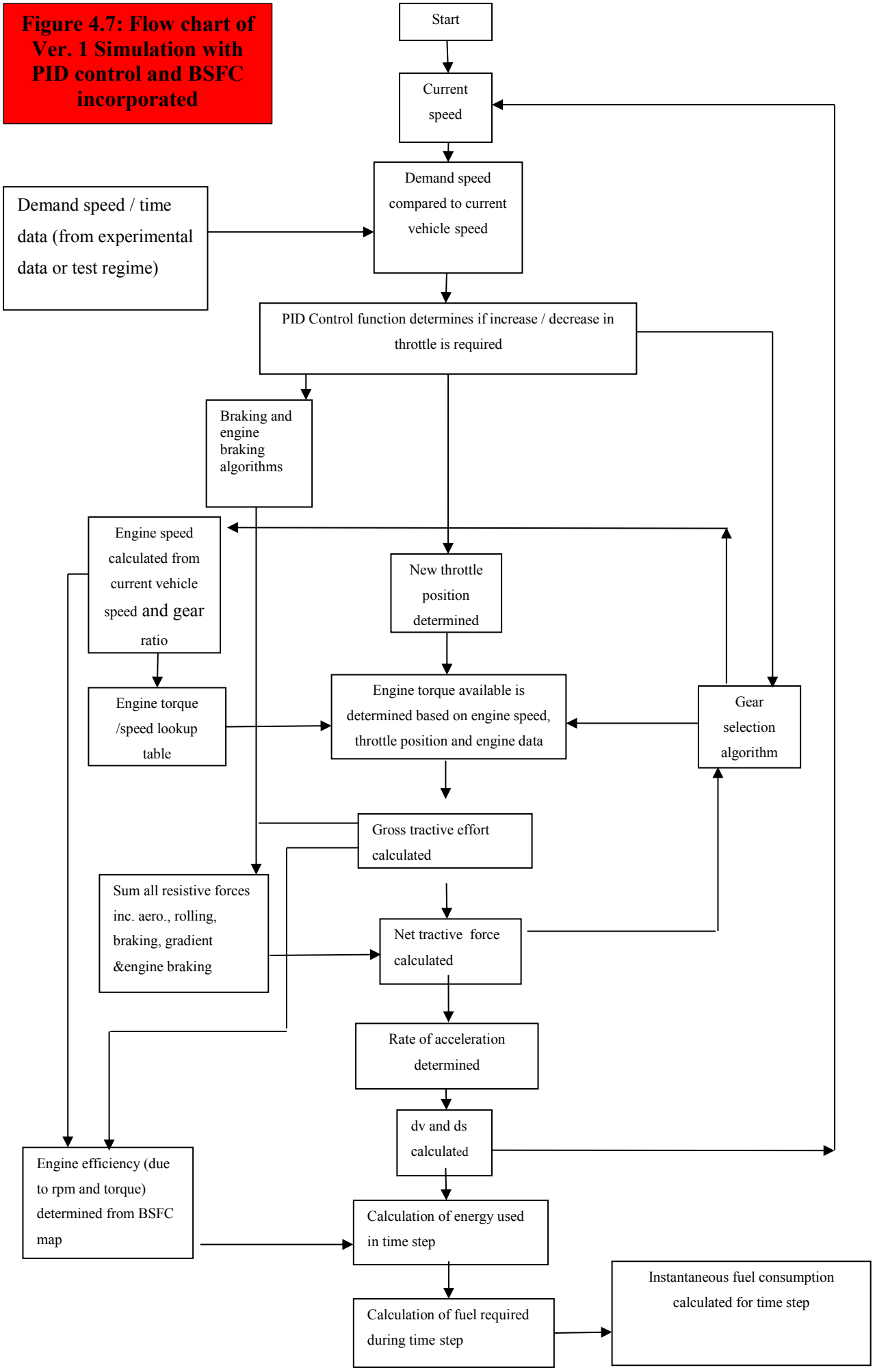

4.3.3 Simulating gear changes

Calculating tractive effort from available engine torque requires knowledge of the overall transmission gear ratio. To achieve this either a gear changing sub-routine was required or a gear changing profile for the whole journey. In the case of the NEDC a gear changing regime (see appendix II) is specified so this feature was disabled for NEDC simulation and the time-based gear changing regime was simply copied into the relevant column. The algorithm used involved a series of nesting logic statements and constants for the engine speed at which a 'down change' was required and the engine speed at which an 'up change' was required. The variables 'change up speed' and 'change down speed' were referenced to remote cells and could easily be adjusted. Changing these two variables allows for the effect of different driving styles to be explored if required. The detail of the logic used in simulating gear changes is shown in the flow chart in Appendix III. An example plot of the gear selected against time (along with road speed and throttle position) during the Artemis road cycle to test functionality is shown in Figure 4.8 (a) & (b). In this version gear changes are assumed to occur instantaneously.

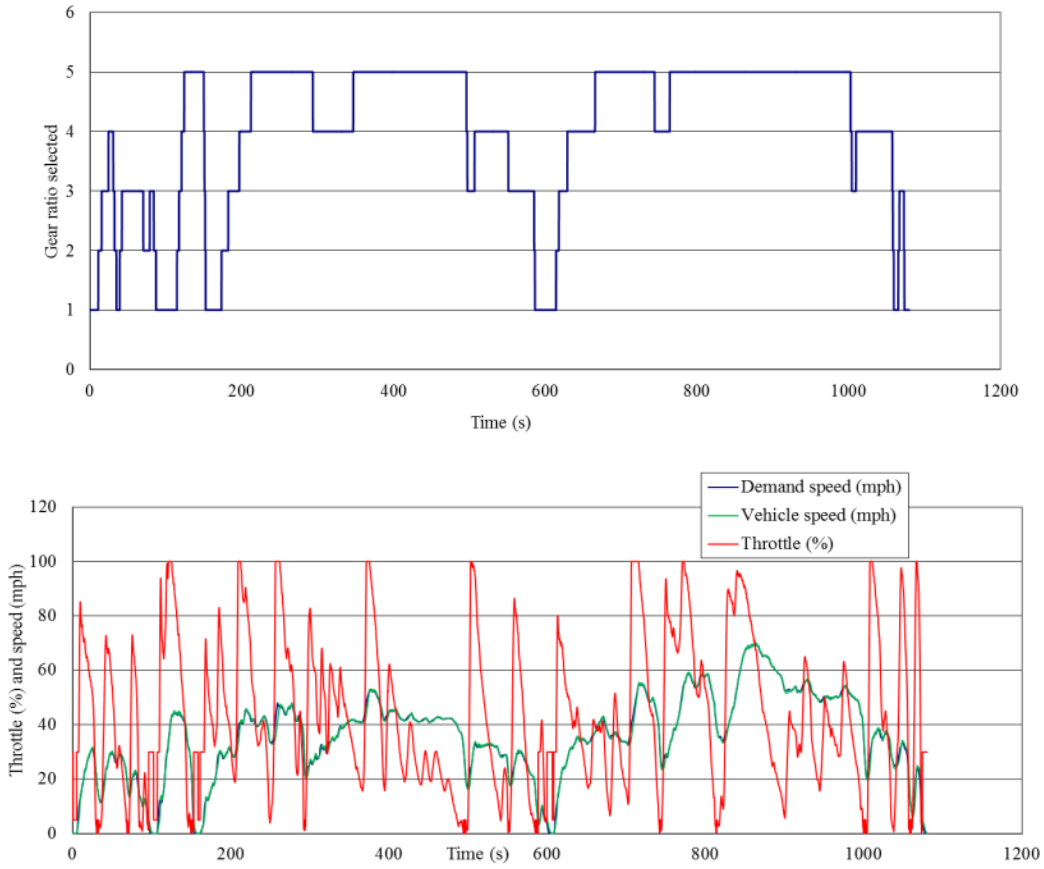

Figure 4.8(a) (Top): Gear changes during the simulated Artemis Road cycle for a Citroen C1 (1.0 l) Chup =3000 rpm Chd = 1500 rpm
Figure 4.8(b) (bottom): Demand speed, vehicle speed and % throttle for the same journey.

4.3.4 Engine braking

Before the introduction of PID control a simplified approach was adopted to account for engine braking where a constant braking force was applied if the vehicle speed exceeded demand speed.

$$If(v_{sim} > v_{demand}), (F_{engbr} = F_{engbrconst}), = F_{engbr} = 0 \qquad (4\text{-}5)$$

With PID control, engine braking was calculated based on the control term and limited to a maximum estimated from engine size. A more realistic method would involve an estimation based on a Willans line where sufficient engine data is available.

4.3.5 Mechanical braking

In addition to engine braking, mechanical (friction) braking was required in the conventional powertrain simulation to deal with larger deceleration rates than could be caused by engine braking alone. In real driving situations a careful driver will apply pressure to the brake pedal in proportion to the required rate of deceleration. In the first instance the braking force, F_{brake}, was defined as shown in equation 4-5 where a simulation over-speed beyond a set level, $F_{brakelim}$, triggered a constant braking force, F_{brake} , to be applied.

$$If\ \left((v_{sim} - v_{dem}) \geq B_{brakelim}\right), \mathrm{F_{brake}}, 0 \qquad (4\text{-}6)$$

This variable $B_{brakelim}$ was referenced to a remote cell and could be altered readily. This oversimplified approach proved inadequate for acceptable following of a demand speed. Proportional braking was introduced, firstly with the use of a linear braking response look up function. Performance was still inadequate and subsequently full PID control of braking was introduced. One control term was used for the throttle and brake control inputs effectively forming a basic 'driver model'.

4.3.6 Calculation of energy used

In early development work, to calculate the instantaneous mpg Figure during each time step the fuel energy required in the time step, E_{fuel}, was calculated by multiplying the

gross force by the distance travelled during the step, and dividing the result by the vehicle engine efficiency.

$$E_{fuel}(J) = \frac{F_{gross}\delta.s}{\eta_{eng}} \quad (4\text{-}7)$$

This was refined to more realistically take account of fuel energy requirements during initial acceleration from a standstill where the clutch slip condition applied.

$$E_{fuel}(J) = \left(\frac{\omega.T\delta.t}{\eta_{eng}}\right) + E_{idle} \quad (4\text{-}8)$$

Further calculations dealt with metres travelled per Joule of energy used. Using the calorific value of pump petrol, this was then converted to km/l and mpg to give an indication of instantaneous mpg. Average fuel consumption figures were calculated from cumulative fuel energy required over a given distance. Engine efficiency was determined from a lookup table based on engine torque and engine speed.

4.3.7 Brake specific fuel consumption

A limitation of the simulation in terms of the realism of energy conversion by the vehicle was the specific efficiency of the ICE. Vehicle manufacturers do not generally release data relating to engine efficiency but from engine dynamometer tests carried out within the Department of Engineering, Design and Mathematics a Figure of approximately 25% is a typical Figure for an early 1990's petrol car engine (Rover 1.4 K series). Based on a range of engines for which BSFC data could be obtained a generally accepted figures for car ICEs range from 25 – 32 % efficiency for petrol engines and from 36 to 41% for diesel engines (estimates based on data from Stone (1989), Reif,(2011) and eco-modder.com (2014)). In the absence of a detailed engine model, engine efficiency can be determined from engine speed and torque with an appropriate look–up table. An example Brake Specific Fuel Consumption (BSFC) plot relating engine torque and speed to fuel consumption is shown in Figure 4.9 below.

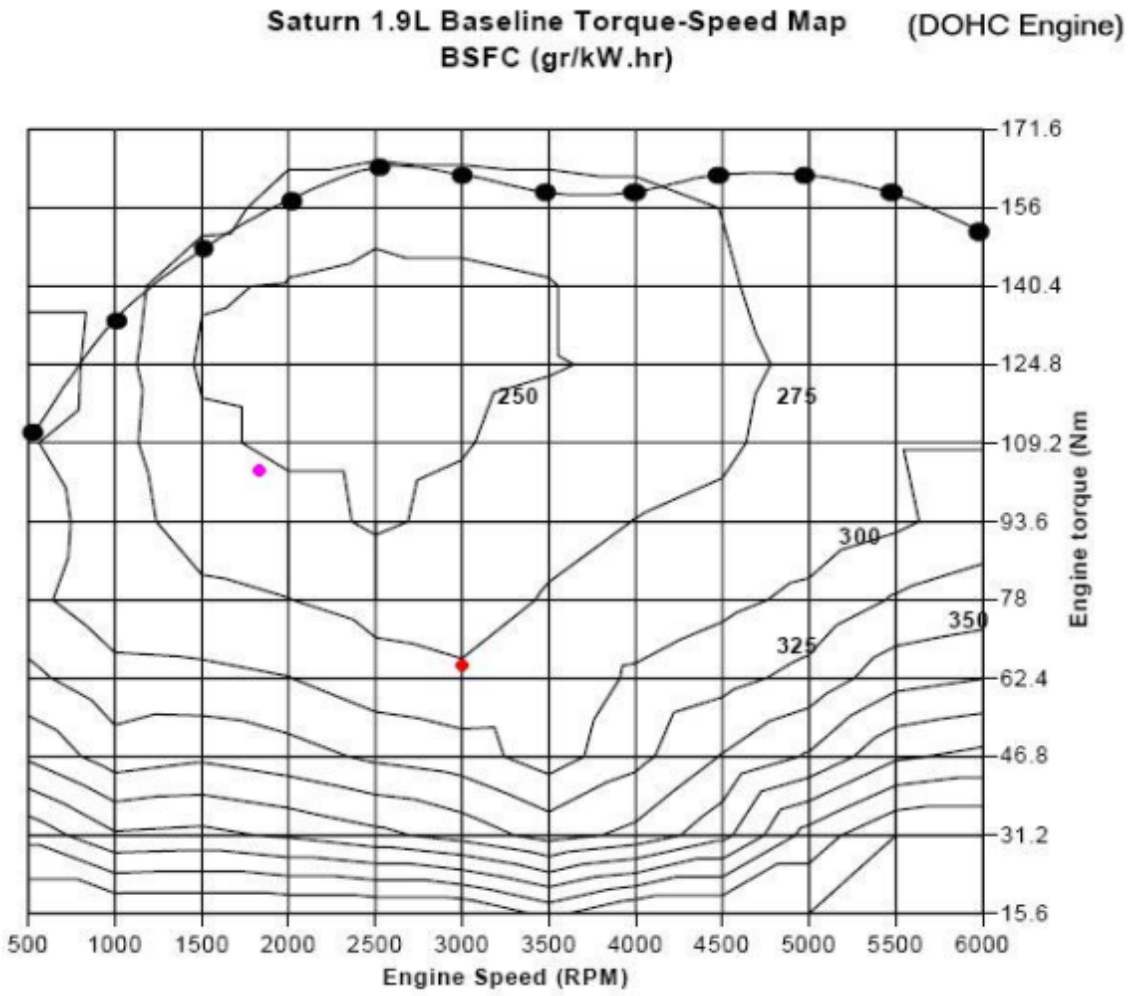

Figure 4.9: An example brake specific fuel consumption plot for a mid- sized car: Saturn 1.9 DOHC petrol engine (ecomodder .com, 2012).

A limited number of BSFC plots are available on-line and from text books but it is difficult to obtain specific data from manufacturers. In response to this the author has adapted and scaled a typical BSFC plot (such as that shown in Figure 4.9) in terms of engine speed and torque to effectively adapt the general characteristics of the map to enable use for a range of petrol vehicles. BSFC data for a range of engine types was available from ADVISOR look-up tables and enabled the closet match to be chosen in each case such that any required scaling was kept to minimum. As shown in Figure 4.9 engine speed has a significant effect on efficiency. For example, at a torque output of 90 Nm, a doubling of engine speed from 2500 rpm to 5000 rpm increases the rate of fuel burn from 250 g/kWh to 300 g/kWh (an increase of 20%). Because engine efficiency is so dependent on engine speed and torque, driving style (which includes engine speeds at which gear changes take place) can have a significant effect on energy use. The forward looking model described in this chapter allows this aspect of driver behaviour to be investigated by adjusting $\omega_{upshift}$ and $\omega_{downshift}$ along with other parameters such as thr_{clutch} (the simulated

throttle response during clutch slip conditions). In addition it is possible to alter the PID terms to alter the responsiveness and reactiveness (or over-reactiveness) of the simulated driver and alter the driver metric of aggressiveness. The driver model inherent in a forward looking model increases the complexity of the simulation but also the range of useful work that can be conducted beyond that which is possible with a backward looking simulation.

4.4 Effect of Time Step Length on Simulation Results

When conducting validation trials (described in section 4.5) a useful comparison study could be made between fuel consumption data recorded on a test journey and data generated from the simulation when it was run using the speed vs time journey profile recorded on the test journey. One difficulty encountered was that, when logging a number of parameters, the data acquisition software would only record data at 1 sample per second rather than the 10 Hz used in the simulation. It is easy to change the time step length *(δt)* in the simulation to 1s rather than 0.1s. However a ten- fold increase in time step length was likely to cause difficulties with the smooth running of the simulation.

During the early stages of the simulation development a time step interval of 0.1 seconds was chosen as a compromise to enable smooth plotting of journey speed vs time profiles without resulting in overly long and cumbersome spread sheet pages.
Later, when a backward looking simulation was developed and a wider range of journey profiles was investigated, it became apparent that the speed against time data for the more realistic and less idealised journey cycles such as the Artemis and EPA cycles was only available in 1 second steps. Ultimately to produce the results shown in chapter 5 these data sets were interpolated to give speed against time with time step $\delta t = 0.1$ s. Once a method for interpolating the journey profiles data had been establish a check was made on the effect of time-step length.
To establish the effect of time step length on the simulation performance a test was undertaken where the fuel consumption in mpg from running the simulation with 0.05, 0.1 0.5 and 1 second time steps was calculated. This was undertaken using the forward looking simulation with the Citroen C1 1.0*l* details entered. The results from this study are shown in figure 4.10 and 4.11.

dt (s)	1.00	0.8	0.50	0.20	0.10	0.05	0.01	0.0050	Citroen quoted
NEDC mpg	45.38	48.05	55.87	57.96	59.18	60.57	60.25	60.01	65.70
Urban mpg	40.44	42.75	47.64	48.38	50.36	51.88	51.60	51.84	55.40
Extra urban mpg	48.92	51.91	62.25	65.57	65.95	66.82	66.84	66.12	74.30

Figure 4.10: Results from the time step length study over NEDC

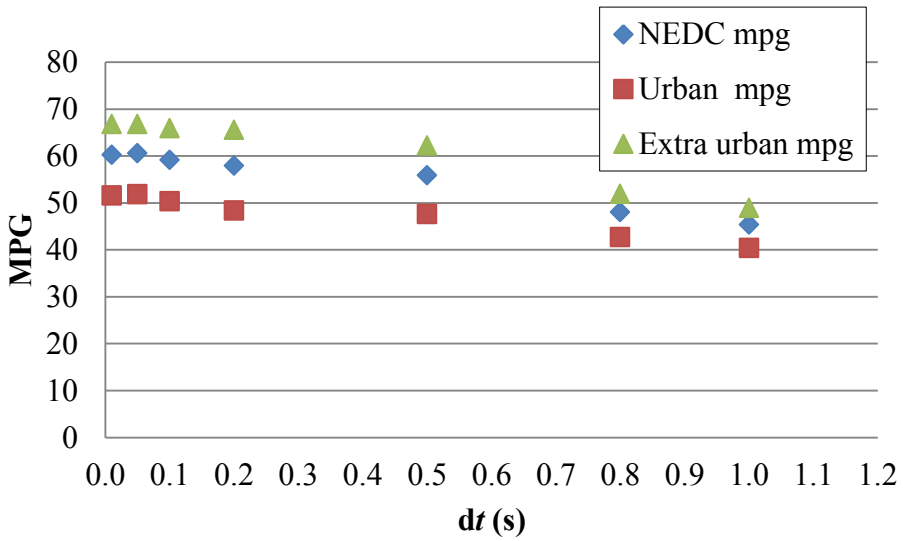

Figure 4.11: Results from the time step length study showing all 3 parts of the NEDC

Figures 4.10 & 4.11 illustrate the influence of time step length on fuel mpg results. Since the results converge as timestep decreased and 0.1 s interval represented a compromise between resolution and convenience of use.

4.5. Validation of Version 1 Simulation

Validation was carried out by comparison with manufacturers' data (for NEDC) as described in 4.5.1 along with long and short term road trials. In long term trials (4.5.2) Torque pro was used to record GPS speed vs time as the car was not OBD (On Board Diagnostic) compatible. On short term trials (4.5.3) the OBD Torque Pro app was used to monitor fuel consumption.

The Torque Pro app was chosen because it was not possible to modify a test vehicle by fitting necessary sensors to measure road speed, engine speed and fuel flow. For validation trials a 'non-intrusive' data monitoring system was required that could be readily set up on any particular test vehicle. Other systems that could have been used include Diagra and Rebel however these were not available to the author. Torque pro uses the OBD (On Board Diagnostic) port that is fitted to all production vehicles built post 2002. A small interface

unit is plugged into the port that can record the parameters that are continuously monitored by the vehicle's built in diagnostic system. This interface uses Bluetooth technology to communicate with the smartphone on which the Torque app is installed and running. The TorquePro app in combination with the OBD Bluetooth interface is purely a monitoring facility and does not allow any changes to be made to vehicle systems.

The benefits of Torque Pro include the ease and simplicity of set up and data capture, the fact that existing on-board monitoring 'built in' sensors are employed and the resultant low cost. An additional attraction is the fact that the smartphone GPS feature is used to monitor vehicle speed from GPS data in addition to any data monitored from the vehicle via the OBD Bluetooth interface. This is useful when logging speed against time data from journeys using a vehicle without an OBD facility. This feature gives the possibility for useful speed vs time data to be acquired for any journey with any vehicle. Limitations include data logging rate, data file size and the level of precision in recorded measurements.

4.5.1 Comparison against published manufacturers' data

The development of the simulation tool was carried out in several stages with evaluation of initial results at each stage as refinements and improvements were introduced. Initially comparison was made between simulation results and vehicle manufacturers' performance data. However, as discussed in sections 3.11 and 3.12, fuel efficiencies claimed by manufacturers for particular vehicles are not always achieved in real world use. A summary of initial validation results is shown in appendix IV.

Further validation work was carried out on a series of short and long term road trials. In addition, bus simulation results were compared with fuel consumption data from independent industrial trials provided by TfL.

4.5.2 An example validation test of vehicle model with respect to fuel consumption (long term trial)

GPS speed vs time data was recorded using the Torque Pro software between N.W Bristol and Minety in Wiltshire. This is a journey that was undertaken daily for 6 months between

April and September 2013 in the 2002 Citroen Xsara 1.4 referred to in section 5.2. An example speed against time profile for the journey is shown in figure 4.12. Several such recorded journey cycles were used to evaluate that the forward looking simulation could follow a realistic profile and predict fuel consumption adequately. The demand speed is the recorded speed / time data from the journey studied.

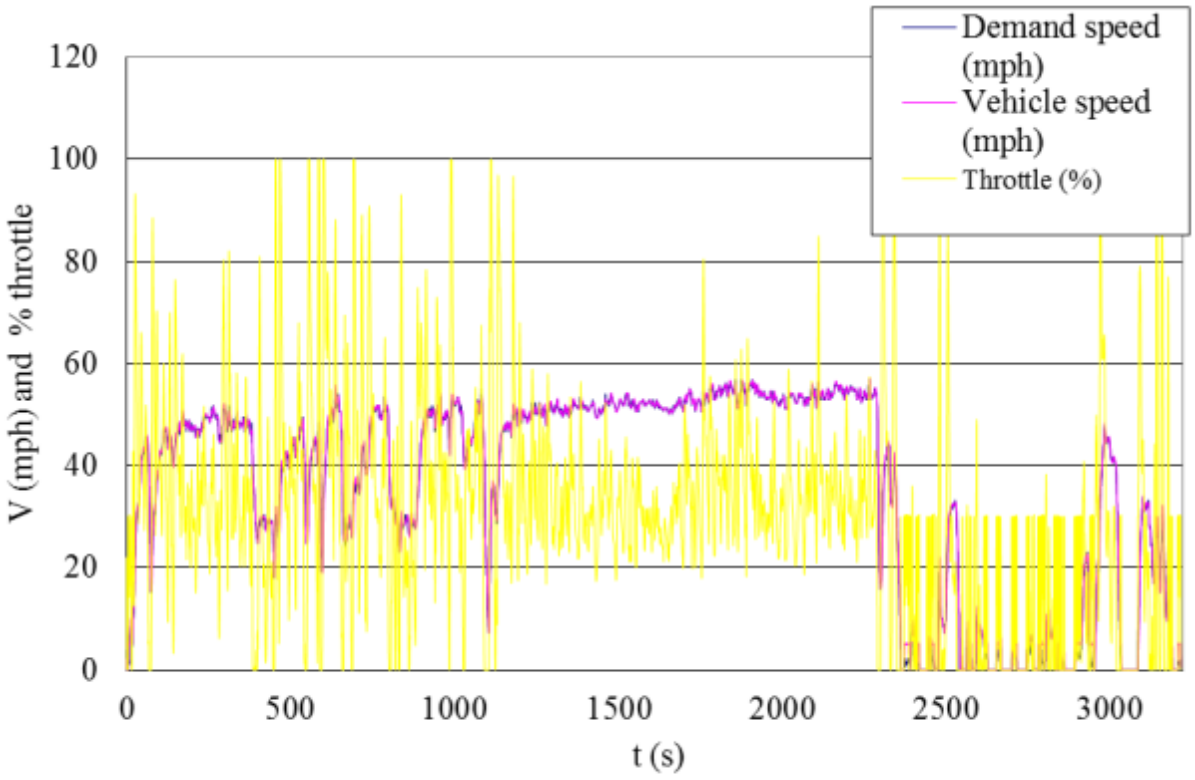

Figure 4.12: Speed against time data (recorded) for extra urban commuting journey between Bristol and Minety (Wiltshire) used as demand speed with simulated vehicle speed and throttle shown for Citroen Xsara 1.4l

The journey represented in Figure 4.12 is illustrated by the map shown in Appendix V. Once recorded, the speed vs time data was entered into the simulation in the 'Demand Speed' column. Since the data recording interval and simulation time step length were both 0.1 seconds the data could be copied straight into the simulation. For the 6 months period, fuel consumption was monitored by logging mileage and fuel used between refills (fill to fill). Long term average fuel consumption could then be calculated for a known journey with one driver with driving style kept consistent as far as practicable. The average fuel consumption over the 6 months was 45.2 mpg. When the Citroen Xsara was modelled in the version 1 simulation (using scaled BSFC data), the fuel efficiency calculated over this journey was 46.71mpg - a difference of 3.8%. It is interesting to note that the comparison

between quoted and simulated mpg data for this model of car vary by a greater amount than the comparison made here between a real journey (where data was recorded for a speed against time over a journey) and simulated fuel consumption over this journey. These findings gave some confidence in the model's realism for this scenario and indicated that the scaled BSFC data was rather better matched for the Citroen Xsara than for the Citroen C1.

4.5.3. Short term validation trial - OBD measurement of fuel consumption on specific real-world journeys for comparison against simulation

The VW Polo 1.2 l petrol (2004 model) was used on a test route local to UWE which included a number of junctions and a range of 30, 40 and 50 mph speed limits. A vehicle profile for a 1.2 VW Polo was set up in the torque pro app. This included data such as the engine capacity, vehicle weight and various other parameters which were used with the measured values to generate some of the non-directly measurable values such as power and torque. Three repeat runs were made in lunchtime traffic and a complete log of the journey data was recorded.

Weather conditions during test were as follows:
Temp: 8 ˚C
Wind: Light breeze < 5kt
Precipitation: None
Rel. humidity < 40%

Journey log files were downloaded to PC via a USB link as .csv files. for use in MS Excel. The recorded speed vs time data could be used for the 'demand speed' in the simulation to compare simulation performance (fuel consumption) could be checked against the recorded vehicle data.

4.5.4 Simulated fuel consumption over a recorded journey profile

With the simulation running, it was possible to evaluate how closely it followed the real journey of the VW Polo. Of particular interest was a comparison between the simulated and measured instantaneous mpg data (see figure 4.13). The average mpg figure over the entire journey was found to be 19.71 mpg from the simulation using the torque data determined from generic toque /speed data and 19.79 MPG when the VW based torque

data was used. The data from the OBD log gave an average of 20.84 MPG over the journey. This difference of around 5% is within acceptable limits, in terms of the overall research aims, concerned primarily with comparison of vehicle and journey types. The general agreement in average fuel consumption over the test journey is also visible in Figure 4.13 although large differences in instantaneous efficiency frequently occur. Such differences are possibly because of the complexities of fuel injection control in S.I engines compared to the simplified simulation. For the purposes of investigating the energy use of vehicles over whole journeys the instantaneous fuel consumption is not necessarily essential. A comparison between the instantaneous fuel consumption recorded from the OBD system and simulated results is shown in Figure 4.13. A map showing the test route is in Appendix V.

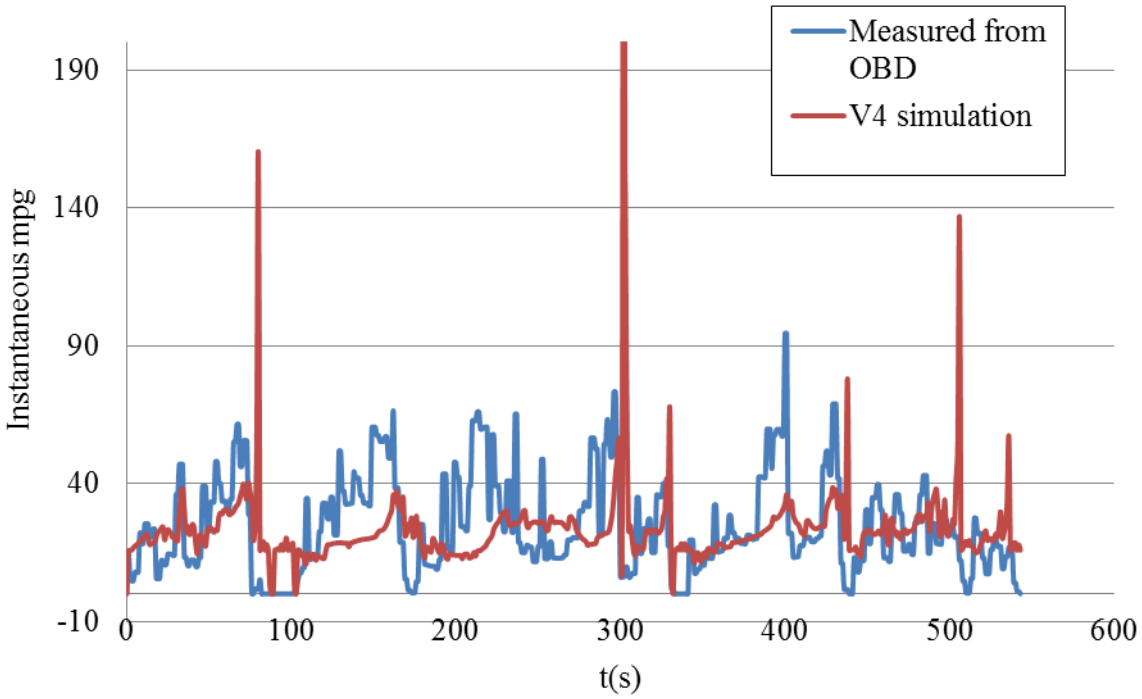

Figure 4.13: Comparison between simulated (ver.4) and recorded (OBD) instantaneous mpg vs time on Filton urban test route with 1.2l petrol VW Polo.

4.6 Incorporating a Hypothetical Regenerative Braking and Energy Storage System into the forward- looking Simulation

To enable the central research question to be addressed a regenerative braking (RB) and energy storage (ES) feature was incorporated into the simulation. A flow chart outlining the algorithm used in the Version 1 simulation to calculate possible energy savings through regenerative braking is shown in Figure 4.14.

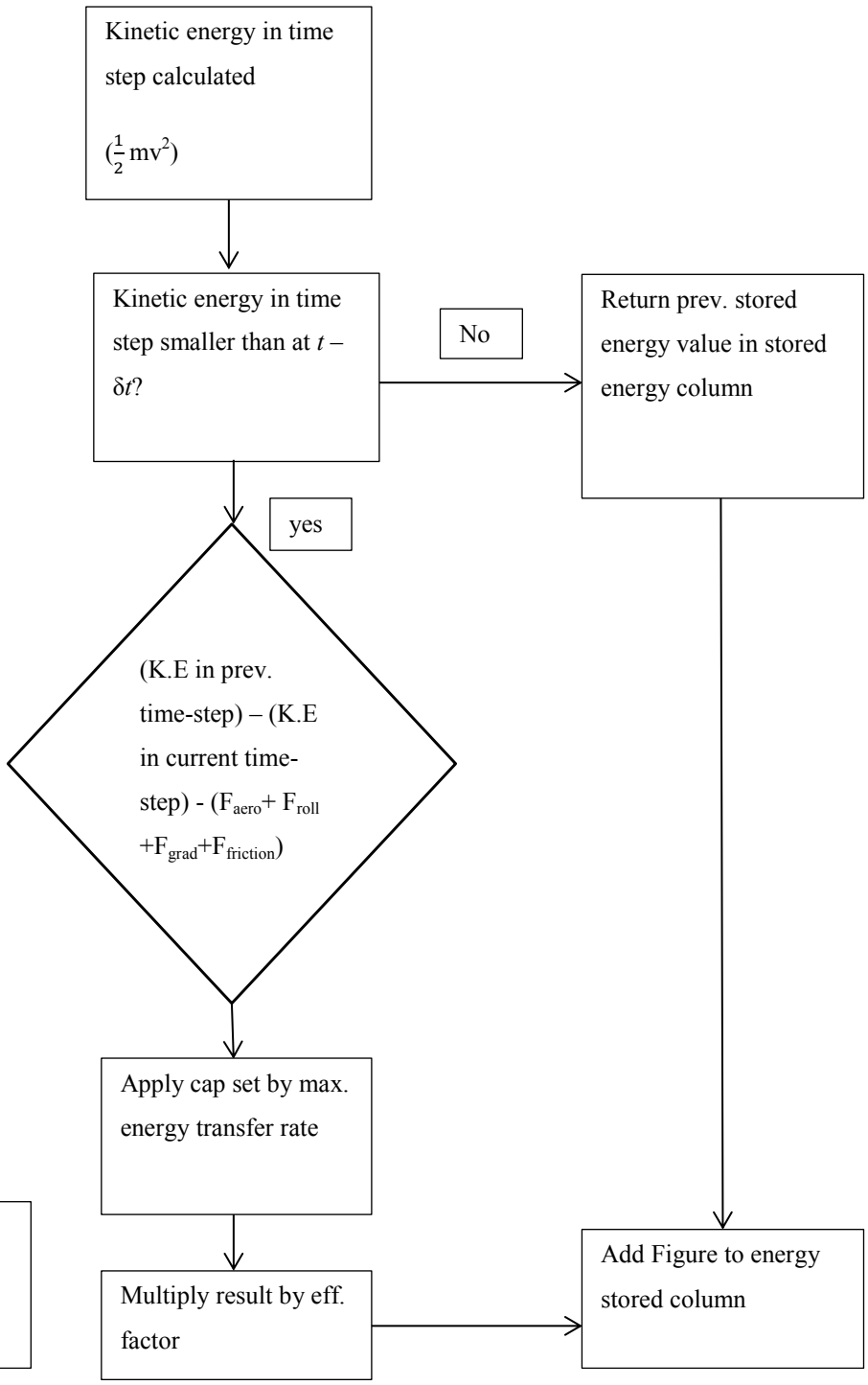

Figure 4.14: RB&ES Flowchart

This algorithm provided a simple method of introducing RB & ES and represented a parallel hybrid system. The overall efficiency factor and the maximum rate of energy transfer were both variables that could be easily adjusted. Initial checks indicated simulated energy savings over the NEDC of up to 18% on the urban and 4% on the extra urban parts of the cycle respectively. Although lower than some manufacturers claim these figures are broadly in line with research carried out by others including Baglione (2007). The regenerative braking algorithm was developed further to take into account the rate of energy transfer between the road wheels/transmission and the energy storage system in each direction and also the energy capacity of the energy storage system. The percentage

energy savings for various scenarios combinations of vehicle type and journey are explored in more detail in chapter 5.

4.7 Development of the Backward Looking (Version 2) Simulation

4.7.1 Simplified backward looking model with engine efficiency related to vehicle speed

Before including the gear changing subroutine, along with relevant gear ratios, into the backward looking model, a simplified approach to dealing with engine efficiency was implemented. This used a look-up table relating engine efficiency to road speed. The data used to generate the lookup table was based on steady state conditions so this was highly simplified although useful for steady state fuel consumption simulation, does not realistically take account of the variable engine loads imposed by the accelerations present in real journeys and standard drive cycles. Flow chart in appendix X.

4.7.2 Incorporating BSFC into the Backward - looking simulation (Version 3)

To enable the use of BSFC data in the backward looking model the gear changing algorithm used in Version 1 was implemented and gear ratio data incorporated, such that in each time step the required engine torque could be found. Engine speed and torque were then used to look-up a BSFC value from a lookup table (as in version1). In the case of the NEDC the gear regime is specified as shown in Appendix III. The MLTB cycle used for the work outlined in Chapter 6 has no gear changing regime specified. Many buses have automatic or semi-automatic transmissions. For these cases the gear changing will depend on several factors including engine load, engine speed road speed and the transmission characteristics. For this work a simplified (engine speed based) approach was used and the gear changing algorithm explained in 4.3.3 was required. Also a function relating road speed to effective tranmsission ratio was used for ‘Bus 1’ and the Optare Solo SR to approximate the behaviour of the torque convertor used when road speeds were below the torque convertor lock-up speed. The effect of incorporating the BSFC look-up vs the previous simplified relationship is shown by the instantaneous engine efficeincy *vs* time graphs in figures. 4.15 and 4.16. A comparison of fuel consumption for a the Citroen C1 (modelled with a conventional powertrain is given in figure 4.17

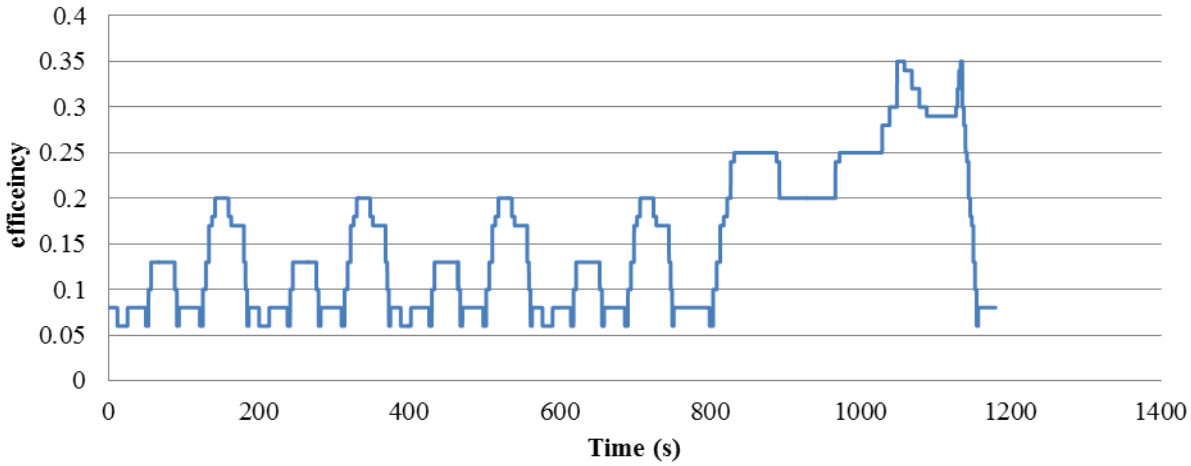

Figure 4.15: Engine efficiency vs time for Citroen C1 (1.0 l) modelled with conventional powertrain using simplified approximation of efficiency used in Version 2 backward looking simulation.

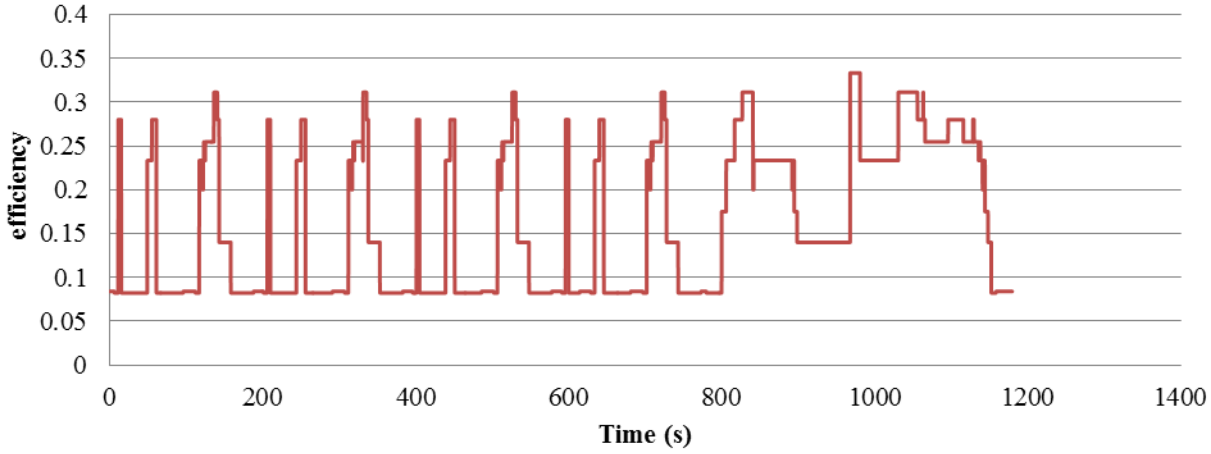

Figure 4.16: Engine efficiency vs time for Citroen C1 (1.0 l) modelled with conventional powertrain using BSFC look-up data used in Version 2 backward-looking simulation.

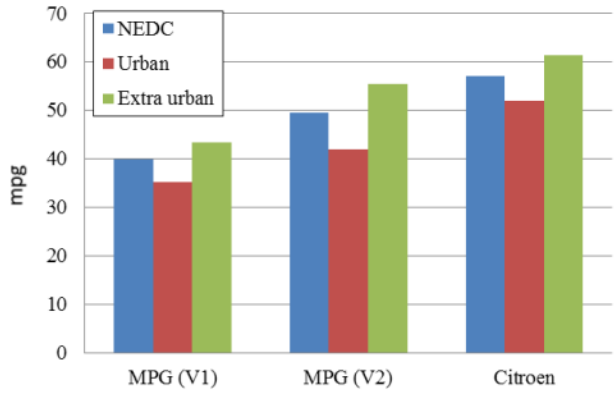

Route	MPG % diff. [sim. (v1) *vs* Citroen]	MPG % diff. [Sim (v2) *vs* Citroen]
NEDC	-30.06	-12.95
Urban	-32.13	-19.10
Extra	-29.46	-9.76
Av. % diff.	-30.55	-13.93

Figure 4.17: Simulation figures compared to Citroen published figures (bar chart), and results shown as percentage difference (table)

Although the data presented in figure 4.17 indicates significant differences between simulated MPG results and official Citroen values, the use of BSFC data to improve realism has reduced the difference to approximately 14% (averaged over NEDC). This difference is broadly in line with Little (2011) suggesting that in general manufacturers' fuel consumption claims are 10 – 15% optimistic.

4.7.3 Incorporating Level of Energy (LOE) / State of Charge (SOC)

For initial work investigating savings that might be achieved through the use of RB & ESS across a range of vehicle types and journey cycles, the ESS LOE (Level of Energy is a 'non-battery specific' term suggested by Ceraolo *et al* (2008)) was not included in the model, as the study was principally comparative and hypothetical in nature (sections 5.2 – 5.4). However in the later, more detailed work described in Chapter 6 it was considered essential to take SOC into account. This was included in the 'Regen' subroutine of the model and the detail is shown in the flow diagram in Appendix XI. As suggested by Schiffer *et al* (2005) to optimize the efficient use of stored energy in HEV it is advantageous to have the SOC inversely proportional to vehicle road speed. This can be achieved using a function such that:

$$KE_{ve} + E_{ESS} = C \qquad (4\text{-}9)$$

Where: KE_{ve} = Vehicle kinetic energy

E_{ESS} = Level of stored Energy

C = constant

Alternatively a LOE or SOC envelope can be used. An example of a SOC performance 'envelope' is shown in figure 4.18. The area between the upper and lower limit lines indicate the envelope within which the ESS operates. The simulation was adapted to include this feature to broaden the utility of the simulation and make investigation of alternative control strategies possible.

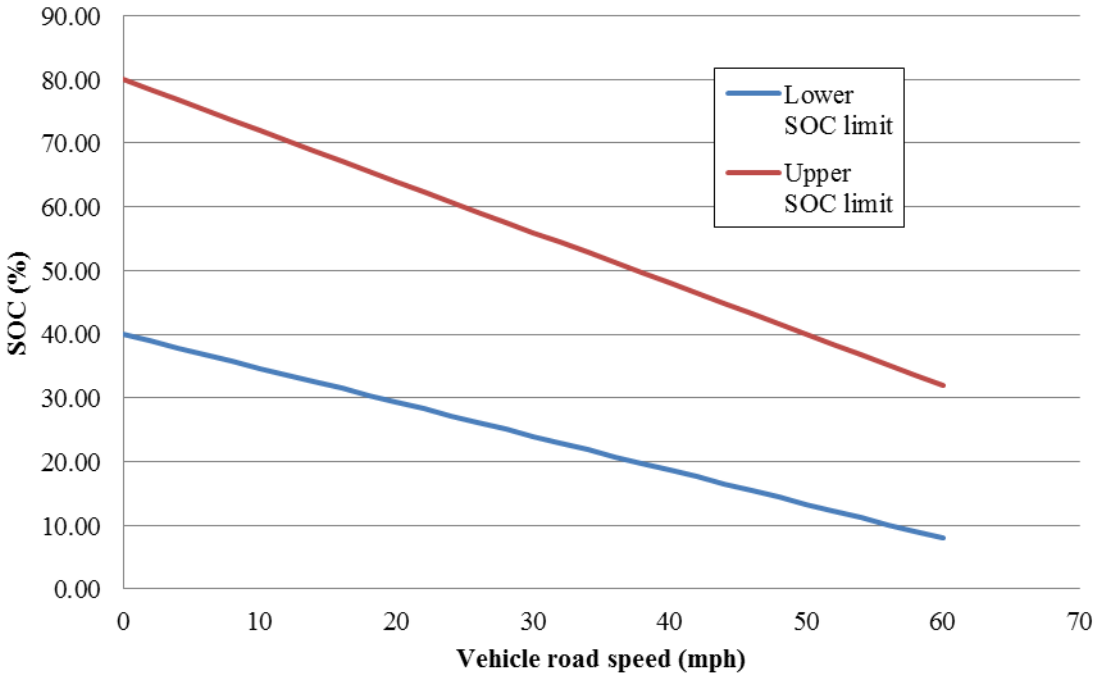

Figure 4.18: An example LOE or SOC operating envelope incorporated in Ver. 3 simulation

The LOE limits defined in the example (figure 4.18) could be applied to the simulation when using the two algorithms shown in figures 4.19 & 4.20.

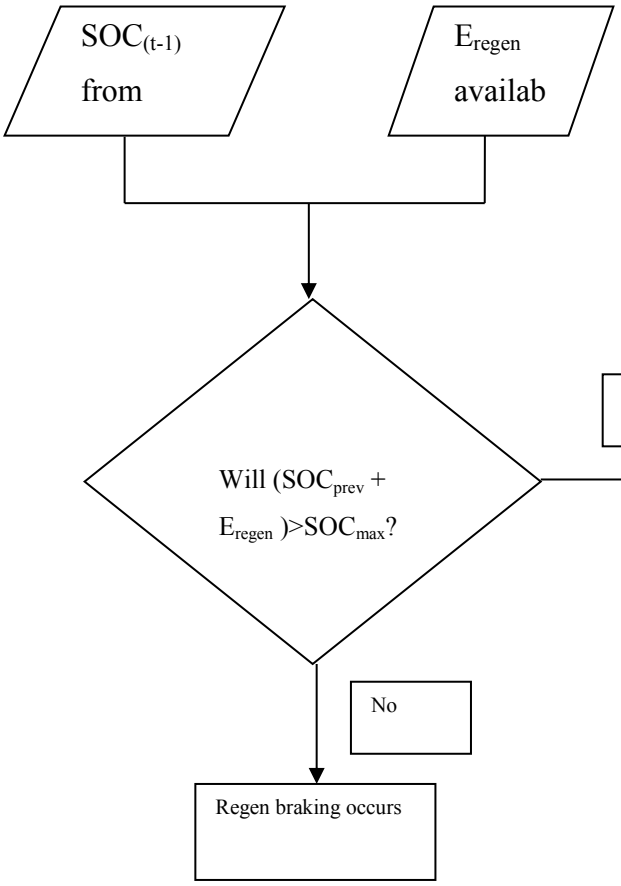

Figure. 4.19: Flow chart detailing how SOC is limited to SOC_{max} in the vehicle model during braking conditions.

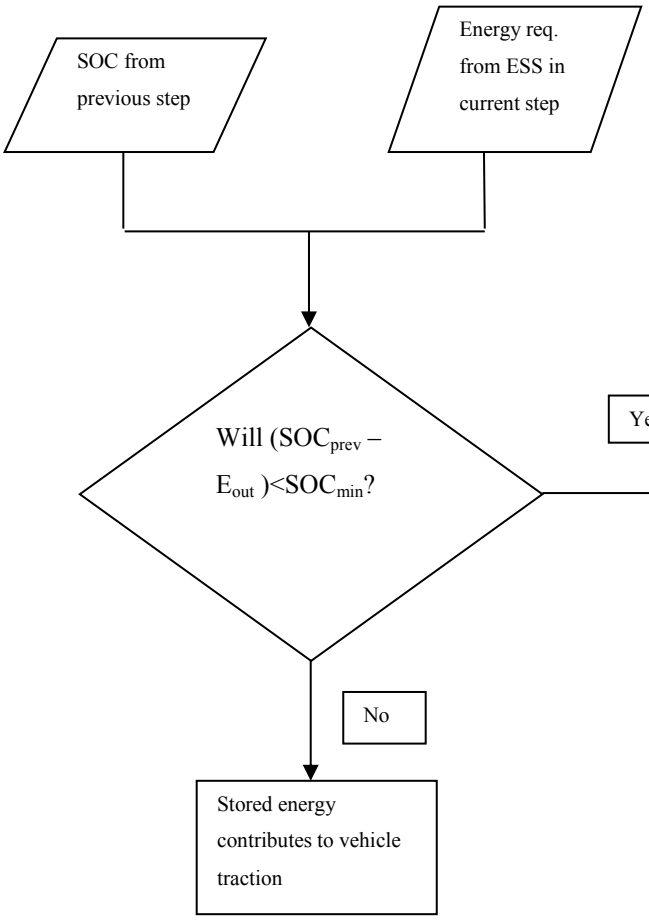

Figure 4.20: Flow chart detailing how SOC is limited to SOC_{min} in the vehicle model acceleration or steady state

4.7.4 Brake specific emissions data

Although much of the work detailed in the following chapter focuses on vehicle energy requirements, once the simulation was validated for predicting fuel use, it was developed further and emissions calculations were included. As covered in chapter 3, for emissions to be calculated, a detailed combustion model or emissions look up data is required for the I.C.E studied. The use of emissions look up tables was considered the most practical method to obtain some useful emissions results whilst keeping the simulation as efficient as possible. It would, in principle, be possible to add a combustion model at some future date but this was beyond the scope of this project.

Obtaining emissions look-up data can be expensive and time consuming however a useful range of emissions data was available from the look-up tables used in the ADVISOR software. Although this data did not specifically relate the engines considered in the vehicles being simulated (Navistar 7.3 l vs Cummins ISB6. 6.7l) it provided a reference example from which some comparative studies could be made. An example of a NO_x emissions map, used in Chapter 5 is shown in figure 4.2.1.

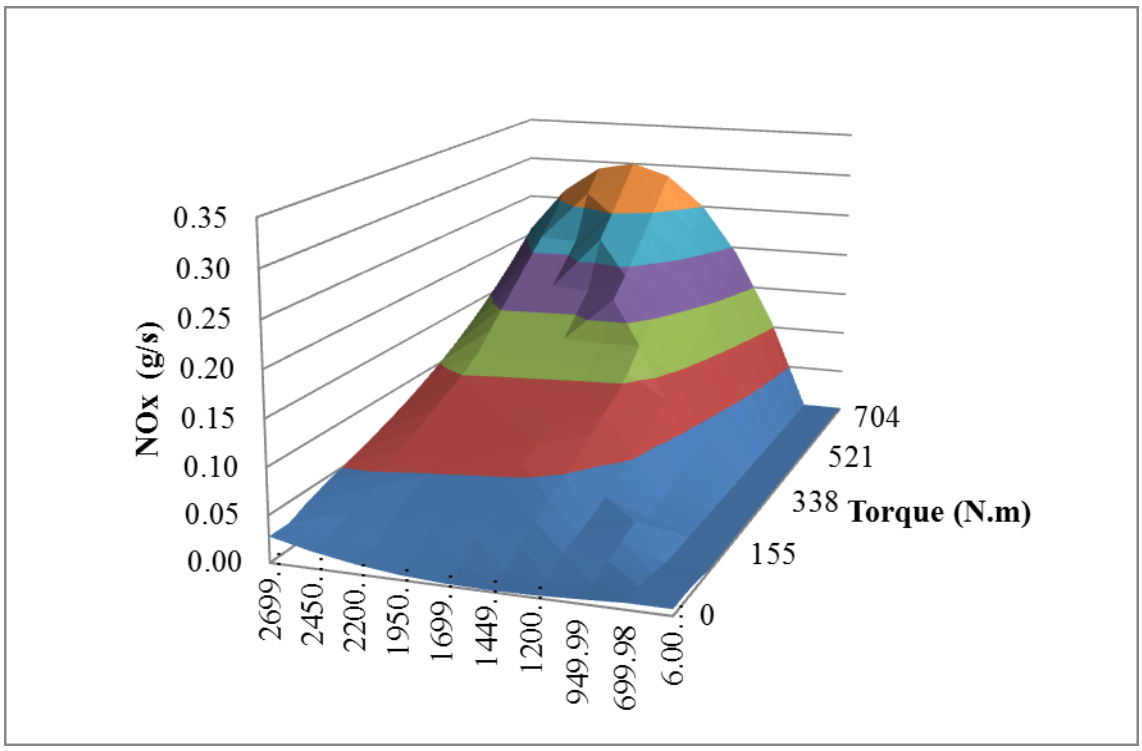

Figure.4.21 An example NOx emissions map for the Navistar 7.3l Diesel (ADVISOR, 2000)

4.7.5 Incorporating engine start / stop

To include this feature, the engine idling condition that comes into effect when the simulated vehicle reaches a standstill, was substituted with a function that reduced energy conversion to zero once the vehicle had been at rest for a set time period. This would be set according to the vehicle data available stating the idle time before the engine shut down occurs. Once the demand speed increased above zero, the normal energy calculations take effect again (as shown in the flow chart, Figure 4.7, and equation 4-8). This feature was only included when vehicle types which have start /stop technology were being simulated or when the effect of incorporating start-stop technology into an existing vehicle type was studied.

4.7.6 Validation of the Ver. 3 simulation

To assess the performance of the ver.3 simulation, data from practical trials conducted on a double decked bus was kindly provided by Coyle (2016). This data was recorded by an independent test establishment working on behalf of TfL using the MLTB cycle to test the bus for fuel consumption and emissions. A comparison of the fuel consumption data from 3 repeated tests and the result from the simulation is shown in figure 4.22.

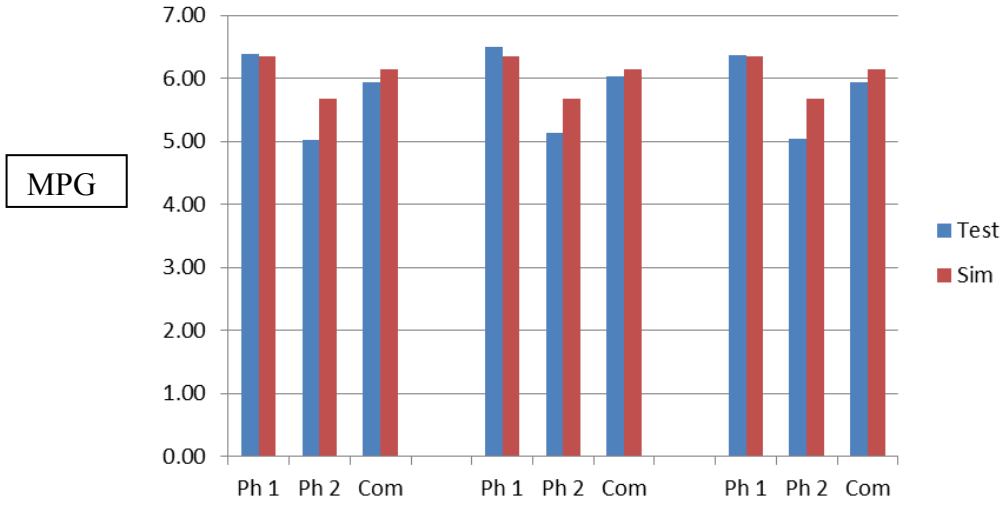

Figure.4.22 Comparison between simulation data practical trials conducted for bus 1

From this comparison it was found that the average difference between the simulation and the averaged test result was as follows: Phase 1 = -1.3%, Phase 2 = +12% and for the combined total cycle = +3%. The comparatively large error in phase 2 is possibly due to the simplification of the torque converter function within the simulation. In phase 2 of the

cycle (inner London) there is a great deal of starting and stopping where the torque convertor is operating much of the time. This may also explain phase why, in phase1, where the gearbox spends more time in lockup there is much better correlation (within 1.5 %) Although the reduced accuracy of the simulation in phase 2 is undesirable it was considered acceptable for this comparative work.

Comparison of measured and simulated emissions showed large differences - in the order of 100% however, as discussed in chapter 3, emissions are subject to significant variation and, owing to limited data available the look-up table for the engine that most closely matching the type used in bus 1 was used. Since the work described in chapter 6 studying emissions reductions possible in buses using a parallel hybrid system with regenerative braking was comparative in nature, the difference in absolute emissions values was considered acceptable. Graphs showing the measured NO_x *vs* power for bus 1 on the MLTB cycle and results generated from the ver. 3 sim using look-up data (as described in 4.7.3) are shown in Appendix IX

4.7.7 Assumptions used in the backward looking simulation

The vehicle data (both from manufacturers and assumed figures) and calculations used in the backward looking simulation were the same as those used in the forward looking ver.1. In addition, since in section 6.6, vehicle fuel energy requirements are calculated taking into account the power density and energy density of currently available energy storage systems the values in figure 5.23 were also used.

Energy storage type	Energy density (J/kg)	Power density (W/kg)	Motor / generator power density (kW/kg)
Litium Ion battery	288000	800	0.2
Lead Acid battery	144000	188	0.2
Composite flywheel	72000	1000	0.2

Figure 4.23: Summary of energy and density values used in the simulation to generate data in figures Chapter 5. Energy and power density from Cheng et al (2008), motor generator power density from Burke et al (1980)

CHAPTER 5

RESULTS FOR SIMULATED PARALLEL HYBRID POWERTRAINS INCORPORATING REGENERATIVE BRAKING AND ENERGY STORAGE

5.1. Introduction

Following on from the simulation development in Chapter 4, the backward looking simulation was used to address the core research question outlined in Chapter 3. Detailed here are the variables studied and results found. Full details of the vehicle data used for each simulation (such as C_d, frontal area and mass) can be found in Appendix 1. Before outlining the simulation work carried out and the results obtained, some performance characteristics of energy storage systems (that were first discussed in Chapter 3) are considered.

5.1.1 Factors limiting energy saved from regenerative braking and energy storage in hybrid vehicles

In terms of technical specification there are several factors which limit the effectiveness of regenerative braking and energy storage in parallel hybrid systems:

(i) The maximum rate of energy transfer between the energy storage system and the vehicle transmission both wheel to storage (braking conditions) and storage to wheel (driving condition). This power rating will be determined by the performance characteristics of the energy storage system and regenerative braking system which typically uses an electrical machine (motor / generator).

(ii) The capacity of energy storage system.

(iii) The effective control of the energy balance (or power split) between energy storage and ICE

The overall vehicle efficiency will also be influenced by the mass of the regenerative braking and energy storage system and of the vehicle as a whole. In addition, there are practical issues relating to the volume of the system in relation to the available space in the vehicle structure.

5.1.2 Energy storage systems investigated

This work was chiefly concerned with a hypothetical hybrid system with an emphasis on the comparison of theoretical energy savings possible in different scenarios. However it

was important to link these findings to real regenerative braking and energy storage systems that are currently available to provide indications of what might be expected from current and emerging technologies. At present, the favoured choice for energy storage in hybrid vehicles is an electrical system, using batteries for energy storage combined with motor generator units in the vehicle wheel hubs. Kinetic energy storage systems are also used but to a lesser extent. Other systems for on-board energy storage such as compressed air and elastomeric materials are, at present not used in commercially available vehicles partly because of some of the practical factors discussed in 3.5.2 .To obtain the results shown in this chapter, the practical performance limitations applied to the hypothetical hybrid system are based on an electrical energy storage system. The vehicle data (both from manufacturers and estimated figures in Appendix I) and calculations used in the backward looking simulation were the same as those used in the forward looking ver.1. In addition, since in section 5.6, vehicle fuel energy requirements are calculated taking into account the power density and energy density of currently available energy storage systems the values in figure 5.1(a)were also used.

Energy storage type	Energy density (J/kg)	Power density (W/kg)	Motor / generator power density (kW/kg)
Litium Ion battery	288000	800	0.2
Lead Acid battery	144000	188	0.2
Composite flywheel	72000	1000	0.2

Figure 5.1(a): Summary of energy and density values used in the simulation to generate data in this chapter. Energy and power density from Cheng et al (2008), motor generator power density from Burke et al (1980)

5.1.3 Electrical energy storage

Hybrid systems using electrical energy storage usually use high performance batteries such as nickel-metal hydride and lithium-ion together with electrical machines working as motor –generators for traction and braking (as per Toyota Prius and Honda Insight and others). Although research into the use of super capacitors has been carried out, Cheung *et al* (2002) suggest that the high cost and weight per MWhr make them impractical for vehicle applications at present.

In any theoretical study of the systems outlined in chapter 5 and 6 the performance of the regenerative braking and energy storage system must be matched to the vehicle being

investigated so that the braking power and energy storage capacity are appropriate for the vehicle type and performance requirements. Since there will always be a maximum possible rate of energy transfer an additional mechanical braking system is always required. The mass of a Regenerative Braking and energy storage system (RB&ESS) will depend on the energy and power density and is likely to contribute significant additional weight to the vehicle. Before applying the performance characteristics of an electrical energy storage system to the simulation a hypothetical system was considered with a fixed efficiency value, and the effects of additional vehicle mass (as a proportion of standard vehicle mass), were simulated. In order to study the *maximum* energy savings possible the hypothetical system was initially considered as having an infinite capacity. Later, as shown in section 5.3 the energy transfer rate (power rating) and energy capacity of the energy storage system were taken into account.

Experience from the literature survey (chapter 3) indicated that for this part of the project the following 3 areas were worthy of investigation. Namely to what extent does the energy saving potential hybrid vehicles depend on:

(i)The vehicle type: The mass of vehicle, cross sectional area, drag coefficient, engine performance and transmission characteristics will all combine to determine the potential energy saving benefit for any given class of vehicle with a hypothetical parallel hybrid system incorporated. In sections 6.2 - 6.6 four vehicle types are considered ranging from a small car to a large coach.

(ii)The type of journey: For example an urban journey with low maximum speed, frequent stops and changes in speed compared with extra urban driving with higher average speeds, sustained periods at high speed and infrequent stops. This aspect is dealt with adequately by various journey profiles. Much of the early simulation work was focussed on the NEDC since this is the cycle specified by the Department for Transport for manufacturers to establish fuel consumption and exhaust emission data. This gave a comparison between early simulation results and data published by manufacturers. In this chapter the Artemis cycle, which is considered to be more representative of real journey cycles, was also applied.

(iii)The Energy storage system: The performance characteristics of the system being studied, in particular maximum rate of energy storage (power rating), energy capacity, energy density and power density. In section 5.3 and 5.4 the effect of energy transfer rate (ETR) and energy capacity were considered separately and independently of mass. For

these studies it is assumed that the hypothetical hybrid vehicle has been designed with reduced mass such that the hybrid system is accommodated with no overall increase in mass. This simplification, whilst not representative of real design constraints, gave a useful basis for initial comparison between vehicle types. For the comparison of energy saving potential the vehicle types shown in Figure 6.1 have been studied with a hypothetical parallel hybrid system built in.

Small car (Citroen C1 1.0*l* petrol)	m = 985 kg
Medium car (Citroen Xsara 1.4*l* petrol)	m = 1280 kg
Large car (Range Rover sport 5.0*l* petrol)	m = 2961 kg
Coach (Volvo B11R)	m = 24745 kg

Figure 5.1(b) Vehicle types simulated to investigate maximum energy transfer rates required

The first study considered how the possible energy saving from a regenerative braking and energy storage system is affected by an increase in vehicle mass. In each instance the fuel energy requirement was compared to that of a standard vehicle. The comparison was carried out for each of the vehicles listed in Figure 5.1 (b)

5.2. Vehicle Mass vs Energy Saved from Regenerative Braking

5.2.1 Results for NEDC case studies

To generate the data presented in Figures 5.2 to 5.5 the fuel energy requirement for the vehicle in question was calculated with the energy capacity and energy transfer rate both set to zero. With these parameters set to zero, the fuel energy requirement was that of a standard vehicle with no regenerative braking and energy storage taking place. To study the effect of increased mass on the likely energy savings from a hypothetical RB&ESS both the energy capacity and the energy transfer rate of the hypothetical hybrid system were set to a level which, within this context, could be considered as infinite. The fuel energy requirement was then compared as a percentage of the requirement for the standard vehicle. With the vehicle mass set as per standard vehicle, and a RB&ESS included in the simulation, the results indicated a net saving in the fuel energy requirement across the NEDC. A series of comparisons were then made with the mass increasing in increments of 0.1% of the standard vehicle mass. Any RB&ESS will have some mass and volume that will contribute to the overall vehicle mass. However, although some ‘retrofit’ systems have been investigated, in most hybrid vehicles the components of the hybrid system are not simply ‘added’ to the vehicle but incorporated into the design from the outset. In designing

a fuel efficient hybrid, manufacturers will, where possible, be keeping vehicle mass to a minimum to offset the mass of the RB&ESS. This makes it difficult to assess the likely total mass of a hypothetical hybrid vehicle of a particular size incorporating these features. Because of this, and keeping in mind the comparative nature of this study, the RB&ESS was simply considered as additional mass above that of the standard vehicle. In each case the backward looking simulation was run with the mass of the RB&ESS set as a percentage of the standard vehicle mass. For the results presented in this section the RB&ESS had an assumed overall efficiency of 50%.

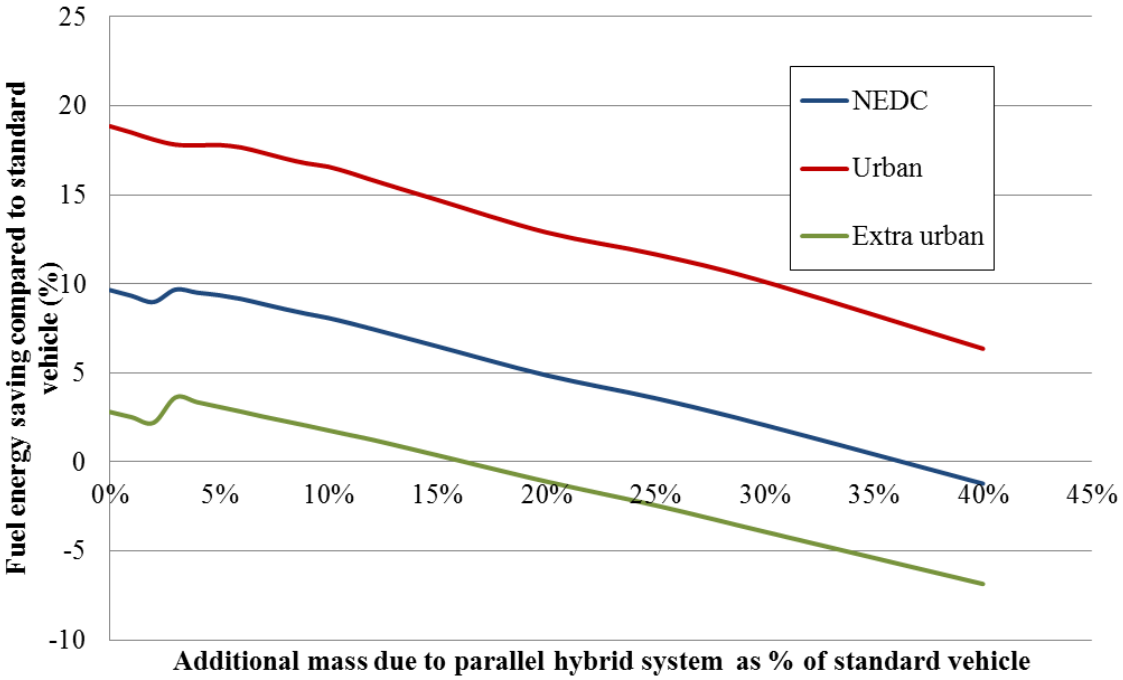

Figure 5.2: Theoretical mass vs energy saving for C1 1.0 (petrol) incorporating a RB&ESS with 50 % efficiency

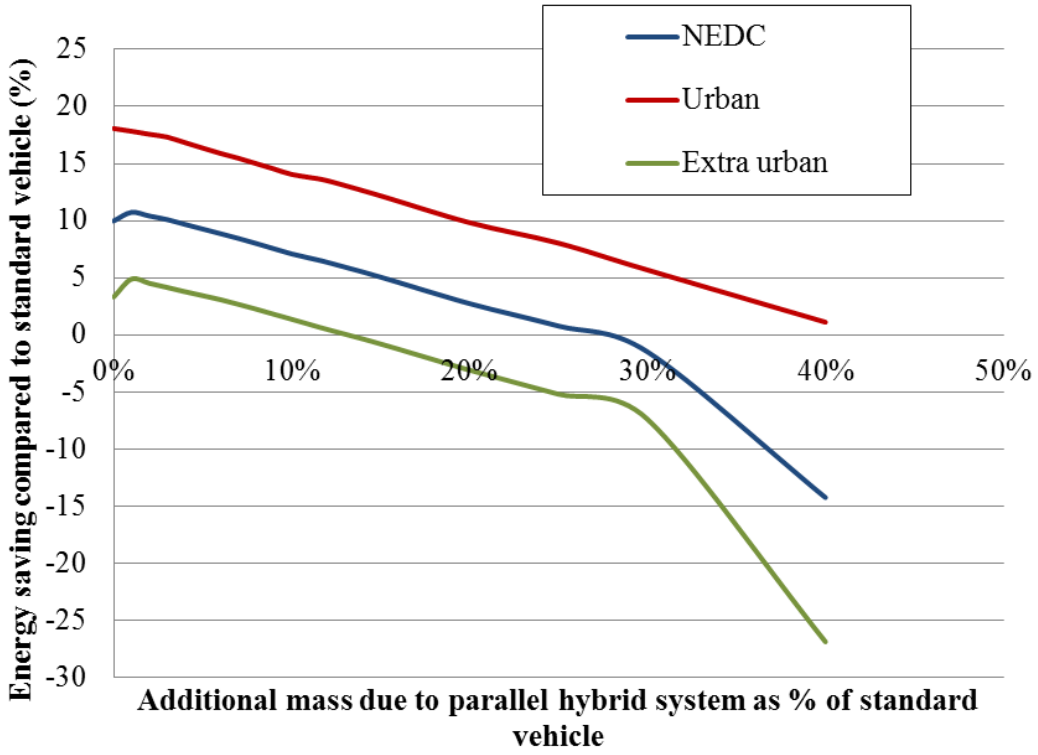

Figure 5.3: Theoretical mass vs energy saving for Citroen Xsara 1.4 (petrol) incorporating a hypothetical RB&ESS with 50 % efficiency

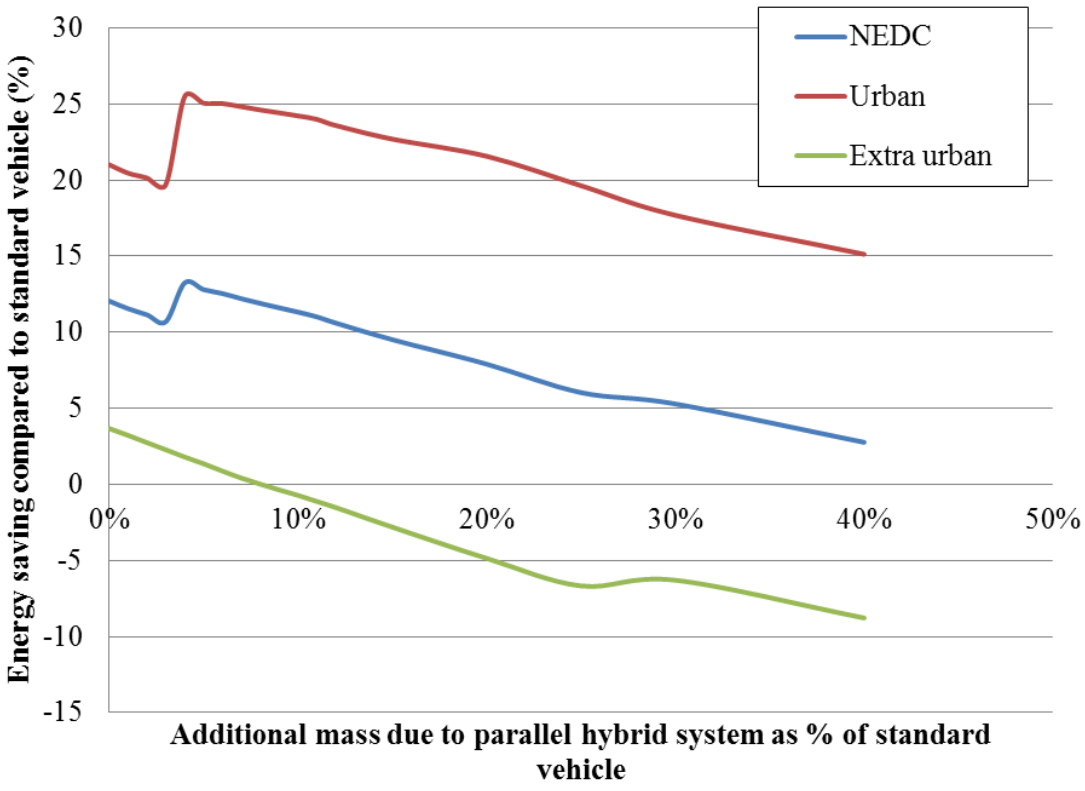

Figure 5.4: Theoretical mass vs energy saving for Range Rover 5.0 (petrol) incorporating hypothetical RB & ESS with 50 % efficiency

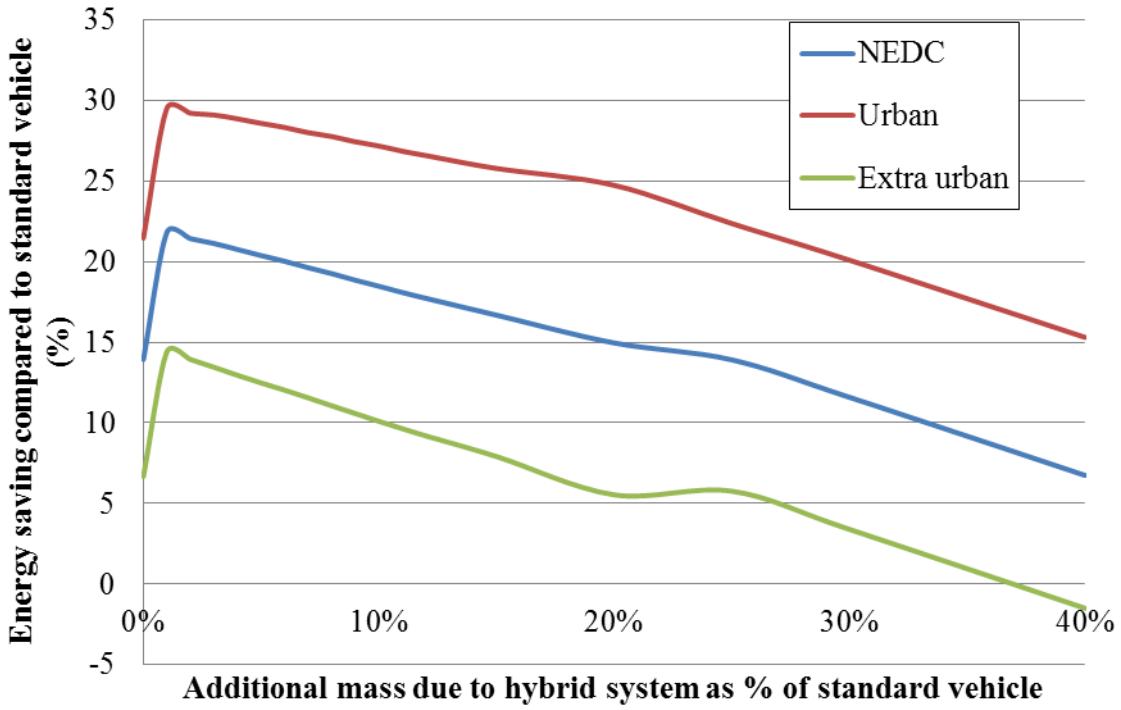

Figure 5.5: Theoretical mass vs energy saving for a Volvo B11R Coach incorporating a hypothetical RB&ESS with 50 % efficiency

For the simulation of the VolvoB11R BSFC data was used from the ADVISOR file for the Detroit Diesel corporation series 60 which is a 12.7 litre diesel with a peak torque of 1800N.m vs 2100 N.m for the VolvoB11R. Data specific to the Volvo engine would have been preferable but it was not possible to obtain this so data for the most closely matched example available from the ADVISOR map was scaled (on the toque and speed axis) then normalised to show η_{eng} for the speed and torque conditions relative to a max efficiency value. An estimate of this was determined from the original plot as 39.57%.

5.2.2 Discussion of simulation results for increased vehicle mass vs possible energy savings

From the results presented in figures 5.2 to 5.5 several observations can be made. Although the data is based on a purely hypothetical idealised case (with unlimited energy transfer rate and energy capacity) some trends are apparent in the results. In each case a linear relationship between theoretical mass increase and the corresponding reduction in energy

saving is shown. The principle forces of resistance acting on a vehicle which are mass dependant are F_{grad}, F_{roll} and F_{acc}. In each case the result of the governing equations (eqt. 4-2, 4-3 and 4-4) is proportional to mass and so this linear relationship is to be expected. For each of the four vehicle types studied here the theoretical savings are greatest on the urban part of the NEDC and lowest on the extra-urban part. Since regenerative braking effectively recovers some kinetic energy during deceleration, journeys where there are many braking episodes, such as urban cycles, can exhibit large savings. Since $F_{aero} \propto \boldsymbol{v^2}$, at typical urban speeds (<35 mph) where F_{aero} is comparatively low, inertial forces constitute a higher proportion of the overall resistive forces acting on a vehicle and a proportion of this may this can be recovered. Extra urban Journeys where there is less variation in speed will offer fewer opportunities for regenerative braking, although occasional changes in speed from say 70 to 50 mph require large resistive forces this happens relatively infrequently and the contribution of aerodynamic drag, F_{aero} , is considerable. The combined result of these factors is that, in general less energy can be recovered. However in real driving conditions where congestion and bunching of traffic occurs on motorways for example, the regular large changes in speed during motorway driving may offer greater saving than those indicated from the simulated extra urban part of the NEDC. The potential energy savings on 'real' journeys could be investigated further using recorded speed / time data. The data in Figures 5.2 to 5.5 suggests a maximum possible saving on the extra urban cycle of up to 14% for a large coach (Volvo B11R) and as little as 3% for a small car (Citroen C1). For the urban part of the NEDC the maximum theoretical savings are ≈ 30% and 18% for the coach and small car respectively.

For each vehicle an increase in mass of ≈ 10% above the standard vehicle mass is sufficient to cancel out any benefit from regenerative braking and energy storage on the extra urban part of the NEDC. For the urban cycle an increase in mass of approximately 40% was recorded before theoretical savings from regenerative braking were cancelled out. This is due to the fact that although any mass increase will require more tractive energy (in order to overcome resistive forces acting on a vehicle) on the urban cycle, a comparatively large proportion of this can be recovered through regenerative braking.

Although this initial study is rather abstract, in the sense that a hypothetical RB&ESS with infinite energy transfer rate and energy capacity is considered, it nonetheless provides some insight into the comparative maximum savings that might be possible across the scenarios considered. To gain some quantitative measure of the influence of energy

transfer rate and energy capacity on the theoretical energy saving potential these two parameters are considered independently in section 6.3 and 6.4.

5.3. The Effect of Energy Transfer Rate on Energy Saving Potential of a Hypothetical Hybrid System

5.3.1 Introduction

The Figures 5.6 to 5.10 show how the maximum possible rate of energy transfer (power rating) of a RB&ESS affects the energy saving potential of a parallel hybrid system. The percentage energy savings shown are relative to the fuel energy requirement of a standard vehicle. For each vehicle type the combined, urban and extra urban parts of the NEDC have been simulated and in each case it was assumed that the mass of the hybrid system did not increase the vehicle mass above that of a standard vehicle (i.e. weight savings have been made elsewhere). A notable example of this being almost achieved in practice is shown by comparison between the 2014 Toyota Prius (hybrid) and Ford Focus (conventional powertrain) which have a quoted mass of 1365 kg and 1333 kg respectively. These figures show that despite being similar in terms of size the Prius typically has only 2.3% greater mass (Toyota, 2014 and Ford, 2014). The effects of increased vehicle mass on vehicle fuel energy saving potential of a RB & ESS were explored section 5.2.1. As in section 5.2 an overall efficiency value of 50% has been used for the RB&ESS. Changing the efficiency value has the effect of scaling the values on the y axis but not changing the overall trend of the data for each journey profile.

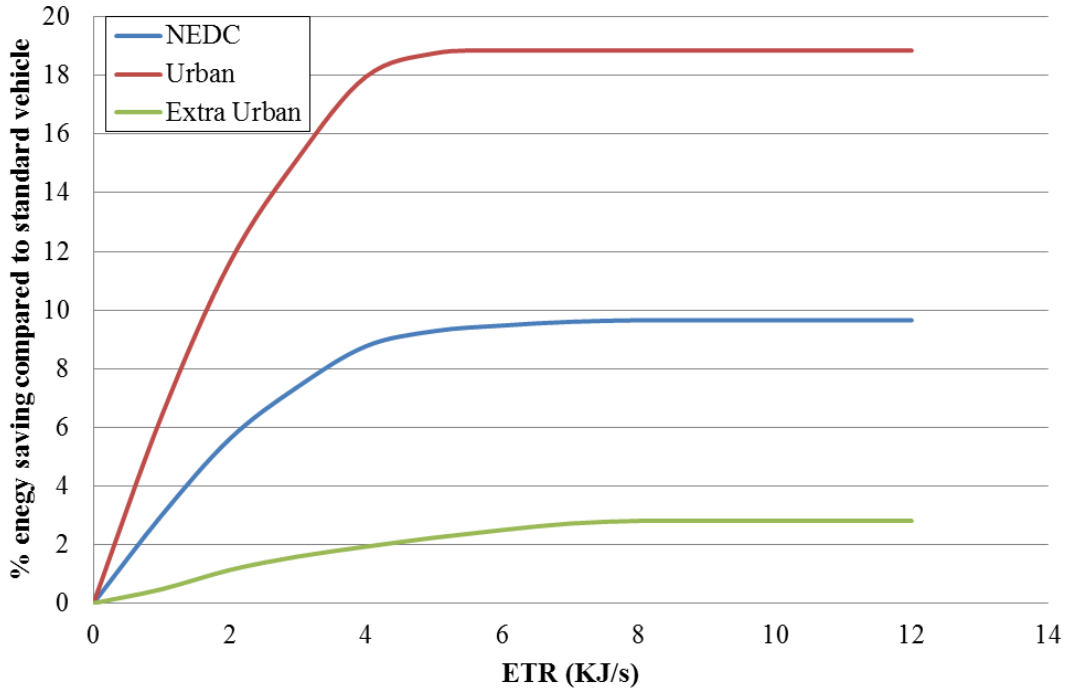

Figure 5.6: Citroen C1 energy saving vs energy transfer rate (standard mass) and RB&ESS, η = 50% (lwr case k)

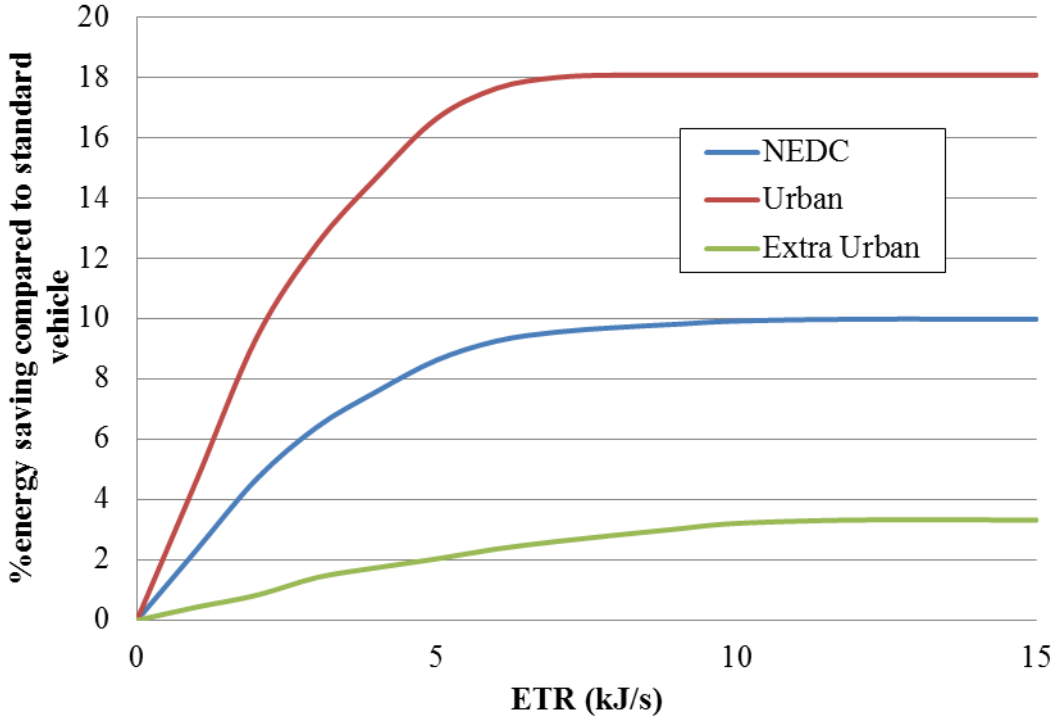

Figure 5.7: Citroen Xsara energy saving against energy transfer rate (Standard mass)

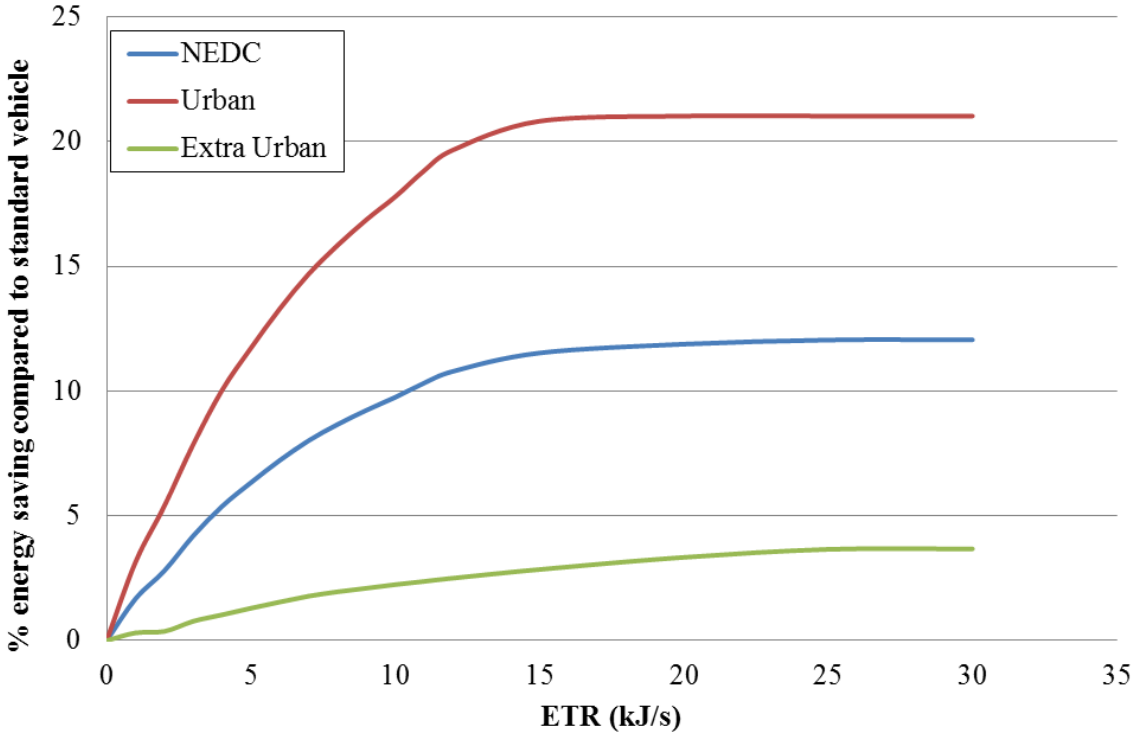

Figure 5.8: Range Rover 5.0 petrol energy saving against energy transfer rate (standard mass)

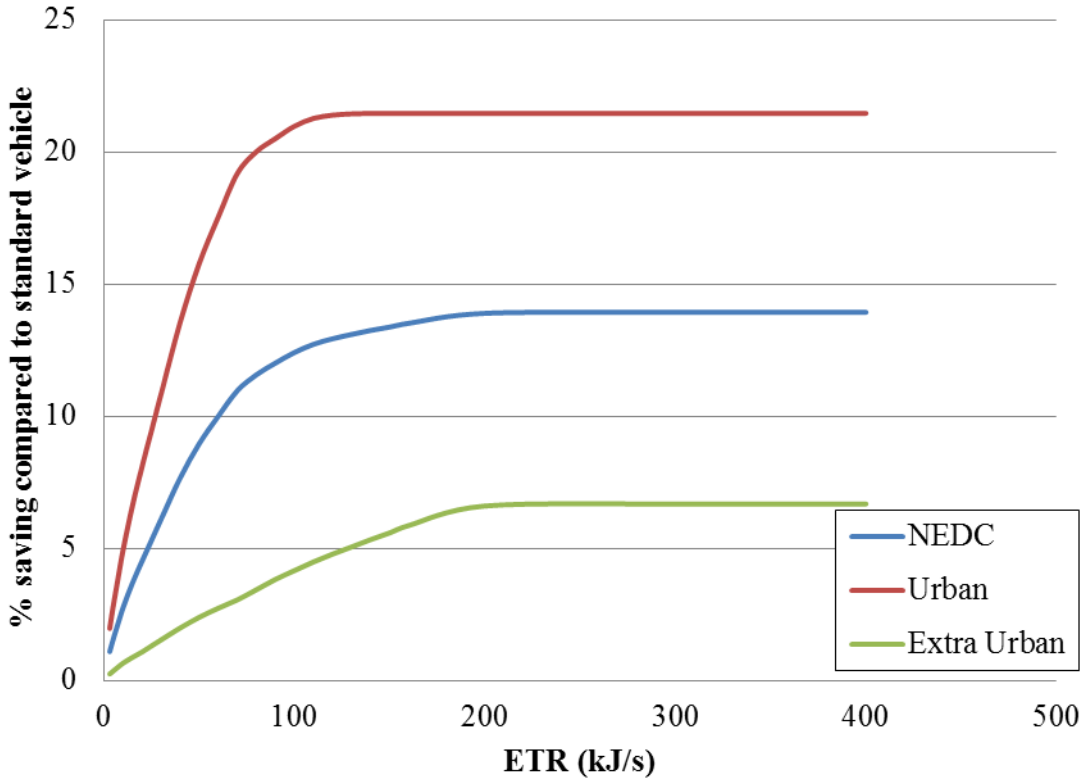

Figure 5.9: Volvo B11R energy saving against energy transfer rate (standard mass)

5.3.2 Discussion of results

From Figures 5.2 to 5.9 it can be seen that for each vehicle type considered there is an optimum maximum energy transfer rate (ETR) (increasing with vehicle size and mass) for any RB&ES system installed. These results provide an insight into the likely power rating required for regenerative braking and energy storage systems in different classes of vehicle for the NEDC.

Vehicle type	Maximum energy transfer rate required
Small car (Citroen C1 1.0 *l* petrol)	8 x 10^3 J/sec
Medium car (Citroen Xsara 1.4 *l* petrol)	10 x 10^3 J/sec
Large car (Range Rover sport 5.0 *l* petrol)	25 x 10^3 J/sec
Coach (Volvo B11R)	200 x 10^3 J/sec

Figure 5.10: Maximum energy transfer rate required to fully utilize recoverable energy available through regenerative braking for different vehicle types over NEDC

To fully specify the power rating for hybrid systems a similar study would be required over a wide range of recognised test journey cycles as well as using recorded speed / time data for a range of real journeys. Although the power rating required increases with vehicle size and mass the relationship is not quite linear. Although kinetic energy is proportional to mass the range of vehicles studied here have different frontal areas and aerodynamic drag coefficients. The result of these different parameters across the range of vehicles is that the aerodynamic drag force does not increase in proportion to the vehicle mass, resulting in the findings shown in Figure 5.10. It is worth considering the magnitudes of the system power rating determined from these results. In the case of the large coach, a required system power rating of 160kW has been predicted. To achieve such capability the contribution, to the vehicle mass, of the necessary electrical machinery and battery units (along with associated hardware) is likely to be considerable. In section 6.4, the predicted performance of a hypothetical hybrid system is considered with respect to the energy capacity of the RB&ESS used.

5.4 The Effect of the Energy Capacity of a System on the Energy Saving Potential of a Hypothetical Hybrid System

5.4.1 Introduction

For these calculations the energy transfer rate (power rating) of the hypothetical system was unlimited so the effect of energy capacity could be studied in isolation. Whilst this may not be a realistic representation of a hybrid system it gave an opportunity to characterise the likely effects of different parameters independently. For each vehicle type considered the simulation repeated a number of times with the energy capacity increased on each run. On each test the total fuel energy required across the three parts of the NEDC was found and the results automatically compared with the equivalent fuel requirement for the standard (non-hybrid) vehicle. From the results presented in Figures 5.11 to 5.14 it is possible to determine the system energy capacity, for each vehicle type, above which no further fuel energy can be saved.

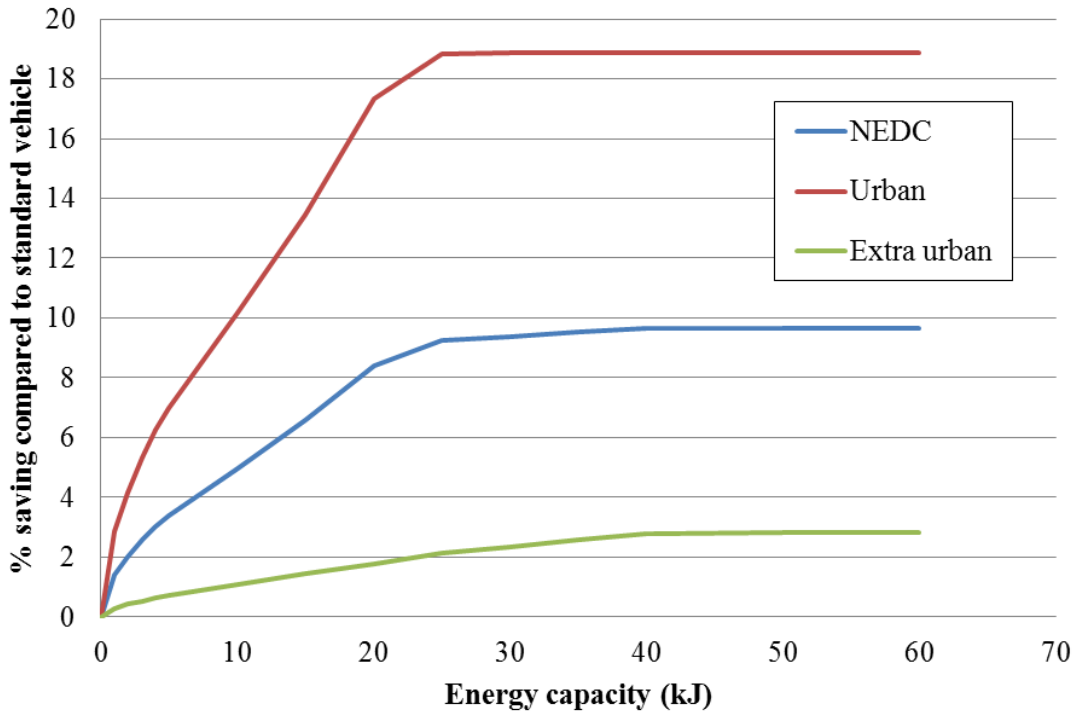

Figure 5.11: The effect of the energy storage system capacity of the energy saving potential for a Citroen C1.

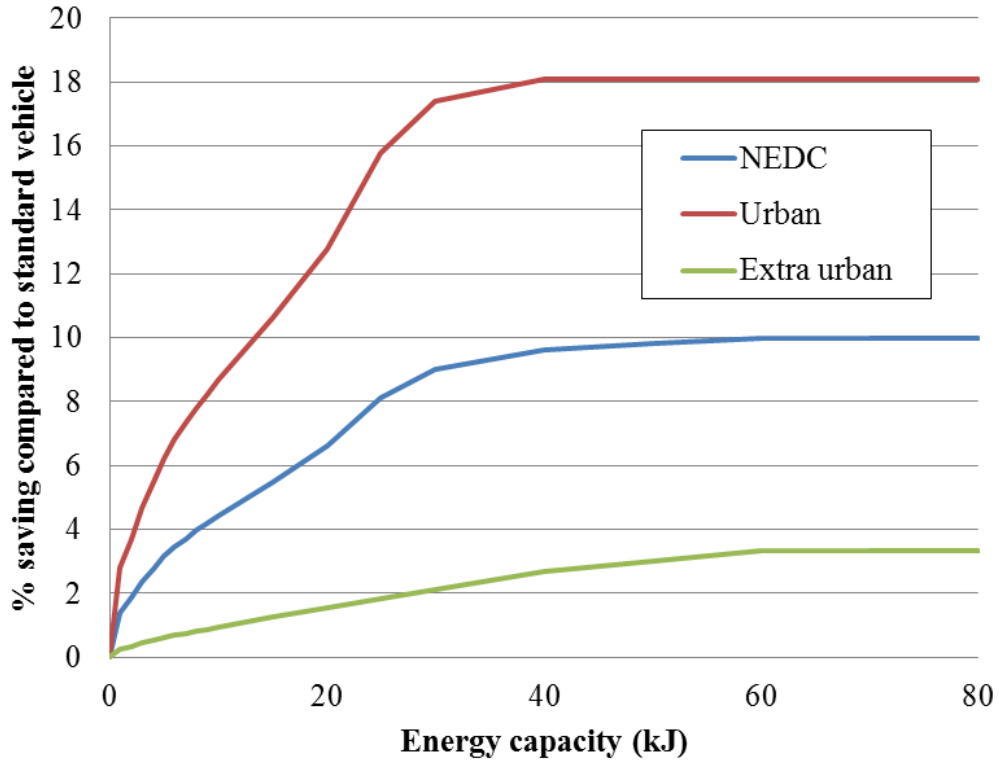

Figure 5.12: The effect of the energy storage system capacity of the energy saving potential for a Citroen Xsara

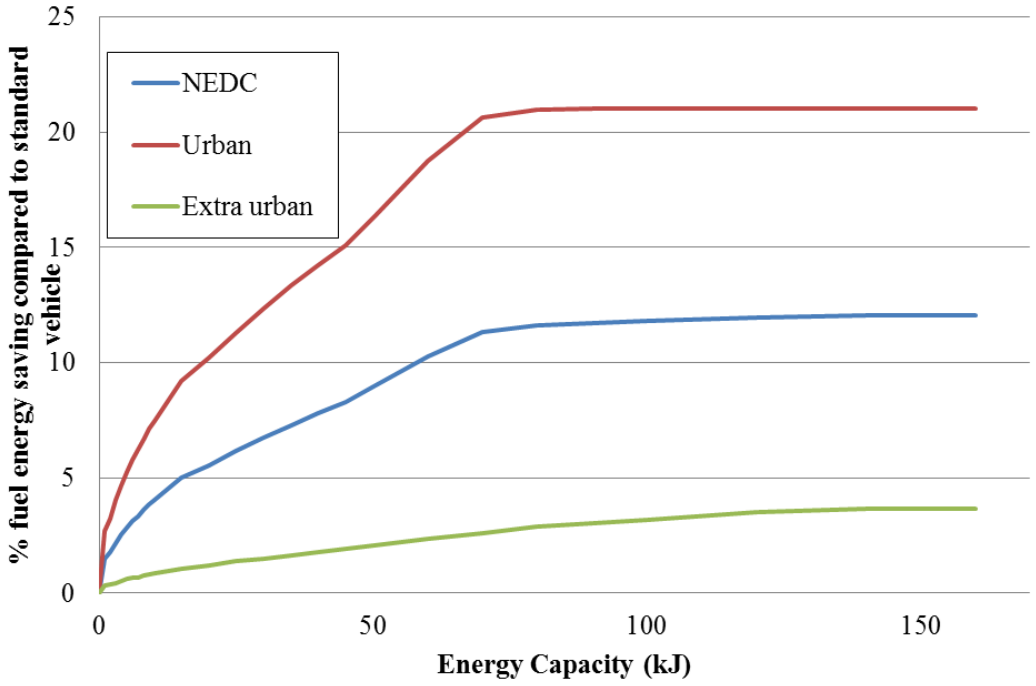

Figure 5.13: The effect of the energy storage system capacity of the energy saving potential for a Range Rover

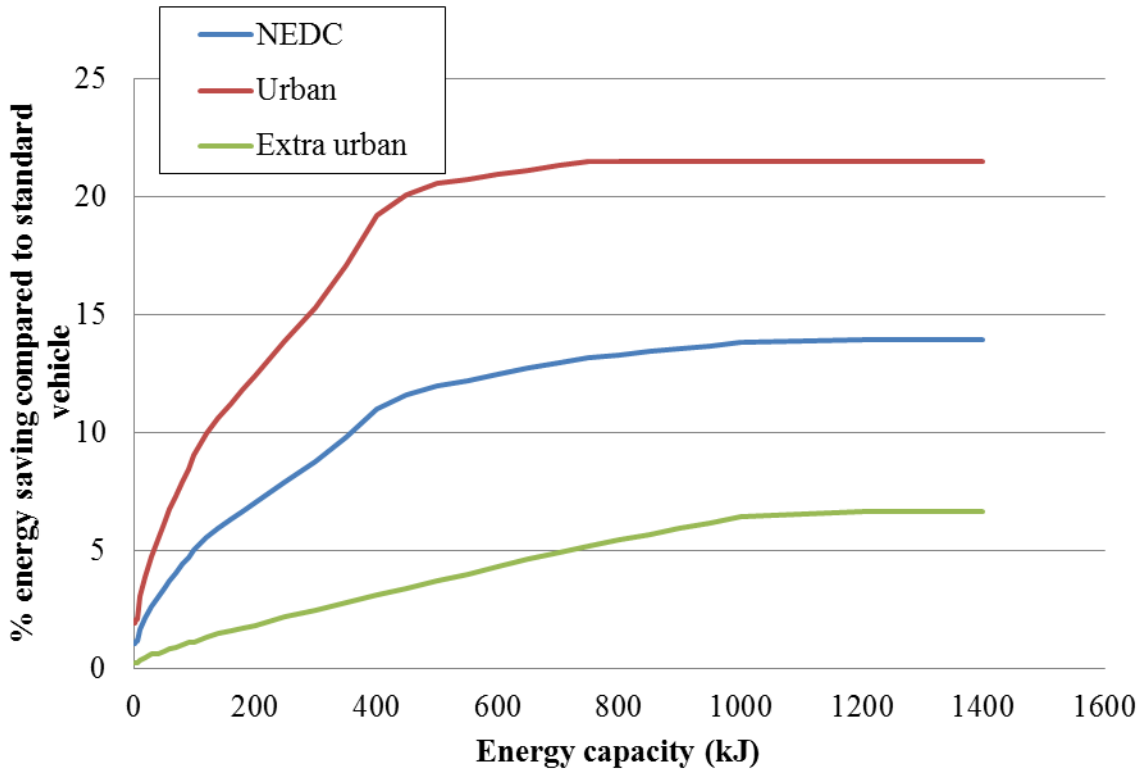

Figure 5.14: The effect of the energy storage system capacity of the energy saving potential for a Volvo B11R Coach

5.4.2 Discussion of results from simulation of energy storage system capacity

From Figures 5.11 to 5.14 it can be seen that in each case the theoretical energy savings available increase in a non-linear fashion with increasing available energy capacity until the energy capacity at which the maximum theoretical saving occurs is reached. These maxima correspond with the values seen in sections 5.2 and 5.3 since for each set of results only one variable was altered. The energy capacity above which no further savings are made increases with vehicle size and mass as expected due to the proportional increase in kinetic energy with mass. The increase in energy capacity required (for maximum savings) does not increase in proportion to vehicle mass due to the additional F_{aero} forces acting on larger vehicles caused by a combination of C_d and A. The energy capacity of batteries is generally proportional to mass. For a system to provide sufficient energy storage (for the regenerative braking energy available over a given journey cycle) it is likely to contribute a significant mass and occupy internal vehicle volume and mass that would otherwise be use for luggage or passengers. The data shown in section 6.4.1 is only based on the NEDC which has a total length of 11,230m. With the simple regenerative braking algorithm shown in appendix VII the repeated periods of deceleration and acceleration on the NEDC mean that energy stored through regenerative braking is soon converted back into tractive

effort. In real driving situations, such as a long descent a far greater energy capacity might be required to store all the regenerative braking energy available. However for a comparison study of this nature the NEDC provides a useful platform for evaluating the hypothetical type of system being considered. In the case of transport systems such as electric trams and locomotives powered by a national grid supply the energy stored could potentially be considered as having infinite capacity due to the size and loading on the system. In addition, since the energy storage is not contained in the vehicle itself, there is no weight or volume penalty to offset the potential savings. A summary of the data shown in Figures 5.11 to 5.14 is shown in Figure 5.15.

Vehicle type	energy capacity required
Small car (Citroen C1 1.0 *l* petrol)	40 kJ
Medium car (Citroen Xsara 1.4 *l* petrol)	60kJ
Large car (Range Rover sport 5.0 *l* petrol)	140 kJ
Coach (Volvo B11R)	1.2 MJ

Figure 5.15: Energy storage capacity required for a hybrid system to achieve maximum possible energy savings on the NEDC for a range of vehicles (based on η =50%)

5.4.3. Summary of maximum theoretical energy savings possible

The energy savings shown in sections 5.2 (and also in 5.3 & 5.4) are collated in figure 5.16.

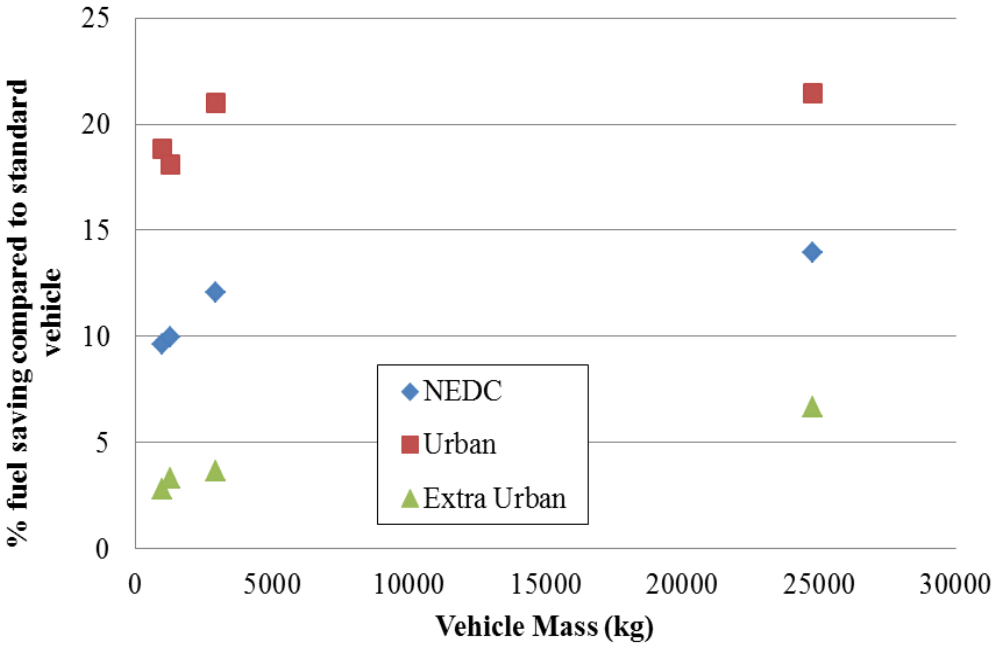

Figure 5.16: Vehicle mass vs maximum potential tractive energy savings from a 50% eff RB&ESS sys (with no weight increase over standard vehicle mass) for NEDC

Note: The use of the NEDC for buses here is considered justified as this is a hypothetical study across vehicle types requiring a uniform cycle. When considering the results shown in Figure. 5.16 it should be borne in mind that this data set represents the *peak* fuel energy savings possible (allowing for a RB&ESS of with η = 50%). Although this does not take into account the practical limitations, in terms of energy density and power density that define the performance of real energy storage systems, it does show a basic comparison of the maximum theoretical saving possible (with an overall system efficiency of 50%). When generating these results it was also assumed that a RB&ESS is incorporated in to the vehicle design with no additional mass compared to a standard (no hybrid power train) vehicle of the same size. In some instances parallel/series hybrid vehicles have been produced with a total mass comparable to non-hybrid vehicles of the same size and similar performance.

5.5 Summary of Results for Theoretical Energy Savings for Hypothetical Hybrid Vehicles with No Weight Penalty Due to Regenerative Braking and Energy Storage System (Using NEDC)

Because designers of hybrid vehicles are particularly concerned with producing energy efficient vehicles it is likely that a variety of features will be incorporated into the design to achieve this. The weight of commercially available mass produced cars is largely influenced by the well- established conventional methods of manufacture and choice of material used and the commercial constraints that limit maximum price. An increasing number of manufacturers are now designing hybrid vehicles starting from completely new designs rather than adapting existing models. This gives the greatest potential for weight saving since the hybrid powertrain is fully integrated into the vehicle design. The percentage savings shown in figure 5.17 represent a best and worst case energy saving based on the simulation study outlined in sections 5.2 to 5.4. The values shown in red relate to η_{regen} = 50% (as shown in Figure 6.16), in green results for η_{regen}= 65%. The general trend shows increased savings for larger vehicles on urban cycles. The energy savings on the urban cycle are around 3 to 4 times greater than those calculated for extra urban cycles.

	Urban	NEDC	Extra Urban
Volvo B11R Coach	32	21.45	8.97
	24.64	16.5	6.9
Range Rover petrol 5.0l	28.8	16.41	5.94
	22.19	12.57	4.57
Citroen Xsara 1.4 Petrol	26.53	15.32	5.7
	20.41	11.79	4.39
Citroen C1 1.0 Petrol	24.05	12.5	4.18
	18.5	9.61	3.22

Figure 5.17: Collated results for backward looking NEDC simulation update numbers

Green = best case, $\eta_{regen} = 65\%$

Red = worst case, $\eta_{regen} = 50\%$

5.6 Simulation Results Taking Into Account the Mass and Performance of a Hypothetical Parallel Hybrid Power-Train

Following the simplified study, outlined in section 6.5, in this section some practical limitations were applied to the RB&ESS. The results here are based on a hypothetical system with Lithium Ion battery energy storage.

Wheel to battery to wheel, η_{regen} = 50%

ESS data*	Li-ion	units
Energy density	288000	J/kg
Power density	800	J/s/kg
Motor generator		
Power density**	0.2	kW/kg
Ancillary mass	10.00	% of motor / gen mass

Figure 5.18 Key parameters of the hypothetical hybrid system modelled to generate results shown in Figures 5.19 to 5.26 * Hitatchi (2008) **Burke (1980)

The ancillary mass represents the mass contribution from the wiring, fixtures control system and other ancillaries required in addition to the battery system and motor generator units. Since the mass of many of these components will increase approximately in proportion with the power rating of the RB&ESS an arbitrary mass is calculated as 10% of the motor / generator mass. To generate each data point on the graphs in this section the mass of the energy storage system (battery) was set as a percentage of the vehicle mass. With the energy density and power density determined by the values shown in Figure 5.18 the capacity and power of the hypothetical battery system could be calculated. From the system power determined, the motor mass was found along with the estimated mass of ancillary equipment needed.

In this section results are shown for both the NEDC and also the more representative Artemis cycle to give a more full and detailed study of estimated performance. It should be noted that the combined part of the NEDC is not an equivalent to the road cycle Artemis cycle since the road part of the Artemis cycle principally represents main road driving whereas the combined NEDC is the urban followed by the extra urban parts of the NEDC.

5.6.1 Citroen C1 simulation results

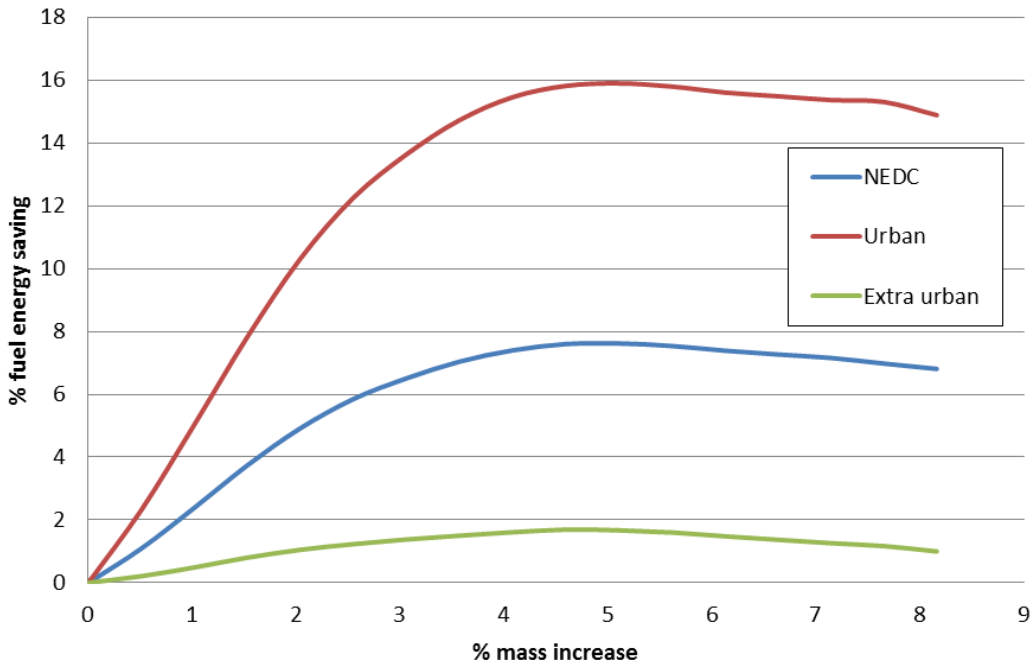

Figure 5.19: C1 % fuel energy saving (comparing to a vehicle with standard mass) vs % mass increase due to parallel hybrid system with RB&ESS (compared to standard vehicle mass) for NEDC drive cycle.

From Figure 5.19 the effect of the additional mass, contributed by the hybrid powertrain components taken into account in this study, was apparent. Peak theoretical savings here were around 16% on the urban part of the NEDC compared with around 18.5% seen from the more abstract study (with no hybrid system mass taken into account) in sections 5.3 – 5.5. The same trend of reduced energy savings was seen across the vehicle types represented in this section using the NEDC cycle. These results suggest that a 5% increase in mass (due to a RB&ESS of the specification outlined in Figure 5.18) would provide optimum energy savings for the Citroen C1. If the mass increases above 5% of the standard vehicle unladen mass energy savings begin to reduce, despite the power rating and energy capacity of the hypothetical hybrid system continuing to increase. The additional power and capacity are of no further benefit yet contribute extra mass which increases the overall tractive energy requirement causing the energy savings to reduce.

Figure 5.20 shows an equivalent plot from the C1 simulation for the Artemis cycles, again an optimum increase in mass is apparent beyond which savings tale off. In this case the peak saving occurs at noticeably different 'percentage additional mass' values across the different cycles. The results also show larger energy savings for the urban journey cycle (compared to NEDC) but lower savings on the Artemis road cycle compared to the combined NEDC. This is likely to be due to the different nature of the cycles outlined at the beginning of section 5.6.

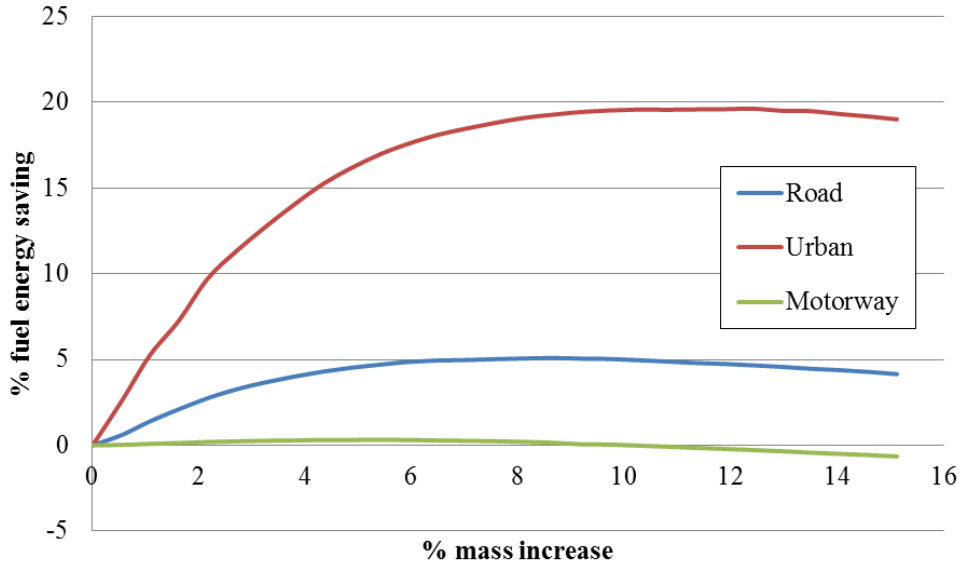

Figure 5.20: C1 % fuel energy saving (compared to a vehicle with standard mass) vs % mass increase due to parallel hybrid system with RB&ESS (compared to standard vehicle mass) for Artemis drive cycle.

5.6.2 Citroen Xsara simulation results

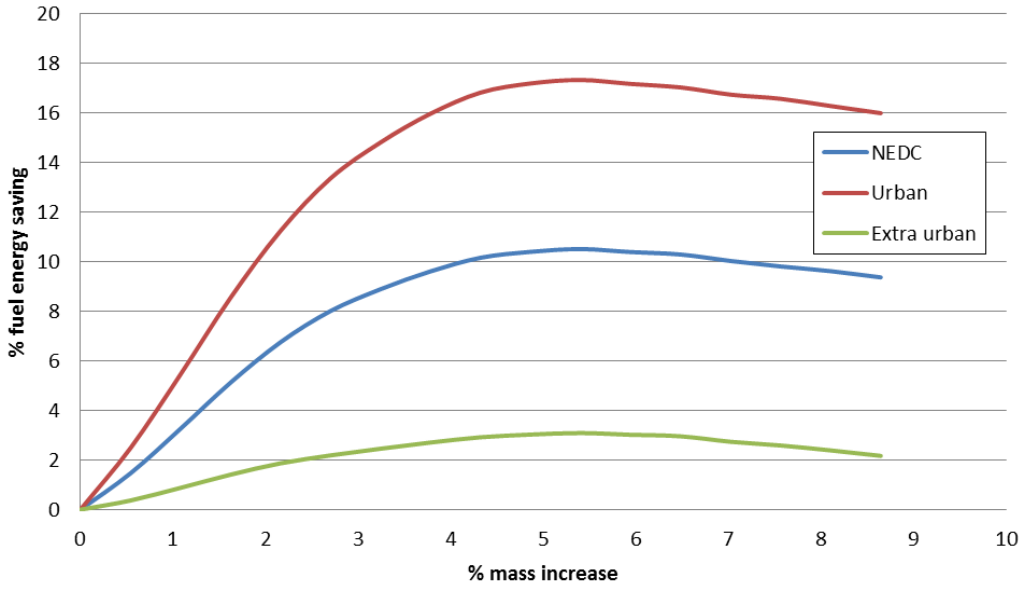

Figure 5.21: Citroen Xsara 1.4 (petrol) % fuel energy saving (compared to a vehicle with standard mass) vs % mass increase due to parallel hybrid system with RB&ESS (compared to standard vehicle mass) for NEDC drive cycles.

Similar trends are apparent in the data shown in Figures 5.21 and 5.22 as in Figures 5.19 and 5.20. Across all four vehicle types simulated here, savings are higher on the Artemis urban cycle by around 2% compared to the NEDC urban cycle. Peak savings in Figure 5.21 are around 17% with only a 5% increase in vehicle mass. Energy savings calculated on the extra urban Artenis cycle are very low at less than 2 %. Peak savings of 20% are apparent in Figure 5.22 with the necessary RB&ESS increasing the vehicle mass by 10% (of standard vehicle mass).

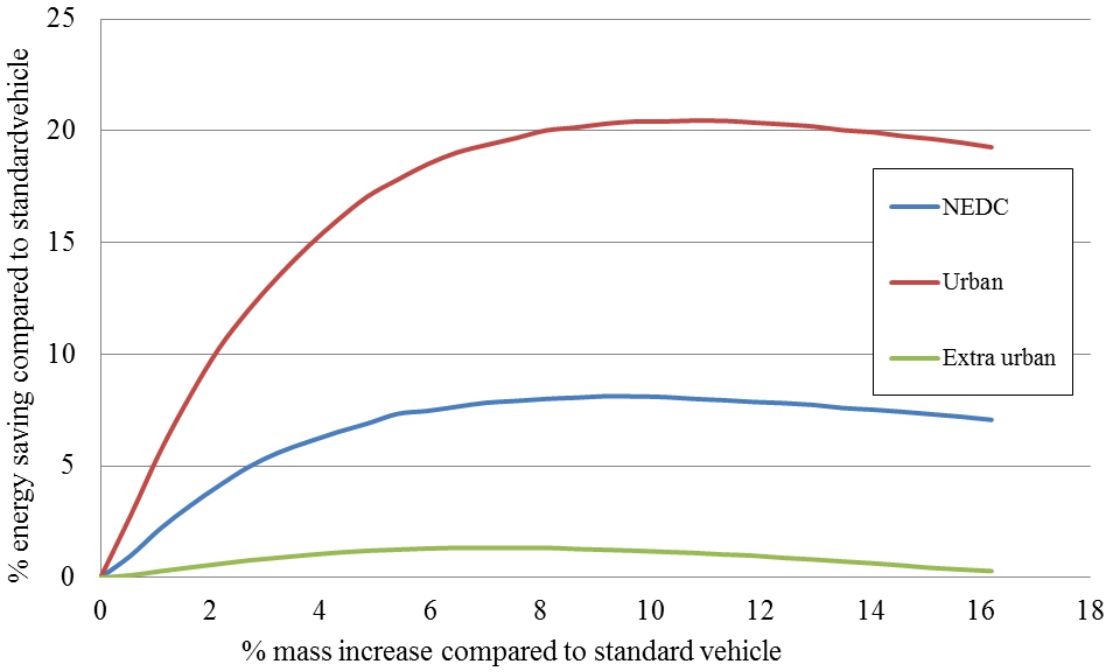

Figure 5.22:Citroen Xsara 1.4 (petrol) % fuel energy saving (comparing to a vehicle with standard mass) vs % mass increase due to parallel hybrid system with RB&ESS (compared to standard vehicle mass) for Artemis drive cycles.

5.6.3 Range Rover simulation results

The results shown in Figures 5.23 and 5.24 show very similar performance trends as seen in section 5.2 but with approximately 2% higher savings across the range of results. The Range Rover has an 'on the road' weight of approximately 3 tons and a 5 litre capacity petrol engine resulting in poor fuel economy. However, the percentage fuel energy savings are comparatively good since inertial forces make up a large proportion of the total force acting on the vehicle. Such vehicles may offer encouraging fuel savings if developed with RB&ESS built in. However, in overall terms, the fuel energy requirement is comparatively large so it is very difficult to justify such vehicles from an environmental perspective even with hybrid power-trains.

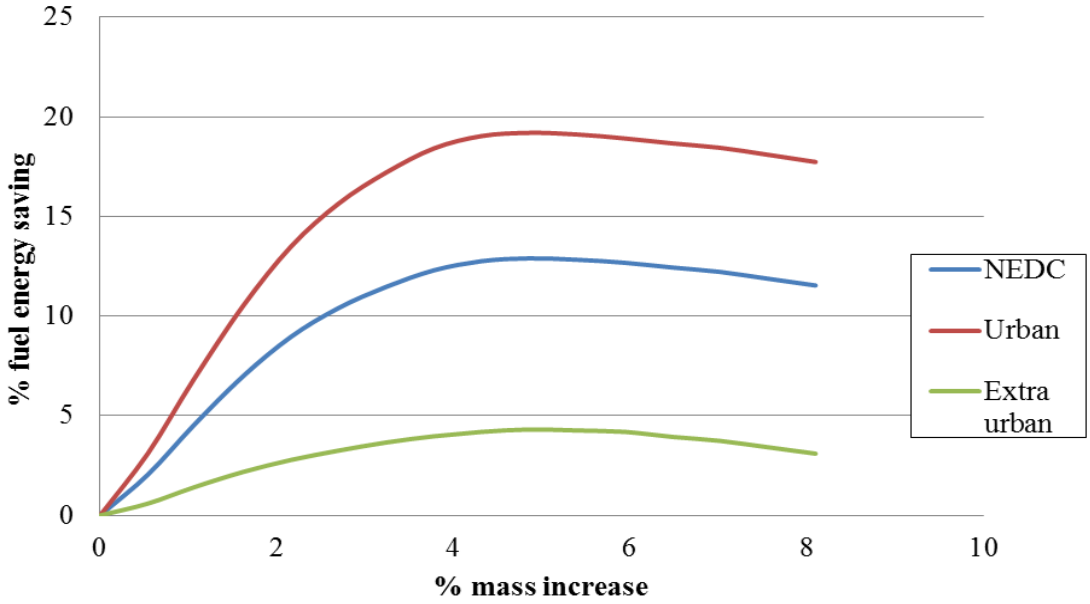

Figure 5.23: Range Rover Sport 5l (petrol) % fuel energy saving (compared to a vehicle with standard mass) vs % mass increase due to parallel hybrid system with RB&ESS (compared to standard vehicle mass) for NEDC drive cycles.

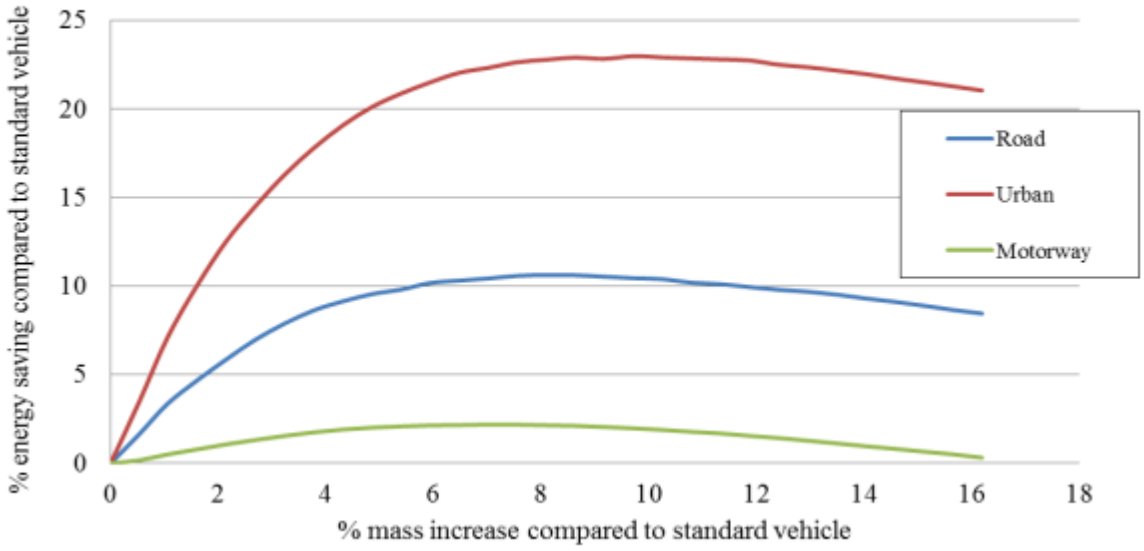

Figure 5.24:Range Rover Sport 5l (petrol) % fuel energy saving (comparing to a vehicle with standard mass) vs % mass increase due to parallel hybrid system with RB&ESS (compared to standard vehicle mass) for Artemis drive cycles.

5.6.4 Optare Solo SR simulation results

Here the MLTB cycle is used to assess possible savings through the use of a parallel hybrid system. Although the NEDC is used on the Volvo bus to give direct comparison here, the MLTB is used since the Optare Solo SR and bus 1 will not achieve the required speeds through the entire NEDC. The indicated fuel savings appear lower than for other vehicles on the NEDC cycle but a direct comparison is not being made so these result are shown for information only.

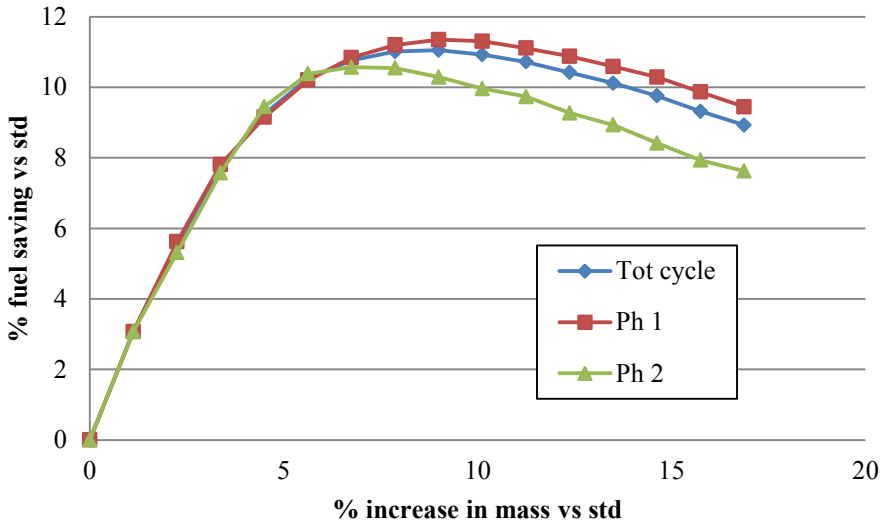

Figure 5.25: Optare Solo SR % fuel saving (comparing to a vehicle with standard mass) vs % mass increase due to parallel hybrid system with RB&ESS using Li-ion ESS (compared to standard vehicle mass) for MLTB drive cycle.

5.6.5 Bus 1 (ADL Enviro 400) simulation results

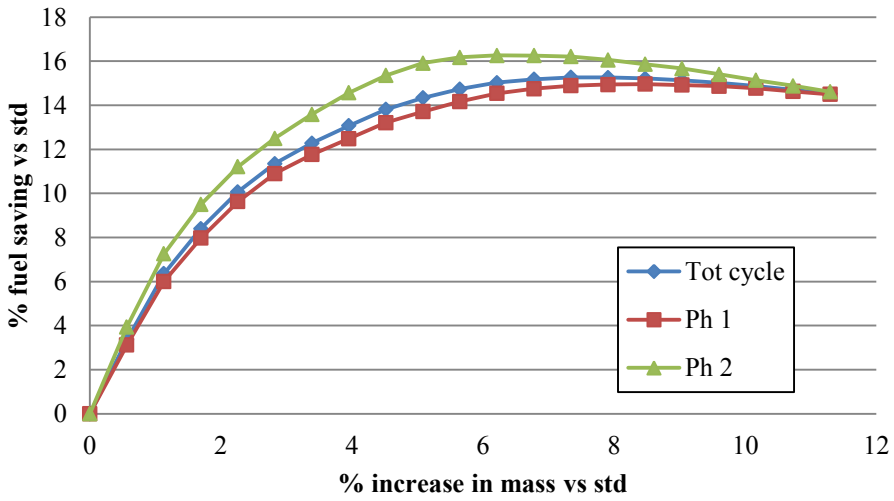

Figure 5.26: % fuel saving (comparing to a vehicle with standard mass) vs % mass increase due to parallel hybrid system with RB&ESS using Li-ion ESS (compared to standard vehicle mass) for MLTB drive.

In the case of the Optare Solo SR the calculated theoretical percentage fuel energy saving was slightly lower in the Phase 2 part of the cycle (inner London) than in Phase 1 (outer London) This is in contrast to the results shown for Bus '1' in figure 5.26. A likely explanation for this is the comparatively low mass of the Optare Solo range of buses. The available kinetic energy that might be recovered through RB is governed by ½ mv^2. During Phase 2 the average speed is relatively low and for a vehicle with relatively low mass (such as the Solo AR) for its size and load bearing capacity this has an overall effect of reducing the potential benefit of the RB&ESS. However, as shown in section 5.8.1, reduction in vehicle mass yields useful fuel energy savings in itself with no requirement for complex mechanical / electrical installations. However in order to achieve such weight savings a great deal of detailed design work is required from the onset. When considering the possible energy savings that might be achieved an important criterion is whether the RB&ESS is to be built in to an existing design as a factory modification or incorporated into the design of a new vehicle type. If the system is being added on then any net savings are of benefit. In the case of completely new designs however, the potential balance between possible fuel savings through weight reduction versus savings through RB&ESS require close consideration.

5.6.6 Volvo Coach simulation results

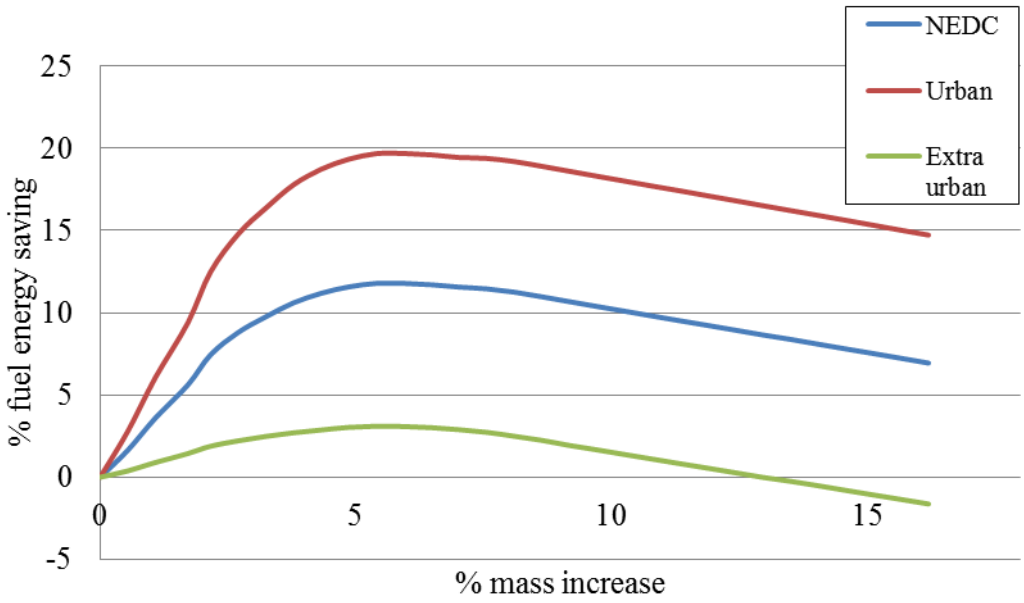

Figure 5.27: Volvo B11R Coach, % fuel energy saving (comparing to a vehicle with standard mass) vs % mass increase due to parallel hybrid system with RB&ESS (compared to standard vehicle mass) for NEDC drive cycles.

The results show in Figures 5.27 and 5.28 show the largest potential energy saving of the range of vehicles considered in this section using the NEDC with a percentage fuel saving of up to 23 % indicated for the Artemis urban cycle. It is worth considering that in urban areas buses, coaches and trams are often in use 24 hours a day. By virtue of the routes they follow and numerous stops it is possible that in practice on some routes with many periods of acceleration and braking even greater savings might be achieved along with the anticipated lowering of exhaust emissions. Any reduction in exhaust emissions, due to hybrid or other systems being used, is particularly welcome in built up areas where air quality is an increasing problem.

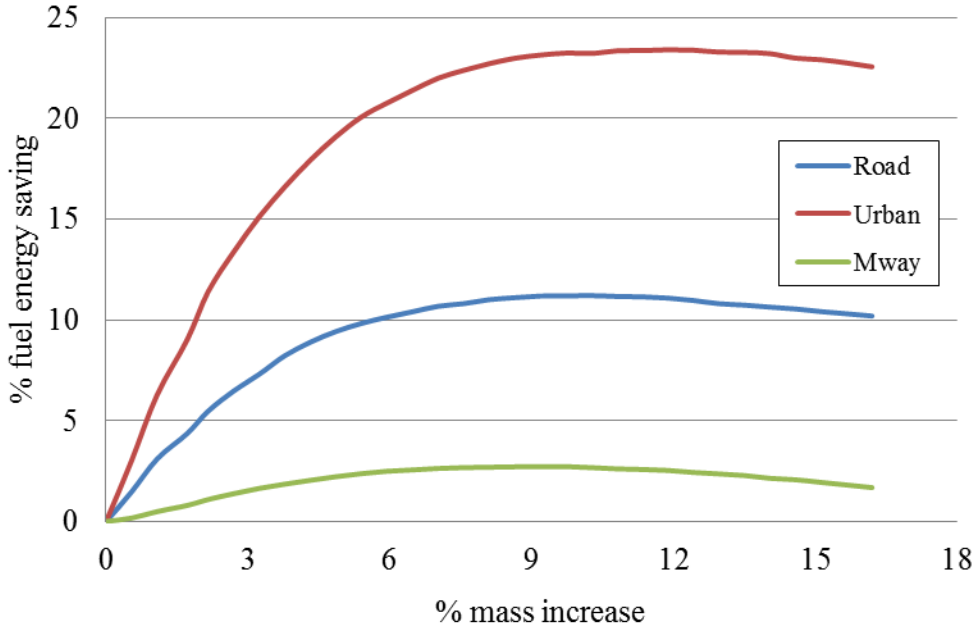

Figure 5.28:Volvo B11R Coach, % fuel energy saving (comparing to a vehicle with standard mass) vs % mass increase due to parallel hybrid system with RB&ESS (compared to standard vehicle mass) for Artemis drive cycles.

The maximum indicated saving for the Volvo B11R on the urban Artemis cycle is ≈ 23% which corresponds closely with the 25% savings possible using regenerative braking with buses claimed by Braess and Seiffert (2005). A summary of the result from section 5.6 are shown in figure 5.29.

Summary of findings from section 6.6	NEDC Urban	NEDC combined	NEDC Extra urban	Artemis Urban	Artemis Road	Artemis M.way
Citroen C1	15.9	7.62	1.67	19.96	4.7	0.32
Citroen Xsara	17.33	10.51	3.09	20.46	8.12	1.33
Range Rover	19.9	12.9	4.31	22.91	63	2.19
Bus	20.61	12.36	3.4	23.39	11.2	2.72

Figure 5.29: Summary of results from section 5.6

The results shown in Figure 5.29 and 5.30 show the same general trend in performance seen in earlier work in section 5.5 and discussion throughout section 5.6. Compared to the results in 5.5 these findings are based on a more realistic hypothetical parallel hybrid system where the mass and performance of the system are accounted for. This still represents a somewhat simplified approach but for the purpose of a quantitative

comparison study the simulation appears to work well. It is interesting to compare the savings summarised in Figure 5.29 with other energy savings that can be achieved using technology commonly found in hybrid vehicles and, increasingly in non-hybrid vehicles. In section 5.7 the possible benefits of start- stop technology are investigated.

5.7 Potential Energy Savings from Engine Stop-Start Technology

To study the energy saving potential of engine start – stop technology across the range of vehicles investigated over the different NEDC journeys the backward looking simulation was run with the changes described in section 4.7.1 such that when the vehicle is stationary for more than 2 seconds idling fuel use is reduced to zero. The results are shown in figure 5.30.

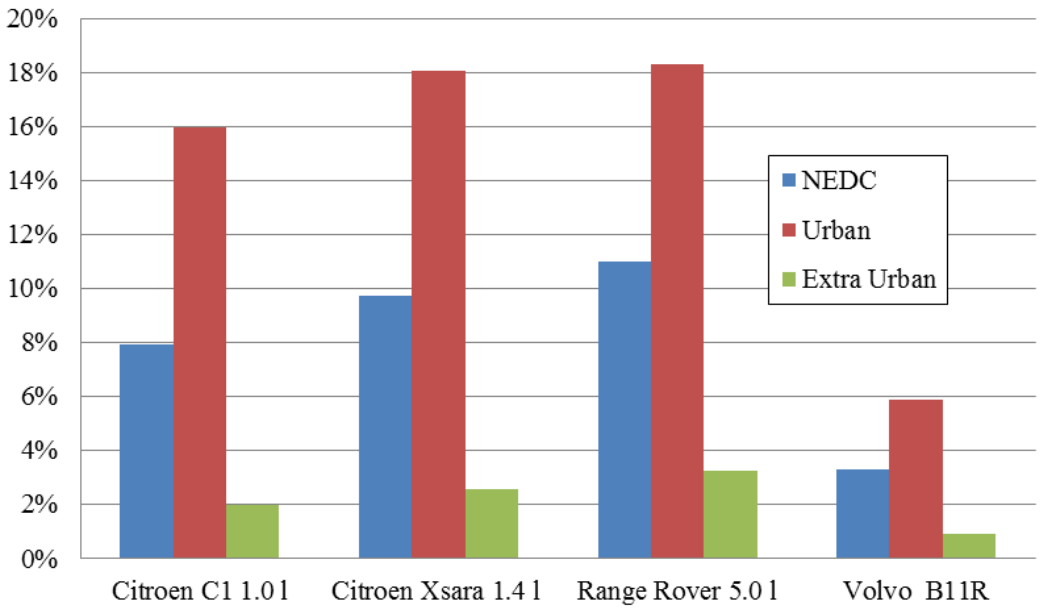

Figure 5.30: The simulated energy saving potential of a simulated start – stop engine system for a range of vehicles on NEDC

The general trend in these results is as one might expect, with greatest indicated energy savings on urban journeys where a comparatively large proportion of the journey time is spent at a standstill. On the extra urban cycle there is a total of 40 seconds idle time which accounts indicated savings from using start stop. It is interesting to note that, of the vehicles studied in this section, the greatest percentage savings appear to be possible with

the Range Rover 5.0 litre Petrol. This type of large luxury off road vehicle typically has high idling fuel consumption because of the large capacity of the engine and this is the principle reason for the comparatively large percentage energy savings indicated. Since the fuel demand during engine starting was not modelled in this work and different systems have different engine shut-down criteria, it is likely that practical savings will be slightly lower than indicated from these results. Human factors may also influence the fuel savings possible.

5.7.1. Start – stop engine technology and human behaviour

Anecdotal accounts and personal experience of the author suggests that drivers find engine start- stop technology quite unsettling when first using it. It can take time for the driver to get used to the engine cutting out each time the vehicle has been at rest for a short time. Most drivers do get used to it in time but the author has heard of examples of people who are so uncomfortable with the engine stopping and starting automatically that they habitually 'dab' the accelerator once their vehicle comes to a standstill and then continue to blip the throttle periodically to prevent the engine cutting out. This highlights the point that in some cases human nature and driving habits of individuals can negate some of the technological and engineering features which are incorporated into modern vehicle design. Some systems such as the one employed in the current Volkswagen *Bluemotion* range de-activates the engine when the car is at a standstill, put into neutral and the clutch released (Volkswagen, 2014). Some drivers are in the habit of leaving a car in gear even when stopped in traffic for quite long periods despite this causing undesirable wear on the clutch. Such behaviour would, of course, prevent the Volkswagen type of system from working as intended.

Reports by the consumer organisation Which (2014), suggest that start – stop technology can result in fuel savings of 5% to 8% in urban usage. As mentioned previously, the effects of start stop technology on fuel consumption can quite simply be assessed using the simulation developed by introducing a feature where fuel consumption falls to zero when the vehicle has been stationary for a set time period. This is essentially how most systems in currently available cars work. The only difference being that in cars, the system also relies on no throttle input from the driver. In the backward looking simulation used here the throttle position is not considered. In the forward looking simulation developed previously throttle position is simulated as part of the control algorithm which, as far as

possible, simulates the response of a driver. In this latter case the simulated throttle response would only rise above zero when the demand speed begins to increase from zero. In either simulation, the difficulty that can occur in real driving situations of drivers 'blipping' the throttle when stationary will not occur unless it is introduced as an extra human behaviour issue. For investigation of the effect of start stop technology on fuel consumption an ideal case was considered where there is no throttle input until demand speed increases above zero. Further investigation of non- ideal scenarios where drivers manually prevent the system working as intended would be worthwhile to reflect the realistic behaviour of some drivers who may be uncomfortable with this technology however this is a separate investigation beyond the scope of this work. As explained in Chapter 4, a benefit of the forward looking model is the possibility to simulate, to some extent, different driving styles. A brief study is included in section 5.7.2.

5.7.2 The effect of driving style on fuel consumption

By altering the engine speeds at which gear changes take place the speed range in which the vehicle's engine operates over the drive cycle can be altered. Some drivers naturally tend to 'race' the engine more than others whilst in some cases a conscious effort is made to drive for optimum economy attempting to keep the engine close to its peak BSFC envelope. The possible effect of increased engine speed range is shown in figure 5.31. In the simulations carried out to produce this plot, downward gear changes were set to occur at 1000 rpm below the engine speed at which upward changes occur – effectively keeping the engine speed within a 100 rpm band.

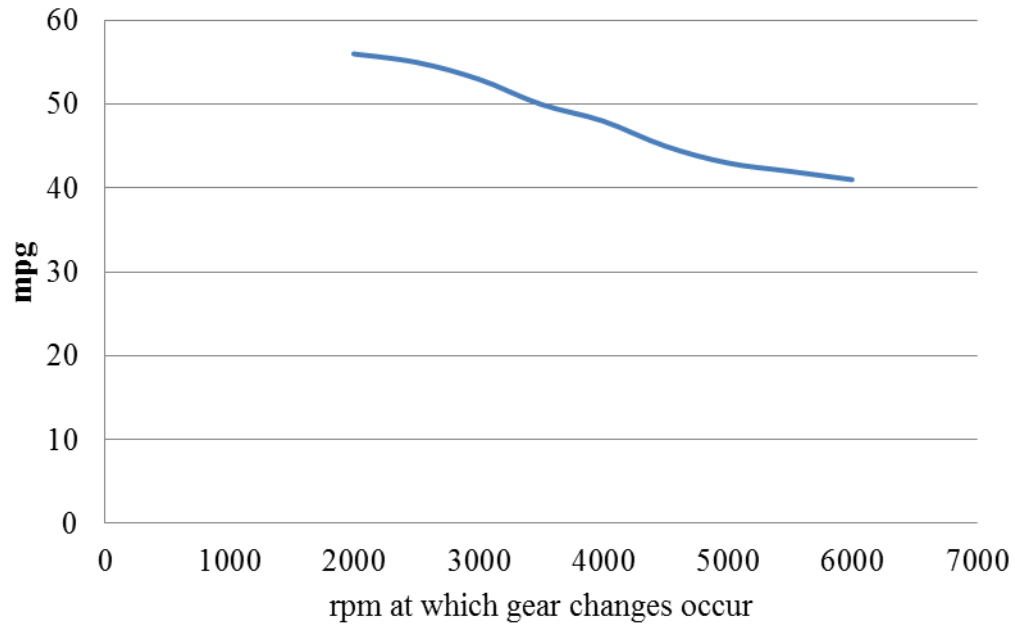

Figure 5.31: The simulated effect of driving style on fuel economy, (mpg / engine speed for upward gear changes) For 2010Citroen C1 1.0l on combined NEDC

The result shown in figure 5.31 suggests that fuel consumption may increase by up to 30% if an aggressive driving style is adopted where the engine is kept at high speeds even though the vehicle is still following the NEDC. Under such conditions the engine (simulated or real) torque and speed fall far outside the peak efficiency region of the BSFC map and typically engine efficiency may reduce to less than half of its peak value (Stone, 1989). This example gives come insight into how the best efforts of automotive engineers and designers may be cancelled out by individual driving style.

5.8 General Discussion

An increasing variety of hybrid vehicles are now available. However, according to collective anecdotal evidence, fuel economy figures claimed by the manufacturer are difficult to achieve in practice, although an improvement over conventional vehicles is likely. The claimed fuel economy of some direct injection diesels (with start-stop technology) is in a similar range to that claimed by Toyota for the Prius. For example the quoted fuel economy for the BMW 320i over a combined cycle is 68.9 (BMW, 2014) compared to 70mpg for the 1.8*l* Prius (Toyota, 2014). An advantage of parallel and series/parallel hybrids is that, for the size of ICE used, comparatively high performance is possible owing to the combined tractive effort of the two drive systems (usually ICE and electrical machines). However if larger savings are to be made in the future it may be necessary for drivers to adjust their expectations for vehicle performance. Anticipated

ongoing developments in battery and other energy storage technologies, resulting in improved energy and power density, may improve the fuel savings illustrated in chapter 5 and exhaust emissions reductions in predicted in chapter 6. However, it is likely a practical limit will be reached for energy storage and, for further savings, a more radical revision of motor vehicle design will be necessary. The reduction of frontal area, C_d, tyre rolling resistance, transmission losses and parasitic losses could all aid further improvement in efficiency. Unfortunately reducing C_d and frontal area both potentially conflict with practical requirements of carrying passengers and/or payload and could also impact on the comfort and ease of use of vehicles. Indeed, reducing these parameters to an absolute minimum would result in a vehicle capable of excellent fuel efficiency but of little practical use for everyday transport. The most successful entrants in the Shell Mileage marathon illustrate this issue clearly. However, current vehicle design is still very conservative as demonstrated by the very gradual change in car design over the past century. The hypothetical studies in Chapter 6 demonstrate that there is still scope for significant improvement in vehicle energy efficiency and that hybrid systems incorporating regenerative braking and energy storage can make a significant contribution.

5.8.1 Discussion on the effect of vehicle mass

A proportion of the fuel energy converted by the ICE of a conventional vehicle is used to overcome rolling resistance (F_{roll}), acceleration forces ($F_{acc} = m.a$) and forces to overcome gradients ($W \cos \alpha$). All three of these parameters are proportional to vehicle mass and, therefore any reduction in mass is expected to result in some improvement in fuel economy. The backward looking simulation was used to study the effect of a reduction in mass on the simulated Citroen C1 1.0l over the Artemis road cycle. In this instance the vehicle modelled was considered as a conventional powertrain with no RB or ESS. The results indicate that a reduction in mass of 20% could save around 9.8% fuel. In a study carried out by Casadei and Broda (2008) fuel savings of 8.4 % were calculated for a small car on the EPA combined cycle suggesting broad agreement with the work presented in Figure 5.32.

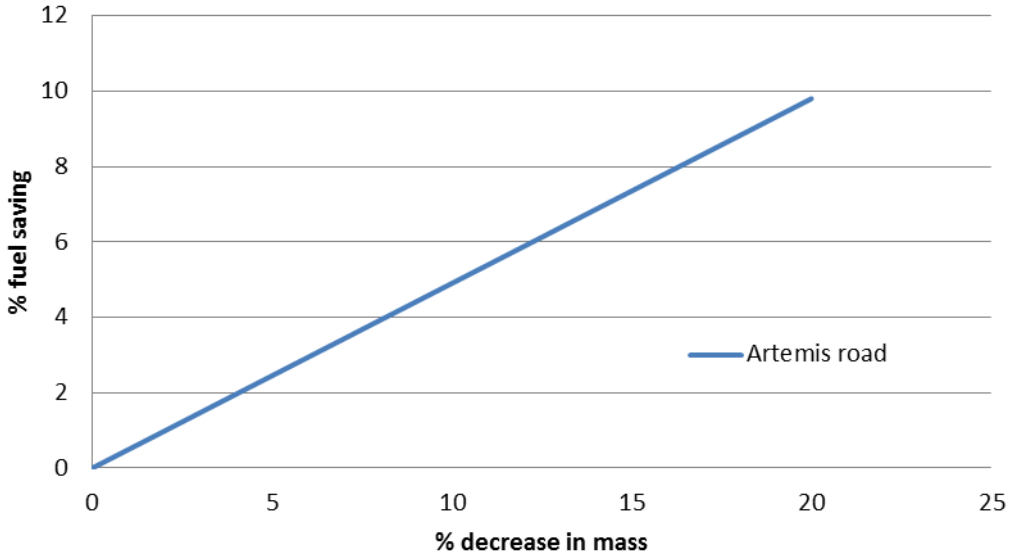

Figure 5.32: The effect of reduced vehicle mass on fuel energy requirement for Citroen C1 1.0 l on the Artemis Road cycle

Clearly, additional mass in vehicles could reduce the energy saving potential of efficiency improvements made by hybrid technologies reducing their impact. Many features that add weight to modern vehicles are mandatory features required by safety legislation (such as airbags, abs and catalytic convertors) but increased levels of driver comfort have also contributed.

5.8.2 The effect of aerodynamic drag coefficient (C_d) on theoretical energy savings from regenerative braking and energy storage

Reductions in vehicle C_d result in a smaller proportion of overall tractive effort being required to overcome aerodynamic resistance. Thus, as C_d increases, a greater proportion of the total tractive effort required is converted to overcome vehicle inertia. It is this portion of the overall energy which is potentially available to recover using a regenerative braking system. The backward looking simulation was used to investigate the possible percentage reduction in fuel burn over the NEDC with C_d reduction from the standard vehicle figure of 0.3 down to 0.2.

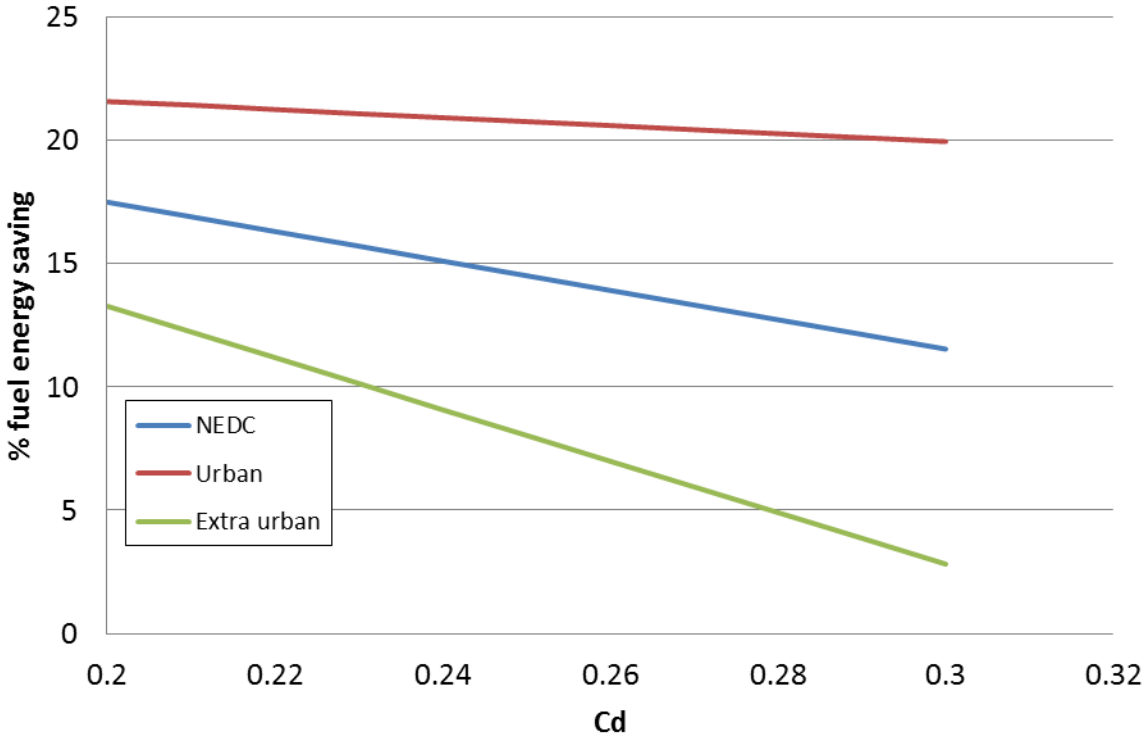

Figure 5.33: The effect of drag coefficient on possible fuel energy savings (shown as a % of standard vehicle fuel requirement) for the Range Rover sport 5.0l (Cd taken as 0.3 for all other modelling with this vehicle type).

From Figure 5.33 it is clear that a reduction in C_d can yield a significant increase in the percentage fuel saving possible with a RB & ESS (compared to standard vehicle). The results show, not surprisingly, that a decrease in drag coefficient for the Range Rover Sport from 0.3 to 0.2, yields the greatest increase in percentage fuel saving over the extra urban cycle (≈ 10%). This large theoretical reduction in drag coefficient only improves the fuel saving on the urban cycle by around 2%. The difference in fuel saving caused by drag reduction is a result of the relatively high average speeds over the extra urban cycle compared to the urban cycle. In practical terms a reduction of C_d from 0.3 to 0.2 would be very difficult with a luxury sport four wheel drive vehicle such as the Range Rover. As a comparison the 2014 Toyota Prius has a drag coefficient of 0.25 and very few production vehicles have a C_d < 0.28. The 2012 Mercedes Benz B Class was a recent notable exception having a C_d of 0.26 or 0.24 with optional aerodynamic extras (Davis, 2012). However whilst a reduction of C_d to 0.2 may not be feasible the data presented in Figure 6.28 indicates that more modest reductions in C_d could result in useful improvements in the effectiveness of a RB & ESS incorporated into the parallel hybrid system that has been modelled. A reduction in C_d and A would be particularly beneficial in the case of small

cars however, because of their relatively short wheelbase and overall length, small cars tend to have a high roof line to accommodate a driver and passengers in comfort. This places a practical limitation on the performance in this regard. The potential to investigate the likely effects on fuel economy of C_d along with other parameters such as C_{roll} and A is a useful additional feature of the simulation.

CHAPTER 6

THE EFFECT OF A HYBRID SYSTEM ON EXHAUST EMISSIONS FROM BUSES

6.1 Introduction

As shown in Chapter 5, maximum likely savings from the use of parallel hybrid powertrains are predicted in the field of public transport, particularly, as might be expected, on urban routes where frequent stops occur. Having produced quantitative estimates of the comparable energy savings on such routes in Chapter 5 here the work moves from a generalised to a more specific study. Emissions look-up tables from ADVISOR (2001) were used to find the engine emissions during each time step. For all results presented in 6.2 the bus payload is set to 50% and all simulation work was based on the MLTB cycle described in 4.1.3

A difficulty with this section of work was obtaining the emissions look-up data since this data is determined from engine dynamometer testing which is dependent on specialist facilities and is expensive and time consuming to conduct. A useful range of emissions data was available from the look-up tables used in the ADVISOR software. Although this data did not specifically relate to the engines in the vehicles being simulated it enabled comparative studies to be conducted.

6.1.2 Exhaust emissions investigated

Owning to the concerns relating to human health effects from exposure to vehicle exhaust emissions outlined in 1.1.4, and the findings outlined in chapter 5, the focus was narrowed to consider public transport applications. Two models of bus, typical of current examples in use around the UK were considered, and NO_x and PM exhaust emissions were simulated over the MLTB cycle described in section 4.1.3 and shown in figure 4.3.

It would be beneficial to explore a wider range of emissions as more data becomes available [Note - Further data was made available in January 2016 and is currently being processed. Findings based on this will be the subject future work]. Alternatively the simulation could be developed to include approximate calculation of engine emissions. Focusing this study on NO_x and PM was considered justified since both are of particular concern in respect of human health as reported in Chapter 1.

6.2 Transport Scenarios Included in the Emissions Study

6.2.1 Bus 1 with Li-Ion Battery ESS

For this study the vehicle considered is referred to as 'Bus 1' this is the same vehicle as considered in the sizing and fuel consumption study in 5.6.5 and is not referred to by its brand and model name at the request of TfL who kindly provided test data from experimental trials. As in 5.6.5, the MLTB cycle is used for this study which includes 2 phases. Phase 1 relating to outer London (details) and Phase 2 relating to inner London (details). The emissions calculations look-up sub-routine described in 4.7.3 along with the brake specific emissions data (in look-up table form) were included in the simulation. The NO_x and PM emissions were then found for the simulated vehicle with a parallel hybrid system incorporating RB&ESS. Although the sizing of the RB & ESS has been previously studied in relation to fuel consumption here the effects of the system sizing (i.e. power rating, energy capacity and hybrid system mass) on NO_x and PM emissions are investigated.

For the first results a hypothetical ESS is included with power and energy density typical for Li-ion batteries (see table in Figure. 6.1) however, for this case initially the energy management is simplified with the SOC limited between 0 and 100%. Although this is a hypothetical case it gives a useful basis for comparison with later results shown in Figures 6.4 to 6.5 and examples throughout this section where the SOC (or LOE in the case of the flywheel study) is taken into account. The characteristics show in Figure 6.1 are by no means the 'best case' example, in fact the motor / generator is a very conservative estimate with power densities of up to 5 -10kW/kg now possible, albeit at high cost. This relatively low value is used here to allow for the fact that in this study the exact mass of the hybrid system is difficult to determine with great accuracy so it is was considered reasonable to use a conservative estimate to account for unknowns. A basic control strategy was employed, as for the work in chapter 5, and outlined in Appendix VI. Essentially, if stored energy is available, within the SOC limits it is used to contribute towards vehicle traction limited by the power rating of the ESS and motor generators.

ESS data	Li-ion Battery	units
Energy density	288000.00	J/kg
Power density	800.00	J/s/kg
Motor /gen		**units**
Power density	0.2	kW/kg

Figure 6.1: Summary of energy and density values used in the simulation to generate data in section 6. Energy and power density from Cheng et al (2008), motor generator power density from Burke et al (1980)

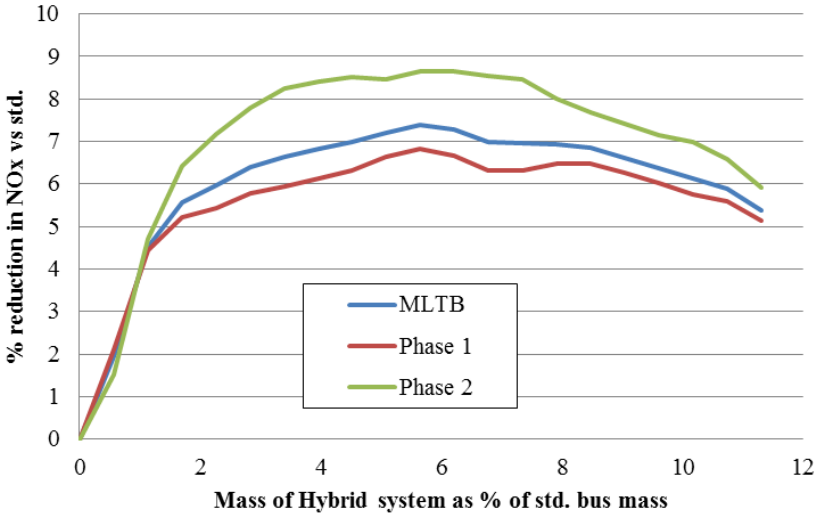

Figure. 6.2: Estimated reductions in NOx with example Li-Ion battery parallel hybrid system (0%<SOC<100%, SOC_{init} = 0%)

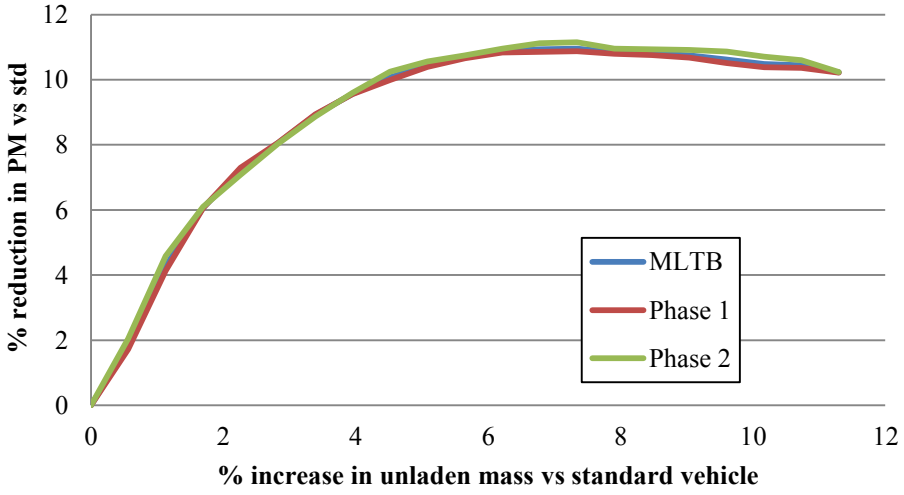

Figure. 6.3: Estimated reductions in PM with example Li-Ion battery parallel hybrid system (0%<SOC<100%, SOCinit = 0%)

Figure 6.2 and 6.3 show that with increased hybrid system size, the emissions of NO_x and PM both increase up to a maximum of around 8.5% and 11% respectively. The greatest benefit predicted to occur with a system weighing corresponding to 6% of the unladen vehicle mass.

For Figures 6.4 and 6.5 SOC_{min} and SOC_{max} limits (40% and 80% respectively) were applied, in these examples SOC_{init} is set at 50%. The simulation calculates the required fuel energy equivalent of the SOC_{init} when calculating fuel energy requirements of a hypothetical hybrid. However in the case of emissions calculations this was not practical owning to the number of unknowns and variables involved and the requirement for a very detailed engine model (even then then this would be difficult). Instead for the data shown the SOC_{init} is assumed to have been generated from previous regenerative braking or the SOC has been raised to this level by a 'plug in' system from mains electricity. In this scenario, unless the electricity was generated by a renewable means then there will be some additional emissions associated with this journey however they will be remote from the point of use. These un-counted emissions, although still of concern on a wider scale, will most likely not effect local air quality at the point of use as in the case with any plug-in EV or HEV.

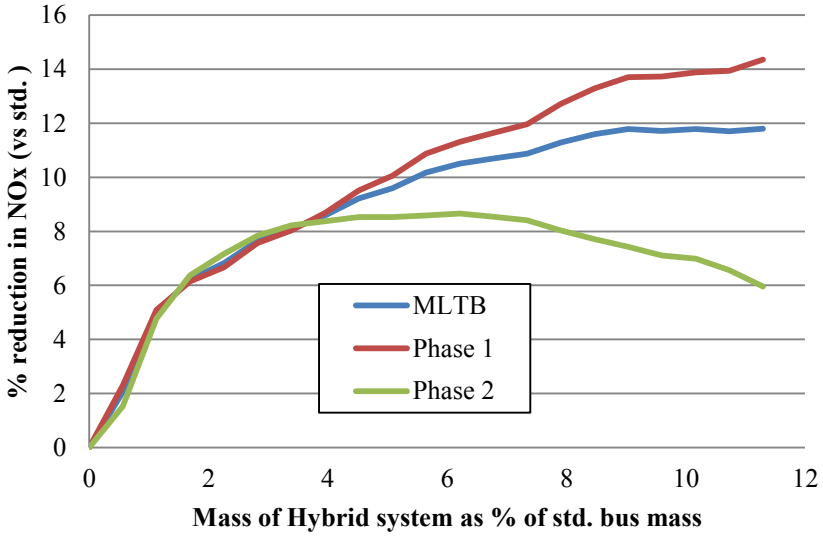

Figure. 6.4: Estimated reductions in NOx with example Li-Ion battery parallel hybrid system (40%<SOC<80%, SOCinit = 50%)

As the modelled hybrid system size is increased the simulated reduction in NO_x emissions across all parts of the journey are found to increase markedly and by similar amounts.

Above a system size weighing approximately 4 % of the vehicle mass the results diverge this can be explained by the fact that the stored energy is dissipated throughout the journey due to the large capacity/ power specification of the ESS. The effect of this is most noticeable on the phase 2 (latter) part of the cycle by which time much of the energy has been dissapated in previous acceleration events. For phase 1 however a reduction of up to 14 % is found. Clearly such a system is not appropriately sized for independent operation relying instead on regular charging at stops which would require significant infrastructure and in many cities would not be feasible.

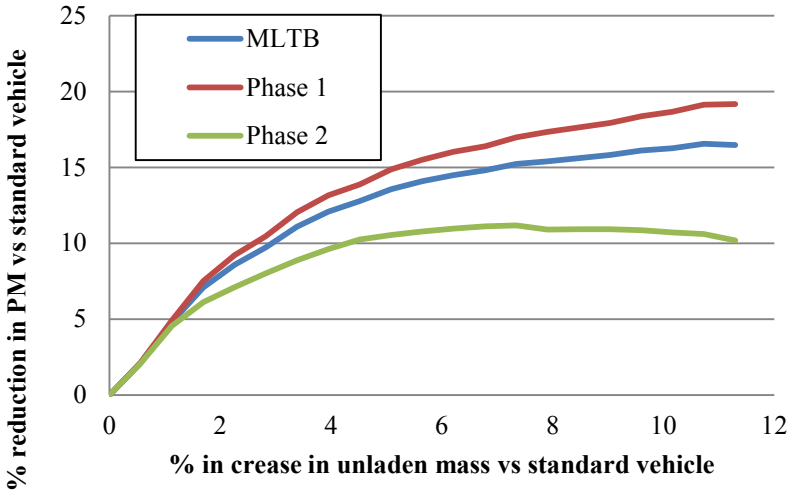

Figure. 6.5: Estimated reductions in PM with example Li-Ion battery parallel hybrid system (40%<SOC<80%, SOC_{init} = 50%)

The results shown in figure 6.5 indicate that the reduction in PM emissions would follow a similar trend to NO_x except with the greatest reduction on phase 1 of the MLTB for the same reasons relating to the reduction in the state of charge throughout the journey.

6.2.2 Bus 1 with High speed composite flywheel ESS

For this study the characteristics of the parallel hybrid system were define as shown in Figure. 6.6. The simulation is used as in section 6.2.1 except in this instance, because a high speed flywheel is used at the ESS a second motor / generator is required (1 is coupled to the vehicle transmission, one to the flywheel) so the mass of this second electrical machine and an estimated mass for associated hardware is taken into account taken in the model.

ESS data	FLYWHEEL	units
Energy density	14000.00	J/kg
Power density	800.00	W/kg
Motor /gen		**units**
Power density	0.2	kW/kg

Figure. 6.6: Hybrid system power and energy densities used for simulation work in section 6.2.2

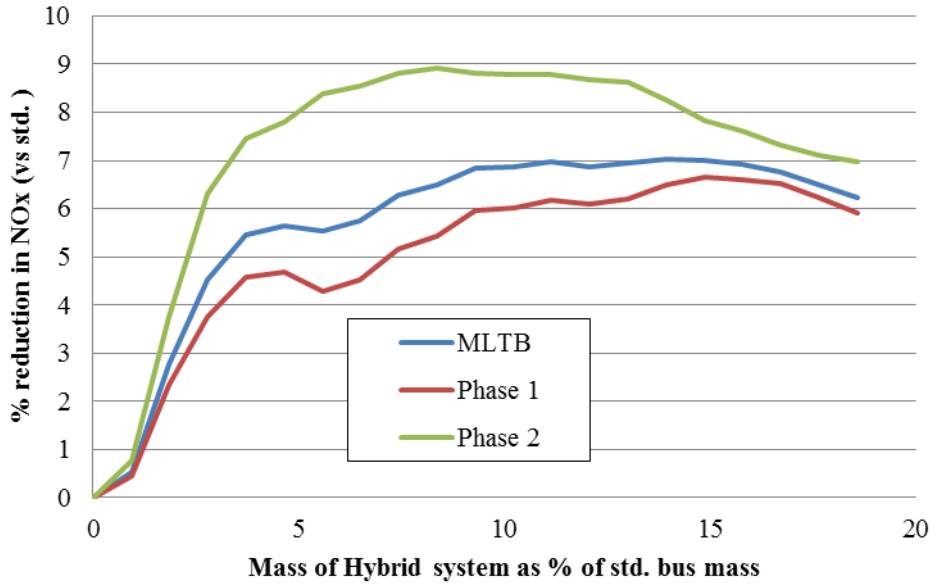

Figure.6.7: Estimated reductions in NOx with flywheel ESS in parallel hybrid system (0%<SOC<100%, initial SOC = 0%)

The data presented above shows the expected trend with maximum reduction (9%) on the phase 2 (inner London) part of the route. A hybrid system sizing of approximately 10% of vehicle unladen mass appears to give the optimal reduction whilst a smaller system of only 5% could still result in useful reductions of around 5%.

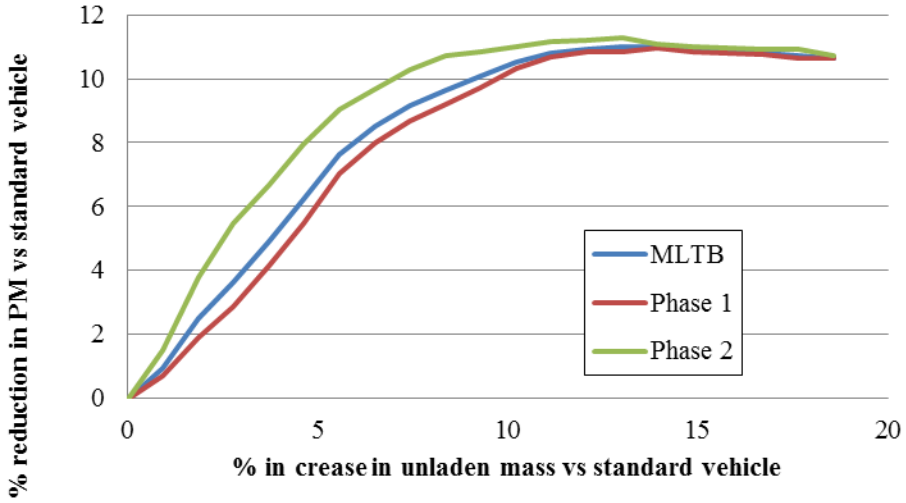

Figure. 6.8: Estimated reductions in PM with flywheel ESS in parallel hybrid system (0%<SOC<100%, initial SOC = 0%)

Figure.6.8 shows that PM reductions are broadly similar across the 3parts of the MLTB and beyond a system mass of 10% of the unladen vehicle no further benefit is predicted.

In the example hybrid system modelled to generate the results in Figure 6.8 the simulation shows that a hypothetical system corresponding to an 18% increase in vehicle mass (vs standard) has a capacity of 0.8MJ. This shows broad agreement with the sizing of the 1 MJ flywheel system used in the Flybrid KERS (Kinetic Energy Recovery System). The corresponding 200 kW power rating calculated by the simulation also corresponds to the 200 - 250 kW power rating claimed for of the Torotrak KERS (Torotrak, 2015). With a higher energy density ESS the peak energy capacity would occur at vehicle mass increase below 18%. Similar trends are observed in figures 6.9 and 6.10 although owing to the SOC_{min} = 10% there is a slightly greater spread in the NO_x result the usable SOC range is reduced.

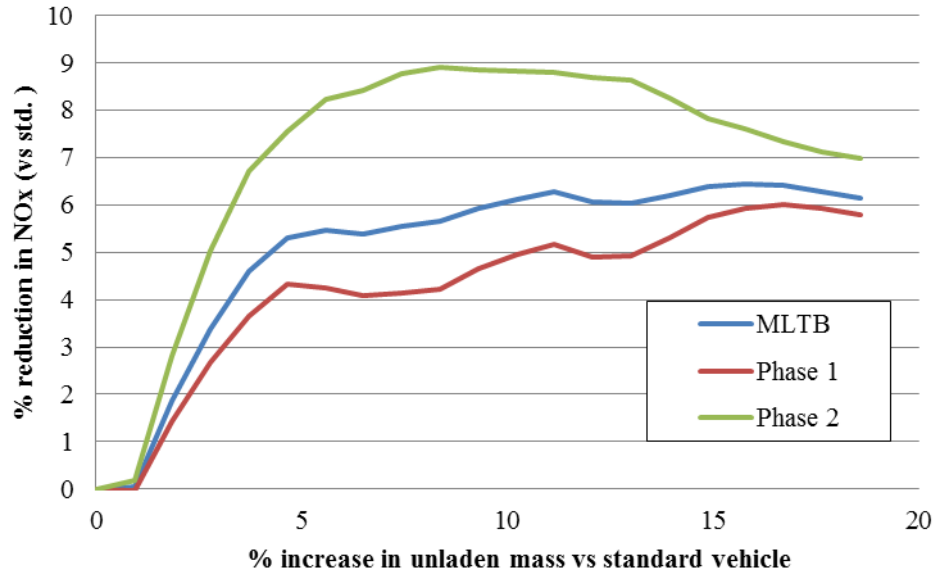

Figure.6.9: Estimated reductions in NOx with flywheel ESS in parallel hybrid system (10%<LOE<100%, initial SOC = 50%)

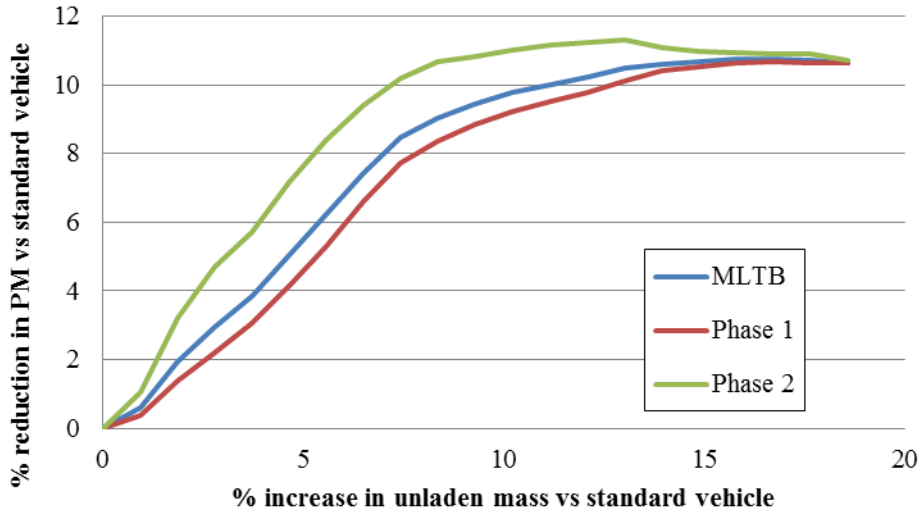

Figure. 6.10: Estimated reductions in PMxx with flywheel ESS in parallel hybrid system (10%<SOC<100%, initial SOC = 50%)

6.3. Study of emissions from an Optare Solo SR

In this section the Optare Solo SR (a single deck example, details listed in Appendix 1) was simulated with a parallel hybrid system using motor generators and a battery system based on the energy and power densities listed in figure 6.1. The performance was first simulated for a hypothetical case with the SOC limits set between 0 and 100% (idealised case)

6.3.1 Optare Solo SR with Li-Ion Battery ESS

In figures 6.11 the improvement in NO_x emission due to the hybrid system is smaller than found for bus 1. The reduction in PM is also not as significant as in the results shown in 6.2. This trend is exhibited throughout the results for the Optare example except in the case of the anomalous results in 6.13 and 6.14 which, judging by appearance, are due an error in data used for this scenario.

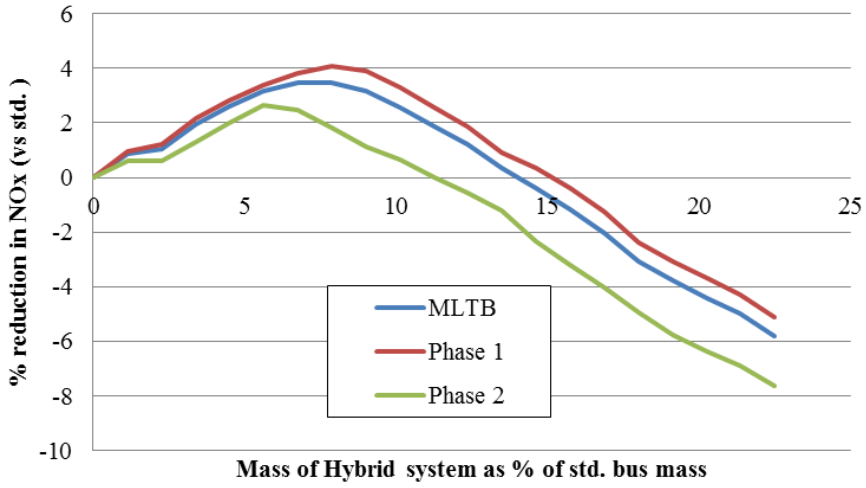

Figure.6.11: Bus 2 Estimated reductions in NOx with Li-ion ESS in parallel hybrid system (0%<SOC<100%, initial SOC = 0%)

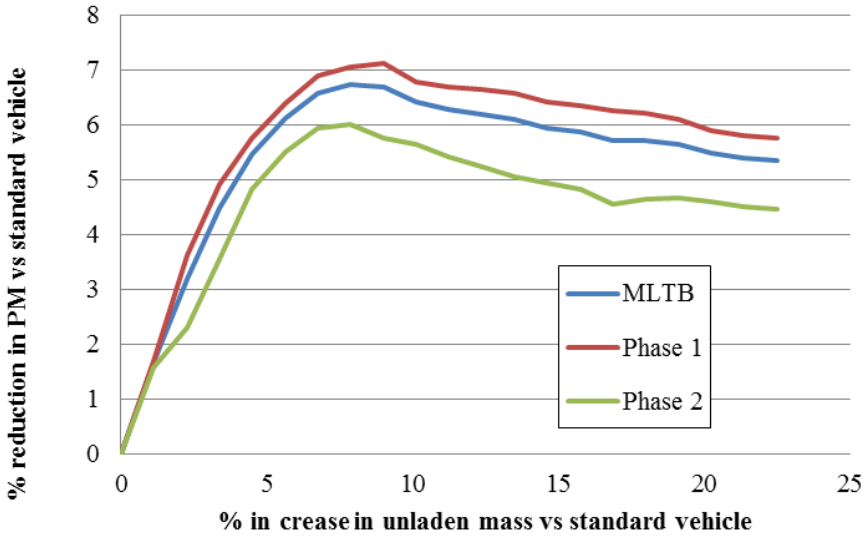

Figure. 6.12: Bus 2 Estimated reductions in PM with Li-ion ESS in parallel hybrid system (0%<SOC<100%, initial SOC = 0%)

The fact that this is a lighter bus, designed for higher speeds, and has a similar engine but different load regime to the 'bus 1' example would lead one to expect rather different results when modelled with a parallel hybrid system. The results shown here (except for 6.13!) indicate very modest reductions in NO_x (approx. 4%) but generally improvements in PM output of 7-8%)

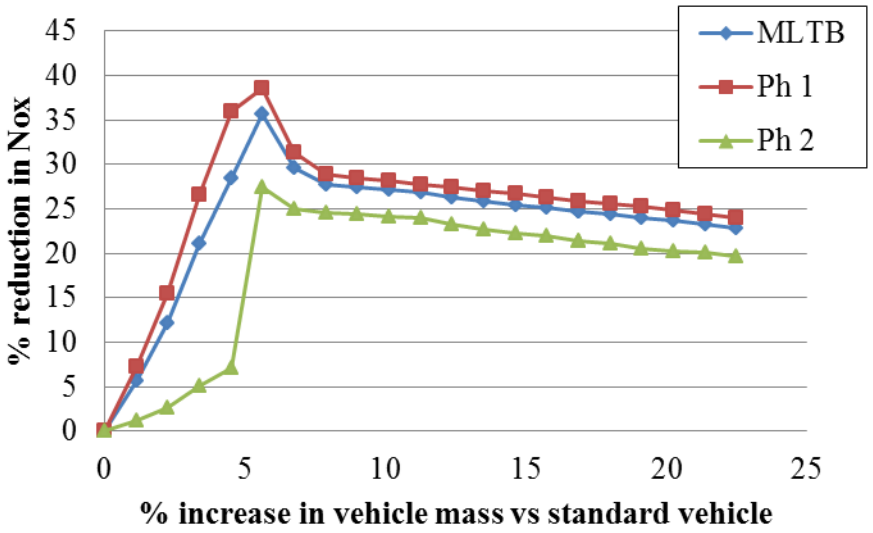

Figure.6.13: Bus 2 Estimated reductions in NOx with Li-ion ESS in parallel hybrid system (40%<SOC<80%, initial SOC = 50%)

The results shown in Figure 6.13 appear anomalous but included hear for completeness, and in the interest of full disclosure. The author is reviewing this particular simulation to double check the input data and settings.

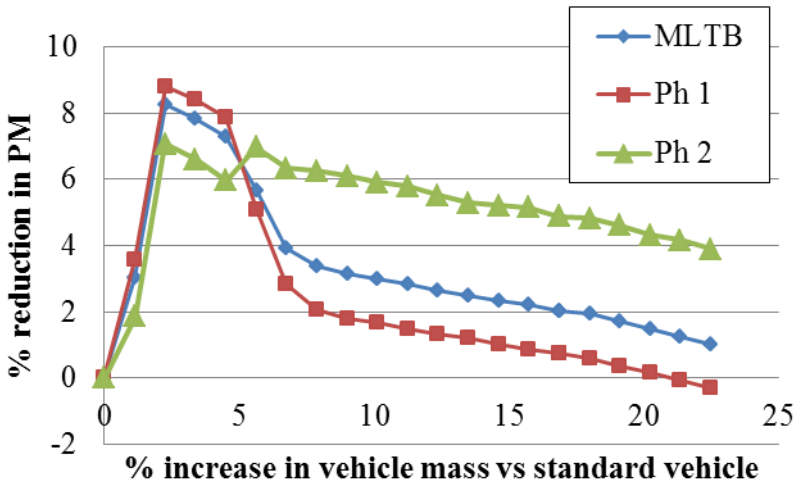

Figure. 6.14: Bus 2 Estimated reductions in PM with Li-ion ESS in parallel hybrid system (40%<SOC<80%, initial SOC = 0%)

.

6.3.2 Optare Solo SR with High speed composite flywheel ESS

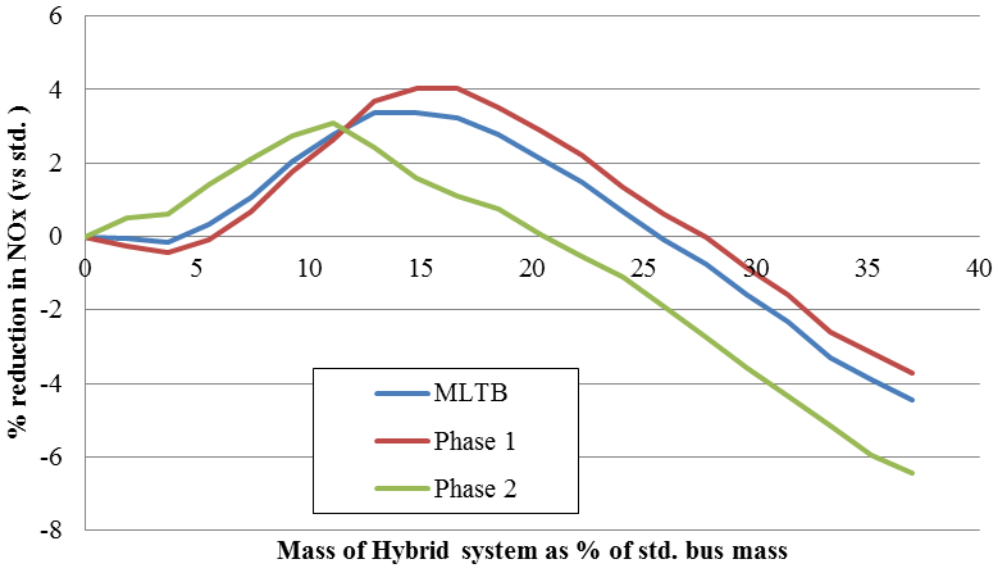

Figure.6.15: Bus 2 Estimated reductions in NOx with flywheel ESS in parallel hybrid system (0%<SOC<100%, initial SOC = 0%)

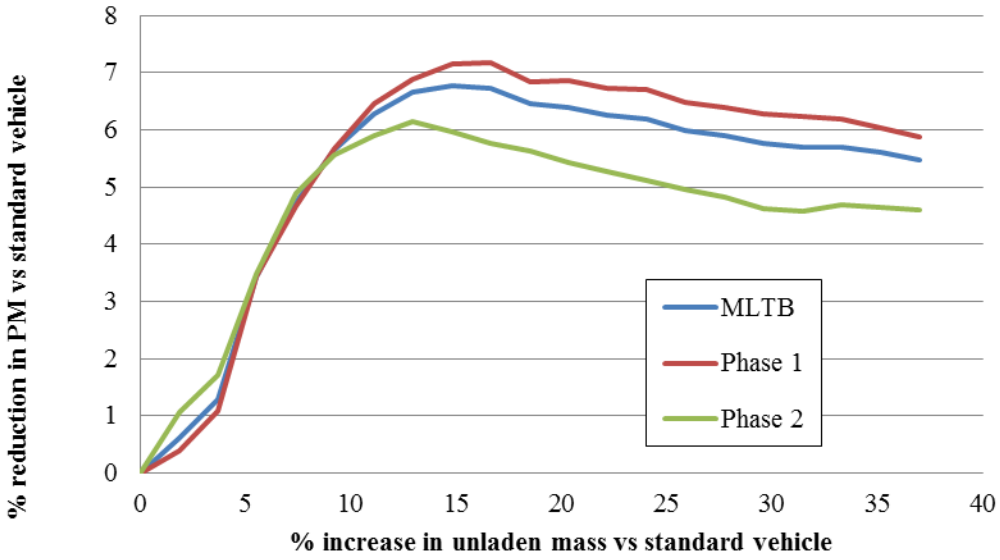

Figure. 6.16: Bus 2 Estimated reductions in PM with flywheel ESS in parallel hybrid system (0%<SOC<100%, initial SOC = 0%)

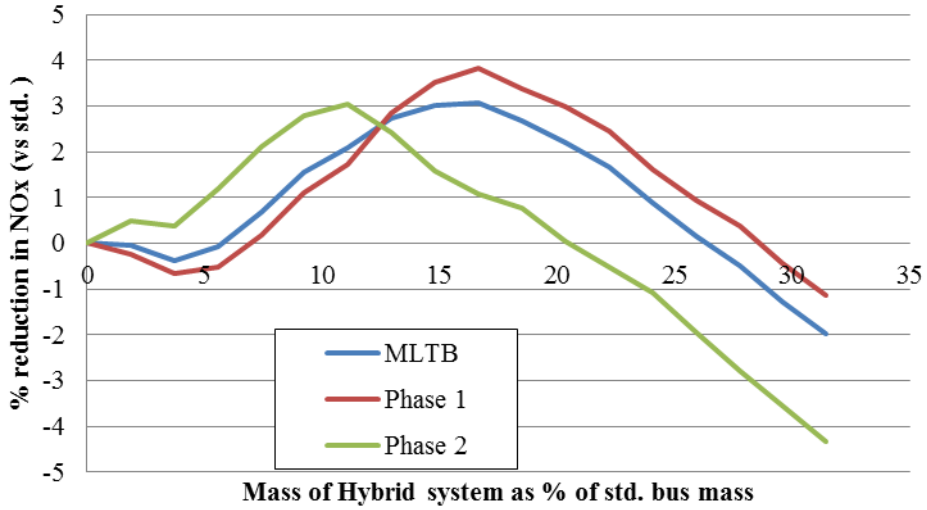

Figure. 6.17: Estimated reductions in NOx with flywheel ESS in parallel hybrid system (10%<SOC<100%, initial SOC = 50%)

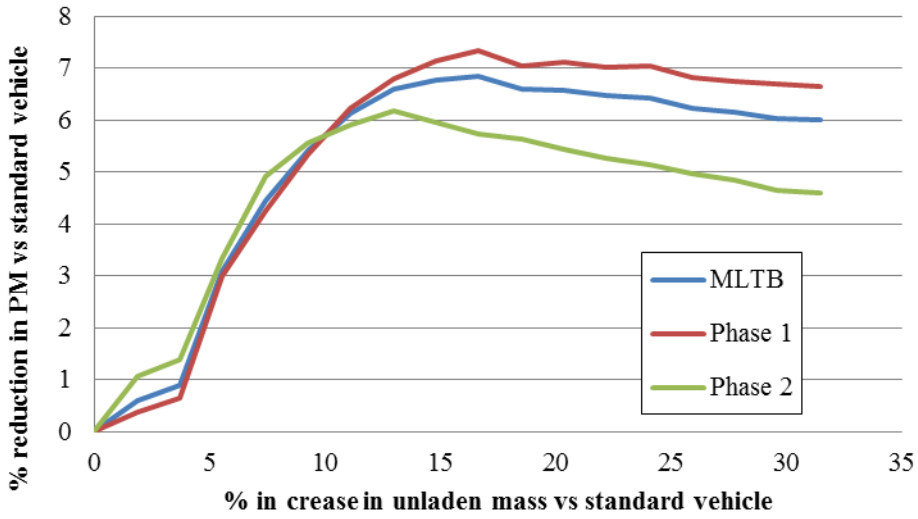

Figure. 6.18: Estimated reductions in PM with flywheel ESS in parallel hybrid system (10%<SOC<100%, initial SOC = 50%)

6.3 Summary of results from emissions study

A summary of the Peak theoretical NO_x and PM reductions achievable from the case studies shown are shown in the figure 6.19. Clearly with the hypothetical parallel hybrid simulated in these case studies useful savings in NO_x and PM ranging from 10 to under 3%. In this idealised study any emissions caused indirectly due to the pre-charging of the ESS when an initial SOC was applied. As described by Heywood (1988) NO_x emissions are increased at high combustion temperatures. In this study the tractive assistance provided by the parallel hybrid system effectively reduces the torque requirement on the ICE and in turn reduces the magnitude of NO_x produced. The relationship between engine loads and PM is less clear and from the look-up table used here it exhibits a more complex topography. However it seems for these example the reduction in engine load has reduced PM emissions noticeably. It is worth noting from the data presented here that reductions of NO_x and PM don't always occur for the same Hybrid system sizing characteristic. Also peak fuel savings can occur at a different system sizing to max reductions in emissions of NO_x and PM.

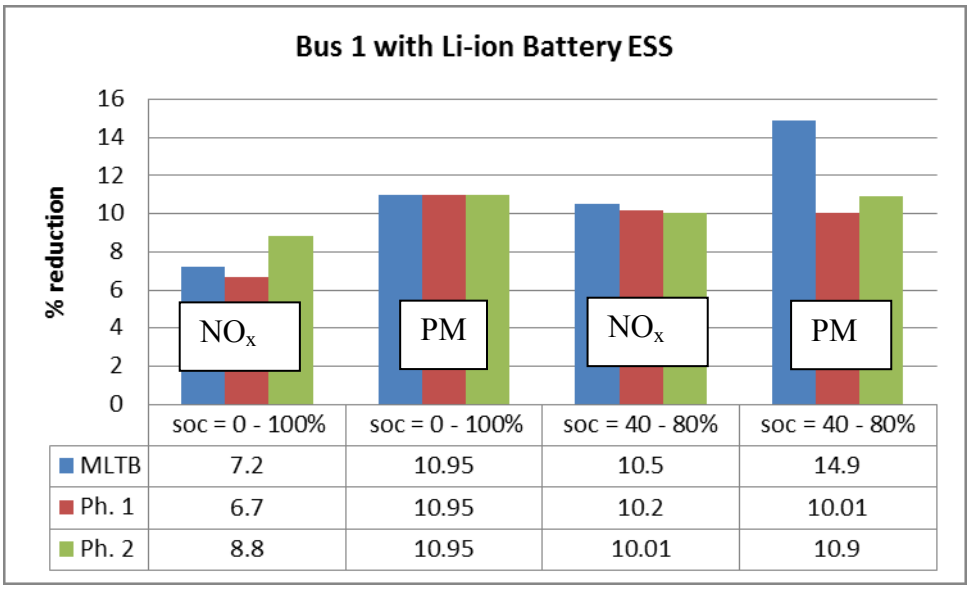

	soc = 0 - 100%	soc = 0 - 100%	soc = 40 - 80%	soc = 40 - 80%
MLTB	7.2	10.95	10.5	14.9
Ph. 1	6.7	10.95	10.2	10.01
Ph. 2	8.8	10.95	10.01	10.9

Figure. 6.19: Summary of results for bus 1 with Li-ion ESS in parallel hybrid system

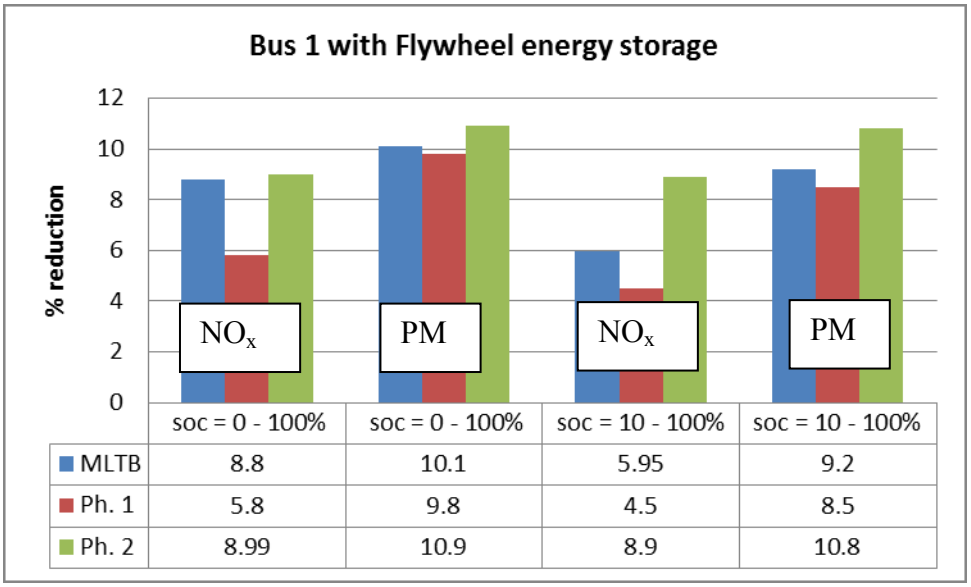

	soc = 0 - 100%	soc = 0 - 100%	soc = 10 - 100%	soc = 10 - 100%
MLTB	8.8	10.1	5.95	9.2
Ph. 1	5.8	9.8	4.5	8.5
Ph. 2	8.99	10.9	8.9	10.8

Figure. 6.20: Summary of results for bus 1 with Flywheel ESS in parallel hybrid system

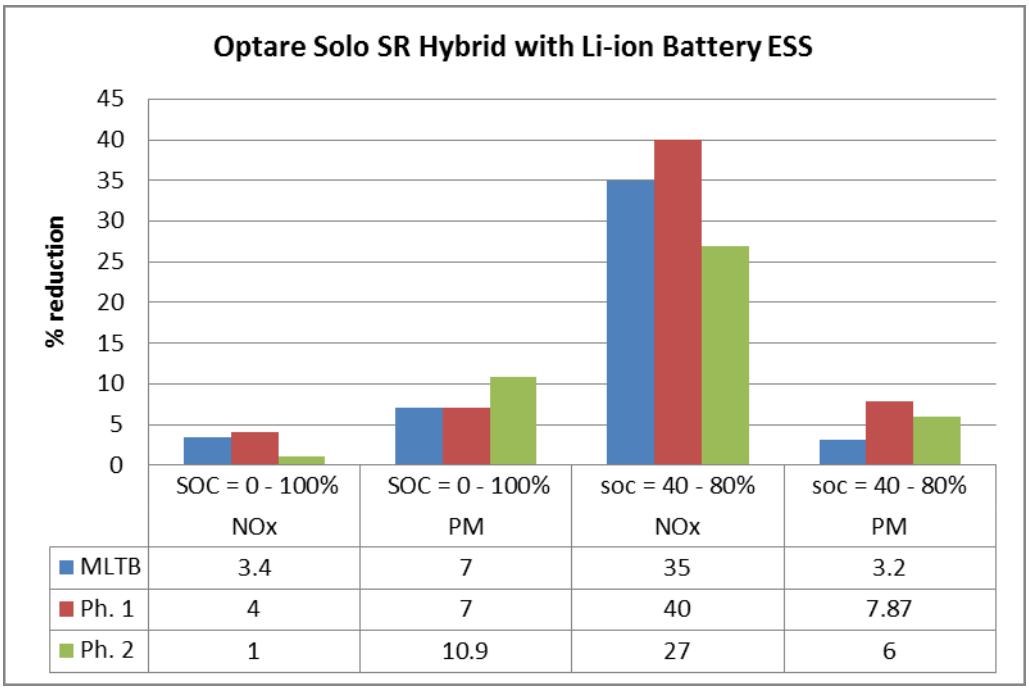

	SOC = 0 - 100% NOx	SOC = 0 - 100% PM	soc = 40 - 80% NOx	soc = 40 - 80% PM
MLTB	3.4	7	35	3.2
Ph. 1	4	7	40	7.87
Ph. 2	1	10.9	27	6

Figure. 6.21: Summary of results for Optare Solo SR with Li-ion ESS in parallel hybrid system

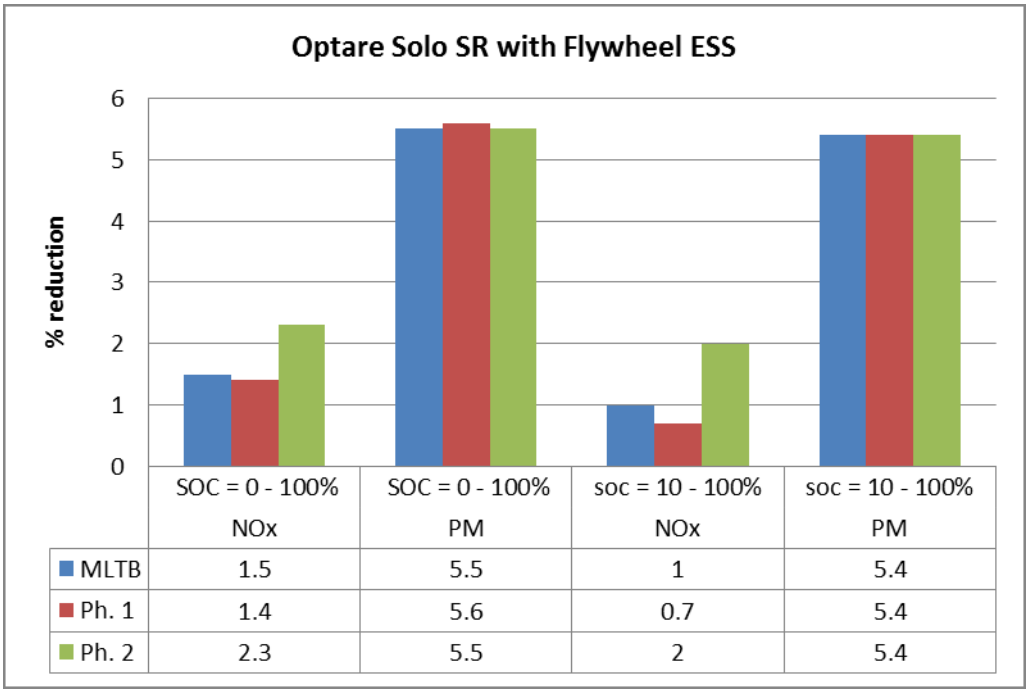

	SOC = 0 - 100% NOx	SOC = 0 - 100% PM	soc = 10 - 100% NOx	soc = 10 - 100% PM
MLTB	1.5	5.5	1	5.4
Ph. 1	1.4	5.6	0.7	5.4
Ph. 2	2.3	5.5	2	5.4

Figure. 6.22: Summary of results for Optare Flywheel ESS in parallel hybrid system

6.4 Energy density and energy capacity in relation to LOE or SOC

An issue when simulating Bus 1 and the Optare Solo SR was found with ratio between the ESS and Energy capacity. This results from the relationship between energy capacity and

energy density for different energy storage types. Based on the performance data shown in fig. 6.1 and 6.2.2 the large energy density / power density ratio results in the simulated Li - ion battery ESS having an excessively large capacity. In the chapter 5 sizing plots for a range of 4 vehicles showing possible energy savings vs hybrid system mass (as a proportion of vehicle unladen mass) the energy capacity and power of the ESS are determined from the energy and power density respectively. To determine each data point on (shown for example in figs 5.25 and 5.26 a regenerative braking power was entered into the simulation and the mass of the electrical machine (motor generator) and ESS were calculated based on their respective power densities. As shown in equations 6-1 and 6-2.

$$m_{ESS} = \frac{P_{regen}}{\rho_{P(ESS)}} \tag{6-1}$$

$$ESS_{cap} = m_{ESS} \cdot \rho_{U(ESS)} \tag{6-2}$$

Where:

m_{ESS} = Energy storage system mass (kg)

P_{regen}= Regenerative braking power of hybrid system (w)

$\rho_{P(ESS)}$= Power density of ESS (W/kg)

ESS_{cap} = Energy capacity of ESS (J/kg)

$\rho_{U(ESS)}$ = Energy density of ESS (MJ/kg)

With the typical values for $\rho_{P(ESS)}$ and $\rho_{U(ESS)}$ used for Li–ion batteries results in an ESS of with a capacity far in excess of the values indicate by the sizing work described in chapter 5. In practice, providing that the physical volume of a proposed Li-ion battery can still be contained within the vehicle structure and its mass does not significantly impede the overall hybrid system efficiency, then an ESS of very large capacity can be viable. However if the ESS capacity is many times higher than the capacity required to recover all the available regenerative braking over a given test cycle (in this case the MLTB) then the system would be most suited to plug-in hybrid systems. A plug-in hybrid configuration

could be suited to some bus (and also tram and train) applications where significant time is spent at stops for loading / unloading and some charging could occur.

A disadvantage of an oversized system is that unless some form of pre-charging occurs before a journey start then there will be no traction contribution to the drivetrain until the minimum SOC is achieved through regenerative braking. If pre-charged to a high level (overnight for example) then an obvious advantage would be the increased opportunity for engine downsizing and, depending on the scaling of the traction motors, electric only (zero emissions operation) . The ratio of the values for used for energy and power density used to characterise the flywheel ESS considered are more closely matched to the minimum power and energy requirements for optimizing regenerative braking over the MLTB. The wide operational LOE range is also beneficial in terms of optimising savings. These findings along with factors discussed in 3.5.3 show that in principle a flywheel system has advantages for energy storage in hybrid applications. Despite the need (in this scenario at least) for a second motor generator the high energy density, good cycle life and ongoing developments to improve efficiency make the technology a possibility as currently being demonstrated by Torotrak (2015). In section 6.5 the effect of passenger load on anticipated emissions when using a flywheel based parallel hybrid system.

6.5 The effect of passenger payload on possible fuel savings and emissions reductions

From the work carried out and fundamental conservation of momentum it is clear that possible energy saving and emissions reductions from the use of hybrids are strongly influenced by vehicle mass. For buses the passenger payload constitutes a significant proportion of the Gross vehicle weight. A full passenger load (82 passengers) on Bus One would contribute approximately 46% of the total vehicle weight. For the Optare Solo SR the equivalent percentage figure is approximately 62%. These calculations are based on an average passenger mass of 68 kg. With these figures in mind the flywheel parallel hybrid system was sized to achieve maximum predicted fuel savings and reduced emissions and the effect of passenger load was simulated. For the simulated results shown in 6.2.3 to 6.2.7 the hybrid system is sized such that it increases the unladen vehicle mass by 10% which corresponds to a system power of 100kW and an energy capacity of 1.75MJ.

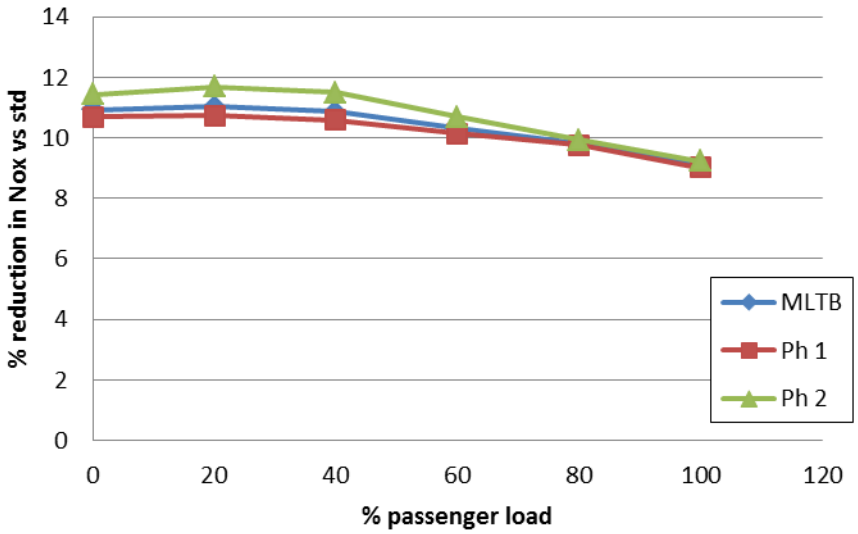

Figure. 6.23: % reduction in NO_x (compared to standard) vs Passenger load for Bus 1

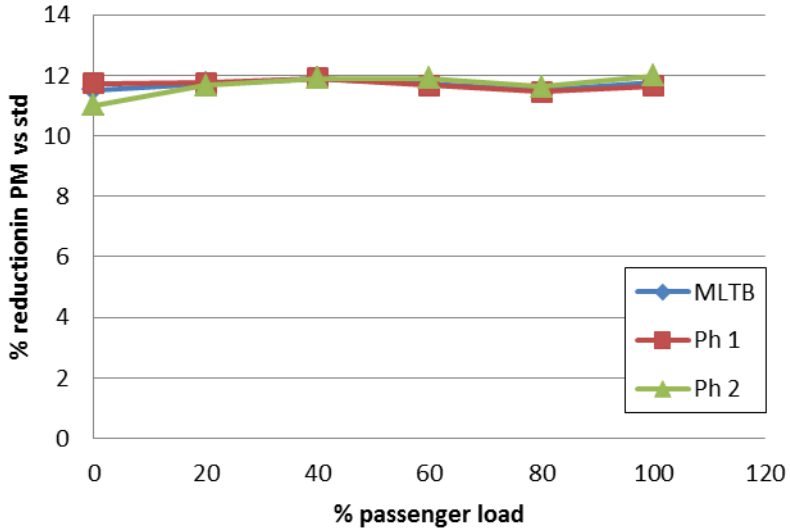

Figure. 6.24: % reduction in PM (compared to standard) in PM vs Passenger load for Bus 1

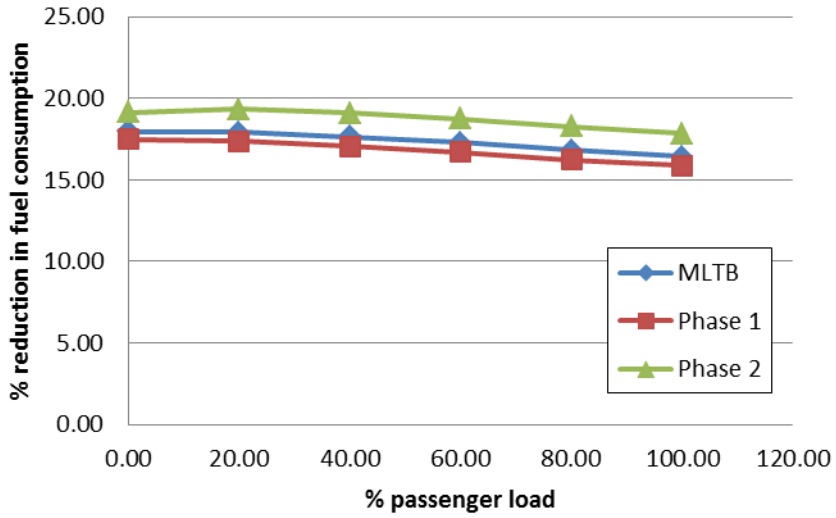

Figure. 6.25: reduction in fuel consumption (compared to standard) in PM vs Passenger load for Bus 1

The effect of a full load of passengers (indicated as 100% in figure 6.25) compared to an empty bus causes the reduction in NOx emission to drop from around 11% to 9% whereas the PM emissions are not significantly altered. The benefit in terms of fuel savings reduces by around 2- 3 %.

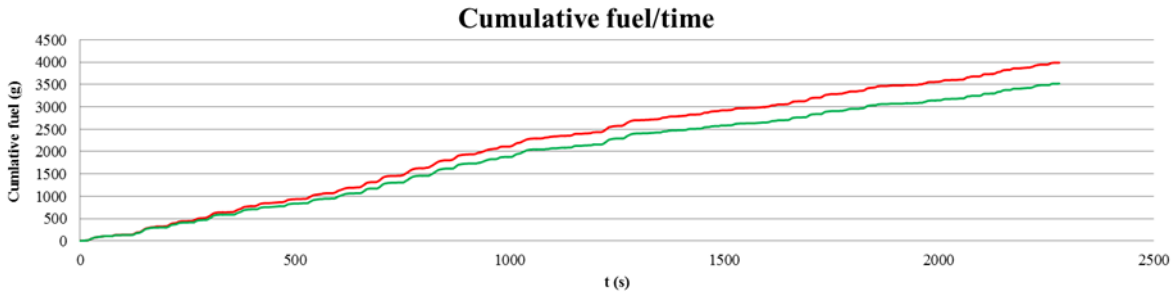

Figure. 6.26: Cumulative fuel consumption (hybrid compared to standard) over the MLTB cycle Red = standard vehicle, green = hybrid

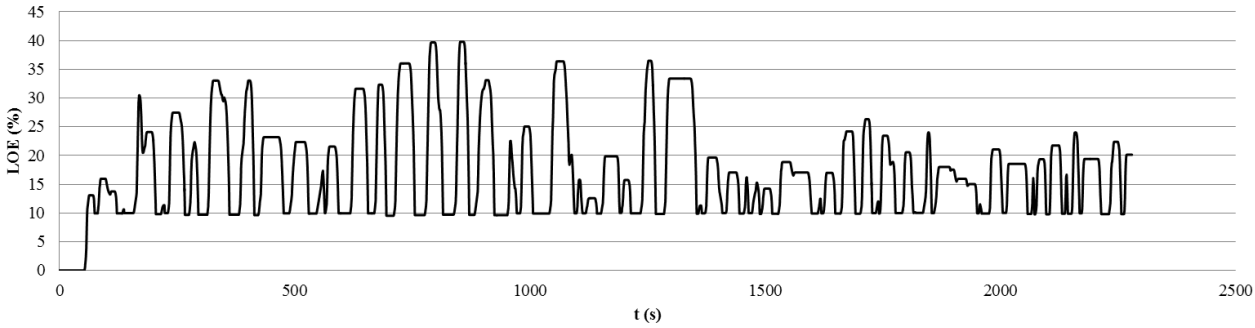

Figure. 6.27: Example LOE plot for bus 1 over the MLTB cycle with no pre-charge and full passenger load. SOC_{min}= 10%

Cumulative fuel consumption over the length of the simulation is shown in 6.26, clearly illustrating the difference in fuel required between the parallel hybrid system and the standard vehicle. A graph indicating the ESS LOE throughout the cycle is also included as an example of the output from the simulation. The fact that the LOE does not exceed 40% over the journey suggests that the system is not optimally sized owing to the energy density / energy capacity ratio discussed in 6.4. As mentioned elsewhere, refinements to the simplified control strategy could improve the predicted reductions in emissions and improvements in fuel economy indicated by the work done to date.

CHAPTER 7

CONCLUSIONS AND RECOMMENDATIONS

7.1 Simulation Performance

The work carried out has demonstrated that a spread-sheet based 'forward looking' time-stepping model can be used to simulate energy use in vehicles but simulated results are sensitive to the stability and optimization of the driver control algorithm. The inclusion of the driver model, necessary for the forward looking approach, adds complexity but could provide scope for investigation into driver behaviour beyond that which is possible from a backward looking model i.e. tuning the PID terms to represent different driving styles.

The PID control function within this model performed adequately, causing the simulated vehicle speed to closely track a given demand profile (either from an industry test cycle or from experimental data). The simplifications made with respect to clutch slipping conditions and particularly engine braking could be refined to improve the smoothness of the simulation response. Although comparison with manufacturers data showed differences of up to 30% correlation with test data from road trials, was more encouraging and was conducted using two methods. Long term fuel consumption over a 'real' combined journey with simulation of the same vehicle type (2002 Citroen Xsara 1.4 petrol) was made which showed a difference of under 5%. Direct fuel flow measurement using the TORQUE app was carried out during road testing over an urban journey in a small hatchback (2004 VW Polo 1.2 petrol). Subsequent simulation of the same vehicle type, over the recorded journey cycle, yielded results that differed by approximately 5%. The development of this model, whilst presenting many challenges, gave a valuable insight into the subtleties of simulating energy conversion in vehicles and proved very useful for the subsequent work on the backward looking model ultimately chosen to remove some complexity.

The backward looking model, Ver.2 (using a simplified engine efficiency function) was used originally used for some of the work outlined in chapter 5. Subsequently, this was revisited using the Ver. 3 simulation which included a conventional BSFC look-up function. Regenerative braking and energy storage feature was incorporated into the backward-looking simulation. Ver.3 includes emissions calculation though using look-up tables. This version also allows LOE / SOC to be limited as required and includes a method for setting LOE / SOC operating envelopes to refine the simplified control strategy that was used for the generalised work in Chapter 5.

Ver. 3 Showed an acceptable correlation with manufacturers' data (within 15% - for a small car). In the case of 'bus 1' fuel simulated consumption differed from independent test data (on the MLTB cycle) by between <2% on the outer London section but 12% on the inner London phase. This is thought to be connected with the difficulties associated with accurately simulating the torque converter. Correlation across the whole cycle was within 3%. The difference warrants further study but considering the comparative nature of this work it was acceptable. Direct comparison between absolute simulated and measured emissions showed large differences but this was considered acceptable within the scope of this work where differences in emissions, due to the use of regenerative braking in a hypothetical parallel hybrid were considered.

7.2 The Effectiveness of Regenerative Braking and Energy Storage In Hybrid Vehicles

7.2.1. Findings from the general study (energy savings)

The novelty in this work lies in the combination of a broad study (using an original spread sheet based model) with the later, more focused case studies considering emissions from buses. Findings presented in this broad study show the significance of the energy transfer rate (power rating) and the capacity of the energy storage system in relation to the amount of regenerative braking energy that can be recovered on different journey types with a range of vehicles.

The potential energy saving benefit of different vehicles and journey profiles has been investigated. In general, findings indicate that regenerative braking and energy storage can be of increasing benefit as vehicle size and mass increases but significant savings of up to 15% are possible even with small cars on urban journeys. For the parallel hybrid simulated, with the mass of a hypothetical RB&ESSS taken into account (using a hypothetical ESS with energy and power densities similar to Li-ion batteries) peak calculated savings ranged from 15% to 23% for a small car (Citron C1) and coach (Volvo BH11R) respectively on the NEDC urban cycle.

Calculated savings over the NEDC and Artemis cycles varied due to the different nature of the journey cycles but produced similar overall findings. The vehicle / journey scenario exhibiting the lowest theoretical energy saving indicated was the Citroen C1 example on the Artemis motorway cycle where a lower than 1 % saving was found.

When considering regenerative braking and energy storage in isolation from other energy hybrid powertrain technologies it is clear that in some cases a relatively small increase in mass (10%) over that of a standard vehicle can cancel out the potential saving incurred with the RB&ESS on extra urban journeys. This highlights the importance of weight saving in any such vehicle. Simulation work to investigate the possible energy savings from start - stop engine technology show that such features can provide a useful contribution towards reduced fuel consumption ranging from over the range of vehicles studied. The greatest benefit was found on vehicles with a significant power surplus (such as large sports 4 wheeled drive) when modelled on the urban NEDC journey profile yielding savings of up to 18%. This was principally due to the idling fuel consumption incurred with a large engine. In extra urban scenarios savings from start - stop technology are predictably small (2-3% from the extra urban part of NEDC) due to the comparatively small amount of time spent at idle. Practical fuel savings may be slightly lower than those indicated here due to some of the simplifications made in this model.

In the specific public transport application considered in Chapter 6, two different bus types: ’Bus 1’ (double deck) and the Optare Solo SR using the MLTB cycle. NO_x and PM emissions were modelled and reductions of between 6 and 10 % for NO_x and PM respectively.

Small differences (in the order of 2-3%) in the predicted fuel saving from a hybrid system were predicted depending on bus payload.

Currently the UK along with many other nations in the developed world is facing serious public health issues related to air quality and pollution related to road traffic. The problem is most prevalent in urban areas with high population and traffic densities. In view of this, opportunities for reductions in emissions, such as demonstrated here by the simulation of a parallel hybrid system, should be given serious consideration. In practice by using an ESS of higher specification than applied in the simulation along with appropriate engine downsizing greater savings could be possible than indicated from the work described in chapter 6. Such improvements in fuel economy and emissions possible from hybrid powertrains and start-stop technology, whilst maintaining vehicle performance, are likely to be difficult to achieve by other existing means in conventional powertrain vehicles whilst maintaining an acceptable level of performance and practicality.

7.3 Recommendations for further work

7.3.1 Further development

(i) The simulation (Ver. 3) could be further developed to include a more refined control strategy / strategies. The possible benefits of such strategies on fuel economy and emissions could then be studied in relation to hybrid buses and or across other vehicle classes.

(ii) A look-ahead strategy could be investigated to optimise energy savings. The control strategy of the hybrid powertrain system would need to be refined taking into account information on the *likely* journey ahead. This could enable the balance between stored energy, and reliance upon the prime motive source to be managed to maximise overall energy efficiency. The findings of such a study would be of benefit for hybrid systems of both a parallel and series type. However any potential benefits from a look-ahead strategy will be greatest where journey cycle is predictable for a relatively long time span such as in the case of tram and train routes and for some urban bus routes.

7.3.2 Further applications

(i) Using data recently obtained, further emissions modelling could include a wider range of exhaust gases and the possible reductions likely due to regenerative braking with a parallel HEV to extend the scope and depth of work on buses (different sizes, models and types of route). A gradient feature is included in the model and could be used to investigate the effectiveness of regenerative braking on hilly routes. Finn Coyle (TfL), who provided test data for 'bus' 1, has asked for a demonstration of the simulation in relation to ongoing work to improve emissions of public transport in London.

(ii) The generalised nature of the simulation, with some simplification of detail, makes it easily adaptable to other types/classes of vehicle. In addition to the existing work on buses other public transport vehicles such as trams and trains could be modelled to assess possible reductions in fuel consumption (or electrical energy) and, where appropriate emissions (i.e. diesel – electric trains). Phil Hinde of Crossrail has expressed interest in the simulation in this regard.

(iii) The effect of engine downsizing could be explored to calculate the predicted savings possible through the use of such methods.

.

REFERENCES

5AT (2015) *Locomotive and Train Resistance*. Available from: http://www.5at.co.uk/index.php/definitions/terrms-and-definitions/resistance.html [Accessed 12 August 2015]

ADVISOR (2001) *Matlab look-up data for BSFC and Emissions* via Dr. Chis Bannister

Afotey, B, Sattler, M. Mattingly, S. and Chen, V. (2013) Statistical Model for Estimating Carbon Dioxide Emissions from a Light-Duty Gasoline Vehicle. *Journal of Environmental Protection*, [online] 4, pp 8-15. Available from: http://www.scirp.org/journal/PaperInformation.aspx?PaperID=35596. [Accessed 10 January 2016].

Ajisman, J. Kobuchi, K. Oobayashi, R. Shimada (1997), Windage Loss Reduction of Flywheel Generator System Using He and **SF** Gas Mixtures. *Proceedings of the 32nd Intersociety Energy Conversion Engineering Conference*. Vol. 3, pp. 1754-1758.

Alstom (2013), *Alstom to supply ground-braking energy recovery system for London Underground*, [online] published 02/05/2013. Available from: http://www.alstom.com/press-centre/2013/5/alstom-to-supply-ground-braking-energy-recovery-system-for-london-underground/ [Accessed 10 July 2014].

Andre, M. (2004) The ARTEMIS European driving cycles for measuring car pollutant emissions, *Science of The Total Environment: Highway and Urban Pollution*. 334–335, pp.73–84.

Baglione, M. (2007), Development of system analysis methodologies and tools for modelling and optimizing vehicle system efficiency, *A dissertation submitted in partial fulfilment of the requirements for the degree of Doctor of Philosophy (Mechanical Engineering)*, University of Michigan 2007.

Bayindir, K., Gozukucuk, M. A., and Teke, A. (2011) A comprehensive overview of hybrid electric vehicle: Powertrain configurations, powertrain control techniques and electronic control units. *Energy Conversion and Management.* (52) pp. 1305–1313.

Barkan, C. (2009) Railroad Transportation Energy Efficiency Presentation from Railroad Engineering Program, Department of Civil and Environmental Engineering, University of Illinois at Urbana-Champaign.

Barlow, T.J. Latham, S. McCrae, I.S. and Boulter, P.G. (2009) *A Reference Book of driving cycles for use in the measurement of road vehicle emissions* 3rd ed. Berkshire: IHS

Barnes, J (2009*) Assessment of World's Supply of Lithium*, U.S Department of Energy, Energy Efficiency and Renewable Energy , Office of Vehicle Technologies. Presentation to the Vehicle Technologies' Annual Merit Review May 19th 2009 [online]. Available from: http://www.energy.gov/sites/prod/files/2014/03/f12/es_13_barnes.pdf [Accessed 15 August 2014].

Barry, B. (2015) Mercedes Concept IAA at Frankfurt 2015: the shape-shifting aero special. *Car* [online]. Published 14 September 2015. Available at: http://www.carmagazine.co.uk/car-news/motor-shows-events/frankfurt/2015/mercedes-releases-teaser-image-of-iaa-concept/ [Accessed 25 February 2016].

Bautus, M. Maciac, A. Oprean, M & Vasiliu, Nicolae (2011) Automotive Clutch Models for Real Time Simulation. *Proceedings of the Romanian Academy, series A*. 12 (2), pp. 109-116.

Bayindir, K., Gozukucuk, M. A., and Teke, A. (2011) A comprehensive overview of hybrid electric vehicle: Powertrain configurations, powertrain control techniques and electronic control units. *Energy Conversion and Management.* (52) pp. 1305–1313.

BBC News Technolgy (2014), *UK to allow driverless cars on public roads in January* [online]. Available from: http://www.bbc.co.uk/news/technology-28551069 [Accessed 30 July 2014].

Ben-Chaim, M. Shmerling, E. & Kuperman, A. (2013) Analytical Modelling of Vehicle Fuel Consumption. *Energies 2013.* (6) pp. 117-127.

Bergsson. K., (2005) *Hybrid-vehicles.org*. Available from: http://www.hybrid-vehicle.org/hybrid-vehicle-history.html [Accessed 22 November 2008].

Bosch, R. (2011) Bosch Automotive Handbook. 8th ed.

Bossel, U. (2006) Does a Hydrogen Economy Make Sense? *Proceedings of the IEEE*. 94 (10), pp.1826 -1837

Borse G. J. (1997) *Numerical methods with Matlab: a resource for scientists and engineers*. Boston, MA: PWS Publishing.

Botes, F. (2014) *Alternative Boosting Systems in Highly Downsized Gasoline Engines.* Project report for MSc in Automotive Engineering, University of Bath. August 2014.

Braess, H. and Seiffert, U. (2005) *Handbook of Automotive Engineering.*Warrendale , USA:SAE International

Brugier-Corbiere, C & deServigny, L. (2013), Hybrid Air – An Innovative petrol full-hybrid solution, PSA Peugeot Citroen Dossier de presse, 22nd January, 2013 . Available from: http://www.psa-peugeot-citroen.com/en/automotive-innovation/innovation-by-psa/hybrid-air-engine-full-hybrid-gasoline (Accessed on 17/7/2013) PSA Peugeot Citroen

Bryant, V (1994) The Origins of the Potter's Wheel. Available from: http://www.ceramicstoday.com/articles/potters_wheel2.htm (accessed on 06/07/2008)

Buttsworth (2002) Spark Ignition Internal Combustion Engine *Faculty of Engineering & Surveying Technical Report* [online]. Available from: https://core.ac.uk/download/pdf/11034602.pdf [Accessed 8 December 2015].

Cai, Z. Worm, J .and Brennan, D.(2012) EXPERIMENTAL STUDIES IN GROUND VEHICLE COASTDOWN TESTING *American Society for Engineering Education*

Cappiello, A. Chabini, I. Nam, E. Luè, A and Abou Zeid, M. (2002) A Statistical Model of Vehicle Emissions and Fuel Consumption. *The IEEE 5th International Conference on Intelligent Transportation Systems.*

Casadei, A and Broda, R (2008) Impact of Vehicle Weight Reduction on Fuel Economy for Various Vehicle Architectures, Research report conducted by Ricardo Inc. for the Aluminium Association, April, 2008.

Ceraolo, M. Donato, A. and Franceschi, G. (2008) A general approach to energy optimization of hybrid electric vehicles, *IEEE Transactions on Vehicular Technology*, vol. (57) (3), pp. 1433–1441.

Chan, C. C (2002) The State of the Art of Electric and Hybrid Vehicles, Proceedings of the IEEE, Vol. 90, No. 2, p247.

Chan. C and Chau, T (1997) An Overview of Power Electronics in Electric Vehicles, IEEE Transactions on Industrial Electronics, Vol. 44, No1, p.11.

Chen, H., Cong, T., Yang, W., Tan, C., Li, Y., and Ding, Y., (2009) Progress in electrical energy storage system: A critical review. Progress in Natural Science Vol. 19, Issue 3, pp 291 – 312.

Clark, S.K. and Dodge, R.N (1979) *A Handbook for the Rolling Resistance of Pneumatic Tires.* Michigan: University of Michigan

Cole, D. Ackerman, M. and Coveney, V. A discussion on the Validity of Car Manufacturers' Fuel Efficiency Claims, *Not yet published*, completed as partial requirement of UWE Research Portfolio Module 2012, pp 1-6

Coveney, V. (2008) Discussion with Dr. V. Coveney, University of the West of England, Bristol.

Coyle, F. (2016) Personal communication via e-mail. Re. transport for London test data for a bus type referred to as 'bus 1' throughout report.

Dargay, J. Gately, G and Sommer, M. (2007) Vehicle Ownership and Income Growth, Worldwide: 1960-2030. *The Energy Journal (Cambridge, Mass.)*. 28 (4), pp.143 -170.

Davis, J. Mercedes(2012) Mercedes-Benz B-Class. Available from: http://www.emercedesbenz.com/autos/mercedes-benz/b-class/mercedes-benz-b-class-aerodynamics-tested-with-paint-video/ (Accessed on 1/2/2013)

Doucette, R. T., and McCulloch, M. D. (2011) A comparison of high-speed flywheels, batteries, and ultra-capacitors on the bases of cost and fuel economy as the energy storage system in a fuel cell based hybrid electric vehicle, *Journal of Power Sources*, 196, pp. 1163–1170.

Ebron, A. and Cregar, R., (2001) Introducing Hybrid Technology. *Altenergymag* [online]. Available from: http://www.altenergymag.com/articles/05.06.01/naftc/contents.html [Accessed 23 October 2008].

Ecomodder.com (2011), *Brake specific fuel consumption maps* Available from: http://ecomodder.com/wiki/index.php/Brake_Specific_Fuel_Consumption_(BSFC)_Maps [Accessed 7/11/09].

Erjavik, J (2013) *Hybrid, Electric and Fuel-Cell Vehicles (2nd Edition)* Cengage Learning

Electricbike.com (2014) *Twike electri-bike / pedal car*. Available from: http://www.electricbike.com/twike/ [accessed on 10/5/2014].

EPA (2013) *Dynamometer Drive Schedules (FTP urban cycle)* Available from: http://www.epa.gov/otaq/emisslab/methods/ftpcol.txt)

Feng, W. Hu, Z. Xiao-Jian, M. Lin, Y. and Bin, Z. (2007) Regenerative braking algorithm for a parallel hybrid electric vehicle with continuously variable transmission, *, 2007. ICVES. IEEE International Conference on Vehicular Electronics and Safety*, pp.1-4.

Formula 1(2014) *Understanding F1 racing, Energy recovery system (ERS)* [online]. Available from: http://www.formula1.com/inside_f1/understanding_f1_racing/8763.html [Accessed 10 May 2014].

Gaelectric (2011) *Larne project update* [online]. Available from: http://www.gaelectric.ie/index.php/energy-storage/larne/ [Accessed 04 July 2012].

Gehring, U., Wijga, A.H., Brauer, M. *et al.,* (2010). Traffic-related Air Pollution and the Development of Asthma and Allergies during the First 8 Years of Life. *American Journal of Respiratory and Critical Care Medicine.* Volume 181. pp 596-603.

Gill, J.D. (1984) *Elastomeric Energy Recovery System, US Patent 4479356* [online]. Available from: https://www.google.com/patents/US4479356 [Accessed 5 May 2014].

Green Car Congress (2013) *BMW's hybrid motor design seeks to deliver high efficiency and power density with lower rare earth use* [online]. Available from: http://www.greencarcongress.com/2013/08/bmw-20130812.html [Accessed 8 August 2015]

Haagen-Smit, A. J., (1952). Chemistry and Physiology of Los Angeles Smog. *Industrial Engineering Chemistry.* Volume. 44, p1342.

Hancock, M. (2006) Impact of regenerative braking on vehicle stability. *The Institution of Engineering and Technology Hybrid Vehicle Conference*, *2006* pp. 173-184.

Hari, D., Brace, C.J., Vagg, C., Poxon, J. and Ash, L. (2012) Analysis of a driver behaviour improvement tool to reduce fuel consumption. In: 1st International Conference on Connected Vehicles and Expo, CCVE 2012, 12-16 December, Beijing

Harrabin, R. BBC (2008) *Five-seat concept car that runs on air* [online]. Available from: http://news.bbc.co.uk/1/hi/sci/tech/7241909.stm [Accessed 23 July 2009].

Hawley, J. G., Bannister, C. D., Brace, C. J., Akehurst, S., Pegg, I. and Avery, M. R. (2010) The effect of engine and transmission oil viscometrics on vehicle fuel consumption. Proceedings of the Institution of Mechanical Engineers, Part D: Journal of Automobile Engineering, 224 (9). Pp. 1213-1228.

Heywood, J., (1988). *Internal Combustion Engine Fundamentals*. Now York: McGraw-Hill Inc.

Hitachi (2008) Lithium-ion battery for transportation [online]. Available from: http://www.hitachi.com/rd/research/hrl/battery_01.html [Accessed 20 August 2008].

Hoimoja, H. (2006) Flywheel energy storage: principles and possibilities, *3rd International Symposium Actual Problems in Energy and Geotechnology*, Kuressaare, pp. 89-92

Hoppie, L. O. (1982) The use of elastomers in regenerative braking systems, Rubber Chemistry and Technology, 55(1), pp 219-232.

Horrein, L., Bouscayrol, A., Delarue, P., Verhille, J. N., Mayet, C. (2012) Forward and backward simulations of a power propulsion system. *Power Plants and Power Systems Control*. 8 (1), pp. 441-446.

Houcque, D (2006), Applications of MATLAB: Ordinary Differential Equations (ODE). Teaching Notes from the Robert R. McCormick School of Engineering and Applied Science – Northwestern University.

Hubbert, M. K., (1956) Nuclear energy and the fossil fuels, American Petroleum Institute Spring Meeting San Antonio, Texas, p. 40.

Hybrid vehicle history website (2005) *More than a century of refinement*. Available from: http://www.hybrid-vehicle.org/hybrid-vehicle-history.html [Accessed 20 October 2011].

Independent (2014) Boris declares war on diesel to boost London air quality, 20 July 2014, p.27.

Jayner, S.J. (1979) *Automotive Energy Absorption, Storage and Retrieval System, US Patent 4159042.* Available from: http://www.google.com/patents/US4159042 [Accessed 05 May 2014].

Jefferson, C. M and Ackerman, M (1996) A flywheel variator energy storage system, *Energy Conversion Management*. 37 (10), pp. 1481 -1491.

Jenson, J. (1980) *Energy Storage*, Newnes Butterworths, 1980, p56 -58.

Kampa, M. and Castanas, E. (2008) Human health effects of air pollution. *Environmental Pollution*, volume 151(2), pp.362-367.

Kim, H. J. Keoleian, G. A. Skerlos, S. J. (2011) Economic assessment of greenhouse gas emissions reduction by vehicle lightweighting using aluminum and high-strength steel. *Journal of Industrial Ecology 2011*, 15 (1), pp 64−80.

Katrasˇnik, T. (2007) Hybridization of powertrain and downsizing of IC engine – A way to reduce fuel consumption and pollutant emissions – Part 1. *Energy Conversion and Management* 48 (2007) pp. 1411–1423.

Lawson, L.J. Koper, J and Cook, L.M. (1981) Wayside energy storage for recuperation of potential energy from freight trains. *Proceedings of the Intersociety Energy Conversion Engineering Conference (USA)*. 1, pp. 875-880.

LowCVP (2014) Low Carbon Vehicle Partnership website: *Testing & Accreditation (LCEB Certification) - Bus Test Cycle* Available from: http://www.lowcvp.org.uk/initiatives/lceb/lceb-testing.htm [Accessed 20 Dec 2015].

Lee, D. (2013) Self-driving car given UK test run at Oxford University, BBC Technology news website, Available from: http://www.bbc.co.uk/news/technology-21462360 [Accessed 24 July 2014].

Leung, D. and Williams, D. (2000) Modelling of Motor Vehicle fuel consumption and emissions using a Power-Based Model. *Environmental Monitoring and Assessment.* 65, pp. 21–29.

Lijun, Q. Nianjiong, Y. Daojun, W (2010) Simulation of Clutch Slipping Control of Automatic Transmission. *Second International Conference on Intelligent Human-Machine Systems and Cybernetics* pp.235 -238.

Little, M (2011), Personal Communication, Ricardo U.K.

Lothian Buses (2012), Hybrid Buses. Available from: http://lothianbuses.com/our-community/environment/hybrid-buses [Accessed 27 September 2012].

Lydall , R.,(2013) End of the free green run... now hybrid cars will have to pay congestion charge too. *London Standard*, [online] 18 January. Available from: http://www.standard.co.uk/news/transport/end-of-the-free-green-run-now-hybrid-cars-will-have-to-pay-congestion-charge-too-8469699.html [Accessed 17 September 2013].

Maslin, M. (2004) *Global Warming, a very short introduction*. Oxford: Oxford University Press. Lenntech [online]. Available from: http://www.lenntech.com/greenhouse-effect/global-warming-history.htm#ixzz2SnLsoqkA [accessed 17 October 2011].

Modak, Prof. Girish S. and Sane, Prof. S. S. (2006) Mechanical Continuously Variable Transmission (CVT) for Parallel Hybrid Vehicle, IEEE, 2006, p1.

Michelin (2016) Michelin Energy Saver For city cars, MPVs and Saloon cars. Available from: www.michelin.co.uk/tyres/michelin-energy-saver [accessed 17/01/2016].

Mierlo, J. and Maggetto, G., (2004) Innovative iteration algorithm for a vehicle simulation program. *IEEE Transactions on Vehicular Technology.* 53, pp.401-412.

Mokaddem, K (2013) PSA Peugeot Citroen Hybrid Air Technology, PSA Peugeot Citroen website. Available from: http://www.psa-peugeot-citroen.com/en/automotive-innovation/innovation-by-psa/hybrid-air-engine-full-hybrid-gasoline [accessed 17/07/2014].

Motavalli, J. (2002) From Stops, Energy to Go, New York Times Automobiles Section, Page F1, 22 March 2002. Available from: http://www.nytimes.com/2002/03/22/automobiles/from-stops-energy-to-go.html [Accessed 18 January 2009].

Mukhitdinov, A.A., Ruzimov,S.K & Eshkabilov, S.L. (2006) Optimal Control Strategies for CVT of the HEV during a regenerative process. IEEE Conference on Electric and Hybrid Vehicles, 2006. pp. 1-12 .

National Bureau for Statistics China (2012) Available from: http://www.stats.gov.cn/tjsj/ndsj/2012/indexeh.htm [Accessed 28 January 2013].

Naunheimer, H., Bertsche, B., Ryborx, J. and Novak, W. (2011) *Automotive Transmissions Fundamentals, Selection, Design and Application.* 2nd ed. New York: Springer Publishing.

Next Green Car (2013) BIK Rates and Company Car Tax. Available from: http://www.nextgreencar.com/company-car-tax/bik-rates/q1.php [Accessed 08 June 2015)].

Parry People Movers Ltd. (2009) *PPM Technology, How the flywheel aids performance*, Available from: http://www.parrypeoplemovers.com/technology.htm [Accessed 06 September 09].

Pederson,V. Italiapseed (2009*) Fiat Regata sedan boasted 'start-stop' technology more than two decades ago.* Available from: http://www.italiaspeed.com/2009/cars/fiat/02/regatta_es/1602.html [Accessed 6 October 2010].

Pendick, Daniel (November 17, 2007). "Squeeze the breeze: Want to get more electricity from the wind? The key lies beneath our feet". *New Scientist* **195** (2623): 4. Retrieved November 17, 2007.

Pour, E. and Golabi, S. (2014) Examining the Effects of Continuously Variable Transmission (CVT) and a new mechanism of planetary gearbox of CVT on Car Acceleration and Fuel Consumption. *International Journal of Application or Innovation in Engineering & Management.* 3 (9), pp. 69-80.

Pusca, R., Ait-Amirat, Y., Berthon, A. and Kauffmann, J.M., (2002) Modelling and simulation of a traction control algorithm for an electric vehicle with four separate wheel drives. *IEEE Vehicular Technology Conference, 2002. Proceedings. VTC 2002-Fall. 2002 IEEE 56th* (3) pp. 1671-1675).

Royal Automobile Club (2009) *Forum, Driving, Buying & Selling Vehicles - Toyota prius.* Available from: http://www.rac.co.uk/forum/showthread.php?3389-toyota-prius [Accessed 02 November 2015].

RailwayPeople.com (2008), Regenerative braking on the third rail DC network, published 15/08/2008), Available from: http://www.railwaypeople.com/rail-news-articles/regenerative-braking-on-the-third-rail-dc-network-1590.html [Accessed 02 July 2014].

Reif, K. and Dietsche, K. *et al* (2011) *Bosch Automotive Handbook.*8th Ed. Cambridge, MA, USA: Bentley Publishers.

Ricardo (2015) *Regenerative braking algorithm for a parallel hybrid electric vehicle with continuously variable transmission*. Wave software information available from http://www.ricardo.com/en-GB/What-we-do/Software/Products/WAVE/Combustion-and-Emissions/ [Accessed 21 March 2015].

Ricardo (2015), *Flybus to start testing first flywheel hybrid bus*. Available from: http://www.ricardo.com/en-GB/News--Media/Press-releases/News-releases1/2011/Flybus-to-start-testing-first-flywheel-hybrid-bus/. [Accessed 15 August 2015]

Roper, D (2014), Roper Highlander Hybrid (HiHy) Plug-In-Supply Conversion, (07/06/14), Available from: http://www.roperld.com/science/HiHyPlugIn.htm [Accessed on 15 July 2014]

Samanuhut, P.(2011) Modeling and Control of Automatic Transmission With Planetary Gears for Shift Quality. *A dissertation submitted in partial fulfilment of the requirements for the degree of Doctor of Philosophy (Mechanical Engineering)*, University of Texas at Arlingon, 2011.

Schaltz, E. (2011). Electrical Vehicle Design and Modeling. In: Soylu, S.Ed., (2011) *Electric Vehicles - Modelling and Simulations*, Rijeka: Intech, InTech, pp. Available from: http://www.intechopen.com/books/electric-vehicles-modelling-and-simulations/electrical-vehicle-design-andmodeling (accessed 10 May 2015)

Schiffer, J. Bohlen, O. De Doncker, R.W. Sauer, D.U.and Kyun Young Ahn, (2005) Optimized energy management for fuelcell-supercap hybrid electric vehicles, *Vehicle Power and Propulsion, 2005 IEEE Conference*, pp.341-348.

Schmidt, S., Eco Test Testing and Assessment Protocol Release 2.0, Available from: http://www.ecotest.eu/html/TestingandAssessmentProtocol.pdf [Accessed 10 January 2012].

Serrarens, A. Dassen, M. and Steinbuch, M (2004) Simulation and Control of an Automotive Dry Clutch. *Proceedings of the 2004 American Control Conference*. 5, pp. 4078 – 4083.

Shah, A.S.V., Lee, K.K., McAllister, D.A., Hunter, A., Nair, H., Whiteley, W., Langrish, J.P., Newby, D.E. & Mills, N.L. (2015) Short term exposure to air pollution and stroke: systematic review and meta-analysis. *British Medical Journal.* Volume 350. p1295.

Schaltz, E. (2011). *Electrical Vehicle Design and Modeling*. In S. Soylu (Ed.), Electric Vehicles - Modelling and Simulations. (1 ed., pp. 1-24). Chapter 1.Croatia: INTECH.

Sugiyama, Y. Fukui, M. Kikuchi, M. Hasbe, K. Nakayama, A. Nishinari, K. Tadaki, S. and Yukawa, S. Traffic jams without bottlenecks –experimental evidence for the physical mechanism of the formation of a jam. *New Journal of Physics* [online]. Available from:

http://iopscience.iop.org/1367-2630/10/3/033001/fulltext/ [Accessed 3 July 2014].

Superconductor Week (2015), *What is Superconductivity?* Available from: http://www.superconductorweek.com/what-is-superconductivity [Accessed 10 December 2015]

Stone, R. (1989) *Motor vehicle fuel economy*. 1st ed. London: Macmillan Education Ltd.

Tahil, W (2006) *The Trouble with Lithium - Implications of Future PHEV Production for Lithium Demand* [online]. Available from: http://www.evworld.com/library/lithium_shortage.pdf [Accessed 10 February 2014]

The Society of Motor Manufacturers and Traders Ltd. (SMMT) *New Car CO_2 Report 2013* [online]. London: SMMT. Available from:

http://www.smmt.co.uk/wp-content/uploads/sites/2/SMMT-New-Car-CO2-Report-2013-web.pdf [Accessed 16 April 2013 and 20 February 2016].

The Society of Motor Manufacturers and Traders Ltd. (SMMT) *Motor Industry Facts 2013* [online]. London: SMMT. Available from:

http://www.smmt.co.uk/wp-content/uploads/sites/2/SMMT-2013-Motor-Industry-Facts-guide.pdf [Accessed 16 April 2013 and 20 February 2016].

The Society of Motor Manufacturers and Traders Ltd. (SMMT) *Motor Industry Facts 2015* [online]. London: SMMT. Available from:

http://www.smmt.co.uk/wp-content/uploads/sites/2/100049_SMMT-Facts-Guide-2015_UPDATES.pdf [Accessed 16 April 2013 and 20 February 2016].

Tesla (2014), *Performance data sheet* [online]. Available from: http://www.teslamotors.com/en_GB/models/features#/performance [Accessed 1 March 2014].

Thomas, S. (2009) Fuel Cell and Battery Electric Vehicles Compared. *International Journal of Hydrogen Energy.* 34 (15) pp 6005–6020.

Torotrak (2015) *Flywheel Hybrids Satisfy the Demands of Drivers and Future Legislation*. Available from: http://www.torotrak.com/flywheel-hybrids-satisfy-the-demands-of-drivers-and-future-legislation/ [Accessed 8 January 2014].

Toyota (2014), Sales brochure and technical data sheet [online]. Available from: http://www.toyota.com/content/ebrochure/2015/prius_ebrochure.pdf and http://www.toyota.co.uk/new-cars/prius-plus-specs-prices [Accessed 6 August 2014].

TRANSform Scotland (2007) Peak Oil and Transport Briefing – Version 1.1.

Transport for London (2012) *Hybrid Buses* [online]. Available from: http://www.tfl.gov.uk/corporate/projectsandschemes/2019.aspx [Accessed 4 May 2012].

Treloar, LRG. (1975) *The Physics of Rubber Elasticity*. UK: Oxford University Press.

Tzirakis, E., Pitsas, K., Zannikos, F., Stournas, S. (2006) Vehicle Emissions and Driving Cycles: Comparison of the Athens Driving Cycle (ADC) with the ECE-15 and European Driving Cycle (EDC), *Global NEST Journal*, 2006, Vol. 8, No. 3, pp 2828-290.

UK Government. *Vehicle tax rates* [online]. Available from: https://www.gov.uk/vehicle-tax-rate-tables/rates-for-cars-registered-on-or-after-1-march-2001 [Accessed 03 March 2013, and 21 February 2016].

UNESCO (2015) Economic Commission for Europe, Inland Transport Committee,

World Forum for Harmonization of Vehicle Regulations. *Proposal for amendments to global technical regulation No. 15 on Worldwide harmonized Light vehicles Test Procedure (WLTP)* Available from: https://www2.unece.org/wiki/download/attachments/29229449/ECE-TRANS-WP29-GRPE-2016-03e_clean.pdf?api=v2 [Accessed 20 Jan 2016)

United Nations Environment Programme (UNEP) (2013) *Urban Air Pollution* [online]. Available from: http://www.unep.org/urban_environment/issues/urban_air.asp [Accessed 3 May 2013].

US Energy Information Administration (2011) *Annual Energy Review, 2011* [online]. Washington: US Energy Information Administration. Available from: https://www.eia.gov/totalenergy/data/annual/pdf/aer.pdf [Accessed 21 February 2016].

US Department of Energy. *Toyota Gen III Prius HEV Accelerated Testing – September 2011* [online]. Available from: http://energy.gov/sites/prod/files/2014/02/f8/toyotapriusIII_ar.pdf [Accessed 21 February 2016].

Vaughan . A (2016). London takes just one week to breach annual air pollution limits. The Guardian [online] 8 January. Available from: http://www.theguardian.com/environment/2016/jan/08/london-takes-just-one-week-to-breach-annual-air-pollution-limits [Accessed 20 January 2016].

Volkswagon (2014) Start /Stop, save every time you stop … [online]. Available from: http://www.volkswagen.co.uk/technology/bluemotion-technologies/stop-start [Accessed 04 August 2014].

Wang, H & Fu, L. (2010) Developing a High-Resolution Vehicular Emission Inventory by Integrating an Emission Model and a Traffic Model: Part 1—Modelling Fuel Consumption and Emissions Based on Speed and Vehicle-Specific Power. *Journal of Air & Waste Manage. Assoc.* 60. pp.1463–1470.

Weart, S, (2013) *The Discovery of Global Warming* [online]. Available from: http://www.aip.org/history/climate/co2.htm [Accessed on 16 April 2013].

West Texas Research Group (WTRG) Website. *Oil Price History and Analysis* [online]. Available from: http://www.wtrg.com/prices.htm [Accessed 21 February 2016].

Wicks, F. Maleszweski, J. Wright, C and Zarybnicky, J (2002) Analysis of Compressed Air Regenerative Braking and a Thermally Enhanced Option, 2002, p 411

Williams, A. Holmes, T. and Lees, G. (1972) Toward the Unified Design of Tire and Pavement for the Reduction of Skidding Accidents, *SAE Technical Paper 720162*, 1972.

Woodbank Communications Ltd. (2007) Electropedia – Battery and Energy Technologies. Available from: http://www.mpoweruk.com/leadacid.htm [Accessed 03 March 2009].

Woodbank Communications Ltd. (2007) Electropedia – Battery and Energy Technologies. Available from: http://www.mpoweruk.com/nicad.htm [Accessed 04 March 2009].

WTRG (2011) Oil Price History and Analysis Available from:

http://www.wtrg.com/prices.htm [Accessed 03 June 2013].

Yim, S. H. L. and Barrett, S. R. H., (2012) Public Health Impacts of Combustion Emissions in the United Kingdom. *Environmental Science Technology*.Volume 46 (8), pp 4291–4296.

York, B (2014) *Lead-Acid Batteries.* Lecture notes from University of California Faculty of Electrical and Computer Engineering. Available from: http://my.ece.ucsb.edu/York/Bobsclass/194/LecNotes/Lect%20-%20Batteries.pdf [Accessed 02 July 2014].

Zemansky, M.W. (1968) *Heat and Thermodynamics*. 5th Ed. Kogakusha:McGraw-Hill. pp 173 – 177.

APPENDIX I : Summary of vehicle data used

Vehicle Data summary	Citroen C1 1.0 (2009)	Citroen Xsara 1.4 (2002)	Range Rover 5.0 (2012)	Optare Solo SR	Bus 1	Volvo B11R (2013)
m (kg)	800	1116	2744	6000*	11949	20000
A (m^2)	2.06	1.98	3.817	6.5	10.807	9.18
Cd	0.3	0.32	0.38	0.6	0.6 est.	0.6 est.
Croll	0.008	0.008	0.008	0.008	0.008	0.008
Max Power (kW)	50@6000 rpm	55	279	150@2300 rpm	187@2100rpm	370 - 460
Max Torque (N.m)	93 @3600	110	310	750@1500 rpm	1000@1200-1600	2150
Fuel type	Petrol	Petrol	Petrol	diesel	diesel	diesel
Eng. type						
Eng. Capacity (l)	1.00	1.40	5.00	6.70	6.70	
Peak eff				36.00	36.00	
Max. No. of occupants	4	4	4	55	75	50
					**wheel to eng.	
Transmission Type				Allison 2100 series	ratios:	
gear ratio 1	11.5	3.636	4.17	3.1	25	2.16
gear ratio 2	7.5	1.95	2.34	1.8	16	3.36
gear ratio 3	5.5	1.28	1.521	1.41	11.7	1.91
gear ratio 4	4.5	0.975	1.143	1	8.7	1.42
gear ratio 5	3.5	0.767	0.867	0.71	6.08	1
gear ratio 6				0.61	4.38	0.72
gear ratio 7						
gear ratio 8						
Torque convertor ratio				1.5	1 **	2.61:1
Final drive ratio	1	4.06:1	3.54:1	4.1:1	1**	1.8:1
Tyre type						
Rolling diameter (m)	0.4856	0.599	0.713	0.769	0.96	0.8

APPENDIX II: Preliminary simulation work

Preliminary simulation work was based on torque/speed data for the vehicle's engine combined with the overall gear ratios for the vehicle to give a theoretical tractive effort / speed relationship purely to verify that the physical equations used gave predicted vehicle performance close to that quoted by manufacturers.

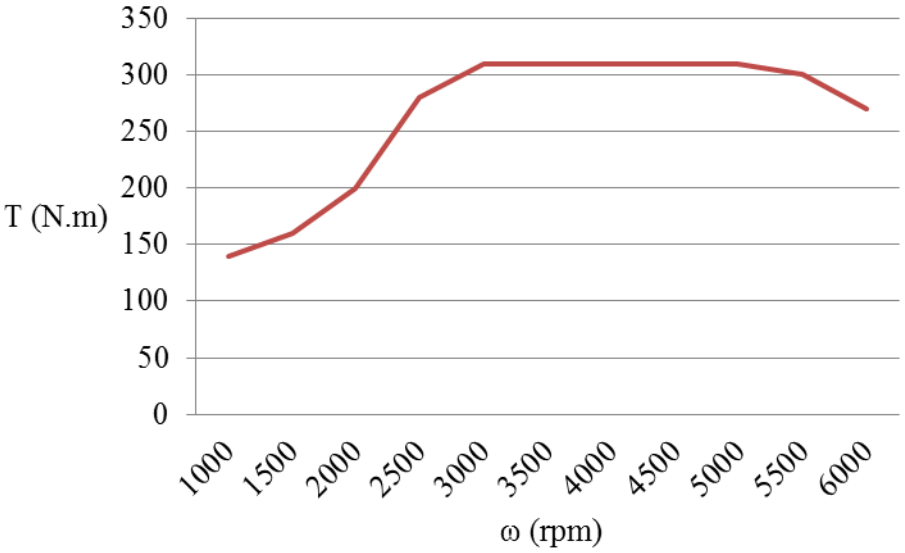

Figure A1.1: A typical T/rpm relationship for a conventional ICE petrol car engine (Volvo C70 engine B5204T3)

The engine torque / speed data was used to simulate vehicle acceleration under optimum conditions. The aim was to compare simulation results with quoted manufacturer's data for acceleration. This simulation involves several assumptions:

(i) The driver of the vehicle controlling the throttle to give peak torque
(ii) The driver changing gear at the optimum time
(iii) Gear changes are instantaneous with no loss of drive

Although these assumptions were unlikely to reflect real everyday driving styles, the simplified nature of the simulation gave a convenient starting point for comparison with experimental data before developing a more realistic vehicle simulation. For a particular vehicle being considered the torque / engine speed data was combined with other vehicle

data such as gear ratios, final drive ratios and wheel/tyre data to generate a graph indicating the tractive effort / speed relationship for the vehicle. An example plot is shown in figure 4.5.

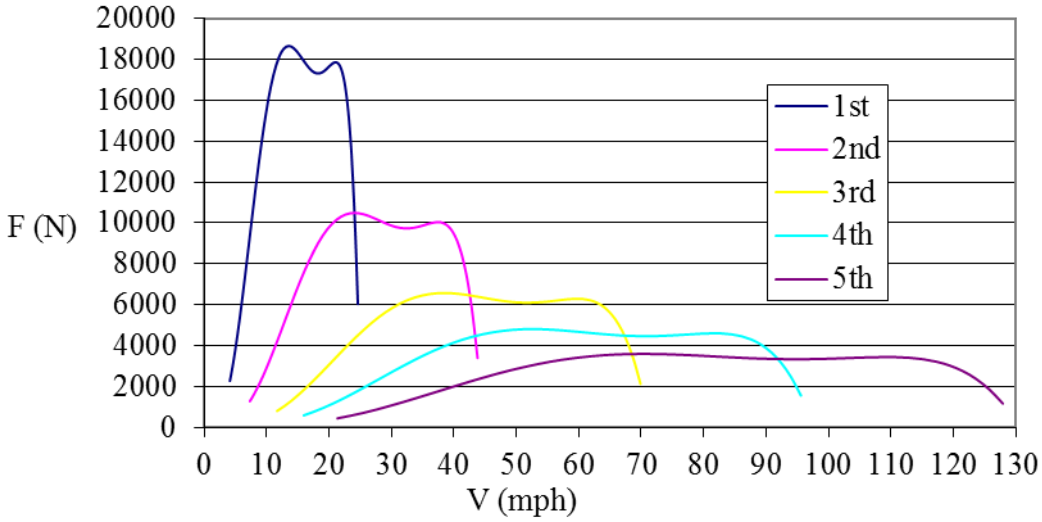

Figure A1.2: *F / V* for the engine and transmission a typical conventional production sports car – The Volvo C70 in gears 1 – 5

To use the data shown in figure A1.2 to find the gross tractive effort of the given vehicle at any speed either a mathematical relationship between speed and tractive effort or a look up table is required. Initially a trend line was manually fitted to the graph, linking the upper regions of the plot for each gear and then plotted in Excel. The trend line function in Excel was then employed to produce a 6 order polynomial relating tractive effort to vehicle speed, an example is shown in figure A1.3

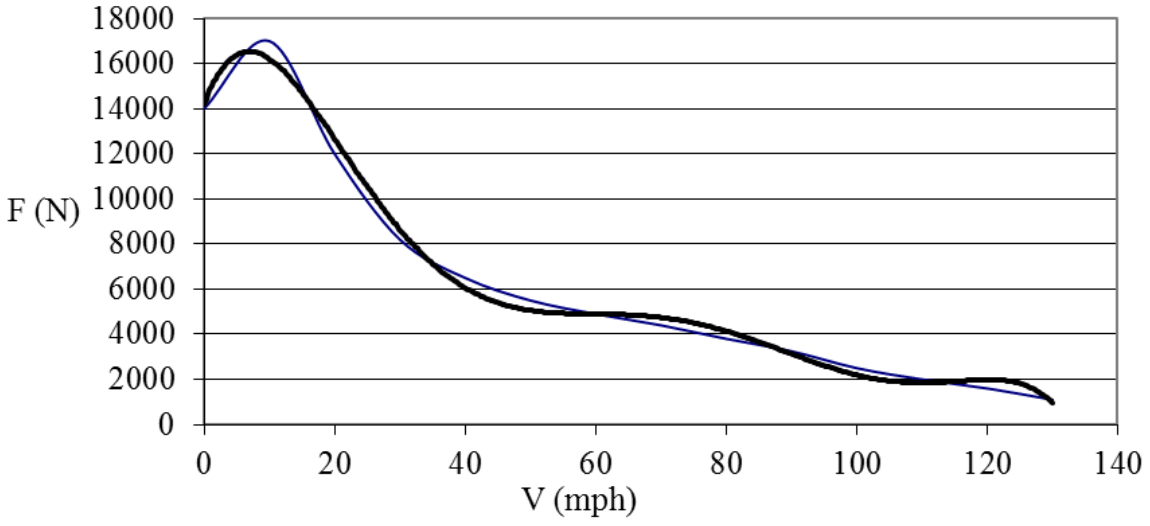

Figure A1.3: Manually plotted trend line (blue) and Excel generated trend line showing the relationship of Gross Tractive effort / road speed for the Volvo C70

This relationship could then be used to calculate the vehicle's theoretical gross tractive effort at any given speed. The forces acting upon the vehicle to resist forward motion such as aerodynamic forces, rolling resistance, frictional losses and gradient scan can be summed to give a total resistive force at a given vehicle speed. The instantaneous net tractive effort can be calculated by subtracting the total resistive force from the theoretical gross tractive effort.

APPENDIX III: NEDC Gear shift regime

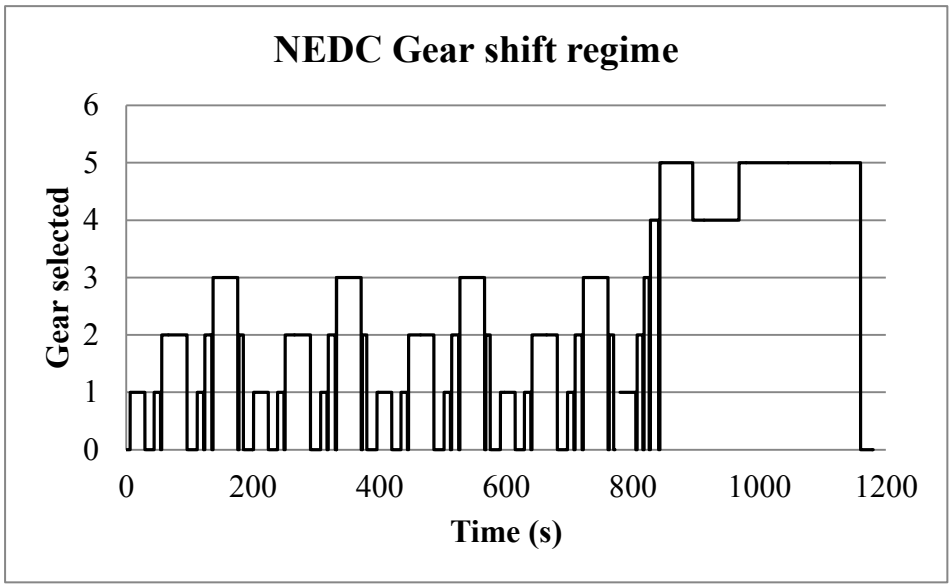

APPENDIX IV: Results from early simulation work

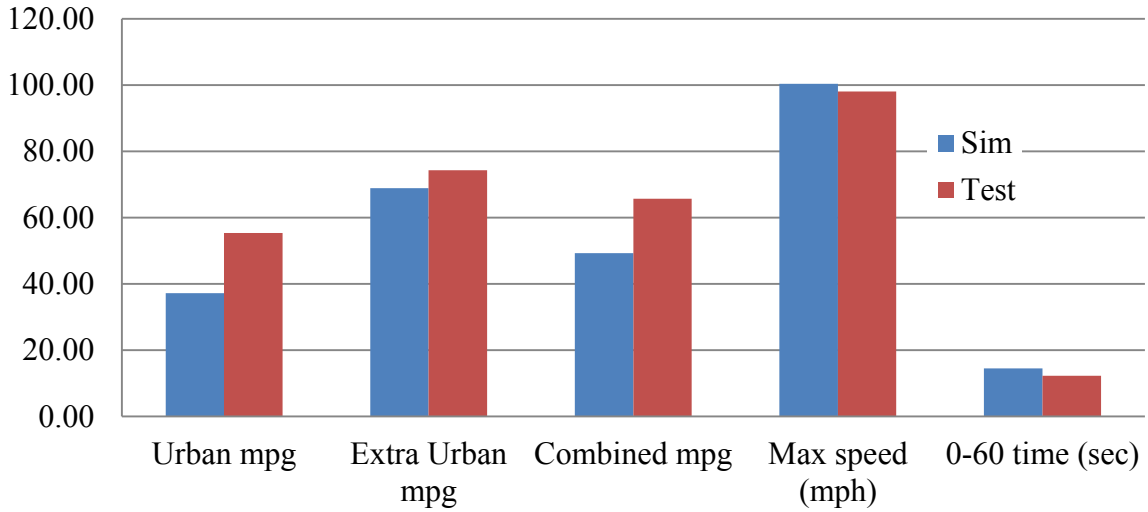

Figure A1: Citroen C1 (1.0*l*) comparison between simulation and manufacturer's data

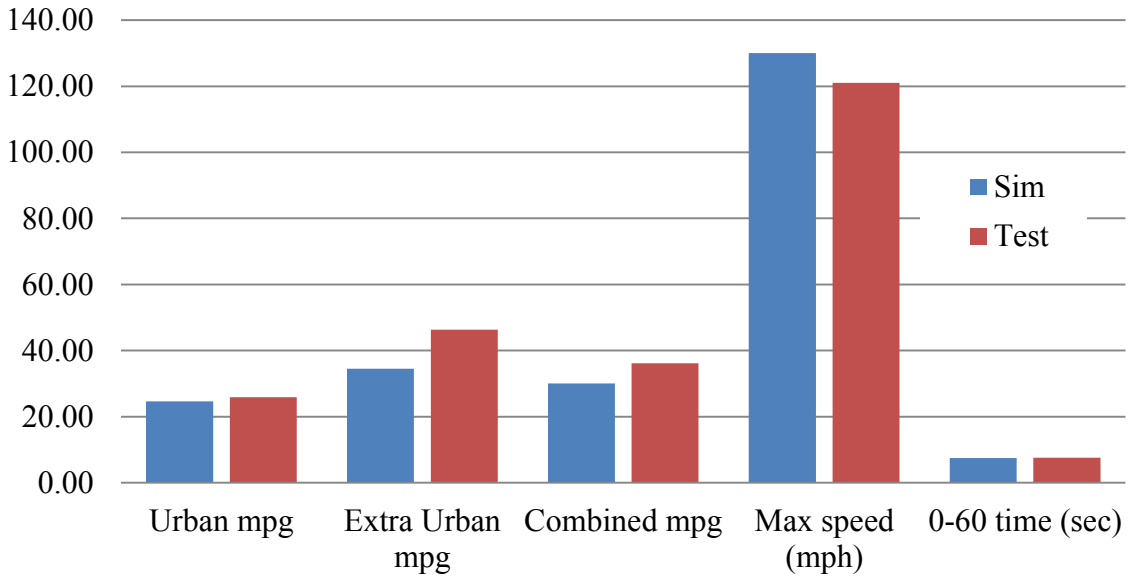

Figure A2: Mazda MX5 (1.8*l*) comparison between simulation and manufacturer's data

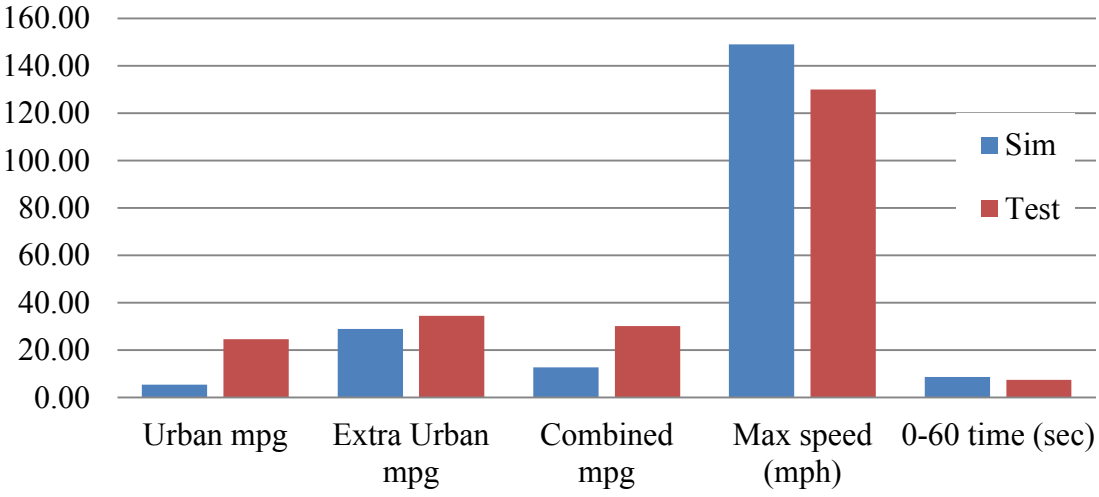

Figure A3: Range Rover (5.0*l*) comparison between simulation and manufacturer's data

APPENDIX V: Urban test route: Bristol, Filton and Extra urban test route, UWE to Minety (Wiltshire)

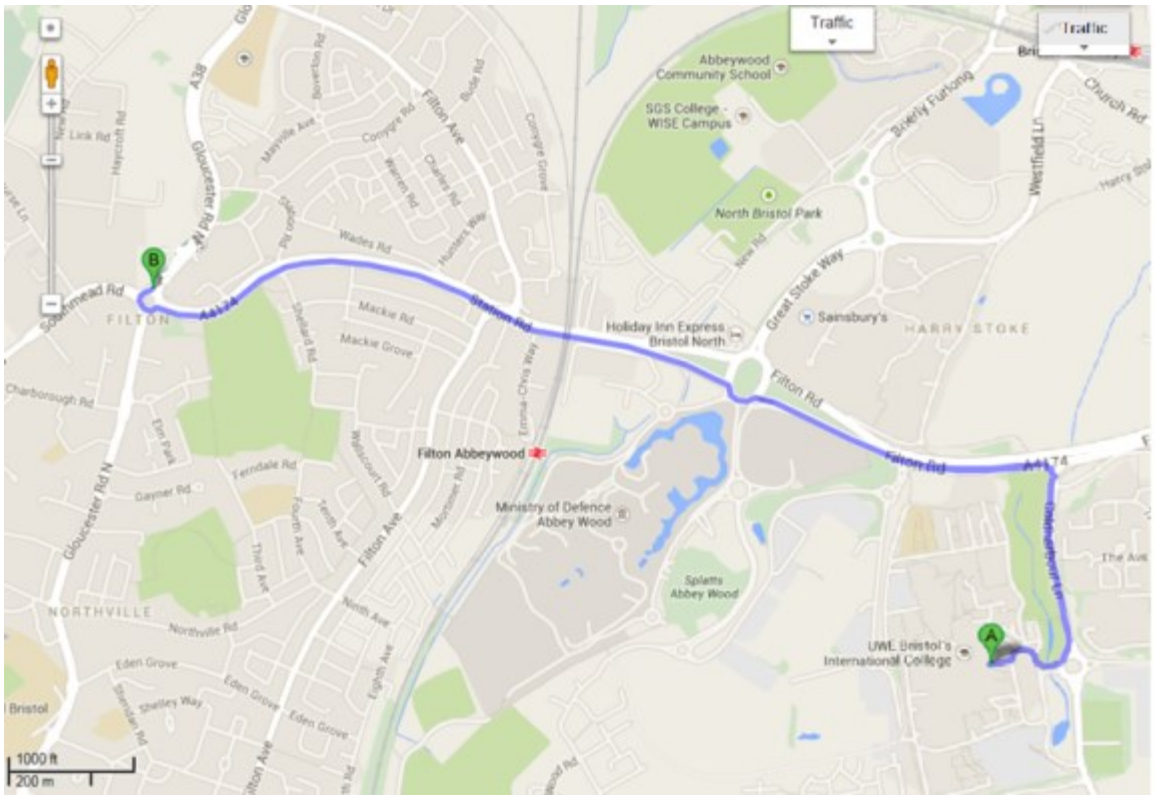

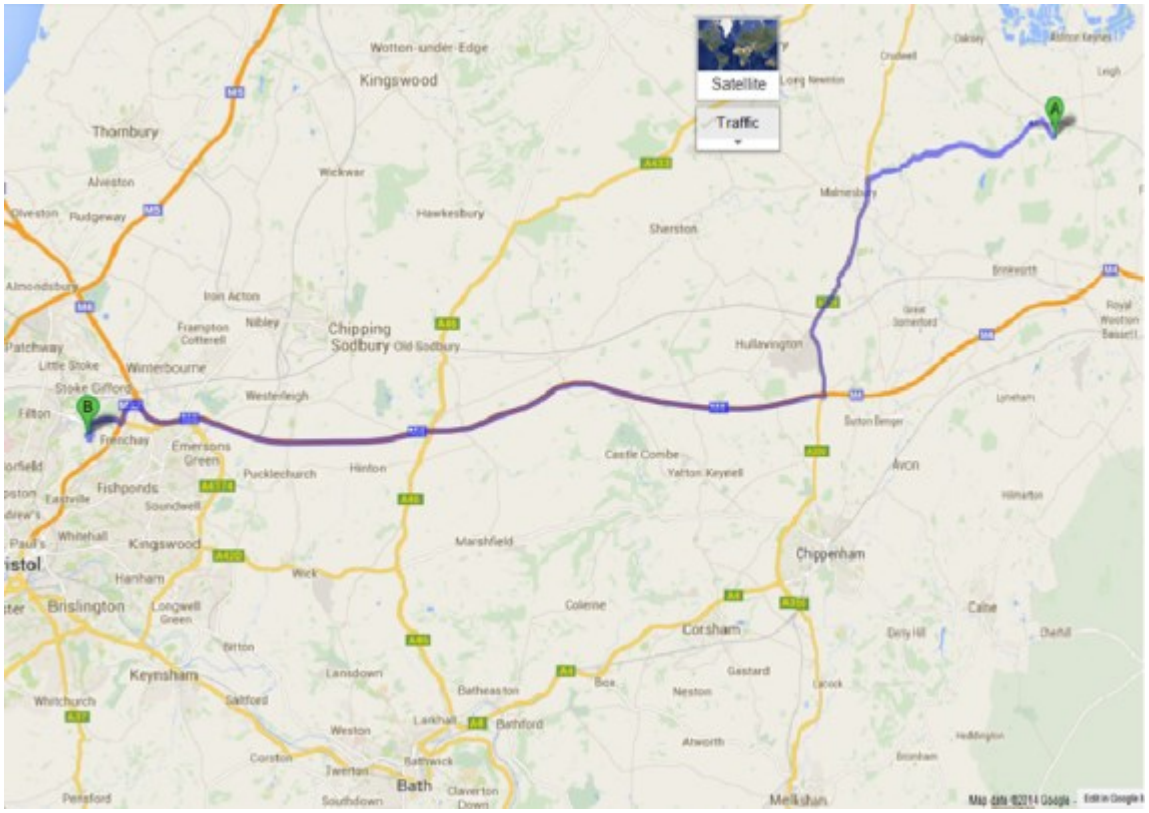

APPENDIX VI: Engine torque data used in simulation work forward looking simulation work

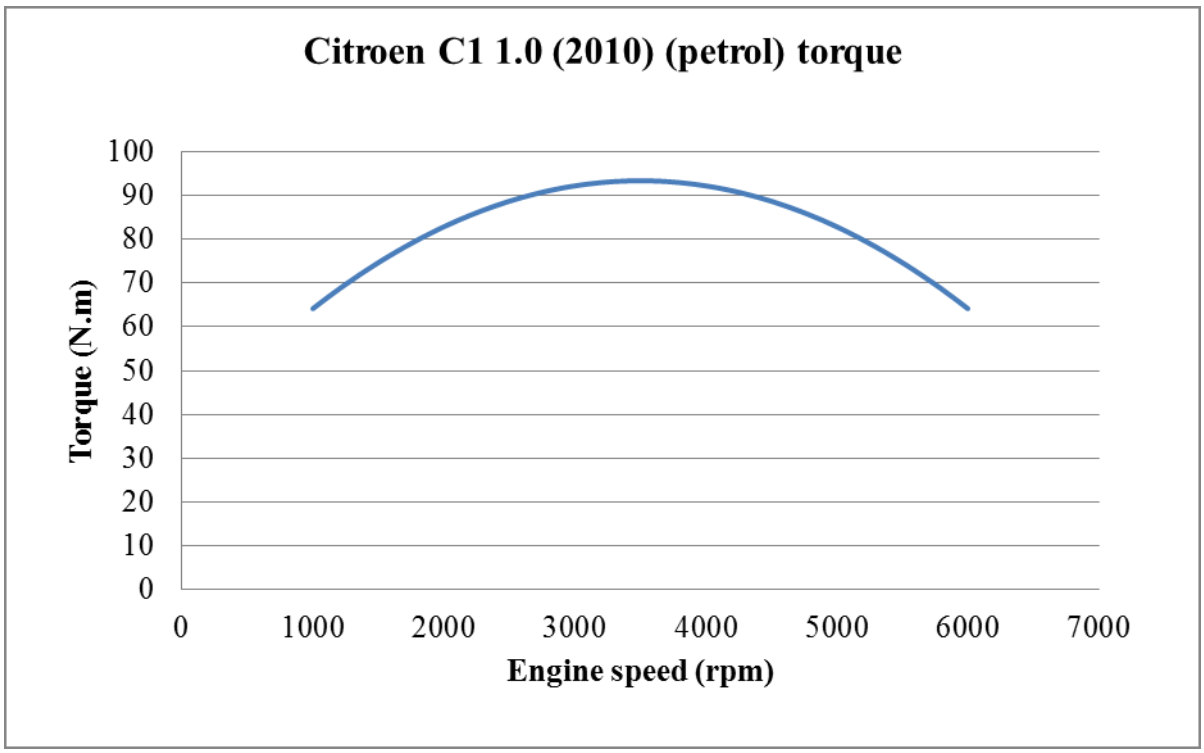

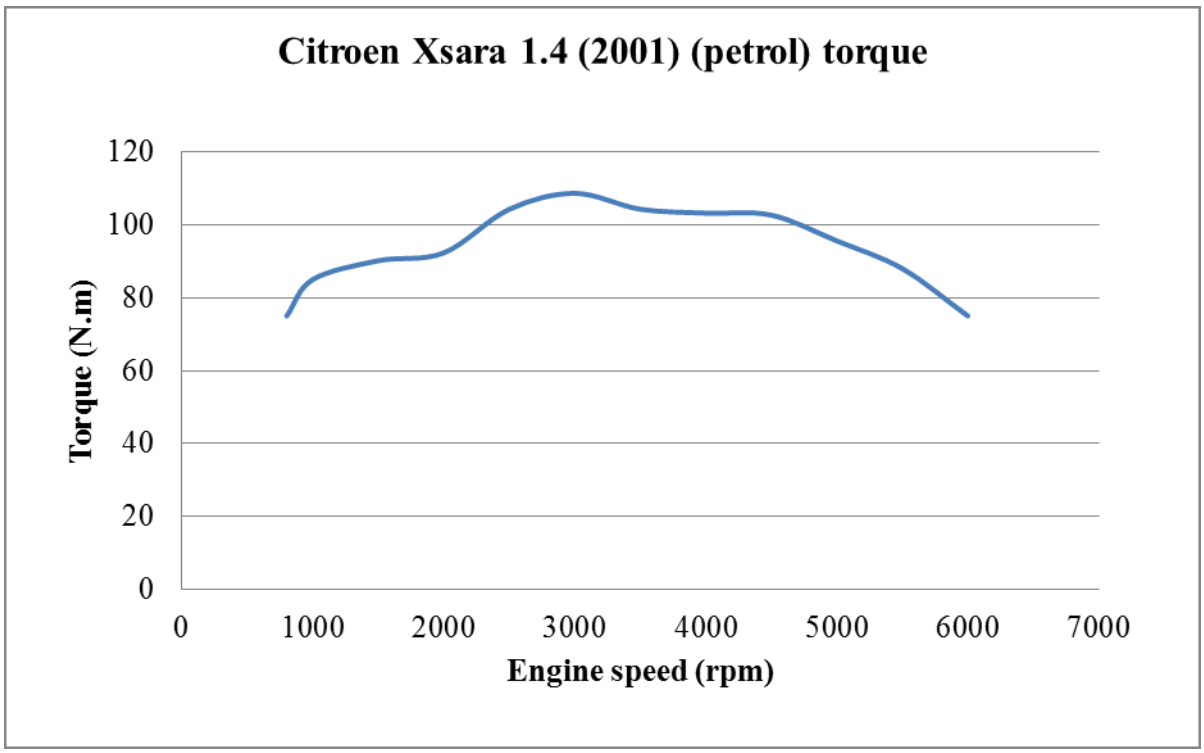

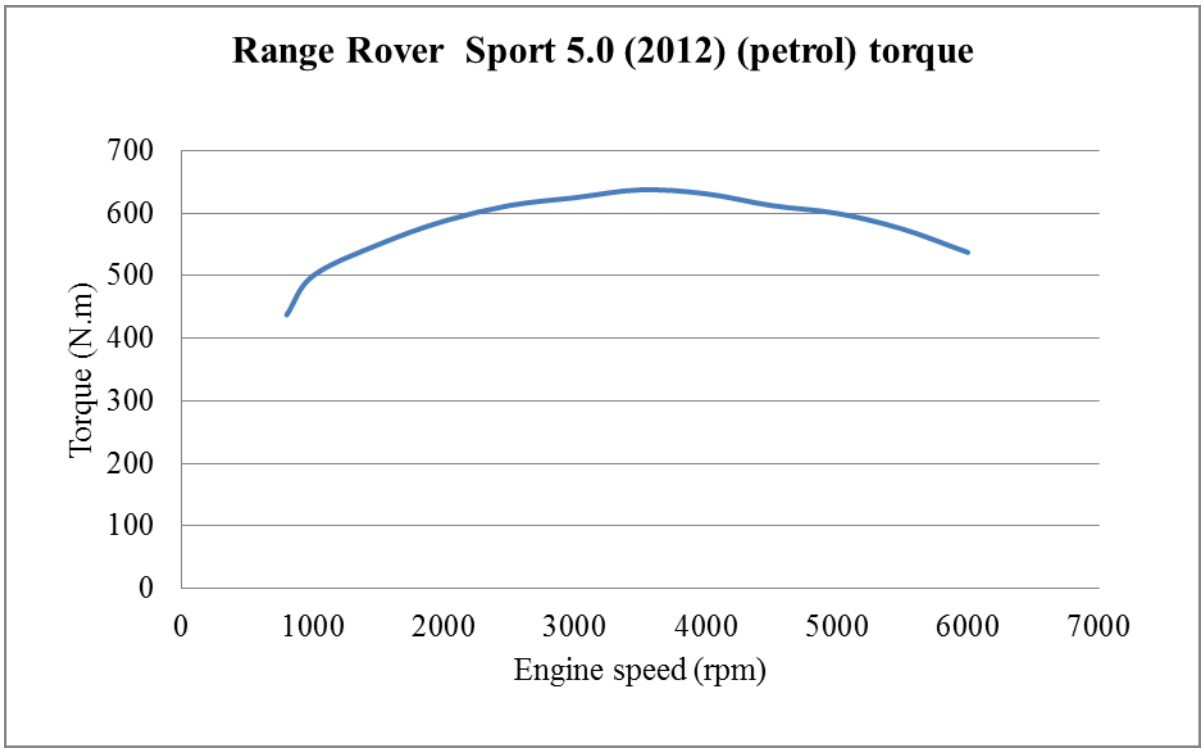
Range Rover Sport 5.0 (2012) (petrol) torque
Torque (N.m)
700
600
500
400
300
200
100
0
0
1000
2000
3000
4000
5000
6000
7000
Engine speed (rpm)

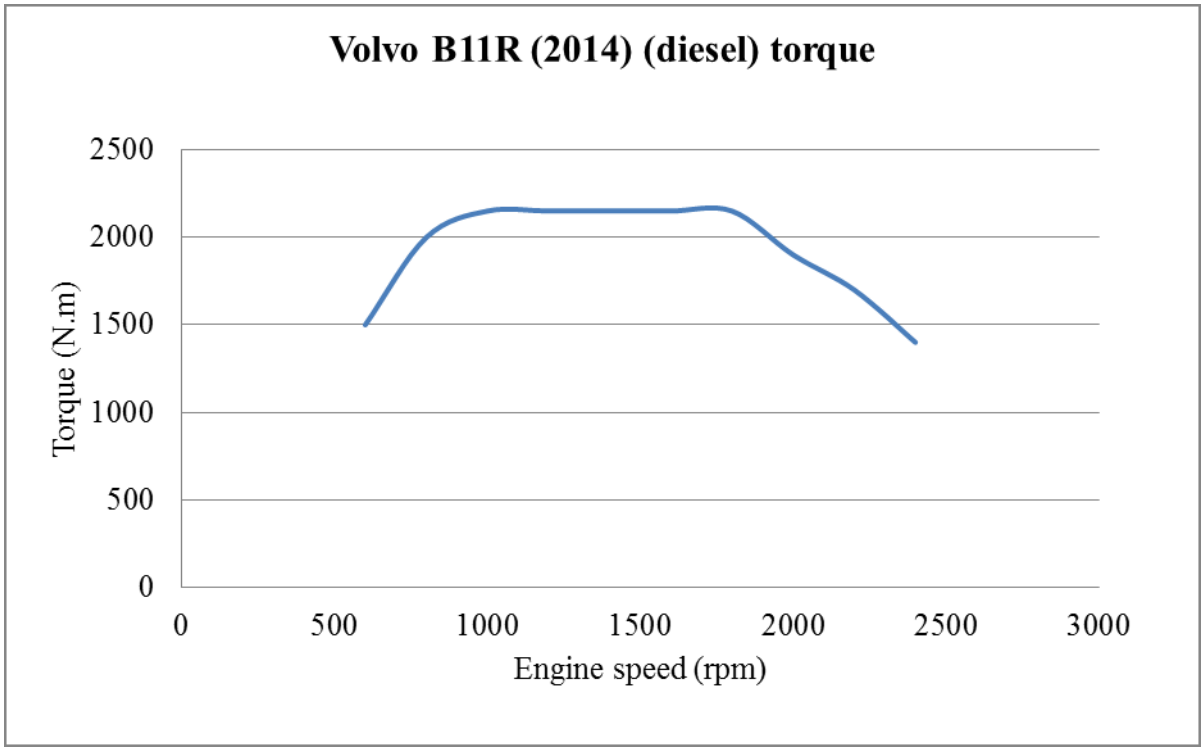
Volvo B11R (2014) (diesel) torque
Torque (N.m)
2500
2000
1500
1000
500
0
0
500
1000
1500
2000
2500
3000
Engine speed (rpm)

APPENDIX VII: Example scaled BSFC plot

eng speed (rpm) / eng load (N.m)	0	3.33	6.67	10	13.3	16.7	20	23.3	26.7	30	33.3	36.7	40	43.3	46.7	50	53.3	56.7	60	63.3	66.7	70	73.3	76.7	80	83.3	86.7	90	93.3
0	0	0	0	0	0	0	0	0	0	0	0	0	0	0	0	0	0	0	0	0	0	0	0	0	0	0	0	0	0
500	0.24	0.24	0.4	0.4	0.5	0.57	0.67	0.67	0.73	0.8	0.8	0.8	0.89	0.89	0.89	0.89	0.89	0.89	0.89	0.89	0.89	0.89	0.89	0.89	0.89	0.89	0.89	0.89	0.89
750	0.24	0.24	0.4	0.44	0.57	0.67	0.67	0.73	0.8	0.8	0.8	0.89	0.89	0.89	0.89	0.95	0.95	0.95	0.95	0.95	0.95	0.95	0.95	0.89	0.89	0.89	0.89	0.89	0.8
1000	0.24	0.24	0.4	0.5	0.57	0.67	0.67	0.73	0.8	0.8	0.89	0.89	0.89	0.89	0.95	0.95	0.95	0.95	0.95	0.95	0.95	0.95	0.95	0.95	0.95	0.89	0.89	0.8	0.8
1250	0.24	0.24	0.4	0.5	0.67	0.67	0.73	0.73	0.8	0.89	0.89	0.89	0.89	0.95	0.95	0.95	0.95	0.95	0.95	0.95	0.95	0.95	0.95	0.95	0.95	0.95	0.95	0.8	0.8
1500	0.24	0.24	0.4	0.5	0.67	0.67	0.73	0.8	0.8	0.89	0.89	0.89	0.89	0.95	0.95	0.95	0.95	1	1	1	1	1	1	0.95	0.95	0.95	0.95	0.95	0.89
1750	0.24	0.24	0.4	0.5	0.67	0.67	0.73	0.8	0.8	0.89	0.89	0.89	0.89	0.95	0.95	0.95	0.95	1	1	1	1	1	1	1	1	0.95	0.95	0.89	0.89
2000	0.24	0.24	0.4	0.5	0.67	0.67	0.73	0.73	0.8	0.89	0.89	0.89	0.89	0.95	0.95	0.95	0.95	1	1	1	1	1	1	1	1	0.95	0.95	0.89	0.89
2250	0.24	0.24	0.4	0.5	0.67	0.67	0.73	0.73	0.8	0.89	0.89	0.89	0.89	0.95	0.95	0.95	0.95	1	1	1	1	1	1	1	1	0.95	0.95	0.89	0.89
2500	0.24	0.24	0.4	0.5	0.57	0.67	0.73	0.73	0.8	0.89	0.89	0.89	0.89	0.95	0.95	0.95	0.95	0.95	1	1	1	1	1	1	1	0.95	0.95	0.89	0.89
2750	0.24	0.24	0.4	0.5	0.57	0.67	0.73	0.73	0.8	0.8	0.89	0.89	0.89	0.95	0.89	0.95	0.95	0.95	0.95	0.95	0.95	0.95	0.95	0.95	0.95	0.95	0.89	0.89	0.89
3000	0.24	0.24	0.4	0.5	0.57	0.67	0.67	0.73	0.8	0.8	0.89	0.89	0.89	0.89	0.89	0.95	0.89	0.89	0.95	0.95	0.95	0.95	0.95	0.95	0.95	0.95	0.89	0.89	0.89
3250	0.24	0.24	0.4	0.44	0.57	0.67	0.67	0.73	0.73	0.8	0.8	0.89	0.89	0.89	0.89	0.89	0.89	0.89	0.95	0.95	0.95	0.95	0.95	0.95	0.89	0.89	0.89	0.89	0.89
3500	0.24	0.24	0.4	0.44	0.57	0.67	0.67	0.73	0.73	0.8	0.8	0.8	0.8	0.89	0.89	0.89	0.89	0.89	0.89	0.89	0.89	0.89	0.95	0.89	0.89	0.89	0.89	0.89	0.8
3750	0.24	0.24	0.4	0.44	0.5	0.67	0.67	0.67	0.73	0.73	0.8	0.8	0.8	0.8	0.8	0.8	0.8	0.89	0.89	0.89	0.89	0.89	0.95	0.89	0.8	0.8	0.8	0.8	0.8
4000	0.24	0.24	0.4	0.44	0.5	0.57	0.67	0.67	0.73	0.73	0.8	0.8	0.8	0.8	0.8	0.8	0.8	0.8	0.8	0.8	0.8	0.8	0.8	0.8	0.8	0.8	0.8	0.8	0
4250	0.24	0.24	0.4	0.44	0.5	0.57	0.67	0.67	0.67	0.73	0.73	0.73	0.8	0.8	0.8	0.8	0.8	0.8	0.8	0.8	0.8	0.8	0.8	0.8	0.8	0.8	0.8	0.8	0
4500	0.24	0.24	0.4	0.44	0.5	0.57	0.67	0.67	0.67	0.73	0.73	0.73	0.73	0.73	0.73	0.73	0.8	0.8	0.8	0.8	0.8	0.8	0.8	0.8	0.8	0.8	0.8	0.8	0
4750	0.24	0.24	0.4	0.44	0.5	0.57	0.67	0.67	0.67	0.67	0.73	0.73	0.73	0.73	0.73	0.73	0.73	0.73	0.73	0.73	0.73	0.73	0.73	0.73	0.73	0.73	0.73	0	0
5000	0.24	0.24	0.4	0.44	0.5	0.5	0.57	0.67	0.67	0.67	0.73	0.73	0.73	0.73	0.73	0.73	0.73	0.73	0.73	0.73	0.73	0.73	0.73	0.73	0.73	0.73	0	0	0
5250	0.24	0.24	0.4	0.4	0.44	0.5	0.57	0.67	0.67	0.67	0.67	0.73	0.73	0.73	0.73	0.73	0.73	0.73	0.73	0.73	0.73	0.73	0.73	0.73	0.73	0	0	0	0
5500	0.24	0.24	0.4	0.4	0.44	0.5	0.57	0.67	0.67	0.67	0.67	0.67	0.73	0.73	0.73	0.73	0.73	0.73	0.73	0.73	0.73	0.73	0.73	0.73	0	0	0	0	0
5750	0.24	0.24	0.4	0.4	0.44	0.5	0.57	0.57	0.67	0.67	0.67	0.67	0.73	0.73	0.73	0.73	0.73	0.73	0.73	0.73	0.73	0.73	0.73	0	0	0	0	0	0
6000	0.24	0.24	0.4	0.4	0.44	0.5	0.57	0.57	0.67	0.67	0.67	0.67	0.67	0.73	0.73	0.73	0.73	0.73	0.73	0.73	0	0	0	0	0	0	0	0	0

Data scaled from Saturn 1.9 (dohc) petrol engine shown in Figure 4.25

An example of normalised BSFC data plot as used in the forward and backward looking model.

Indicates engine efficiency relative to peak efficiency, i.e. 1 = max. full load efficiency

APPENDIX VIII: Engine efficiency vs steady state speed

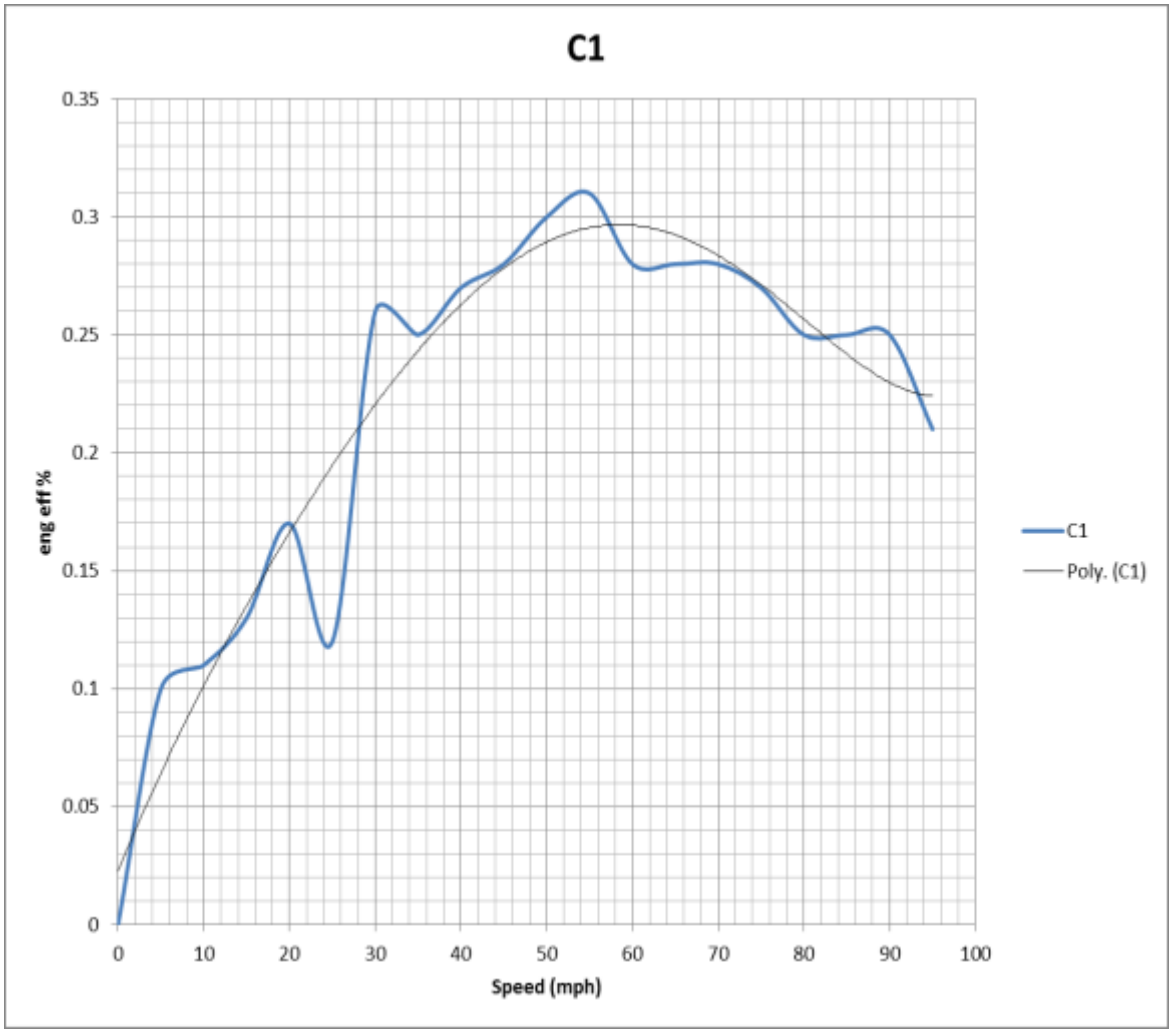

APPENDIX IX: Example plot of NOx *vs* power

Experimental data (top), simulation data (below) Data from TfL, via Coyle (2016)

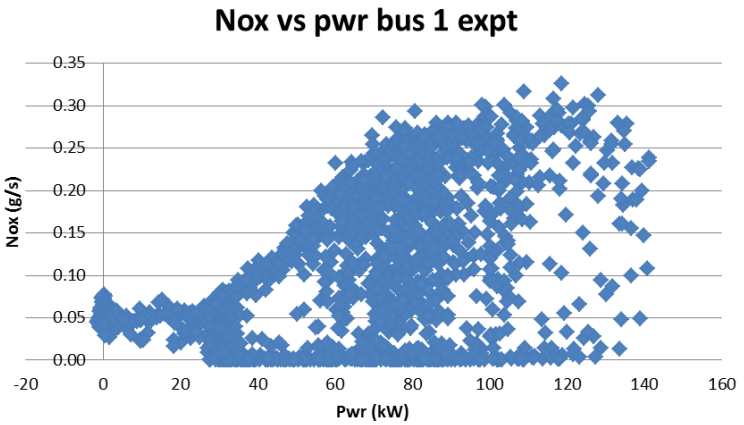

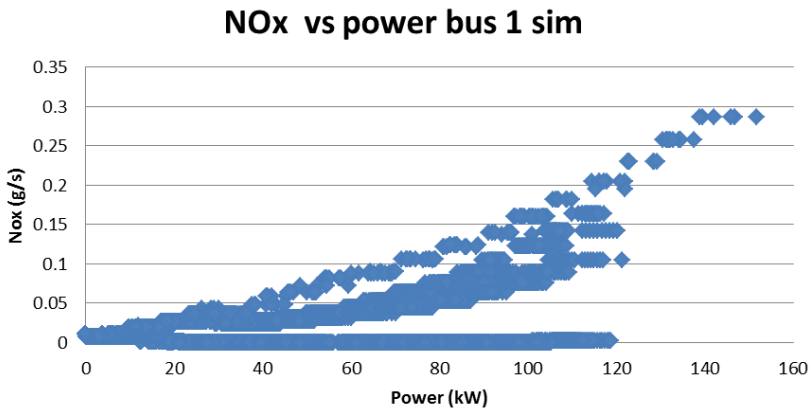

APPENDIX X: Flowchart for backward looking simulation

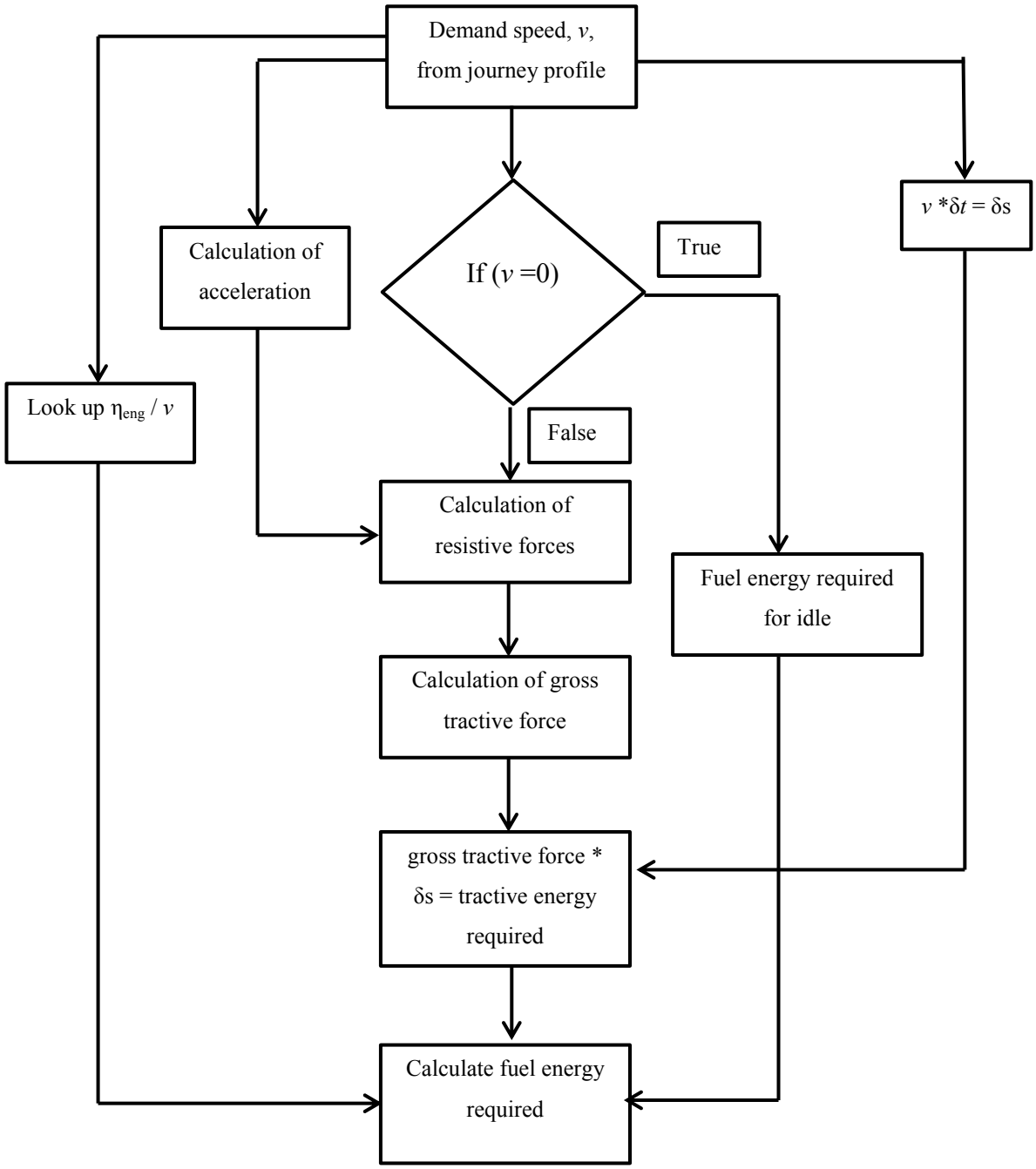

APPENDIX XI: Regenerative braking and energy storage algorithm

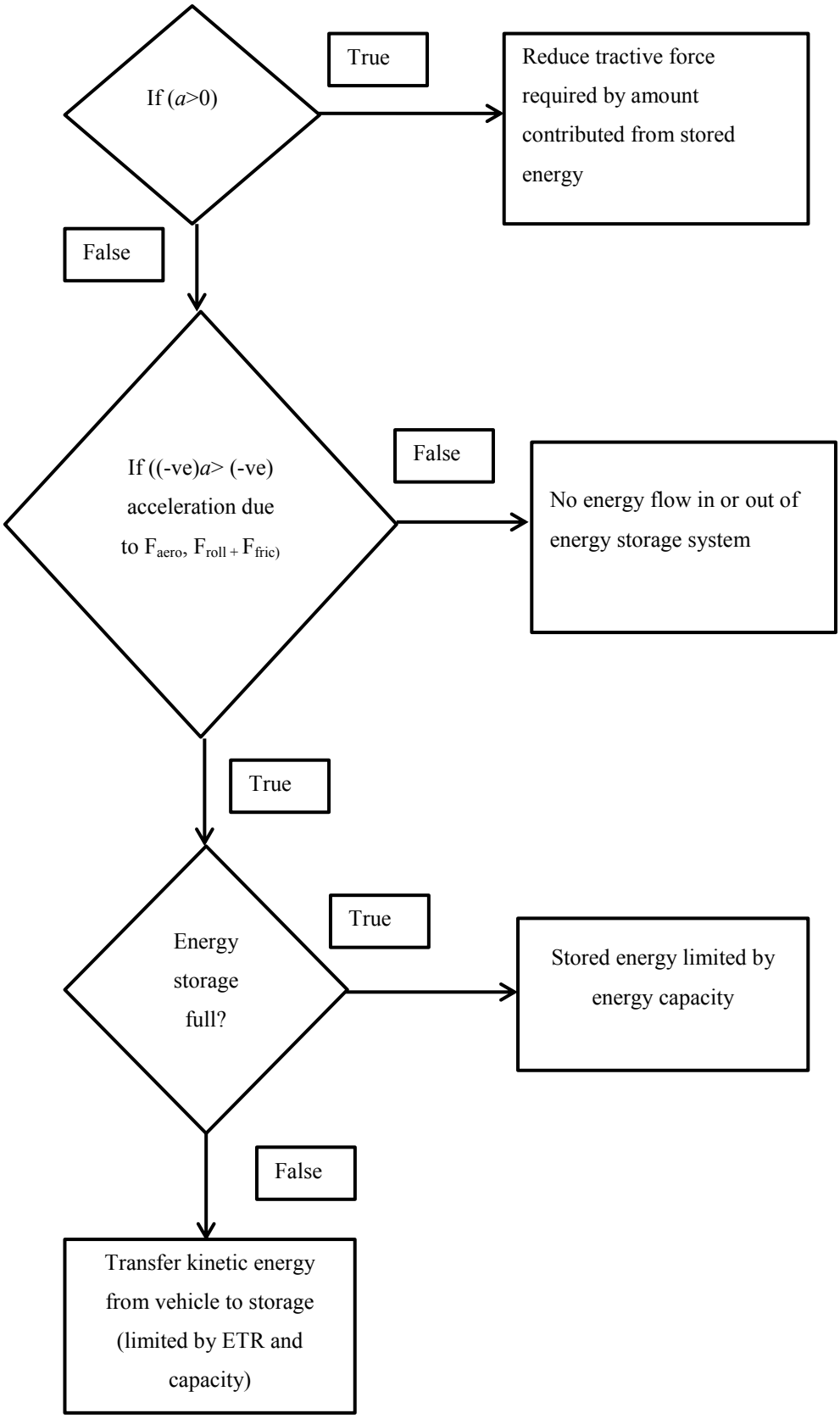

APPENDIX XII: Contribution from stored energy towards traction effort in backward looking model

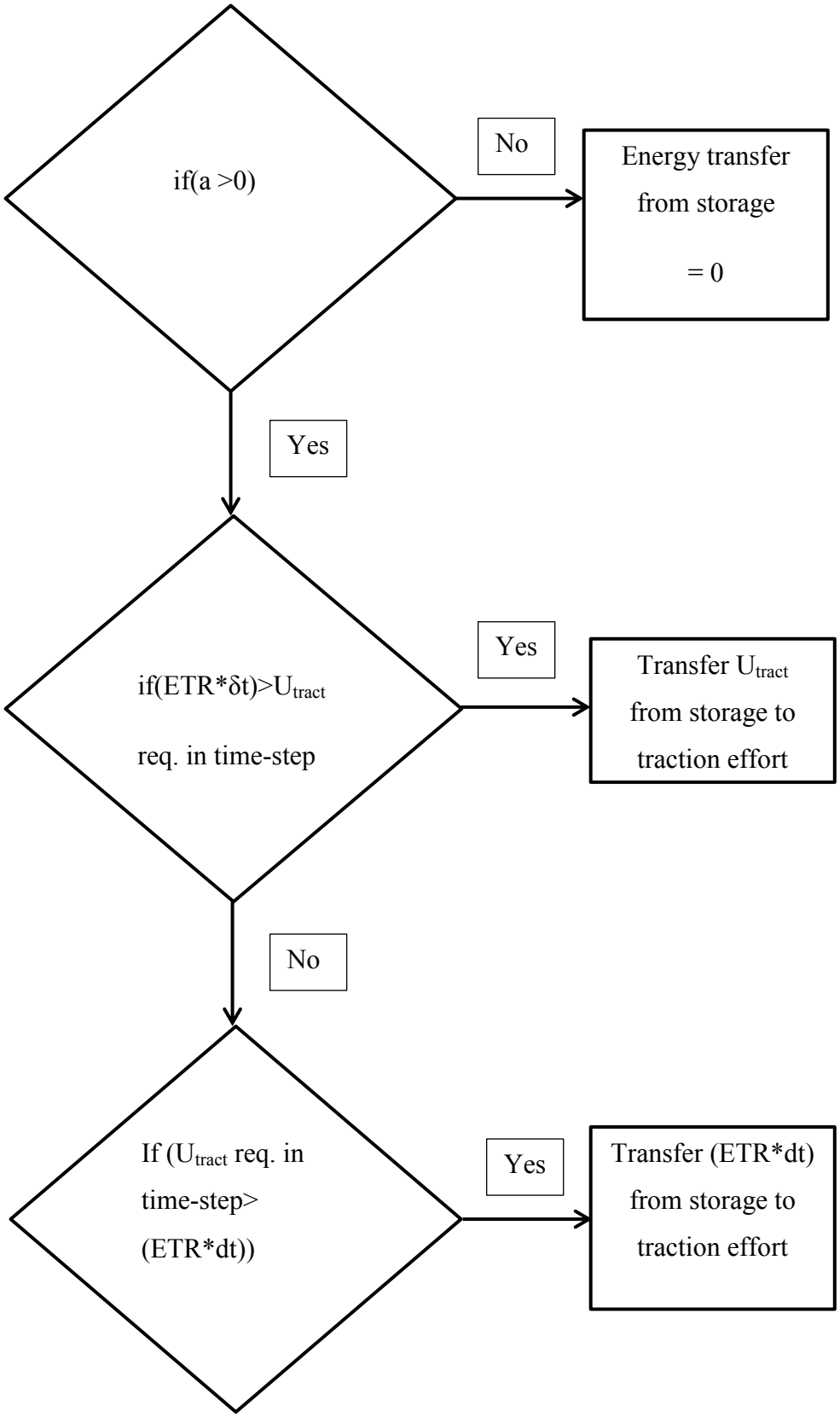

APPENDIX XIII: Limiting total stored energy in backward looking model